



University
of Glasgow

Wallace, Lynsey J.M. (2004) Biochemical and molecular characterisation of purine transporters of *Trypanosoma brucei brucei*. PhD thesis

<http://theses.gla.ac.uk/6546/>

Copyright and moral rights for this thesis are retained by the author

A copy can be downloaded for personal non-commercial research or study, without prior permission or charge

This thesis cannot be reproduced or quoted extensively from without first obtaining permission in writing from the Author

The content must not be changed in any way or sold commercially in any format or medium without the formal permission of the Author

When referring to this work, full bibliographic details including the author, title, awarding institution and date of the thesis must be given.

**Biochemical and Molecular Characterisation of Purine
Transporters of *Trypanosoma brucei brucei***

Lynsey J. M. Wallace

**Division of Infection and Immunity
Institute of Biomedical and Life Sciences**

**This thesis is submitted for the Degree of Doctor of Philosophy
Faculty of Biomedical and Life Sciences
University of Glasgow
June 2004**

Declaration

The results presented in this thesis are my own work, except where there is a statement to the contrary.



Lynsey J. M. Wallace

Abstract

Human African trypanosomiasis (HAT), a lethal disease caused by infection with *Trypanosoma brucei rhodesiense* or *Trypanosoma brucei gambiense*, is responsible for an estimated 500,000 fatalities every year in sub-Saharan Africa. Veterinary trypanosomiasis caused by related trypanosome species have also retarded agricultural and economic development in one of the world's poorest areas. Current control methods rely heavily on flawed trypanocides that have been in use for over 50 years. The inherent limitations of existing drugs have been compounded further by reports of increasing rates of treatment failure.

Trypanosomes are incapable of *de novo* synthesis of the purine ring, and since purines are essential for many cellular functions (e.g. nucleic acid synthesis, energy metabolism) this means the parasites have an absolute requirement for exogenous purines. Several transporters have been identified in *T. brucei brucei* that allow the salvage of purine nucleosides (P1 and P2 transporter) and nucleobases (H1, H2, H3 and H4 transporter) from the host environment. Whilst mammalian cells can also internalise purines from their surroundings, most can synthesise the purine ring from other precursor molecules and this is generally reflected in their less efficient uptake systems.

The P2 nucleoside transporter has also been shown to facilitate entry of arsenical and diamidine trypanocides, and loss of this transporter appears to confer resistance to some of these drugs *in vitro*. Given the need for new drugs in the battle against African trypanosomiasis and that, possible role in drug resistance notwithstanding, a purine transporter has proven an ideal conduit in the past for empirically-applied chemotherapy, it has been proposed that other parasite nucleoside and nucleobase transporters could be exploited for entry of rationally designed trypanocides. Furthermore, a large reservoir of purine compounds exists as a consequence of their widespread use in many other medical conditions – the identification of an effective trypanocide from this resource could contribute to rapid and cost-effective deployment.

This thesis describes the elucidation and comparison of substrate recognition relationships for the H2 nucleobase transporter of *T. b. brucei* and the main nucleobase transporter of

human erythrocytes. Using standard transport kinetics, application of the Cheng-Prusoff equation and a derivation of the Nernst equation, it was possible to determine the Gibbs free energy (ΔG°) for the interactions of purine analogues with each transporter, which allowed predictions about the nature of the interactions that are essential for uptake. A range of unusual tricyclic and “fleximer” purine analogues was also assayed for ability to interact with the various purine transporters in *T. b. brucei* and human erythrocytes. This provided further insights into the extent that the substrate-binding pocket can accommodate unusual and large substrates.

Some of the purine analogues used for the substrate-recognition study also displayed limited trypanocidal activity *in vitro*. More importantly, these results provide a foundation for the design and development of purine nucleobase analogues with anti-trypanosomal action that are efficiently and selectively accumulated by the parasite.

One of the main aims of the project was to clone and characterise nucleobase transporters from *T. b. brucei*. The initial functional complementation strategy in nucleobase-transport deficient trypanosomes proved unsuccessful due to the presence of an additional, previously uncharacterised purine transporter in the trypanosome selection background and other technical obstacles.

Homology searching of the *T. b. brucei* genome database led to the identification of a sequence with substantial similarity to the Adenosine Transporter 1 (*TbAT1*) gene previously shown to be responsible for the P2 nucleoside transport activity. The AT-like sequence was cloned, functionally expressed in heterologous systems (*Saccharomyces cerevisiae* and *Xenopus* oocytes), and characterised as the high-affinity Nucleobase Transporter 1 (TbNBT1). This also marked the first time a nucleobase-specific transporter had been cloned and characterised from any protozoan.

Several other AT-like sequences were identified in the genome database and some of these were also cloned and partially characterised by heterologous expression in yeast. The AT-like D sequence was found to encode a very high-affinity nucleoside transporter.

This project has significantly increased our understanding of the biochemical and molecular nature of purine transporters in *T. b. brucei*.

Acknowledgements

Without doubt my greatest appreciation must go to my supervisor Harry de Koning who has been supportive throughout, despite some *very* difficult times – I genuinely couldn't have done this without him.

I also wish to express my appreciation to Professor Graham Coombs for allowing me to undertake my Ph. D research in his department and for acting as my assessor.

Everyone in North lab, past and present, has contributed to my Ph. D in some way, whether this was as a source for technical advice, by being there as sounding-boards for scientific ideas or general grumbling, or just by being there. I'm incredibly lucky to have worked with such great people.

My roll-call of people I'd particularly like to acknowledge: thanks to my Lab 3 cohorts Denise Candlish and Mohammed Al-Salabi; thanks to Richard Burchmore for his indispensable advice on molecular techniques; a special thank you to Dorothy Armstrong who forms the heart of North lab (and who is very good at putting things back in perspective); and an extra special thank you with kisses and hugs to Mhairi Stewart and Fiona Seow who have been exceptional friends over the past (...how many...?!!) years – eternal thanks guys!

Thank you to my loving husband Alan for his not-so-never-ending patience (it did tend to wear a bit thin occasionally)! Everything must come to an end eventually – and thankfully this has. I wonder which one of us is more relieved?

Thank you to my mum and Gerry for everything (!) and to my little sister Jaclyn (who has suddenly and scarily become an adult). I love you all very much indeed.

TABLE OF CONTENTS

Declaration	ii
Abstract	iii
Acknowledgements	v
Table of Contents	vi
List of Figures	xiv
List of Tables	xix
List of Abbreviations	xxi
Chapter I – Introduction	1
<hr/>	
<i>1.1 African trypanosomiasis</i>	2
1.1.1 The problem	2
1.1.2 Historical perspectives	3
1.1.3 Geography and prevalence	5
1.1.4 The disease	8
1.1.5 Surveillance and diagnosis	9
1.1.6 Chemotherapy	12
<i>1.1.6.1 Treatment of early-stage disease</i>	<i>12</i>
<i>1.1.6.2 Treatment of late-stage disease</i>	<i>15</i>
<i>1.1.6.3 Limitations of current chemotherapy</i>	<i>17</i>
1.1.7 Vector control	20
<i>1.2 Trypanosomes</i>	22
1.2.1 Taxonomy	22
1.2.2 Life-cycles and morphologies	26
1.2.3 Molecular biology of trypanosomes	31
1.2.4 Purine salvage and metabolism in trypanosomes	33
<i>1.2.4.1 Purine metabolic pathways</i>	<i>33</i>

1.2.4.2	<i>Purine transport activities</i>	37
1.2.4.3	<i>Molecular biology of purine uptake</i>	40
1.2.5	The role of transporters in drug targeting and drug resistance	43
Chapter II – Materials and Methods		47
<hr/>		
2.1	<u>Parasite strains</u>	48
2.2	<u>Bacterial strains</u>	48
2.3	<u>Yeast strains</u>	48
2.4	<u>Chemicals</u>	49
2.4.1	Purine analogues and radiolabelled compounds	49
2.4.2	Other chemical reagents	49
2.4.3	Oligonucleotides and molecular biology enzymes	49
2.5	<u>Growth and maintenance of parasites</u>	50
2.5.1	Bloodstream form trypanosomes <i>in vitro</i>	50
2.5.2	Bloodstream form trypanosomes <i>in vivo</i>	50
2.5.3	Procyclic form trypanosomes <i>in vitro</i>	50
2.6	<u>Growth and maintenance of <i>Saccharomyces cerevisiae</i></u>	51
2.7	<u>Growth and maintenance of <i>Escherichia coli</i></u>	51
2.8	<u>Transport assays in trypanosomatids</u>	51
2.8.1	Collection and purification of bloodstream form <i>Trypanosoma brucei</i> <i>brucei</i> from experimental rodents	51
2.8.2	Preparation of cells for uptake assay	52

2.8.3	Transport assays in trypanosomatids	52
2.9	<u>Transport assays in human erythrocytes</u>	53
2.9.1	Preparation of cells for uptake assay	53
2.9.2	Transport assays in human erythrocytes	53
2.10	<u>Transport assays in <i>Saccharomyces cerevisiae</i></u>	54
2.10.1	Preparation of cells for uptake assay	54
2.10.2	Transport assays in <i>Saccharomyces cerevisiae</i>	54
2.11	<u>Transport assays in <i>Xenopus laevis</i> oocytes</u>	55
2.11.1	Preparation of cells for uptake assay	55
2.11.2	Transport assays in <i>Xenopus laevis</i> oocytes	55
2.11	<u>Analysis of data from transport assays</u>	55
2.12	<u>Alamar Blue assays</u>	56
2.13	<u>Molecular cloning techniques</u>	57
2.13.1	Preparation and purification of genomic DNA from <i>Trypanosoma brucei</i>	57
2.13.2	Plasmid vectors	58
2.13.3	Restriction enzyme digestion of DNA	59
2.13.4	Agarose electrophoresis of DNA	59
2.13.5	Purification of DNA from agarose gel	60
2.13.6	Ligation	60
2.13.7	Preparation of chemically-competent <i>Escherichia coli</i>	60
2.13.8	Preparation of electrocompetent <i>Escherichia coli</i>	61
2.13.9	Transformation of <i>Escherichia coli</i>	62
2.13.9.1	Heat-shock method	62
2.13.9.2	Electroporation	62

2.13.10 Mini-, midi-, and maxi-preps of plasmid DNA	63
2.13.11 Polymerase chain reactions	63
2.13.12 A-tailing of PCR products	63
2.13.13 Transformation of chemically-competent <i>Saccharomyces cerevisiae</i>	64
2.13.14 Growth of <i>Saccharomyces cerevisiae</i> in selective media	64
2.13.15 Preparation and purification of total RNA from <i>T. brucei</i>	65
2.13.16 Radiolabelling of probes	65
2.13.17 Northern hybridisation	65
2.14 <u>Software and web resources</u>	67

Chapter III – Substrate recognition models for the H2 purine transporter of *Trypanosoma brucei brucei* **68**

3.1 <u>Introduction</u>	69
3.1.1 Why study the H2 transporter?	69
3.1.2 Mechanisms of molecular recognition	70
3.1.3 Recognition models and use of analogues to characterise transporters or enzymes	73
3.2 <u>Results</u>	80
3.2.1 Structure-activity relationships	80
3.2.2 Trypanotoxicity of purine analogues	86
3.3 <u>Discussion</u>	88

Chapter IV – Substrate recognition models for the equilibrative nucleobase transporter of human erythrocytes **91**

4.1 <u>Introduction</u>	92
--------------------------------	-----------

4.1.1	The human erythrocyte as experimental model	92
4.1.2	The facilitative nucleobase transporter	93
4.2	<u>Results</u>	94
4.2.1	Confirmation of basic kinetics of hFNT1 in human erythrocytes	94
4.2.2	Structure-activity relationships	96
4.3	<u>Discussion</u>	101
 Chapter V – Recognition of unusual potential trypanocides by the purine transporters of <i>Trypanosoma brucei brucei</i>		104
<hr/>		
5.1	<u>Introduction</u>	105
5.1.1	Tricyclic purine compounds – origins	105
5.1.2	Thieno-separated tricyclic and fleximer purine analogues	106
5.2	<u>Results</u>	110
5.2.1	Analogues	110
5.2.2	Inhibition of H2 activity by thieno-separated purine nucleobases	110
5.2.3	Inhibition of P1 activity by thieno-separated and fleximer purine analogues	113
5.2.4	Inhibition of P2 activity by thieno-separated and fleximer purine analogues	115
5.2.5	Inhibition of hFNT1 activity by thieno-separated purine nucleobases	116
5.2.6	Trypanotoxicity of thieno-separated and fleximer purine analogues	118
5.3	<u>Discussion</u>	120

Chapter VI - Functional complementation strategy for cloning of nucleobase transporter genes from *Trypanosoma brucei brucei* **124**

6.1 <u>Introduction</u>	125
6.1.1 Functional complementation in <i>Trypanosoma brucei</i>	126
6.1.2 Functional complementation in <i>Aspergillus nidulans</i>	128
6.2 <u>Results</u>	129
6.2.1 <i>Trypanosoma brucei</i> genomic DNA libraries	129
6.2.1.1 Optimisation of technique	132
6.2.1.2 Validation of DNA libraries	133
6.2.2 Growth of <i>Trypanosoma brucei</i> procyclics in allopurinol in attempt to obtain H1-deficient line	135
6.2.3 <i>Aspergillus</i> screening	137
6.3 <u>Discussion</u>	138

Chapter VII – Characterisation of a novel ENT family member as the first protozoan nucleobase transporter **141**

7.1 <u>Introduction</u>	142
7.1.1 Identification of sequence in the <i>Trypanosoma brucei</i> genome database with homology to <i>TbAT1</i>	142
7.1.2 Yeast expression systems	144
7.1.3 <i>Xenopus laevis</i> oocyte expression systems	147
7.2 <u>Results</u>	148
7.2.1 Sub-cloning of AT-like putative transporter gene into pDR195	148
7.2.2 Sub-cloning of AT-like putative transporter gene into pGEM-HE	149

7.2.3 Selection of yeast colonies expressing the AT-like gene	151
7.2.4 Characterisation of uptake by AT-like permease expressed in <i>Saccharomyces cerevisiae</i> MG887.1	151
7.2.5 Characterisation of uptake by TbNBT1 expressed in <i>Xenopus laevis</i> oocytes	155
7.2.6 Reconciliation of heterologous system results with transport activities <i>in situ</i>	156
7.3 <u>Discussion</u>	157

Chapter VIII – Cloning and characterisation of AT-like transporter genes

161

8.1 <u>Introduction</u>	162
8.2 <u>Results</u>	162
8.2.1 Polymerase chain reactions and cloning of AT-like sequences	162
8.2.2 Sequencing	165
8.2.3 Prediction of transmembrane domains	166
8.2.4 Sub-cloning of AT-like sequences into pDR195	170
8.2.5 Selection of yeast colonies expressing the AT-like A, B or D gene	174
8.2.6 Preliminary characterisation of uptake by AT-like permeases expressed in <i>Saccharomyces cerevisiae</i> MG887.1	174
8.2.7 Northern hybridisation	177
8.2.8 Overview of ENT family members identified in the <i>Trypanosoma brucei</i> genome database	179
8.3 <u>Discussion</u>	184

Chapter IX – General Discussion

188

References	195
-------------------	------------

Appendices**A1**

A: Media, Buffers and Solutions***A2******B: Restriction Enzyme Recognition and Incision Sites******A10******C: Publications******A11***

List of Figures

Chapter I. Introduction

Figure 1.1	Regions of the African continent at risk from HAT.	5
Figure 1.2	Diagnosis of trypanosomiasis.	11
Figure 1.3	Structures of trypanocides.	13
Figure 1.4	The tsetse fly.	20
Figure 1.5	Taxonomic classification of trypanosomes.	23
Figure 1.6	Morphologies of <i>Trypanosoma brucei rhodesiense</i> .	27
Figure 1.7	Bloodstream form <i>Trypanosoma brucei gambiense</i> .	28
Figure 1.8	Events during a single "wave" of parasitaemia caused by <i>Trypanosoma brucei brucei</i> .	28
Figure 1.9	The <i>Trypanosoma brucei</i> life-cycle.	30
Figure 1.10	Organisation of the bloodstream expression site.	33
Figure 1.11	Origins of the atoms present in the purine ring following <i>de novo</i> synthesis.	34
Figure 1.12	The main pathways of purine salvage in <i>Trypanosoma brucei</i> .	35
Figure 1.13	Nucleobase and nucleoside transporters of <i>Trypanosoma brucei</i> .	41
Figure 1.14	Uptake of trypanocidal drugs.	44

Chapter III. Substrate recognition models for the H2 purine transporter of *Trypanosoma brucei brucei*

Figure 3.1	The geometry of a hydrogen bond.	72
Figure 3.2	Recognition of DHF and MTX by DHFR.	73
Figure 3.3	Analogues used to characterise substrate recognition by the H2 transporter.	76-79
Figure 3.4	Inhibition of H2-mediated [³ H] hypoxanthine transport in <i>Trypanosoma brucei brucei</i> bloodstream forms by purine analogues.	81

Figure 3.5	Model of the interactions between purines and the <i>Trypanosoma brucei</i> H2 transporter.	85
Figure 3.6	Trypanocidal activity of purine analogues.	87

Chapter IV. Substrate recognition models for the equilibrative nucleobase transporter of human erythrocytes

Figure 4.1	Uptake of [³ H] adenine by human erythrocytes as a function of time.	95
Figure 4.2	Michaelis-Menten plot for transport of 1 μM [³ H] adenine by human erythrocytes.	95
Figure 4.3	Inhibition of FNT1-mediated [³ H] adenine transport in human erythrocytes by purine analogues.	98
Figure 4.4	Model of the interactions between purines and the hFNT1 transporter.	100

Chapter V. Recognition of unusual potential trypanocides by the purine transporters of *Trypanosoma brucei brucei*

Figure 5.1	Original benzoadenine compounds.	105
Figure 5.2	Tricyclic analogues of purine nucleosides.	107
Figure 5.3	Tricyclic analogues of purine nucleobases.	108
Figure 5.4	Fleximer analogues of purine nucleosides.	108
Figure 5.5	The 3-dimensional structure of TRI-B-004 compared to the parent molecule 6-methylthiopurine.	109
Figure 5.6	Inhibition of transport of 0.1 μM [³ H] hypoxanthine by <i>Trypanosoma brucei</i> bloodstream forms by TRI-B-001, TRI-B-002 and TRI-003.	110
Figure 5.7	Model of the interactions between tricyclic purines and the <i>Trypanosoma brucei</i> H2 transporter.	113
Figure 5.8	The normal P1 substrate recognition motif.	114
Figure 5.9	The normal P2 substrate recognition motif.	115
Figure 5.10	Inhibition of transport of 1 μM [³ H] adenine by human erythrocytes by TRI-B-001, TRI-B-002 and TRI-003.	116

Figure 5.11	Example of Alamar Blue assay graph.	118
-------------	-------------------------------------	-----

Chapter VI. Functional complementation strategy for cloning of nucleobase transporter genes from *Trypanosoma brucei brucei*

Figure 6.1	Functional complementation strategy in <i>Trypanosoma brucei</i> .	127
Figure 6.2	Plasmid vector pTSO-HYG4.	130
Figure 6.3	The UapA transcriptional cassette of plasmid vector pNS328.	130
Figure 6.4	Gel electrophoresis of <i>T. b. brucei</i> genomic DNA partially digested using <i>Sau3A</i> .	131
Figure 6.5	Ligation of <i>Sau3A</i> fragments and plasmid vector.	131
Figure 6.6	Nine random library colony minipreps digested with <i>HindIII</i> .	132
Figure 6.7	PCR reactions using library as template.	135
Figure 6.8	Effect of allopurinol on growth of <i>Trypanosoma brucei</i> procyclics.	136

Chapter VII. Characterisation of a novel ENT family member as the first protozoan nucleobase transporter

Figure 7.1	Alignment comparing predicted amino acid sequences of <i>TbAT1</i> and AT-like gene.	144
Figure 7.2	Nucleotide and amino acid sequence of AT-like sequence.	145
Figure 7.3	Transient expression of exogenous permease genes in <i>Xenopus laevis</i> oocytes.	147
Figure 7.4	Vector pDR195 for expression in <i>Saccharomyces cerevisiae</i> .	148
Figure 7.5	Orientation of AT-like sequence in pDR195 multicloning site.	149
Figure 7.6	Orientation of the AT-like insert in pDR195.	149
Figure 7.7	<i>Xenopus</i> oocyte vector pGEM-HE.	150
Figure 7.8	Orientation of AT-like sequence in pGEM-HE.	150
Figure 7.9	Orientation of AT-like insert in pGEM-HE.	151
Figure 7.10	Uptake of [³ H] purine permeants versus time for <i>TbNBT1</i> expressed in <i>Saccharomyces cerevisiae</i> strain MG887-1.	152-153

Figure 7.11	Transport of [³ H] hypoxanthine by <i>TbNBT1</i> in <i>Saccharomyces cerevisiae</i> strain MG887-1.	154
Figure 7.12	Purine and pyrimidine transport in <i>Xenopus</i> oocytes injected with RNA transcripts encoding protozoan and mammalian members of the ENT family.	156

Chapter VIII. Cloning and characterisation of AT-like transporter genes

Figure 8.1	Primers used for amplification of AT-like sequences from total <i>Trypanosoma brucei</i> genomic DNA.	163
Figure 8.2	Polymerase chain reaction.	163
Figure 8.3	Digest of AT-like A:pGEM-T Easy.	164
Figure 8.4	Digest of AT-like B:pGEM-T Easy.	164
Figure 8.5	Digest of AT-like D:pGEM-T Easy.	165
Figure 8.6	Sequencing.	166
Figure 8.7	Nucleotide and amino acid sequence of AT-like A.	167
Figure 8.8	The nucleotide and amino acid sequence of AT-like B.	168
Figure 8.9	The nucleotide and amino acid sequence of AT-like D.	169
Figure 8.10	Hydropathy plots for AT-like amino acid sequences.	171
Figure 8.11	Orientation of AT-like A in pDR195.	172
Figure 8.12	AT-like A:pDR195 digested with <i>Bam</i> HI/ <i>Hind</i> III.	172
Figure 8.13	Orientation of AT-like B in pDR195.	172
Figure 8.14	AT-like B:pDR195 digested with <i>Xho</i> I.	173
Figure 8.15	Orientation of AT-like D in pDR195.	173
Figure 8.16	AT-like D:pDR195 digested with <i>Bam</i> HI.	174
Figure 8.17	Uptake of adenine by <i>Saccharomyces cerevisiae</i> MG887.1 transformed with AT-like D:pDR195.	175
Figure 8.18	Uptake of adenosine by <i>Saccharomyces cerevisiae</i> MG887.1 transformed with AT-like D:pDR195.	176

Figure 8.19	Inhibition of adenosine uptake by <i>Saccharomyces cerevisiae</i> MG887.1 transformed with AT-like D:pDR195.	176
Figure 8.21	Transfer of RNA to membrane for Northern analysis.	178
Figure 8.22	Northern hybridisation using the full-length AT-like B ORF as probe.	178
Figure 8.23	Multiple alignment of ENT gene family members in <i>Trypanosoma brucei</i> .	180-181
Figure 8.24	Tree showing how <i>Trypanosoma brucei</i> ENTs relate to each other.	182

Chapter IX. General Discussion

Figure 9.1	Model of the interactions between purines and the <i>Leishmania major</i> NBT1 transporter.	190
Figure 9.2	Structure of the immunosuppressant azathioprine.	191

List of Tables

Chapter I. Introduction

Table 1.1	Comparison of the number of reported cases of HAT in four African countries in 1976 and 1997.	7
-----------	---	---

Chapter III. Substrate recognition models for the H2 purine transporter of *Trypanosoma brucei brucei*

Table 3.1	K_i and ΔG° values for the inhibition of hypoxanthine uptake by the <i>Trypanosoma brucei</i> H2 nucleobase transporter.	83
-----------	---	----

Chapter IV. Substrate recognition models for the equilibrative nucleobase transporter of human erythrocytes

Table 4.1	K_i and ΔG° values for inhibition of adenine uptake by the human facilitative nucleobase transporter.	99
Table 4.2	Specificity ratio table.	103

Chapter V. Recognition of unusual potential trypanocides by the purine transporters of *Trypanosoma brucei brucei*

Table 5.1	Inhibition of <i>Trypanosoma brucei</i> nucleobase uptake by thieno-separated tricyclic nucleobases.	112
Table 5.2	Inhibition of <i>Trypanosoma brucei</i> P1- transport activity by fleximer and tricyclic nucleoside analogues.	114
Table 5.3	Inhibition of <i>Trypanosoma brucei</i> P2- transport activity by fleximer and tricyclic purine analogues.	115
Table 5.4	Inhibition of hFNT1- transport activity by tricyclic purine nucleobase analogues.	117
Table 5.5	Anti-trypanosomal activity of purine analogues.	119
Table 5.6.	The selectivity indices of thieno-separated tricyclic purine nucleobases for uptake by the H2 transporter and hFNT1.	121

Chapter VI. Functional complementation strategy for cloning of nucleobase transporter genes from *Trypanosoma brucei brucei*

Table 6.1	Primers used for polymerase chain reactions using library as template.	134
Table 6.2	Effect of various purine analogues and trypanocides on <i>Trypanosoma brucei</i> WT procyclics and <i>Trypanosoma brucei</i> procyclics exposed to allopurinol.	137
Table 6.3	Kinetic parameters of procyclic hypoxanthine transporters in control and long-term allopurinol exposed cells.	139

Chapter VII. Characterisation of a novel ENT family member as the first protozoan nucleobase transporter

Table 7.1	K_m or K_i values obtained for <i>TbNBT1</i> expressed in <i>Saccharomyces cerevisiae</i> MG887.1.	155
-----------	--	-----

Chapter VIII. Cloning and characterisation of AT-like transporter genes

Table 8.1	Affinity constants for AT-like D expressed in <i>Saccharomyces cerevisiae</i> MG887.1.	177
Table 8.2	Similarities and identities of <i>T. b. brucei</i> ENT-family members.	183

List of Abbreviations

ΔG°	Gibbs free energy
$\delta(\Delta G^\circ)$	difference in Gibbs free energy
μ	micro
μF	micro Faraday
μg	microgram
μl	microlitre
μM	micromolar
π	pi
Ω	Ohm – unit of resistance
	angstrom
ADH	alcohol dehydrogenase
AIDS	Acquired Immunodeficiency Syndrome
AMP	adenosine 5'-monophosphate
APRT	adenine phosphoribosyltransferase
AT	adenosine transporter
ATP	adenosine triphosphate
BBB	blood brain barrier
B-ES	bloodstream expression site
bp	basepair
BSF	bloodstream form
CATT	card agglutination test for trypanosomiasis
CBSS	Carter's balanced salt solution
Ci	Curie
CIAP	calf intestinal alkaline phosphatase
CNS	central nervous system
CSF	cerebrospinal fluid
CTC	capillary tube centrifugation
dATP	deoxyadenosine triphosphate
dCTP	deoxycytidine triphosphate
DDT	dichloro-diphenyl-trichloroethane

DEAE	diethylaminoethyl-
DEPC	diethylpyrocarbonate
DFMO	difluoromethylornithine
dGTP	deoxyguanosine triphosphate
DHF	dihydrofolate
DHFR	dihydrofolate reductase
DMSO	dimethylsulphoxide
DNA	deoxyribonucleic acid
dNTP	deoxynucleotide triphosphate
DRC	Democratic Republic of Congo
dTTP	deoxythymidine triphosphate
EATRO	East African Trypanosomiasis Research Organisation
EDTA	ethylenediamine tetra acetic acid
ENT	equilibrative nucleoside transporter
ESAG	expression site associated gene
FCS	foetal calf serum
g	gram
GMP	guanosine 5'-monophosphate
GPI	glycosylphosphatidylinositol
gRNA	guide RNA
h	hour
HAPT1	high affinity pentamidine transporter
HAT	human African trypanosomiasis
H-bond	hydrogen bond
HEPES	N-2-hydroxyethylpiperazine-N'-2-ethanesulphonic acid
HGPRT	hypoxanthine guanine phosphoribosyltransferase
hs DNA	herring sperm DNA
IC ₅₀	50% inhibitory concentration
IMP	inosine 5'-monophosphate
IPTG	isopropylthio-β-D-galactoside
kb	kilobase
kg	kilogram
K _i	inhibition constant
kJ	kilojoule

K_m	Michaelis constant
LAPT1	low affinity pentamidine transporter
LB	Luria-Bertani medium
LDL	low-density lipoprotein
LS	long-slender
m-AECT	mini anion exchange column technique
Mb	megabase
M-ES	metacyclic expression site
mg	milligram
ml	millilitre
mM	millimolar
mmol	millimole
MOPS	3-[N-morpholino] propane-sulphonic acid
mRNA	messenger ribonucleic acid
MTX	methotrexate
mV	millivolt
NAT	nucleobase/ascorbate transporter
ng	nanogram
nm	nanometer
OD	optical density
ODC	ornithine decarboxylase
ORF	open reading frame
PARP	procyclic acidic repetitive protein
PC	procyclic
PCR	polymerase chain reaction
PEG	polyethylene glycol
PFGE	pulsed field gel electrophoresis
PFTM	purine-free trypanosome medium
<i>Pfu</i>	<i>Pyrococcus furiosus</i>
PGND	phosphogluconate dehydrogenase
PMA1	yeast plasma membrane ATPase
pmol	picomole
PRP	purine-related transporter
PRPP	5'-phosphoribosyl-1-pyrophosphate

PRTase	phosphoribosyltransferase
PSG	phosphate buffered saline, 1% glucose
PTRE	post treatment reactive encephalopathy
PUP	plant purine-related transporter
RBC	red blood cell
RFLP	restriction fragment length polymorphism
RIME	ribosomal insertional mobile element
RNA	ribonucleic acid
rpm	revolutions per minute
RPMI	Roswell Park Memorial Institute
rRNA	ribosomal RNA
s	second
SAT	sequential aerial technique
SC-URA	synthetic complete drop out mix minus uracil
SDS	sodium dodecylsulphate
SE	standard error
SIT	sterile insect technique
SRA	serum resistance associated
SS	short-stumpy
SSC	saline sodium citrate
SS-DNA	single-stranded DNA
<i>Taq</i>	<i>Thermus aquaticus</i>
TbAT1	<i>Trypanosoma brucei</i> adenosine transporter
TBE	tris-borate-EDTA
TbNBT1	<i>T. brucei</i> nucleobase transporter
TbNT2-7	<i>T. brucei</i> nucleoside transporter
TE	tris-EDTA
TLF	trypanolytic factor
TREU	Trypanosome Research Edinburgh University
U	unit
UV	ultraviolet
V	volts
VAT	variant antigen type
V_{\max}	maximum velocity

VSG	variant surface glycoprotein
WHO	World Health Organisation
WT	wild-type
X-Gal	5-bromo-4-chloro-3-indolyl- β -D-galactoside
XMP	xanthosine 5'-monophosphate
XPRT	xanthine phosphoribosyltransferase
YPAD	yeast extract-peptone-dextrose and adenine medium

Chapter One

Introduction

1.1 African trypanosomiasis

1.1.1 The problem

The diseases caused by parasitic protozoans of the genus *Trypanosoma* are responsible for the devastation of large regions of the African continent. In the absence of treatment, or in the event of treatment failure, infection of the human bloodstream and central nervous system by these parasites leads inexorably to death. As well as the casualties directly attributable to human African trypanosomiasis (HAT), the decimation of the domestic cattle population by the related disease known as nagana (the Zulu word for “poorly”) also contributes to the profound poverty and malnutrition experienced in sub-Saharan Africa.

Two distinct types of HAT, also known rather innocuously as “sleeping sickness”, can be differentiated on the basis of the organism involved, the geographical location and how quickly the disease progresses. The causative agent of the East African disease is *Trypanosoma brucei rhodesiense* and the infection typically runs a rapid course usually terminating within six months in the absence of any medical intervention. Meanwhile, infection with the related species *Trypanosoma brucei gambiense* leads to the chronic disease seen in West and Central Africa. *Gambiense* disease can persist for up to two years before final lethal involvement of the central nervous system (Welburn, *et al.*, 2001).

Although HAT can be managed with a combination of timely medical treatment and control of the tsetse fly vector, due to several factors the disease has made a comeback in recent years. In the last 20-30 years there has been a rise in the number of reported cases which has coincided with a drop in the number of people under surveillance (WHO, Report on Global Surveillance of Epidemic-prone Infectious Diseases, 2000). This means that the number of reported cases does not reflect the real magnitude of the problem. It is estimated that up to 60 million people are at risk of infection but less than 7% of these are subject to surveillance. Therefore, although 40,000 was the number of official cases in 1999 the actual victims are much more likely to number 300,000 - 500,000 (Seed, 2000).

The direct agricultural toll due to the occurrence of trypanosomiasis in domestic livestock is the death of an estimated 3 million cattle annually. *T. vivax*, *T. congolense* and *T. brucei brucei* are the main causative agents of bovine trypanosomiasis across Africa. Infection of

cattle is also responsible for a 20% decrease in calving and a 25% decrease in milk production (Seed, 2000). As well as the obvious direct loss of livestock and dairy produce the presence of animal disease also has other consequences for the development of rural communities. Infestation by disease-carrying tsetse flies leads to otherwise farmable land being unusable and lack of draught power is also disadvantageous to progress (Kuzoe, 1993; Seed, 2000).

Factors which have led to the re-emergence of both human and animal disease are numerous. The changing political landscape in many areas with the inevitable concurrent conflicts and social upheaval has often led to the collapse of health provision services and the cessation of control practices. Existing chemotherapy can be effective but is inadequate in terms of toxicity, cost and ease of administration, and is further complicated by an increasing number of treatment failures in the field.

1.1.2 Historical perspectives

The genus *Trypanosoma* was inaugurated by Gruby in 1843 with the discovery of the first trypanosome in frogs (*Trypanosoma sanguinis*). Observations by David Bruce that led to the association of *T. b. brucei*, the tsetse fly and the animal disease nagana were preceded by the observations of Evans and of Smith & Kilbourne. In 1880, Evans made the connection between the animal disease sura and the organism later known as *Trypanosoma evansi*. Meanwhile, the transmission of babesia by the tick was elucidated by Smith & Kilbourne in 1893 to provide the first known example of a communicable disease spread by insect vectors (Vickerman, 1997).

Trypanosomes and tsetse flies co-evolved with humans and historical accounts suggest that although the cause of the disease was unknown prior to the end of the 19th century, the symptoms were well known long before. Slave traders would use the presence of characteristic neck swellings to reject slaves who would become ill with “sleepy distemper” (Barrett, *et al.*, 2003). The role of the tsetse in causing sickness in animals had also been observed in the mid 19th century by the renowned explorer David Livingstone who surmised that the flies administered some kind of venom in their bite (Vickerman, 1997).

In 1895, while posted in Zululand in South Africa David Bruce outlined the links between the tsetse fly, the trypanosome and the cattle scourge named nagana (Smith, *et al.*, 1998). Bruce, who also elucidated the cause of brucellosis, later gave his name to the *Trypanosoma brucei* parasite. Several years later, Bruce also worked on the human disease in Uganda identifying the causative agent as the *Trypanosoma gambiense* (later *Trypanosoma brucei gambiense*) parasite that had been isolated from a patient by Dutton in 1902 (Vickerman, 1997).

By the time David Bruce was researching the role of *T. b. gambiense* in human sleeping sickness, the number of people suffering from the disease was reaching epidemic proportions. The extent of the epidemic in the early 1900's is now estimated to have involved more than one million human cases with approximately three quarters of a million deaths in central Africa – and over 250,000 fatalities occurring in Uganda alone (Seed, 2000; Smith, *et al.*, 1998). According to the World Health Organization, the 20th century went on to witness two other periods of extraordinarily high epidemic levels of HAT (WHO, Report on Global Surveillance of Epidemic-prone Infectious Diseases, 2000). The second epidemic occurred in the 1920's and 1930's, with an all-time high of 33,562 human cases reported in Zaire in 1930 (Ekwanzala, *et al.*, 1996).

Following the devastating epidemics of the first quarter of the century, the colonial powers-that-be enforced enthusiastic control measures that included mass-screening and treatment of the population, eradication of tsetse flies using insecticides, the destruction of tsetse fly habitat and culling of the animal reservoirs of disease (Seed, 2000). By 1959 the number of reported cases in Zaire had fallen to around 1,000 (Ekwanzala, *et al.*, 1996); the number of cases in Angola also fell from 5,000 in the 1950's to only 3 reported cases in 1974 (Smith, *et al.*, 1998). By the 1970's, with 10,000 to 20,000 cases across the tsetse fly belt it appeared as if the war on HAT was slowly but surely being won (Seed, 2000). With no significant involvement of animal reservoirs in the transmission cycle of *T. brucei gambiense* the eradication of the *gambiense* disease in particular seemed tantalisingly close.

Unfortunately, the last thirty years have seen the re-emergence of HAT, with epidemics caused by *T. brucei gambiense* arising in Zaire (now the Democratic Republic of Congo), Uganda, Sudan and Angola.

Many factors have contributed to this recrudescence. The advent of independence for many African countries, bringing with it the almost obligatory accompanying civil unrest and conflict, led to the disruption of HAT control strategies. Following independence in Zaire in 1960, for example, there was a five year civil war, during which there was no surveillance of the population (Ekwanzala, *et al.*, 1996). Despite renewed surveillance projects from 1965 to 1990, there were around 5,000 to 10,000 cases of HAT annually. The toll has continued to rise throughout the last 15 years compounded by another civil war in 1996, and the DRC is now in the unenviable position of being the country worst-affected by HAT (Smith, *et al.*, 1998).

1.1.3 Geography and prevalence

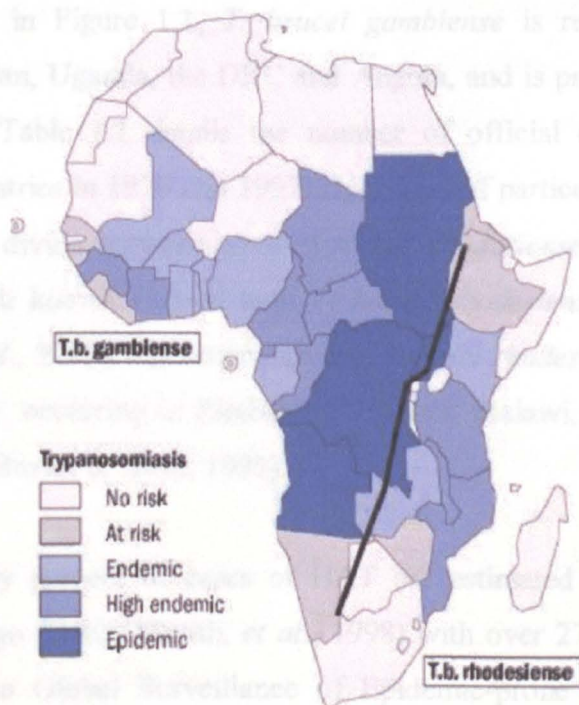


Figure 1.1. Regions of the African continent at risk from HAT. Reproduced from WHO Report on Global Surveillance of Epidemic-prone Infectious Diseases.

Thirty-six of the fifty-two nations making up the continent of Africa are affected by human-infective *Trypanosoma* species (Figure 1.1). Four hundred million people live in countries considered to be part of the "tsetse belt" and it is estimated that between 55 and 60 million people are at risk of infection with *Trypanosoma* (Barrett, 1999). The

distribution of *rhodesiense* and *gambiense* disease very much depends on the distribution of the *Glossina* species that carry the causative agents. The Rift Valley running through Africa roughly divides the areas of occurrence of the two types of HAT – *gambiense* in West and Central Africa and *rhodesiense* in the East (Welburn, *et al.*, 2001). *T. brucei gambiense* is mainly passed by tsetse flies of the *G. palpalis* group which inhabit riverine territories, while *T. brucei rhodesiense* parasites are transmitted by woodland tsetse flies such as *G. morsitans*, *G. pallidipes*, and *G. swynnertoni* (Brown & Neva, 1993). Since tsetse flies obviously do not respect international boundaries the regions of endemic and epidemic disease often spill indiscriminately across borders.

The dependence of the disease on tsetse fly transmission means that HAT is almost exclusively rural in nature. It also tends to occur in discrete foci usually centring on a few villages with almost 300 known active foci (Barrett, *et al.*, 2003). As can be seen from the distribution map in Figure 1.1, *T. brucei gambiense* is responsible for the on-going epidemics in Sudan, Uganda, the DRC and Angola, and is present endemically in several other countries. Table 1.1 details the number of official cases present in these four epidemic-hit countries in 1976 and 1997. Uganda is of particular interest since it straddles the geographical divide between *gambiense* and *rhodesiense* disease areas, and it is the only country with known foci of both *T. brucei rhodesiense* and *T. brucei gambiense* (Hutchinson, *et al.*, 2003). The incidence of *T. brucei rhodesiense* is lower than that of *T. brucei gambiense*, occurring in Zimbabwe, Zambia, Malawi, Mozambique, Tanzania and eastern Uganda (Brown & Neva, 1993).

Seventy to eighty percent of cases of HAT are estimated to arise in the Democratic Republic of Congo (DRC) (Smith, *et al.*, 1998) with over 27,000 cases reported in 1998 (WHO Report on Global Surveillance of Epidemic-prone Infectious Diseases, 2000). Considering the limitations of the screening and reporting processes the actual number of cases may be double the official figure. It is estimated that approximately 2% of the entire population of the DRC may be suffering from the disease (Barrett, 1999). According to Ekwanzala, *et al* (1996), the prevalence of sleeping sickness in some foci in the DRC approaches a phenomenal 70%. In Bandundu and Equateur provinces, HAT is the most significant cause of mortality (WHO Report on Global Surveillance of Epidemic-prone Infectious Diseases, 2000).

Country	Number of cases of HAT reported in 1976	Number of cases of HAT reported in 1997
Angola	83	8,610
Democratic Republic of Congo	3,818	25,200
Sudan	431	737
Uganda	52	1,300

Table 1.1. Comparison of the number of reported cases of HAT in four African countries in 1976 and 1997. Reproduced from the WHO Report on Global Surveillance of Epidemic-prone Infectious Diseases (2000).

Embroiled in civil war since the mid-1970's, Angola has seen an exponential rise in the cases of HAT. Despite the weak surveillance systems in place, Angola is second only to DRC in terms of the number of officially-recorded HAT cases (Ruiz, *et al.*, 2002). Over 12,000 cases were recognised in 2001 but this may have only represented around 10% of the actual incidence (Stich, *et al.*, 2003). A prevalence of 60% has been indicated in some areas (Seed, 2000).

Between 1976 and 1990 there were over 40,000 confirmed cases of HAT in Uganda. In the last decade of the 20th century the implementation of more rigorous surveillance and control strategies resulted in some improvement of the situation. Fly populations were reduced using traps, and a higher proportion of HAT cases were detected while in the more-easily-treated early stage of the disease (Smith, *et al.*, 1998). Despite the improvements Uganda is still subject to the consequences of civil unrest in the 1980's – a new focus of *T. brucei rhodesiense* disease was recently identified in a previously-unaffected region. The appearance of this Soroti focus is thought to have been the result of the introduction of cattle from affected areas as part of a re-stocking exercise following the resettlement of the region (Hutchinson, *et al.*, 2003).

A prevalence of 40-60% has been observed in some villages in southern Sudan with more than half of cases in late stage disease at first presentation (Seed, 2000). Large numbers of cases that have already progressed to the advanced stages have been detected in many epidemic foci across Africa.

1.1.4 The disease

Parasites are introduced into the mammalian host when an infected tsetse fly takes a blood meal. A palpable painful ulcer known as a trypanosomal chancre sometimes develops at the site of the bite and is the first sign of infection – these chancres are more common in *T. brucei rhodesiense* infection. The chancre is usually self-resolving within a month of infection (Barrett, *et al.*, 2003). Trypanosomes can be isolated from aspirations of animal chancres before the parasites have become apparent in the bloodstream. The trypanosomes can make their way into the bloodstream via dermal venules in the vicinity of the original inoculation or via the lymphatic system – the first specific antibody response usually arises at this stage (Poltera, 1985).

In the early stages of the disease the parasites remain confined to the bloodstream, lymphatic system and interstitial spaces. The duration of this stage is dependent on the infecting species – in East African HAT caused by the more virulent *T. brucei rhodesiense* the disease progresses beyond the early stage within weeks; in West African HAT the disease can persist as a chronic early stage infection for years (Barrett, *et al.*, 2003). HAT in the early stages produces a variety of non-specific symptoms, the most common of which is a cycling febrile illness accompanied by general weakness and rapid weight loss. Host-mediated reactions lead to anaemia. There is often a swelling of the postcervical lymph nodes known as Winterbottom's sign and, in *T. brucei rhodesiense* infections particularly, a more diffuse lymphadenopathy (Poltera, 1985).

Late stage trypanosomiasis is characterised by parasitic invasion of the central nervous system. Exactly how the trypanosomes gain entry into the central nervous system has not been determined – they must somehow traverse the defensive blood-brain and/or blood-cerebrospinal fluid barriers that ordinarily protect the brain (Enanga, *et al.*, 2002). Whatever the mechanism of entry, the invasion and the ensuing host responses lead to a diffuse meningoencephalitis and meningomyelitis with a subsequent increase in protein and leucocytes in the CSF (Brown & Neva, 1993). The progression of early stage to late stage HAT brings with it a host of escalating neurological symptoms. Apathy, personality changes and unrelenting headache are often the first signs of CNS involvement. Profound disruption of circadian rhythms leads to an inversion of the sleep-wake cycle. Many patients exhibit Parkinson's disease-like tremors and dyskinesia. Without treatment the

neurological damage continues and the disease eventually culminates in coma and death (Cowan & Heap, 1993).

If HAT is diagnosed and treated whilst in the early stage or before serious neural damage has occurred, prognosis is generally good. There is some evidence that once late stage disease has progressed past a certain point, the injury to the brain is irrevocable and treatment at this time is unlikely to facilitate cure (Barrett, *et al.*, 2003).

1.1.5 Surveillance and diagnosis

An essential part of trypanosomiasis control is the screening of the at-risk population and the treatment of people found to be carrying the disease. This is particularly important in regions affected by *T. b. gambiense* because there is a long, largely asymptomatic period in which the patient is infective to feeding tsetse flies. Animal reservoirs are not thought to play a significant role in the epidemiology of *gambiense* disease with human-fly-human transmission the most likely scenario. Surveillance and treatment programmes are central to the reduction of the human reservoir of disease.

The World Health Organization launched a programme in 1984 for the prevention and control of trypanosomiasis; 22 of the 36 countries at risk from trypanosomiasis are actively involved in this programme (WHO web-site). Several countries potentially vulnerable to HAT, including Ghana, Nigeria, Sierra Leone and Liberia, do not have any surveillance system in place and the current picture of HAT in these countries is unclear.

Surveillance is defined by the World Health Organization as “continuing scrutiny of all aspects of the occurrence and spread of a disease that are pertinent to effective control”. Mass screening of populations for disease is not commonly undertaken due both to the cost and difficulty in the implementation of active programmes (WHO Report on Global Surveillance of Epidemic-prone Infectious Diseases, 2000). Despite recognition of the importance of surveillance, the infrastructure required to carry out the testing and screening often does not exist or the necessary resources are scarce. Other factors can impede the functioning of surveillance workers in areas often ravaged by military conflict. In one epidemiological study in Angola, for example, some villages were unreachable due

to mine-fields (Ruiz, *et al.*, 2002). This provides a stark illustration of how the difficulty of HAT surveillance can be exacerbated by local circumstances.

Since most victims of sleeping sickness will succumb to the disease many miles from the nearest hospital or other health services, it is necessary for mobile surveillance teams to venture out into the field for the purpose of active case-finding (WHO Report on Global Surveillance of Epidemic-prone Infectious Diseases, 2000; Cattand, *et al.*, 2001). In the study of Ruiz and colleagues in Angola (2002) only 19.3% of patients sought medical attention out-with the active surveillance network. The population under threat is not compelled to participate in screening and it is estimated that the participation rate is only around 50% compared to the 95% participation once seen in compulsory colonial screening programmes (Ekwanzala, *et al.*, 1996).

Given the potential consequences of treatment it is imperative to establish that the individual patient is indeed suffering from trypanosomiasis and to determine what stage of the disease the patient has progressed to. It is important to try to identify patients while they are in the first haemolymphatic stage of the disease since the drug treatments are less dangerous. In some regions in the mid-1990's up to 90% of confirmed cases of HAT were first identified when the patients were already in the late stage of the disease (Smith, *et al.*, 1998).

A definitive diagnosis of HAT can be reached only after demonstration of parasites in the blood, lymph or cerebrospinal fluid but parasitaemias can be extremely low, particularly in *gambiense* disease (Brown & Neva, 1993). Several techniques have been developed to aid in the diagnosis of HAT. The card agglutination test for trypanosomiasis (CATT) is a serological test for the presence of anti-trypanosomal antibodies which is useful for identifying possible cases of HAT but it is not specific enough to be used on its own (WHO Report on Global Surveillance of Epidemic-prone Infectious Diseases, 2000). If parasites are not apparent on examination of whole blood smears concentrative techniques such as capillary tube centrifugation, quantitative buffy coat analysis, and mini-anion exchange columns can be utilised (Barrett, *et al.*, 2003). Figure 1.2 shows a schedule used for diagnosis of HAT in Angola.

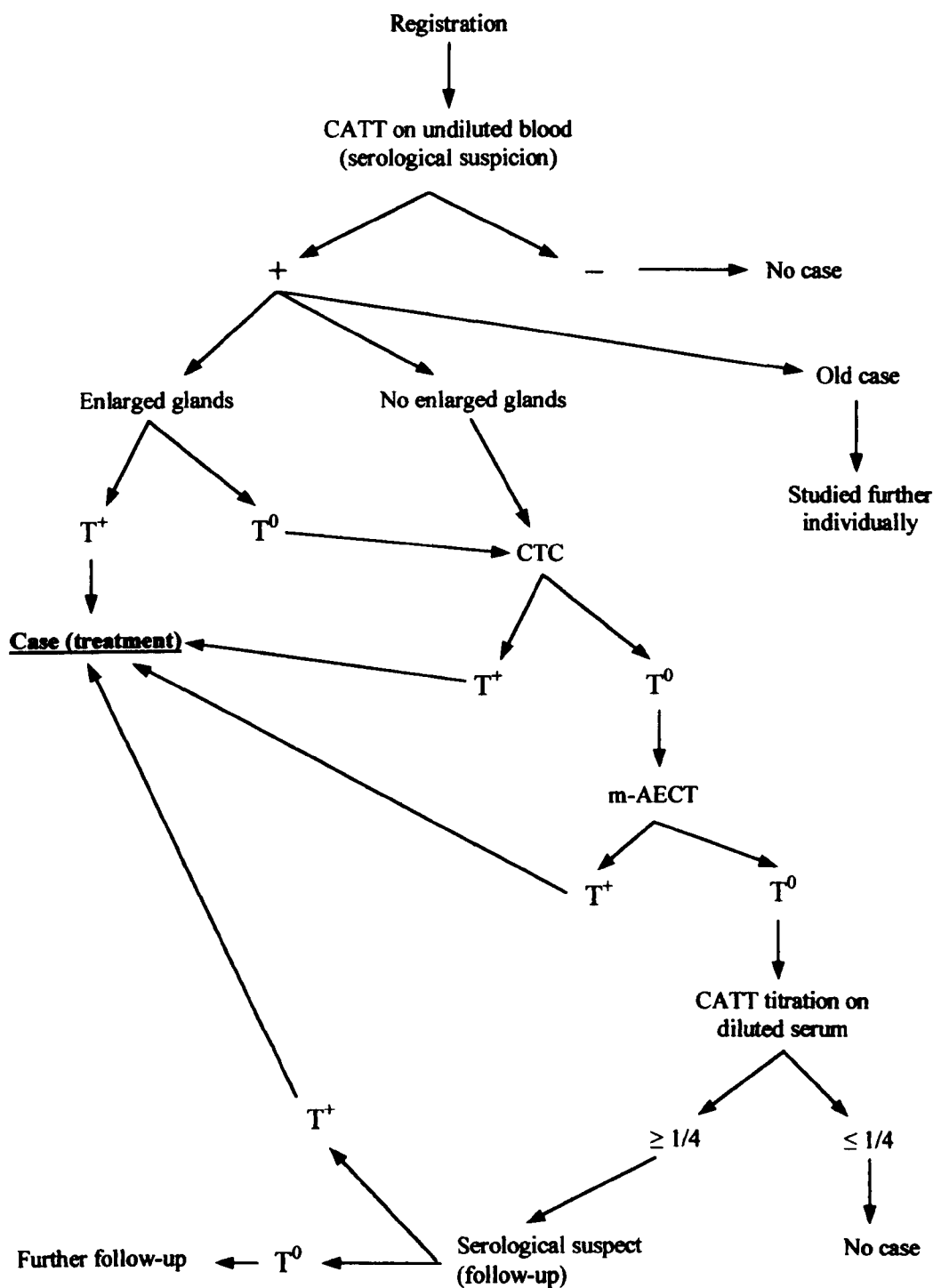


Figure 1.2. Diagnosis of trypanosomiasis. CATT – card agglutination trypanosomiasis test, T⁺ - trypanosome positive, T⁰ – trypanosome negative, CTC – capillary tube centrifugation, m-AECT – mini-anion exchange centrifugation technique. Reproduced from Ruiz, *et al.*, 2002.

For identification of late stage disease the cerebrospinal fluid must be examined necessitating a potentially dangerous, invasive lumbar puncture. Since trypanosomes are not often visualised in the CSF from lumbar punctures, increased white cell numbers (>5 cells/ μ l) and heightened protein levels (>25 mg/100 ml) are used to confirm involvement of the CNS (Barrett, *et al.*, 2003).

1.1.6 Chemotherapy

Since the ability of trypanosomes to evade the host immune response by periodically changing their protein covering has so far prevented viable vaccination strategies management of HAT relies on chemotherapy. The main weapons in the “current” arsenal against HAT consist of four drugs, three of which have been in use for more than fifty years. The use of these four drugs is further complicated since two are only suitable for early-stage disease (pentamidine and suramin) and another is only active against *T. brucei gambiense* (difluoromethylornithine (DFMO), also known as eflornithine). Figure 1.3 shows the chemical structures of suramin, pentamidine, melarsoprol, DFMO, and the veterinary trypanocide, berenil.

1.6.1.1 Treatment of early-stage disease

The oldest drug still in use is the polysulphonated naphthylamine suramin, first used in 1922 (Wang, 1995). Suramin is active against both *T. b. rhodesiense* and *T. b. gambiense* and is the preferred treatment for the early-stage East African disease. With six negative charges this drug interacts with many different serum components and is actually taken up by the trypanosome LDL receptor as a complex with low-density lipoproteins (Vansterkenburg, *et al.*, 1993; Kirchhoff, *et al.*, 2000). As with most of the other trypanocides, the intracellular target of suramin has not been definitively identified. The drug has been shown to inhibit several different trypanosomal enzymes including dihydrofolate reductase, thymidine kinase, and those involved in glycolysis. The trypanocidal action of suramin is likely to be the result of inhibitory effects on a range of enzymes *in situ* (Wang, 1995).

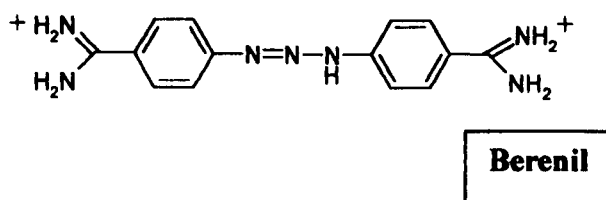
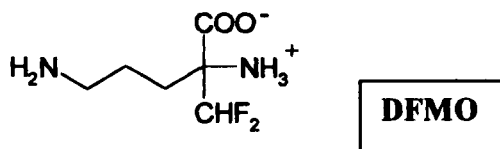
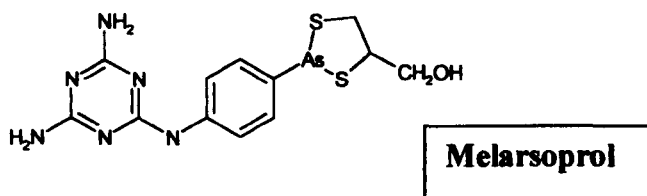
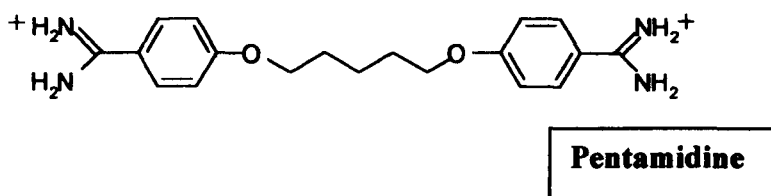
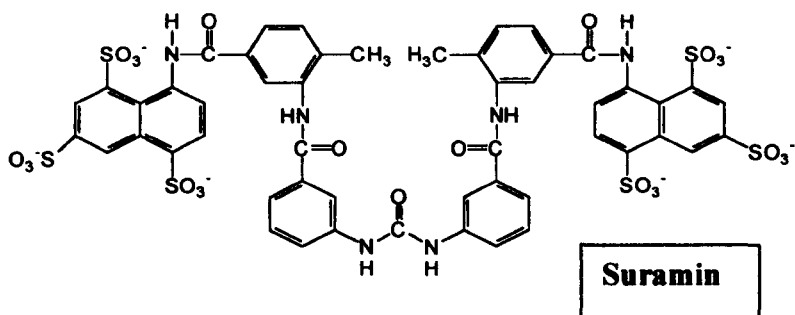


Figure 1.3. Structures of trypanocides. Suramin and pentamidine are used against early stage disease. Melarsoprol and DFMO are used against late stage sleeping sickness. Berenil is the most commonly-used veterinary trypanocide.

The recommended suramin regimen includes an initial test-dose of 100-200 mg since the drug can precipitate an anaphylactic reaction in a small proportion of patients. Thereafter, one gram of drug is delivered by slow, intravenous infusion on day 1, 3, 7, 14 and 21 (Kirchhoff, *et al.*, 2000). Suramin has a range of toxic side-effects, the most common of which is renal damage, resulting in proteinuria - although this is usually mild (Pépin & Milord, 1994).

Pentamidine was first used against HAT in 1940 and continues to be used to treat early-stage *T. brucei gambiense* infections (Legros, *et al.*, 2002). It is an aromatic diamidine compound that associates with the DNA contained within a trypanosomal organelle known as the kinetoplast. The drug possesses a range of activities which could contribute to its anti-trypanosomal action but, as with suramin, the trypanocidal mechanisms are not fully understood. Pentamidine has been shown to inhibit adenosyl-L-methionine carboxylase, mitochondrial topoisomerase II, Ca²⁺ transport, and amino acid transport, as well as precipitating a partial degradation of the kinetoplast minicircle network (Wang, 1995; Pépin & Milord, 1994). Pentamidine also has activity against *Leishmania* species and has proven useful in the treatment of AIDS-related *Pneumocystis carinii* pneumonia (Wang, 1995).

The treatment schedule for pentamidine involves 7-10 intramuscular injections of 4 mg per kg of body weight either daily or on alternate days (Kuzoe, 1993). The side-effects associated with pentamidine are mostly transient in nature and include nausea, tachycardia and arterial hypotension. More serious problems can follow treatment with pentamidine: damage to the pancreas can lead to diabetes and liver damage can also be triggered (Kirchhoff, *et al.*, 2000).

Another aromatic diamidine closely related to pentamidine is the veterinary trypanocide berenil used for the treatment of livestock infected with *T. congolense*, *T. vivax* and *T. b. brucei* (Peregrine & Mamman, 1993). The active component of berenil is diminazene aceturate which has been shown to be active against human-infective parasites (Williamson, 1970). Berenil has never been licenced for human usage but it has been used in cases where other drugs were not available or were ineffective (Atouguia & Costa, 1999; Bacchi, 1993).

1.6.1.2 Treatment of late-stage disease

Arsenic-containing drugs have played a major role in anti-trypanosomal therapy since the first treatments were attempted (Williamson, 1970). Most of the arsenical drugs have fallen out of usage due to excessive toxicity, development of resistance or other limitations. Melarsoprol, a melaminophenyl arsenical active against both *T. b. gambiense* and *T. b. rhodesiense*, was developed by Friedheim in the 1940's and until the introduction of eflornithine was the only available treatment for late-stage HAT (Pépin & Milord, 1994). The ability of the drug to cross the blood-brain barrier and reach trypanosomes in the CNS is assumed to be due to its lipophilic nature. Levels of melarsoprol in the CNS only reach about 2-5% of those seen in plasma and this is thought to be due to the rapid metabolism of melarsoprol to melarsen oxide which is less able to traverse the BBB (Enanga, *et al.*, 2002; Keiser, *et al.*, 2000).

Although it is known that parasites are quickly lysed in the presence of the drug, in what has become a familiar story regarding trypanocides, the mode of action of melarsoprol has not been elucidated. Arsenicals have been shown to inhibit glycolytic enzymes (Van Schaftingen, *et al.*, 1987; Denise, *et al.*, 1999) and to inhibit trypanothione reductase by forming stable adducts with trypanothione (Fairlamb, *et al.*, 1989) but these effects have probably not advanced to an appreciable level prior to the lysis of the parasites. In 1993, a study by Carter & Fairlamb revealed that arsenical-resistance in trypanosomes could be linked to the absence of the P2 purine nucleoside transporter (see later). This transporter was shown to mediate uptake of melarsoprol and related compounds and was also capable of transporting diamidines such as pentamidine.

Due to insolubility in most other solvents, melarsoprol is administered as a 3.6% solution in propylene glycol, contributing to the painfulness of the injection. Drug regimens were determined empirically and traditionally consist of 3 or 4 series of 4 daily intravenous injections (3.6 mg/kg) with a period of one week separating each series (Kuzoe, 1993). Unsurprisingly, as well as leading to the clearance of parasites from the CNS, administration of melarsoprol leads to a host of collateral toxic effects. The most serious side-effect is the post-treatment reactive encephalopathy (PTRE) that affects up to 10% of patients. These reactions are fatal in approximately 50% of patients in whom they occur (Kennedy, 2004). Other side-effects include abdominal pain, vomiting, diarrhoea, and

damage to the myocardium, kidneys and liver (Kirchhoff, *et al.*, 2000). The administration of the anti-inflammatory drug prednisolone throughout the entire treatment course can help to reduce the incidence and severity of PTRE (Ruiz, *et al.*, 2002).

Difluoromethylornithine (DFMO), also known as eflornithine, was first licensed for use against HAT in 1990. It is active against *T. b. gambiense* and due to its ability to cross the BBB continues to be effective even when the disease is at an advanced state. Unfortunately, this drug is not very effective against *T. b. rhodesiense* and so the arsenicals remain the only therapeutic option for the late stages of the East African disease.

As well as being the newest drug DFMO is novel amongst trypanocides because its mode of action is known. A suicide inhibitor of ornithine decarboxylase (ODC) originally intended for use in neoplastic conditions, DFMO interferes with polyamine synthesis leading to a cessation of trypanosome proliferation (Bacchi, *et al.*, 1983; Barrett & Barrett, 2000; Kirchhoff, *et al.*, 2000). The suspension of normal cell function also affects the parasite's ability to change its protein coat. Since the drug does not kill the trypanosome cells outright immunocompetency is required to clear the parasites from the bloodstream and CNS.

The reason for the selective action of eflornithine on *T. b. gambiense* and not on *T. b. rhodesiense* or mammalian cells, despite the fact that ODC is also a valid target in these cell types, has also been elucidated. Mammalian ODC has a much shorter half-life than trypanosomal ODC, e.g. murine ODC has a half-life of less than one hour compared to the > 18 hour half-life of *T. b. gambiense* ODC (Phillips, *et al.*, 1987; Ghoda, *et al.*, 1990). So although mammalian ODC is sensitive to inhibition by DFMO, the rapid turnover of the enzyme combined with the relatively short half-life of the drug itself abrogates any negative effects on the cells. The natural insensitivity to DFMO observed in *T. b. rhodesiense* would also appear to be due to differences in both turnover and specific activity of ODC. Recombinant enzymes from both *T. b. rhodesiense* and *T. b. gambiense* are inhibited to a similar degree by DFMO, but the specific activity of the *T. b. rhodesiense* enzyme was three times that of its *T. b. gambiense* counterpart, and the half-life of *T. b. rhodesiense* ODC was approximately 4 hours compared to the 18 hours obtained for the *T. b. gambiense* ODC (Iten, *et al.*, 1997).

In terms of toxic side-effects, eflornithine is actually well tolerated by patients. The real problem with the administration of the drug is the massive amounts required for each patient, the duration of the individual intravenous infusions and the length of the entire course. The standard treatment protocol is 4 intravenous 100 mg/kg infusions daily for 14 days – since the drug is provided commercially as a 200 mg/ml solution almost 1.5 litres of drug solution requires to be infused over the course (WHO, Human African Trypanosomiasis – A Guide for Drug Supply, 2002).

1.6.1.3 Limitations of current chemotherapy

The pharmaceutical industry has long been seemingly indifferent to the real need for new drugs against neglected diseases such as African trypanosomiasis. In the period 1975-1997 a total of 1223 drugs were licensed for use globally, but only 13 of these were destined for use against tropical diseases (Veeken & Pécou, 2000). Eflornithine, the only new trypanocide to be developed for almost 50 years was not even intended for use against HAT. It's clear that profit-driven pharmaceutical companies have more invested in the afflictions of the developed nations, such as erectile dysfunction (8 drugs in development), obesity (7 drugs) and, ironically, sleep disorders (4 drugs), than they do in the diseases suffered by the world's poorest people (1 drug for trypanosomiasis and 1 drug for malaria are currently in development) (reported in *The Scientist*, May 13th 2002).

Despite this lack of interest from the drug companies, the fact remains that most of the trypanocides currently in use are woefully inadequate in terms of toxicity, cost and availability, the logistics of treatment and follow-up, and a further complication is emerging resistance in the field.

Although the anti-trypanosomal activity of suramin, pentamidine and melarsoprol were discovered empirically, it is quite extraordinary that their mode(s) of action are still shrouded in mystery more than 50 years after their inaugural application. Given the toxicity of melarsoprol (discussed above), it is highly unlikely that this drug would be accepted under the current strict safety guidelines (Fairlamb, 1990).

The process of simply getting the drugs to the right geographical location can be daunting. This highlights the need for socio-economic interventions, such as the rebuilding of

infrastructure in post-conflict areas – even the perfect drug is useless if it can't be administered to patients. Provided they are available, all of the drugs used against HAT require the patient to remain in hospital for the entire duration of the course, and adequate follow-up consists of a lumbar puncture procedure every six months for two years – unsurprisingly, patient compliance can be problematic (Atouguia & Costa, 1999). Efforts have been made to adapt the empirically designed treatment regimens to reduce the course duration and/or quantities of drug administered, both as an attempt to cut costs and to reduce toxic effects. A shorter course of melarsoprol was found to be just as effective as traditional schedules (Burri, *et al.*, 2000), but attempts to reduce the eflornithine course from 14 days to 7 days resulted in less encouraging results (Pépin, *et al.*, 2000). Another possible path to improving current treatment with the limited resources available is combinatorial chemotherapy (Keiser, *et al.*, 2001), but more studies are required.

It is one thing for pharmaceutical companies to drag their heels on research and development of new trypanocidal drugs, but even more worrying is their continuing reluctance to even continue production of the four current drugs. Inevitably, this is due, at least in part, to the poor profitability of these agents, but environmental groups have also lobbied for tighter regulations extending to an outright ban on the use of arsenic (Veeken & Pécoul, 2000). By-products of suramin manufacture and the hazardous process of fluorination necessary for the production of DFMO have also contributed to the unwillingness of companies to continue supplying trypanocides (WHO, Human African Trypanosomiasis Treatment and Drug Resistance Network: Report of the second and third meetings, 2001).

Use of trypanocides in other disease conditions, particularly “Western diseases”, can be a mixed blessing. It means the drug is more likely to be available and often leads to a more concerted effort to establish a mode of action and improve toxicity data (Barrett, 2000). But it also leads to an inevitable increase in cost – when pentamidine found an application in AIDS-related *Pneumocystis carinii* pneumonia there was an immediate escalation in price. It was necessary for the WHO to intervene in order to secure even a limited supply of pentamidine from Aventis for HAT usage at a reasonable cost (Veeken & Pécoul, 2000).

DFMO would not be available for the treatment of HAT at all if it weren't for an alternative use. In the late 1990's Hoechst, Marion, Roussel withdrew eflornithine due to

lack of profit and the remaining stocks were quickly used up (Veeken & Pécou, 2000). The company also donated the license to the WHO, effectively divorcing themselves from any responsibility for future production. There was therefore outrage when Vaniqua – a depilatory cream with DFMO as the main active component – appeared on the US market a few years later (Stich, *et al.*, 2003). The situation of having eflornithine available for a purpose as frivolous as hair removal, whilst unavailable for melarsoprol-refractory HAT was untenable. Thanks largely to the involvement of the WHO and Médecins Sans Frontières, pentamidine, melarsoprol, and eflornithine will now be manufactured and supplied free-of-charge by Aventis until 2006, and Bayer has also pledged supplies of suramin (Barrett, *et al.*, 2003).

Considering that there are only four drugs currently licensed for HAT, and that only 1-2 (depending on which species of parasite is involved) of these are effective against late-stage disease, the emergence of drug resistance is extremely disturbing. The existence of resistance to all three of the most commonly used veterinary trypanocides (isometamidium, homidium, berenil) has also been acknowledged (Anene, *et al.*, 2001). In the treatment of early-stage HAT, there have been no significant reports of resistance to pentamidine or suramin, with occasional treatment failures assumed to be misdiagnosed early late-stage disease (Kaminsky & Mäser, 2000). Unfortunately, the number of treatment failures following administration of melarsoprol is on the rise – current figures show that 15-30% of patients suffer relapse (WHO Report on Global Surveillance of Epidemic-prone Infectious Diseases, 2000). Although arsenical resistance can be induced by exposing parasites to sub-curative doses in the laboratory, the precise reasons for the treatment failures in the field have still not been elucidated. The contribution of host-related factors has not been ruled out, and might include sequestration of parasites in sites not available to melarsoprol or a reduced movement across the BBB (Kaminsky & Mäser, 2000). Yet, such factors do not easily explain the recent sharp increase in treatment failure rates in specific foci.

Loss or alteration of the P2 adenosine transporter has been implicated in resistance to arsenicals and some diamidines due to a decrease in uptake of the drug by the parasite (Carter & Fairlamb, 1993). The role of the P2 transporter and other trypanosomal transport proteins in drug targeting and drug resistance is discussed in more detail later.

Investigation of a limited number of field isolates by the group of Reto Brun and colleagues (Brun, *et al.*, 2001) found that most of the *T. b. rhodesiense* samples displayed significant resistance to arsenicals, both *in vitro* and in animal models *in vivo*. Despite a clear resistant phenotype, some of the isolates possessed a wild-type P2 transporter. Clearly, although the P2 transporter has been linked to resistance, it is not the only significant factor. In the same study, a correlation between reduced melarsoprol sensitivity of *T. b. gambiense* isolates and the relapse or cure status of the patient was not apparent. Given that drug-resistant parasites exhibit a range of very different phenotypes, the pathways through which resistance develops may take a while to fully elucidate (Kaminsky & Mäser, 2000).

1.1.7 Vector control



Figure 1.4. Tsetse fly, *Glossina morsitans*, feeding on a human arm (WHO/TDR/Petana). Obtained from <http://www.who.int/tdr/media/image.html> (Image ID # 9104108)

There are seven different tsetse species capable of carrying and transmitting African trypanosomes (Figure 1.4). There are barriers to the survival of trypanosomes within the invertebrate host - the gut of the insect contains lectins that inhibit colonisation by the parasites – and this is reflected in the relatively low proportion of infected flies (2-4%) even in endemic areas (Aksoy, *et al.*, 2001; Brown & Neva, 1993).

It is estimated that tsetse flies are present over more than 40% of the land area in countries at risk from human and/or veterinary trypanosomiasis (Allsop, 2001). As a means of disrupting disease transmission, reduction of the tsetse population in areas vulnerable to zoonotic *T. b. rhodesiense* infection has been particularly useful. Historically, vector control measures took the form of destruction of tsetse habitat and culling of reservoir game animals whose blood formed the tsetse diet (Schofield & Maudlin, 2001). For obvious ecological reasons these measures are no longer considered acceptable.

With the advent of organochlorine compounds such as DDT, application of insecticides by aerial or ground spraying became the mainstay of vector control methods from the 1940's onwards. Originally, insecticides were applied residually at high concentrations to maximise the duration of the anti-tsetse effect, but it soon became clear that this approach was harmful to other wildlife in the treated areas (Grant, 2001). A new spraying protocol known as the sequential aerial drift technique (SAT) using much lower doses at appropriate intervals went a long way to minimising this collateral damage but many environmentalists still express concern about the wide-spread use of insecticides (Grant, 2001).

A more environmentally friendly approach to vector control is the use of fabric traps and targets. As the name suggests, traps can simply incarcerate the flies or can lead to direct killing if the material is impregnated with insecticide. In Uganda, the organised use of fly-traps managed to reduce the tsetse populations by around 95% (Smith, *et al.*, 1998). Targets are simple insecticide-saturated screens designed to attract tsetse flies using visual stimuli or olfactory stimuli such as carbon dioxide or acetone (Schofield & Maudlin, 2001). The use of non-toxic pyrethroid insecticides in animal dips or as pour-on formulations in "live-bait" techniques has gained in popularity (Allsop, 2001). Pyrethroid insecticides used in this way also prevents ticks and other biting flies from feeding on the treated cattle (Grant, 2001). Although the use of insecticides, traps and targets lead to reductions in tsetse populations, all tsetse control strategies have sustainability issues. Breakdown of spraying programmes or poor maintenance or theft of traps and targets can lead tsetse flies to quickly reclaim the cleared areas (Allsop, 2001).

Ambitious plans to rid Africa of the tsetse/trypanosomiasis scourge by the implementation of the sterile insect technique (SIT) have received much publicity. The basis of the

technique is the mass release of male flies made sterile by exposure to gamma-radiation. The over-abundance of sterile males compared to indigenous male fly populations favours the interlopers in terms of mating opportunities, with mating events between these males and wild-type females being unproductive (Aksoy, *et al.*, 2001). The technique was successfully used to eliminate *Glossina austeni* from the island of Zanzibar (Vreysen, *et al.*, 2000), but many scientists remain sceptical of the current proposals to clear tsetse from the African mainland using the technique (Rogers & Randolph, 2002).

1.2 Trypanosomes

1.2.1 Taxonomy

Trypanosomes are eukaryotic, protozoan parasites of the order Kinetoplastida. The possession of only one flagellum distinguishes the Trypanosomatina from their other Kinetoplastida relatives, the biflagellate Bodonina. Whilst many of the Bodonina are free-living, all the Trypanosomatina are dependent on their parasitic associations with a wide range of multicellular organisms. As a result, Trypanosomatid parasites are the aetiological agents of several diseases of medical and veterinary importance, including of course the African trypanosomiases. There are at least nine genera making up the family Trypanosomatidae: five which are monoxenous (*Leptomonas*, *Herpetomonas*, *Crithidia*, *Blastocrithidia* and *Rhynchoidomonas*) meaning they have only one host, usually an arthropod or other invertebrate; and four that are heteroxenous (*Phytomonas*, *Endotrypanum*, *Leishmania* and *Trypanosoma*) with different hosts depending on the life-cycle stage. *Phytomonas* is a parasite of plants, whilst *Endotrypanum*, *Leishmania*, and *Trypanosoma* infect a wide variety of vertebrate species, being transmitted by insect or leech vectors (Kreier & Baker, 1987). The full taxonomic classification of the *Trypanosoma* genus is shown in Figure 1.5.

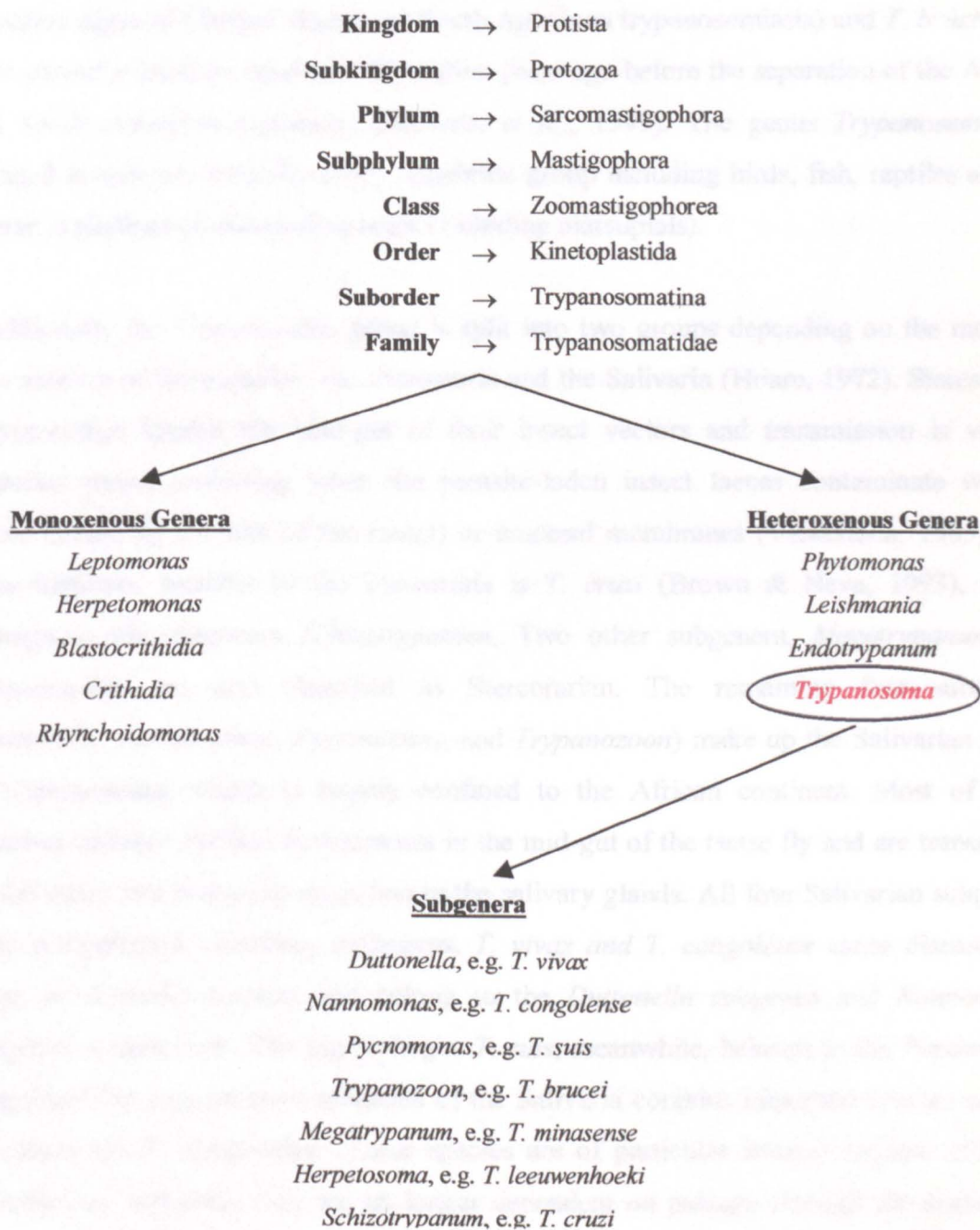


Figure 1.5. Taxonomic classification of trypanosomes.

Studies of the evolutionary relationships within the Trypanosomatidae have indicated that the *Trypanosoma* genus is monophyletic – that is, they are all descended from a single common ancestor (Stevens, *et al.*, 2001). The phylogenetic data shows that *T. cruzi* (the causative agent of Chagas' disease or South American trypanosomiasis) and *T. brucei* may have shared a common ancestor 100 million years ago before the separation of the African and South American continents (Stevens, *et al.*, 1999). The genus *Trypanosoma* has radiated to colonise virtually every vertebrate group including birds, fish, reptiles and, of course, a plethora of mammalian hosts (including marsupials).

Traditionally the *Trypanosoma* genus is split into two groups depending on the mode of transmission of the parasites: the Stercoraria and the Salivaria (Hoare, 1972). Stercorarian trypanosomes inhabit the hind-gut of their insect vectors and transmission is via the posterior station occurring when the parasite-laden insect faeces contaminate wounds (often caused by the bite of the insect) or mucosal membranes (Vickerman, 1985). The most infamous member of the Stercoraria is *T. cruzi* (Brown & Neva, 1993), which belongs to the subgenera *Schizotrypanum*. Two other subgenera, *Megatrypanum* and *Herpetosoma*, are also classified as Stercorarian. The remaining four subgenera (*Duttonella*, *Nannomonas*, *Pycnomonas*, and *Trypanozoon*) make up the Salivarian group of trypanosomes, which is largely confined to the African continent. Most of these parasites undergo cyclical development in the mid-gut of the tsetse fly and are transmitted by the tsetse bite following migration to the salivary glands. All four Salivarian subgenera contain significant veterinary pathogens. *T. vivax* and *T. congolense* cause disease in a range of domestic animals and belong to the *Duttonella* subgenus and *Nannomonas* subgenus, respectively. The pig pathogen *T. suis*, meanwhile, belongs to the *Pycnomonas* subgenus. The *Trypanozoon* subgenus of the Salivaria contains important species such as *T. evansi* and *T. equiperdum*. These species are of particular interest because although classified as Salivarian they are no longer dependent on passage through the insect, and consequently are not limited solely to areas infested by tsetse flies. *T. evansi* is mechanically transmitted on the contaminated mouth-parts of various biting flies and *T. equiperdum* is transmitted venereally (Kreier & Baker, 1987). These intriguingly different lifestyles notwithstanding, the *Trypanozoon* subgenus has arguably received the most attention since it contains the *T. brucei* subgroup.

As discussed earlier in this chapter, *T. b. brucei* is responsible for disease in animals, including cattle, while *T. brucei gambiense* and *T. brucei rhodesiense* cause different clinical manifestations of HAT. In addition, *T. b. rhodesiense* is clearly zoonotic in that it infects a range of domestic and wild animals forming a reservoir for human-infective pathogens (Njiru, *et al.*, 2004). Although *T. b. gambiense* is largely regarded as a human parasite with little or no animal reservoir, there have been reports of the parasite infecting animals such as pigs (Mehlitz, *et al.*, 1982). The three subspecies of *T. brucei* are morphologically indistinguishable from one another and various techniques have been devised to allow the proper identification of isolates.

Isoenzyme analysis established *T. b. gambiense* as a bonafide subspecies, but it was not possible to separate *T. b. brucei* and *T. b. rhodesiense*, giving rise to the hypothesis that *T. b. rhodesiense* represents a “host-range variant” of *T. b. brucei* (Tait, *et al.*, 1984; Tait, *et al.*, 1985; Gibson, 2002). Molecular techniques such as restriction fragment length polymorphism (RFLP) (Welburn, *et al.*, 2001) and minisatellite marker analysis (MacLeod, *et al.*, 2000) can distinguish *T. b. rhodesiense* from *T. b. brucei*.

For obvious reasons, the factors accounting for the human-infectivity of *T. b. gambiense* and *T. b. rhodesiense* have come under close scrutiny. *T. b. brucei* is unable to establish infections in man because it is sensitive to a trypanolytic factor (TLF) present in human serum, but *T. b. gambiense* and *T. b. rhodesiense* both appear to have an innate resistance to this serum constituent (Raper, *et al.*, 2001). *T. b. rhodesiense* has been shown to possess a serum resistance associated (SRA) gene that encodes for a molecule related to the variant surface glycoproteins making up the protein coat of the trypanosome (De Greef, *et al.*, 1992; Van Xong, *et al.*, 1998; Milner & Hajduk, 1999). The SRA gene is not found in serum-sensitive *T. b. brucei*, and also is not found in serum-sensitive *T. b. rhodesiense* isolates (De Greef, *et al.*, 1992). It is unclear exactly how exposure to TLF leads to lysis of *T. b. brucei* and, equally, the mechanism by which the SRA protein prevents lysis in *T. b. rhodesiense* has not been elucidated. However, TLF must be internalised by the trypanosome to exert its lytic effect and there is some evidence that this internalisation is somehow disrupted in the serum-resistant *T. b. rhodesiense* parasites (Raper, *et al.*, 2001). *T. b. gambiense*, a very efficient parasite of humans, is clearly able to resist the action of TLF, but the SRA gene has not been identified in this parasite. Other mechanisms are obviously involved in the human serum-resistance trait of human-infective parasites.

1.2.2 Life-cycles and morphologies

The trypanosome assumes different morphological forms throughout its life-cycle as it adapts to the different environmental conditions encountered. It is usually elongate in shape and is highly motile due to the action of the single flagellum and the presence of the undulating membrane. This undulating membrane is the result of a fold of the pellicle bordered by the attached flagellum, which arises from the posteriorly-located flagellar pocket, runs the length of cell and, depending on the life-cycle stage, extends to form the free flagellum (Brown & Neva, 1993). The trypanosome also possesses several unusual organelles including the kinetoplast that is the defining feature of all the Kinetoplastidae (Lukeš, *et al.*, 2002), and also the glycosome which is the site of the compartmentalised glycolytic processes (Opperdoes, *et al.*, 1984; Opperdoes & Michels, 1993). The basic morphology of *T. b. brucei* is illustrated in Figure 1.6.

In the mammalian bloodstream *T. b. brucei* exists as a pleiomorphic mixture with proliferative long-slender (LS) forms giving rise to non-dividing short-stumpy (SS) forms. As the names suggest these two populations can be identified by their different morphologies – typically, LS forms are ~30 μm by 1.5 μm , whereas the SS form are ~18 μm by 3.5 μm (Kreier & Baker, 1987). The rapidly dividing LS trypanosomes are responsible for the establishment and maintenance of the mammalian infection. Bloodstream *T. b. gambiense* is shown in Figure 1.7. In the glucose-rich environment of the blood the energy metabolism of the trypanosome is dependent solely on glycolysis, and this is reflected in the large number of glycosomes (>200 per cell) and the simplified mitochondrial architecture (Vickerman, 1985; Opperdoes, *et al.*, 1984). As an organism swimming free in the bloodstream, the trypanosome is fully exposed to the mammalian immune system. The entire cell surface is covered with a variant surface glycoprotein (VSG) coat that shields antigenic membrane components (Donelson & Rice-Ficht, 1985), and due to the ability to spontaneously change this protein coat by the process of antigenic variation (Barry & McCulloch, 2001) parasites are repeatedly able to evade host responses.

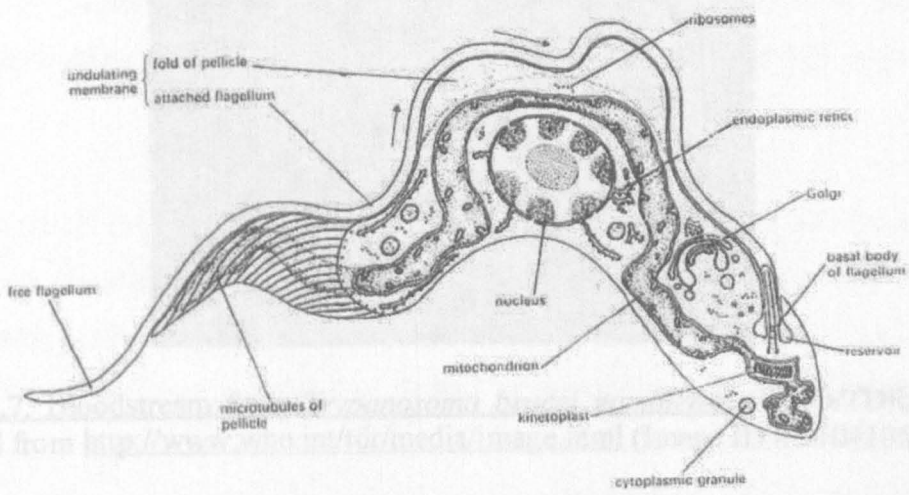


Figure 1.5. *Trypanosoma rhodesiense* in the trypomastigote stage. Reproduced from Mulligan, 1970.

A combination of host immune reactions and antigenic variation in the trypanosome is responsible for the characteristic fluctuating parasitaemia during each "wave" of parasitaemia. Figure 1.6 shows the morphology of the parasite during the initial modification of *L3* trypanosomes – a few days after infection. The initial modification during this ascending phase. The role of the host immune response in the development of *L3* forms to the non-proliferative 5S form is still unclear. The immune response appears to be directed against the

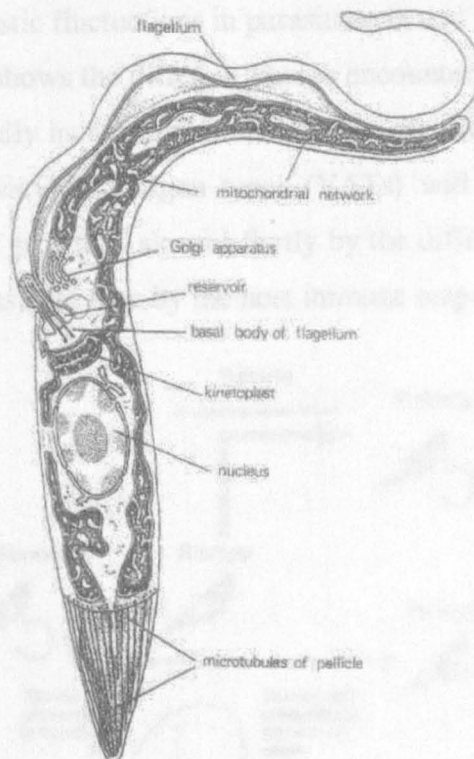


Figure 1.6. Morphologies of *T. b. rhodesiense*. The upper diagram represents the trypomastigote stage and the lower diagram illustrates the epimastigote form. Reproduced from Mulligan, 1970.

Figure 1.8. Events during a "short wave" of parasitaemia. Reproduced from Mulligan, 1970.

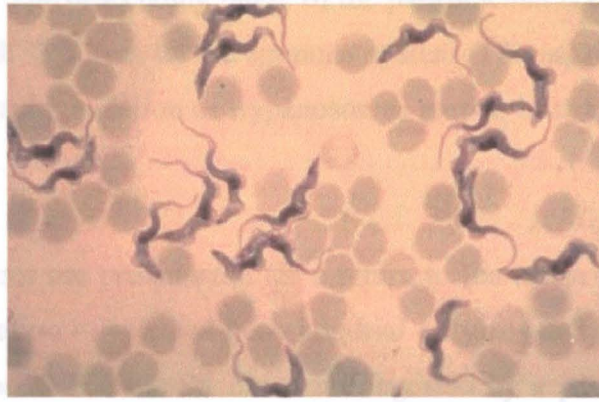


Figure 1.7. Bloodstream form *Trypanosoma brucei gambiense* (WHO/TDR/Molyneux). Obtained from <http://www.who.int/tdr/media/image.html> (Image ID # 9104106)

A combination of host immune reactions and antigenic variation in the trypanosome is responsible for the characteristic fluctuations in parasitaemia and the consequent cycling of HAT symptoms. Figure 1.8 shows the different phases encountered during each "wave" of parasitaemia. The initial rapidly increasing parasitaemia is due to the rapid proliferation of LS trypanosomes – a few variable antigen types (VATs) will predominate during this ascending phase. The rate of growth is slowed firstly by the differentiation of LS forms to the non-proliferative SS forms, and then by the host immune responses targeted against the

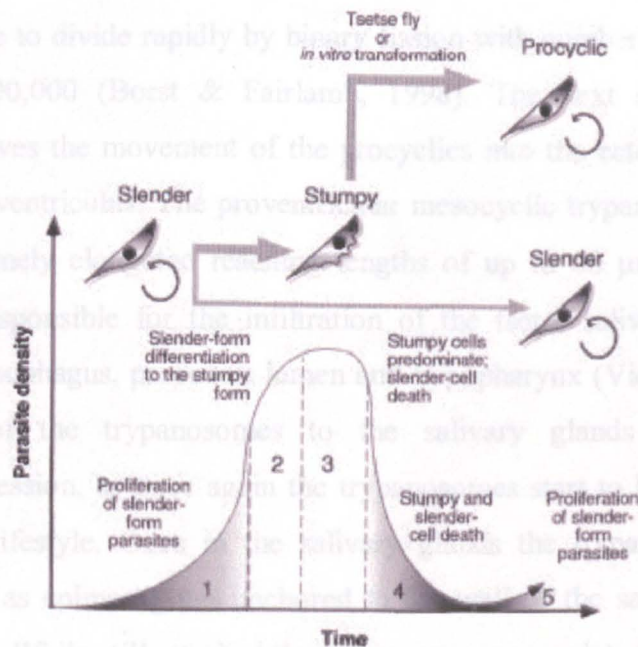


Figure 1.8. Events during a single "wave" of parasitaemia caused by *T. b. brucei*. Reproduced from Matthews, 1999.

predominant VATs. The descending phase of the parasitaemia is characterised by the mass clearance of LS and SS forms by the immune system. The next wave of parasitaemia is initiated by a small subpopulation of trypanosomes garbed in a new VSG coat (Matthews, 1999).

Bloodstream SS forms are pre-adapted for a return to the tsetse fly and in large part this involves the reactivation of selected mitochondrial enzymes and the reorganisation of the mitochondrial cristae. When the SS forms are ingested by a potential tsetse vector, it is essential that they quickly convert to alternative energy sources since glucose is rapidly removed from the bloodmeal. The energy requirements of the mid-gut procyclic form of the parasite are met by the amino acid proline (Vickerman, 1985), and succinate and oxoglutarate can also be utilised (Vickerman, *et al.*, 1988). The change in metabolic substrate is also reflected in reduced numbers of glycosomes with a general flattening of the retained organelles. The VSG coat is rapidly shed as the ingested SS parasites differentiate into the proliferative procyclic trypomastigotes (Vickerman, *et al.*, 1988) and it is replaced by a layer of procyclic acidic repetitive proteins (PARP), or procyclins. There are two different types of procyclin molecule: EP and GPEET, named for their signature amino acid repeat motifs (Roditi, *et al.*, 1998).

Procyclics continue to divide rapidly by binary fission with numbers in the mid-gut of the tsetse reaching 300,000 (Borst & Fairlamb, 1998). The next stage of trypanosome development involves the movement of the procyclics into the ectoperitrophic space and forward to the proventriculus. The proventricular mesocyclic trypanosomes do not divide and become extremely elongated reaching lengths of up to 60 μm (Vickerman, 1985). These cells are responsible for the infiltration of the tsetse salivary glands which are reached via the oesophagus, proboscis lumen and hypopharynx (Vickerman, *et al.*, 1988). The movement of the trypanosomes to the salivary glands is accompanied by mitochondrial regression, as once again the trypanosomes start to brace themselves for a major change in lifestyle. Once in the salivary glands the trypanosomes enter a new proliferative stage as epimastigotes anchored to the wall of the salivary glands by their flagellar structures. While still attached the trypanosomes complete their development into mammalian-infective forms by the acquisition of the VSG layer and further changes in mitochondrial and glycosomal structure. The 12-15 nm-thick protein coat consists of $\sim 10^7$ copies of a single GPI-linked VSG unit and there are usually around 15-20 different VATs

present in the entire mature metacyclic population (El-Sayed, *et al.*, 2000). Final maturation is marked by the detachment of the non-dividing metacyclic into the lumen of the gland, with each fly harbouring up to 50,000 metacyclics (Donelson & Rice-Ficht, 1985). The time taken for the passage of the trypanosome through the fly is usually around 3-5 weeks (Vickerman, *et al.*, 1985). The life-cycle continues when the trypanosomes are injected into the unfortunate provider of the tsetse's next bloodmeal.

The complete life-cycle of the trypanosome is illustrated in Figure 1.9.

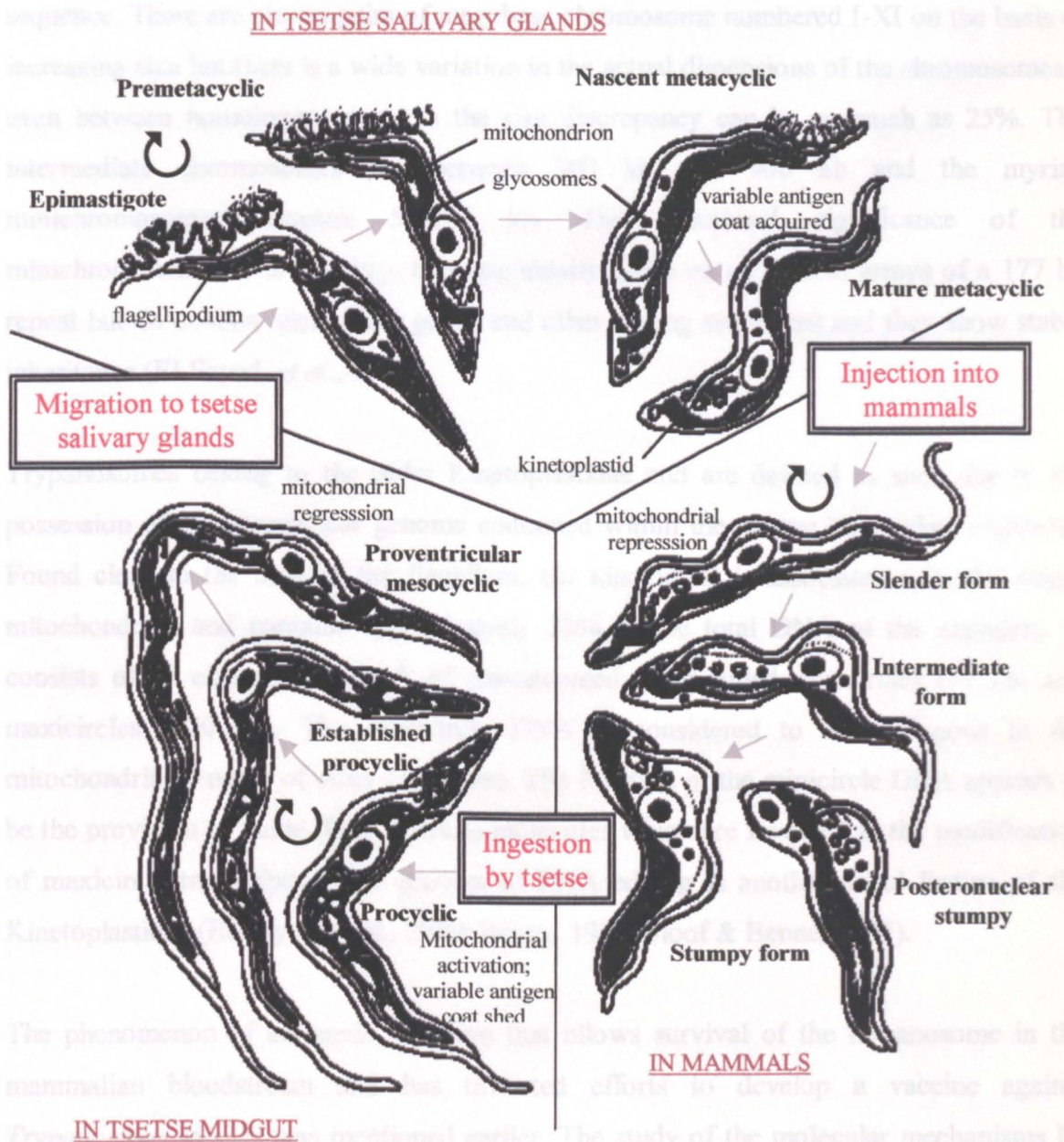


Figure 1.9. Diagrammatic representation of the *T. b. brucei* life-cycle. Reproduced from Vickerman, 1985.

1.2.3 Molecular biology of trypanosomes

The entire DNA content of each individual *T. b. brucei* parasite is in the region of 0.1 ng (Kreier & Baker, 1987) and the interphase nucleus measures ~3 μm in diameter (Ersfeld, *et al.*, 1999). The genome is considered to be diploid and may contain more than 12,000 genes. The haploid nuclear genome of *T. b. brucei* is around 35 Mb and is made up of several different chromosome types distinguished by their comparative mobilities in pulsed field gel electrophoresis (PFGE) (Ersfeld, *et al.*, 1999). The main megabase chromosomes are between 1 Mb and 6 Mb and are thought to contain the majority of the coding sequence. There are eleven pairs of megabase chromosome numbered I-XI on the basis of increasing size but there is a wide variation in the actual dimensions of the chromosomes – even between homologous partners the size discrepancy can be as much as 25%. The intermediate chromosomes are between 200 kb and 900 kb and the myriad minichromosomes measure 50-150 kb. The functional significance of the minichromosomes is uncertain – they are mostly made up of tandem arrays of a 177 bp repeat but do contain silent VSG genes and other coding sequences and they show stable inheritance (El-Sayed, *et al.*, 2000).

Trypanosomes belong to the order Kinetoplastidae and are defined as such due to the possession of an extranuclear genome contained within the unique kinetoplast organelle. Found close to the base of the flagellum, the kinetoplast is associated with the single mitochondrion and contains approximately 20% of the total DNA of the organism. It consists of an extensive network of concatenated super-coiled minicircles (~1 kb) and maxicircles (~20 kb). The maxicircle DNA is considered to be analogous to the mitochondrial genome of other organisms. The function of the minicircle DNA appears to be the provision of guide RNA (gRNA) molecules which are involved in the modification of maxicircle transcripts – this process of RNA editing is another novel feature of the Kinetoplastidae (El-Sayed, *et al.*, 2000; Benne, 1994; Sloof & Benne, 1997).

The phenomenon of antigenic variation that allows survival of the trypanosome in the mammalian bloodstream and has thwarted efforts to develop a vaccine against *Trypanosoma* species was mentioned earlier. The study of the molecular mechanisms by which the parasite effects the periodic changes in the VSG covering has been one of the most studied and most intriguing aspects of trypanosome biology (Donelson & Rice-Ficht,

1985; Barry & McCulloch, 2001). The trypanosome genome codes for many different VSGs (~1000) that are often expressed in a characteristic sequence with certain VATs associated with metacyclic populations and others making an appearance early in the infection course (Turner, 1999). The parasites accomplish the complete re-garbing of the cell by changing which VSG is expressed from an active expression site located at one of the telomeres – only one VSG is actively expressed at any one time. It is estimated that trypanosomes are capable of making 10^6 - 10^2 switches of VSG per doubling time of 5-10 hours (El-Sayed, *et al.*, 2000; Turner & Barry, 1989).

Figure 1.10 shows the structure of a typical telomeric bloodstream expression site (B-ES). It consists of the sequence between the VSG promoter and the characteristic repeats that make up the telomere and is between 45-60 kb in length. Between the promoter and the actual VSG gene is a series of 76 bp repeats and several expression site associated genes (ESAGs) that include the trypanosomal transferrin receptor which is also subject to variation (Borst & Fairlamb, 1998). Downstream of the B-ES is a series of 50 bp repeats, and then characteristic RIME (ribosomal insertional mobile elements) and *ingi* motifs that vary in size and number. There are thought to be around 20 B-ES present in the trypanosome genome, and also another 20 metacyclic expression sites (M-ES) which are smaller and simpler in terms of structural organisation (El-Sayed, *et al.*, 2000).

A range of different molecular switching mechanisms can lead to the expression of a new VSG. A silent telomeric B-ES can become active leading to the expression of its constituent VSG gene although this process of *in situ* activation leads to a limited number of combinations and is not thought to be the most important route of antigenic variation. Various recombinatory processes such as gene conversion, telomere conversion and telomere exchange which lead to the integration of new VSG genes into active B-ES are probably the most common pathways of antigen switching (El-Sayed, *et al.*, 2000; Barry & McCulloch, 2001).

The mechanisms that prevent the expression of the multitude of silent VSG genes and allow exclusive transcription of the VSG residing in the active expression site have yet to be fully elucidated. There have been reports of a RNA pol I involved in the expression of the active VSG (Navarro & Gull, 2001).

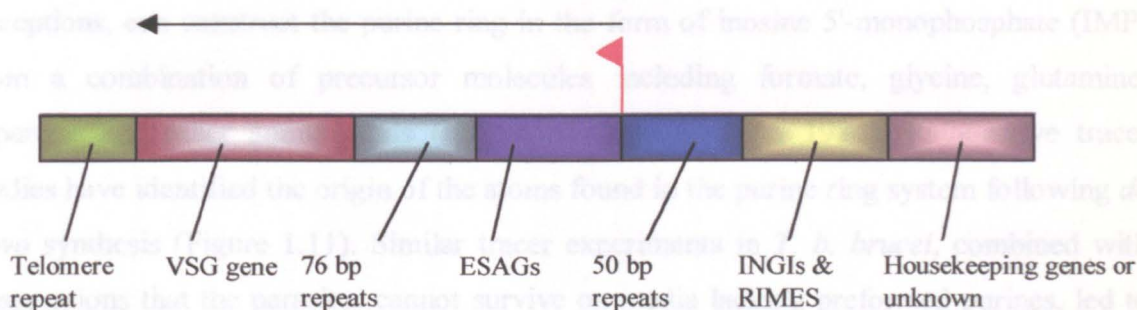


Figure 1.10. Organisation of the bloodstream expression site (B-ES). Adapted from El-Sayed, *et al.*, 2000.

Very few promoter sequences have been identified in trypanosomes with genes being transcribed as large polycistronic messages which are then processed into individual functional transcripts. Consequently, much of the regulation of protein synthesis in *T. brucei* is thought to occur at the level of mRNA stability or translationally (Clayton, 2002).

1.2.4 Purine salvage and metabolism in trypanosomes

1.2.4.1 Purine metabolic pathways

In many ways, trypanosomes and other parasites are "metabolically lazy" since they require the host to furnish them with energy-rich molecules such as glucose and ready-made cellular building blocks such as purines (Fairlamb, 1989). In the glucose-rich environment of the bloodstream trypanosomes rely totally on glycolysis and do not even make full use of the appropriated sugar molecules, generating only 2 ATP from each salvaged glucose. This opportunism, brought about by an abundant supply of nutrients, is wholly to the parasite's benefit, as it reduces the number of metabolic pathways it needs to maintain, allowing it to concentrate on vital functions such as immune-response evasion and rapid proliferation. Moreover, *de novo* biosynthesis of the purine ring costs three ATP molecules, so it is more energy efficient to salvage them instead.

Purine salvage in protozoan parasites has received much attention since they are generally incapable of the *de novo* synthesis of purines. Mammalian cells, with a few notable exceptions, can construct the purine ring in the form of inosine 5'-monophosphate (IMP) from a combination of precursor molecules including formate, glycine, glutamine, aspartate and other amino acids (Hammond & Gutteridge, 1984). Radioactive tracer studies have identified the origin of the atoms found in the purine ring system following *de novo* synthesis (Figure 1.11). Similar tracer experiments in *T. b. brucei*, combined with observations that the parasites cannot survive on media lacking preformed purines, led to the conclusion that rapidly proliferating trypanosomes depend on the scavenging of purines from their environment to satisfy their high demand for nucleic acid constituents (Hassan & Coombs, 1988).

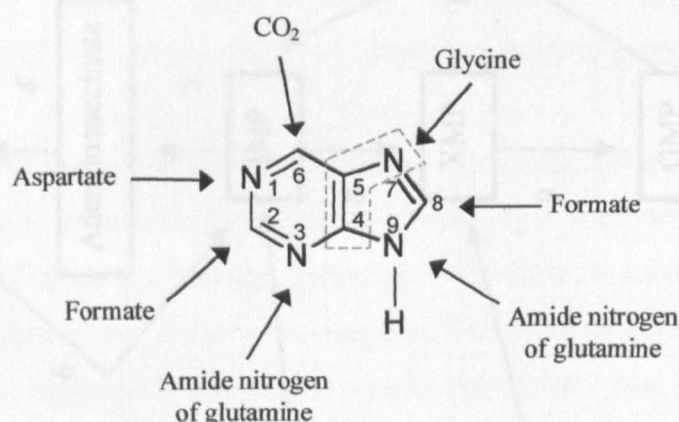


Figure 1.11. Origins of the atoms present in the purine ring following *de novo* synthesis. Reproduced from Gutteridge & Coombs (1977).

The survival of trypanosomes on media containing any one of the natural purines indicates that there must be pathways for interconversion of these molecules and this is indeed the case (Hammond & Gutteridge, 1984; Hassan & Coombs, 1988). Figure 1.12 shows the main routes of purine metabolism in trypanosomes.

Trypanosoma brucei possesses three different phosphoribosyltransferases with different substrate specificities: adenine phosphoribosyltransferase (APRT), xanthine phosphoribosyltransferase (XPRT) and hypoxanthine-guanine phosphoribosyltransferase (HGPRT). Only HGPRT has been cloned and characterised in detail (Allen & Ullman, 1993). These enzymes are responsible for the formation of nucleoside 5'-monophosphates from the appropriate base and 5'-phosphoribosyl-1-pyrophosphate (PRPP). Nucleoside

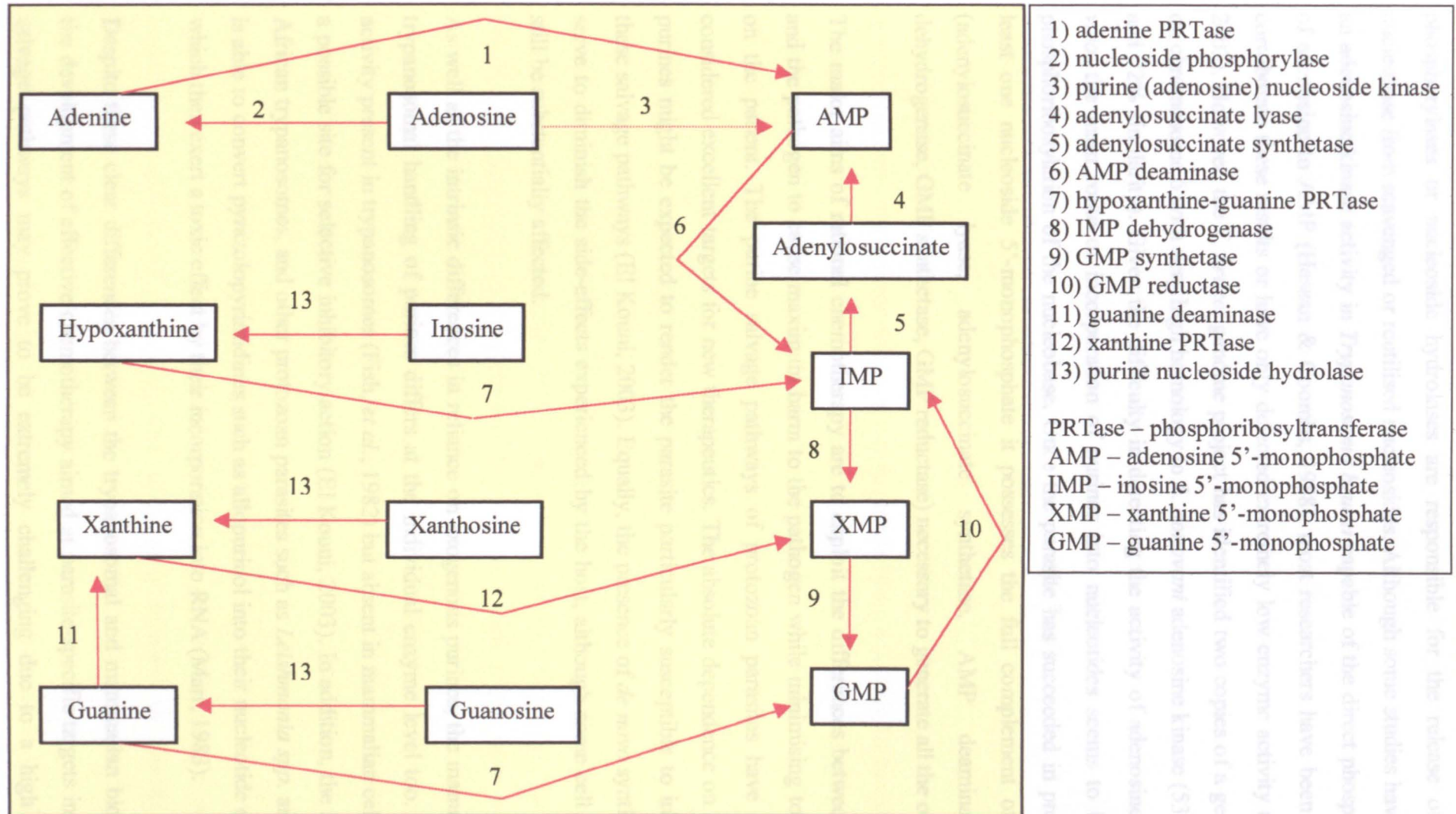


Figure 1.12. The main pathways of purine salvage in *Trypanosoma brucei*. The enzymes responsible for the interconversion of purines are numbered 1-13 and are listed in the legend.

phosphorylases or nucleoside hydrolases are responsible for the release of the free nucleobase from scavenged or reutilised nucleosides. Although some studies have reported an adenosine kinase activity in *Trypanosoma brucei* capable of the direct phosphorylation of adenosine to AMP (Hassan & Coombs, 1988), most researchers have been unable to corroborate these results or have only detected extremely low enzyme activity (El Kouni, 2003). However, the *T. brucei* genome project has identified two copies of a gene located on chromosome 6 with very high homology to *L. donovani* adenosine kinase (53% identity and 72% similarity). Given the difficulty in detecting the activity of adenosine kinase *in vivo*, the main route of incorporation of purines into nucleotides seems to be via the phosphoribosylation of the nucleobase. Once the parasite has succeeded in producing at least one nucleoside 5'-monophosphate it possesses the full complement of enzymes (adenylosuccinate lyase, adenylosuccinate synthetase, AMP deaminase, IMP dehydrogenase, GMP synthetase, GMP reductase) necessary to generate all the others.

The major aims of rational chemotherapy are to exploit the differences between the host and the pathogen to cause maximum harm to the pathogen while minimising toxic effects on the patient. The purine salvage pathways of protozoan parasites have long been considered excellent targets for new therapeutics. The absolute dependence on exogenous purines might be expected to render the parasite particularly susceptible to inhibitors of these salvage pathways (El Kouni, 2003). Equally, the presence of *de novo* synthesis could serve to diminish the side-effects experienced by the host, although some cell types may still be substantially affected.

As well as the intrinsic differences in reliance on exogenous purines, the mammalian and trypanosomal handling of purines differs at the individual enzyme level too. An XPRT activity present in trypanosomes (Fish, *et al.*, 1982) but absent in mammalian cells presents a possible site for selective inhibitory action (El Kouni, 2003). In addition, the HGPRT of African trypanosomes, and other protozoan parasites such as *Leishmania spp.* and *T. cruzi*, is able to convert pyrazolopyrimidines such as allopurinol into their nucleotide equivalents which then exert a toxic effect by their incorporation into RNA (Marr, 1983).

Despite these clear differences between the trypanosomal and mammalian biochemistry, the development of effective chemotherapy aimed at parasite-specific targets in the purine salvage pathways may prove to be extremely challenging due to a high degree of

redundancy integral to the system. Blocking the xanthine phosphoribosyltransferase activity would certainly seem to exert a selective effect on the trypanosome compared to the host, but the presence of other functioning conversion enzymes would negate any nucleotide deficiency caused. In some other protozoans, the salvage relies more heavily on the action of a single enzyme (e.g. the hypoxanthine-guanine-xanthine phosphoribosyltransferase in *Tritrichomonas foetus*) and there has been speculation that purine salvage could be more easily blocked in these systems (Somoza, *et al.*, 1998). In order to circumvent the problem of redundancy in trypanosomes it would be necessary to administer a cocktail of different inhibitors specific for different enzymes – currently, this does not seem practicable and is likely to increase the likelihood of undesirable side-effects.

As the “selective inhibitor” approach appears problematic, the “subversive substrate” approach becomes more accessible, as multiple pathways are available for the activation of nucleoside or nucleobase pro-drugs. Allopurinol is one example in trypanosomatid parasites and thioxanthine is another for the apicomplexan parasite *Toxoplasma gondii* (Pfefferkorn, *et al.*, 2001).

1.2.4.2 Purine transport activities

Although purines can be fed into the salvage pathways from other intracellular processes, such as nucleic acid degradation or ATP hydrolysis, the first step in purine salvage is usually the uptake of preformed purines from the host milieu. For most purines, this requires the action of specific transport permeases present in the plasma membrane of the parasite. The uptake of purines by nucleoside and nucleobase transporters in trypanosomes has been well studied, particularly in the past 15 to 20 years following revelations about the central role they play in parasite viability and their participation in drug uptake.

Prior to the identification of the first purine transporter gene in 1999, the study of purine uptake in *Trypanosoma brucei brucei* relied almost exclusively on the detection of internalised radiolabelled permeants. One early study reported the uptake of purine nucleotides by *T. b. brucei* (Sanchez, *et al.*, 1976), but this was highly controversial since the ability to transport these molecules across biological membranes is very rare. The consensus opinion seemed to be that the results obtained were due to the activity of a

nucleotidase present at the exofacial side of the plasma membrane followed by uptake of the resultant nucleoside. A recent review by Landfear and co-workers, however, reported some preliminary findings regarding the possible uptake of AMP by *T. b. brucei* and the related trypanosomatid parasite *Leishmania donovani*, and so this is one area that may need re-examination (Landfear, *et al.*, 2004).

James & Born (1980) showed that bloodstream form *T. b. brucei* and *T. congolense* could accumulate adenosine, guanosine, inosine, hypoxanthine and adenine. The discovery in the early 1990's that an adenosine transporter was involved in the uptake of arsenical drugs in *T. b. brucei* led quickly to the characterisation of two separate nucleoside transport activities designated P1 and P2 (Carter & Fairlamb, 1993).

The P1 transporter displayed very high affinity for [³H] adenosine with a K_m value of 0.15 μM and could be inhibited by other purine nucleosides but had very little affinity for the purine nucleobases. The P1 carrier also had a high capacity for its adenosine permeant (V_{max} value of 1.06 pmol (10^7 cells)⁻¹ s⁻¹) and was responsible for up to 80% of the adenosine flux in *T. b. brucei* bloodstream forms (Carter & Fairlamb, 1993; De Koning & Jarvis, 1999). Addition of 1 μM melarsen oxide or melarsoprol failed to inhibit uptake of adenosine by the P1 transporter (Carter & Fairlamb, 1993), indicating that this transporter was not involved in the uptake of these chemotherapeutic agents. The P1 transporter was shown to be the only adenosine or inosine transporter present in procyclic parasites and was the first purine transporter in *T. b. brucei* to be identified as a nucleoside/proton symporter (De Koning, *et al.*, 1998).

By completely saturating the P1 transport activity with unlabelled inosine, the uptake of [³H] adenosine by the P2 transporter could be studied in isolation. It displayed rigorous substrate preference for the 6-aminopurines adenosine and adenine (K_m value for adenosine uptake of 0.59 μM ; K_i value for inhibition of adenosine uptake by adenine of 0.38 μM) (Carter & Fairlamb, 1993; De Koning & Jarvis, 1999). Its mixed nucleoside/nucleobase transport function has been confirmed by the measurement of [³H] adenine uptake in bloodstream form trypanosomes (De Koning, unpublished) and also following expression of the *TbAT1* gene (see next section) in *Xenopus* oocytes (Baldwin & De Koning, unpublished). As expected, uptake by the P2 transporter accounted for the

remaining 20-40% of adenosine flux (Carter & Fairlamb, 1993; De Koning & Jarvis, 1999). In contrast to the P1 transport component, the P2-mediated uptake of adenosine was inhibited by the addition of melarsen oxide or melarsoprol, implicating this transporter in uptake of trypanocidal agents. The observation that a melarsen-resistant parasite line had completely lost the ability to accumulate adenosine via the P2 transporter further endorsed the idea that P2 was involved in the selective targeting of melaminophenyl arsenical drugs to the parasite (Carter & Fairlamb, 1993). To complicate the situation even further, the P2 transporter was later shown to also mediate the uptake of the diamidine class of drugs which includes pentamidine and berenil (Carter, *et al.*, 1995; Barrett, *et al.*, 1995; De Koning, 2001b).

T. b. brucei also exhibits several different purine nucleobase transport activities which are differentially expressed according to life-cycle stage. The H1 hypoxanthine transporter is present in the procyclic form of the trypanosome, and was shown to be driven by the protonmotive force using similar techniques used to determine the proton-dependence of the P1 nucleoside transporter (De Koning & Jarvis, 1997a). The H1 transporter was specific for purine nucleobase permeants with affinities of between 1.8 μM and 9.3 μM . The existence of an additional nucleobase transport component in procyclics was discovered in the course of my research project. This transport activity was designated H4 and is described in Chapter 6, Chapter 7 and in Burchmore, *et al.*, 2003.

When *T. b. brucei* procyclics were exposed to different purine levels there was a concordant change in purine uptake systems. In response to purine starvation first hypoxanthine and then adenosine transport components displayed increased capacities as indicated by a rise in V_{max} values – the K_{m} values were unchanged. The differential control of the purine transporters in *T. b. brucei* in response to different growth conditions mirrors similar phenomena in the monoxenous insect parasite *Crithidia spp.* (De Koning, *et al.*, 2000).

Uptake of purine nucleobases in the bloodstream form parasites was found to be due to the activity of two distinct transporters, which could be distinguished on the basis of their substrate preference, their affinities for their permeant and their differential sensitivity to guanosine. The H2 transporter mediated uptake of hypoxanthine with a K_{m} value of 123 nM, and this transporter was affected by a range of purine nucleobases and pyrimidines,

and was inhibited by guanosine with a K_i of 10.9 μM . The guanosine-sensitive H2 component accounted for ~90% of hypoxanthine transport, whilst the H3 transporter mediated the remaining 10% of transport. The lower affinity H3 hypoxanthine transporter was more stringent in its choice of substrate – it accepted the four natural purine nucleobases (hypoxanthine, adenine, guanine, and xanthine) with affinities in the range of 4.7 μM to 28.8 μM , but was not inhibited by other purines and pyrimidines (De Koning & Jarvis, 1997b).

In addition to the purine transporters described above, *T. b. brucei* also possesses the high-affinity U1 uracil transporter that is expressed in procyclics and is also a proton-symporter (De Koning & Jarvis, 1998). There is also evidence for the existence of a separate transporter in bloodstream forms for S-adenosylmethionine (Goldberg, *et al.*, 1997).

The proton-dependence of the *T. b. brucei* purine transporters is in contrast with the transporters in mammalian cells and tissues. Purine uptake in animal cells is by one of two mechanisms: facilitated diffusion/equilibrative transport or alternatively sodium-dependent active transport (Plagemann, *et al.*, 1988; Griffith & Jarvis, 1996). It is hoped that such fundamental differences in the function of the transport processes can be exploited to target trypanocides selectively to the trypanosome (Landfear, *et al.*, 2004).

Figure 1.13 shows the range of transporters expressed in *T. b. brucei* bloodstream forms and procyclics.

1.2.4.3 Molecular biology of purine uptake

The characterisation of transporters in intact parasites using radiolabelled permeants was obviously necessary in the absence of genetic information but the techniques used had many drawbacks, particularly as the multitude of transporters with overlapping specificities can confound efforts to dissect the function of the individual transport components.

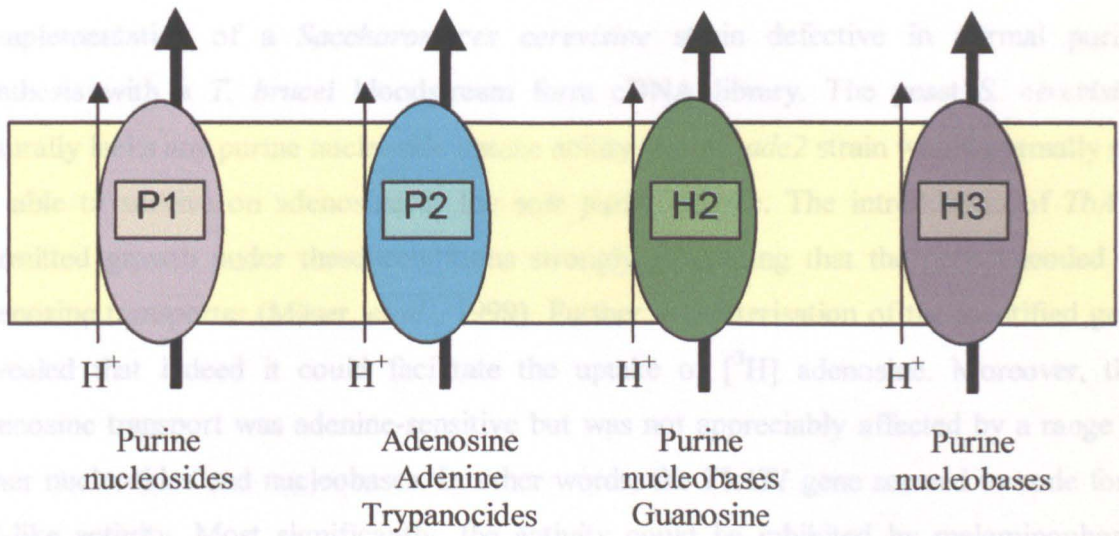
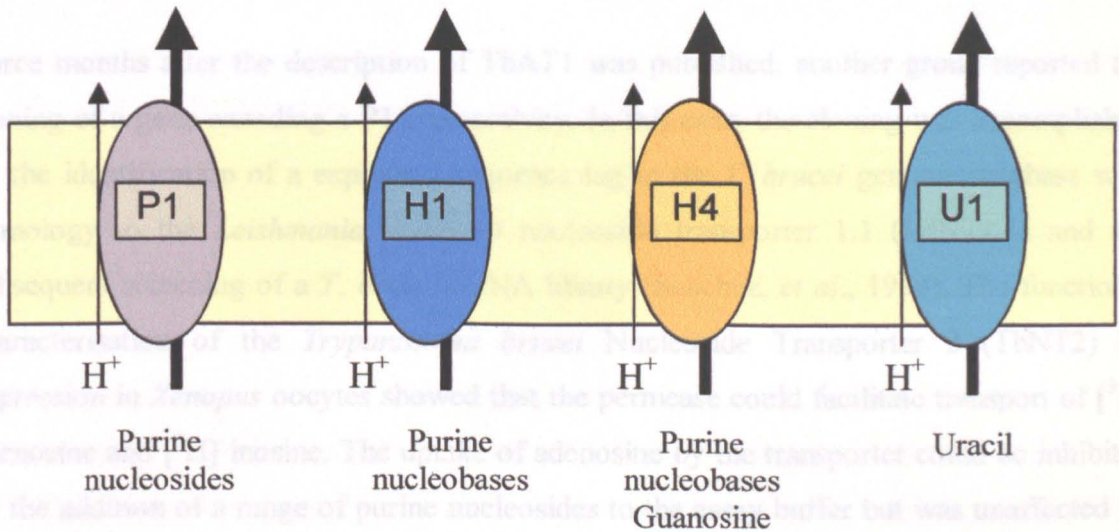
T. b. brucei* long-slender bloodstream form**T. b. brucei* procyclic form**

Figure 1.13. The complement of nucleoside and nucleobase transporters present in the plasma membrane of *T. b. brucei* at different life-cycle stages. The P1 nucleoside transport component is found in both bloodstream form and procyclic *T. b. brucei* and seems to be encoded by the *TbNT* cluster of genes found on chromosome 2. The P2 transport activity is present in bloodstream form parasites only and is encoded by the *TbAT1* gene. The expression of the *TbNBT1* protein is responsible for the procyclic H4 hypoxanthine transport activity (see Chapter 7 and Burchmore, *et al.*, 2003). The other transporters shown in this figure have been detected biochemically but have yet to be characterised at the molecular level.

The cloning of the first purine nucleoside transporter gene from *T. b. brucei* heralded a new molecular age in the study of purine uptake. The gene encoding the *Trypanosoma brucei* Adenosine Transporter 1 (TbAT1) was identified by the functional complementation of a *Saccharomyces cerevisiae* strain defective in normal purine synthesis with a *T. brucei* bloodstream form cDNA library. The yeast *S. cerevisiae* naturally lacks any purine nucleoside uptake ability and the *ade2* strain would normally not be able to survive on adenosine as the sole purine source. The introduction of *TbAT1* permitted growth under these conditions strongly suggesting that the gene encoded an adenosine transporter (Mäser, *et al.*, 1999). Further characterisation of the identified gene revealed that indeed it could facilitate the uptake of [³H] adenosine. Moreover, this adenosine transport was adenine-sensitive but was not appreciably affected by a range of other nucleosides and nucleobases. In other words, the *TbAT1* gene seemed to code for a P2-like activity. Most significantly, the activity could be inhibited by melaminophenyl arsenicals and the complemented yeast strain became sensitised to the drugs compared to the non-complemented controls (Mäser, *et al.*, 1999).

Three months after the description of TbAT1 was published, another group reported the cloning of a gene encoding a P1-type activity. In this case, the cloning was accomplished by the identification of a expressed sequence tag in the *T. brucei* genome database with homology to the *Leishmania donovani* nucleoside transporter 1.1 (LdNT1.1) and the subsequent screening of a *T. brucei* cDNA library (Sanchez, *et al.*, 1999). The functional characterisation of the *Trypanosoma brucei* Nucleoside Transporter 2 (TbNT2) by expression in *Xenopus* oocytes showed that the permease could facilitate transport of [³H] adenosine and [³H] inosine. The uptake of adenosine by the transporter could be inhibited by the addition of a range of purine nucleosides to the assay buffer but was unaffected by purine nucleobases paralleling the substrate preferences of the P1 transporter characterised *in situ*. Southern blots in this initial study strongly suggested the existence of an array of closely related genes and this was confirmed in a further report identifying 5 more NT2-like genes present at the NT2 locus (Sanchez, *et al.*, 2001). The predicted amino acid sequences of TbNT3, TbNT4, TbNT5, TbNT6 and TbNT7 exhibited > 80% identity to TbNT2. Expression in *Xenopus* oocytes revealed that TbNT5, TbNT6 and TbNT7 encoded permeases capable of mediating transport of typical P1 nucleoside substrates. Intriguingly, expression of TbNT5, and to a lesser degree TbNT6 and TbNT7, conferred some

hypoxanthine transport ability on the oocytes. No substrates were identified for TbNT3 and TbNT4.

As part of this project *Trypanosoma brucei* Nucleobase Transporter 1 (*TbNBT1*), the first nucleobase-specific trypanosomal transporter gene to be identified, was cloned and its function was characterised (see Chapter 7; Burchmore, *et al.*, 2003). An almost identical transporter was cloned by Henriques and co-workers (Henriques, *et al.*, 2003) and the first *Leishmania* nucleobase transporter was also recently cloned and characterised (Sanchez, *et al.*, 2004).

1.2.5 The role of transporters in drug targeting and drug resistance

Like the purine salvage enzymes, the purine transporters of *T. b. brucei* have potential as drug targets because they are essential for parasite survival and have been shown to be functionally different from the purine transporters possessed by the host. However, chemotherapeutic strategies aimed at inhibiting the uptake of purines and thus depriving the parasite of essential nutrients would require all the transporters to be blocked simultaneously. It has been shown that parasites that have lost a single purine transporter (*i.e.* the *TbAT1* gene knockout) suffered no perceivable loss of viability (Matovu, *et al.*, 2003). With the range of purine transporters with different substrate preferences and affinities present in *T. b. brucei* it would likely be very difficult to achieve total suppression of uptake – and of course the purine salvage enzymes would be able to convert any purine substrate that evaded the transport blockade. Furthermore, adenine may be able to diffuse across the membrane to some degree, and trypanosomes that are subjected to absolutely purine-free conditions *in vitro* undergo a reversible growth arrest rather than cell death for the first few days at least (De Koning, *et al.*, 2000; Natto, *et al.*, submitted).

The purine transporters, along with other transporter and receptor classes in *T. b. brucei*, have garnered interest for their potential or actual ability to act as gateways for trypanocides. Figure 1.14 shows the different pathways through which existing trypanocides can enter the trypanosome. Although lipophilic drugs can diffuse across the plasma membrane to gain access to their intracellular targets they can be limited by their

lack of selectivity with drugs flooding into host cells as well as into the parasite target. The entry of DFMO into host cells by passive diffusion (Bitonti, *et al.*, 1986) is not problematic

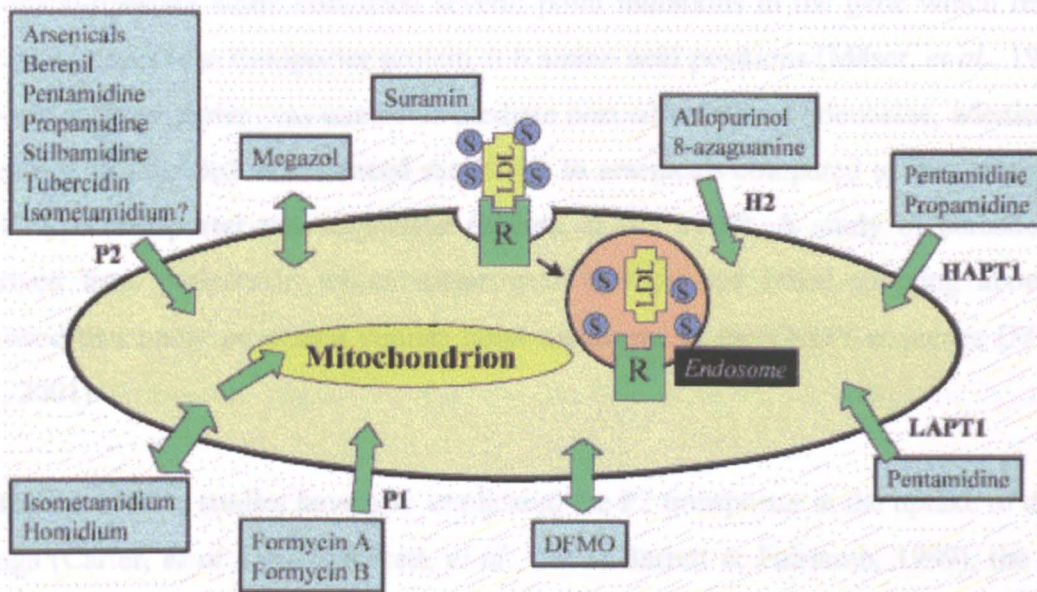


Figure 1.14. Uptake of trypanocidal drugs. Reproduced from De Koning, 2001a.

because pronounced differences in the properties of the host and parasite ODC account for the selectivity of the drug. Other drugs require specific transport processes to allow their entry into cells and/or across other membranes such as the BBB, and their selective action can often be mediated at the level of uptake. Suramin is taken up as a complex with LDL by receptor-mediated endocytosis mediated by the trypanosomal LDL receptor (Vansterkenburg, *et al.*, 1993). The P2 purine nucleoside transporter has already been shown to be involved in the selective uptake of existing trypanocidal agents, as discussed. The purine transporters of *T. b. brucei* could be further exploited to facilitate the selective and concentrative accumulation of novel trypanocides, whether these are subversive purine substrates intended to disrupt normal incorporation of purines into nucleic acids, or molecules engineered to be taken up by the purine transporters, but with an intracellular target unrelated to purine salvage (El Kouni, *et al.*, 2003; Landfear, 2001; Wallace, *et al.*, 2002).

There have been many studies reinforcing the link between the P2 transporter and the uptake of arsenical drugs. Observations that arsenical-resistant parasites accumulated lower levels of diamidines and other drugs gave an indication that resistance could be due to

reduced uptake of the trypanocides (Frommel & Balber, 1987). The original P2 transport study showed that an arsenical-resistant strain had lost the P2 transport function (Carter & Fairlamb, 1993). Following the identification of the *TbAT1* gene it was discovered that an arsenical-resistant strain contained several point mutations in the gene which resulted in the alteration of the transporter protein at 6 amino acid positions (Mäser, *et al.*, 1999). The altered P2 transporter was unable to mediate normal uptake of adenosine, adenine and its presence in yeast led to a reduced sensitivity to arsenicals compared to that seen when the wild-type transporter was expressed (Mäser, *et al.*, 1999). A study of parasite isolates derived from patients in whom melarsoprol therapy had failed to bring about a cure showed that many possessed similar point mutations in the *TbAT1* sequence (Matovu, *et al.*, 2001).

Although several studies have also implicated the P2 transporter in the uptake of diamidine drugs (Carter, *et al.*, 1995; Barrett, *et al.*, 1995; Barrett & Fairlamb, 1999), the situation has been somewhat complicated with the discovery that alternative transporters are also involved in the internalisation of a number of these drugs (De Koning, 2001b). Barrett and co-workers demonstrated that a berenil-resistant *T. equiperdum* line possessed a P2 transport activity with reduced affinity for its substrates (Barrett, *et al.*, 1995). On the other hand, the arsenical-resistant parasites described by Carter & Fairlamb (1993) as having lost the P2 transport function were hardly resistant to pentamidine at all (Fairlamb, *et al.*, 1992). Although adenosine uptake by the P2 transporter could be inhibited by pentamidine, a 100-fold excess of adenosine failed to inhibit uptake of pentamidine, and other diamidine drugs could only partially inhibit uptake of radiolabelled pentamidine (Carter, *et al.*, 1995). The P2 activity introduced into yeast by the expression of the *TbAT1* gene also could not be inhibited with pentamidine (Mäser, *et al.*, 1999).

The existence of two additional pentamidine transporters, designated as the high affinity pentamidine transporter (HAPT) and the low affinity pentamidine transporter (LAPT) are now known to be responsible for the conflicting data regarding uptake of diamidines in *Trypanosoma* species (De Koning, 2001b). The high level of cross-resistance between the arsenicals and the veterinary diamidine berenil is a consequence of the two drugs sharing the same main route of uptake through the P2 transporter (De Koning, *et al.*, 2004; Witola, *et al.*, 2004), although there is some evidence for a residual uptake of arsenicals via the HAPT (Matovu, *et al.*, 2003). The surprisingly low levels of cross-resistance observed for

melarsoprol and pentamidine (Fairlamb, *et al.*, 1992) are explained by the transport of pentamidine by HAPT and LAPT even in the absence of the P2 transporter (De Koning, 2001b).

Given the scarcity of effective trypanocides and the dearth of novel anti-trypanosomal lead compounds, the importance of understanding both normal and aberrant targeting of the essential HAT chemotherapeutics melarsoprol and pentamidine to the parasite cannot be understated. The inherent limitations of these drugs, however, call for the development of new or re-engineered trypanocides. Since the uptake of drugs by the trypanosome is likely to be important for selective action an increased understanding of how the many different purine transporters of *Trypanosoma brucei* function at the molecular and biochemical level must also be imperative.

This Ph. D. project was initiated with the issues stated above very much in mind. The main focus of the project was to improve our knowledge of previously-identified transport components with particular emphasis on nucleobase-specific transporters, but also to catalogue transporter genes emerging from the *T. brucei* genome project. The initial aims were to quantitatively characterise the substrate recognition motifs of the *T. brucei* H2 transporter and the human erythrocyte nucleobase transporter. This also led us to investigate some of the compounds used in this study as potential trypanocides. Circumstances also allowed us to investigate some novel purine compounds for trypanocidal activity. Another primary aim was to clone *T. brucei* purine permease genes and characterise their function in an heterologous system, again with an emphasis on the identification of genes responsible for nucleobase-specific transporters.

Chapter Two

Materials and Methods

2.1 Parasite strains

Two strains of *Trypanosoma brucei brucei* were used during the project. It is a peculiarity of African trypanosome research that biochemical studies have tended to focus on the EATRO 427 strain, while the molecular analyses, including the genome sequencing project, have been carried out on the TREU 927 strain; the work described here has mostly kept to this custom, except where noted. Both bloodstream form parasites and procyclic form parasites were used for various stages of the study. Stabilates were maintained on-site as liquid nitrogen stocks and these were prepared as described in Appendix A.

2.2 Bacterial strains

The JM109 and TOP10 strains of *Escherichia coli* were used for routine cloning and subcloning of *T. b. brucei* genomic sequences. *E. coli* JM109 (endA1, recA1, gyrA96, thi, hsdR17 (r_K - m_K +), relA1, supE44, Δ (lac-proAB), F' [traD36, proAB, lacI^qZAM15]) competent cells were purchased from Promega initially but were subsequently prepared “in-house” using the method described in section 2.14.7, below. *E. coli* TOP10 (F-, mcrA, Δ (mrr-hsdRMS-mcrBC), ϕ 80lacZAM15, Δ lacX74, deoR, recA1, araD139, Δ (ara-leu)7697, galU, galK, rpsL (Str^R), endA1, nupG) electrocompetent cells were also prepared in the laboratory (see section 2.14.8).

2.3 Yeast strains

Saccharomyces cerevisiae MG887.1 (Gillissen, *et al.*, 2000) was used as a heterologous expression system for the cloned *T. b. brucei* nucleobase transporters. This strain is an *fcy2* mutant and thus does not possess a functional endogenous uptake system for adenine, guanine, hypoxanthine or cytosine (Horak, 1997). The strain has also been engineered by replacement of the *ura3* gene with a truncated version, thus generating uracil auxotrophy.

2.4 Chemicals

2.4.1 Purine analogues and radiolabelled compounds

[8-³H] hypoxanthine (1.18 TBq/mmol) was purchased from Amersham Pharmacia Biotech, UK. [2,8-³H] adenine (1.2 TBq/mmol) was obtained from NEN, USA. [2,8-³H] adenosine (1.2 TBq/mmol) was manufactured by Perkin Elmer. [2,8-³H] inosine (592 GBq/mmol) and [³H] allopurinol (44.4 GBq/mmol) were both purchased from Moravek.

Natural purines and purine analogues were purchased from Sigma (adenine, hypoxanthine, guanine, xanthine, thymine, uracil, adenosine, guanosine, inosine, acycloguanosine, allopurinol, 6-thioguanine, 2-aminopurine, 8-azaguanine, 7-deazaguanine, 2,6-diaminopurine, ARA-hypoxanthine, inosine, 6-methoxypurine, 1-methyladenine, 3-methyladenine, purine, theophylline, 8-azaadenine, and lumazine,), Fluka (1-methylguanine and 9-methylguanine), Aldrich (aminopurinol, 1,3-dideazapurine, 6-benzyloxypurine, 6-chloropurine, 1-deazapurine, 2,6-dichloropurine, 6-dimethylaminopurine and 4(3H)-pyrimidone), and ICN (7-azaindole). 9-deazaadenine was a kind gift from John A. Secrist III of the Southern Research Institute. 9-deazaguanine was generously provided by Howard Cottam of the University of California, San Diego. The novel purine compounds described in Chapter Five were synthesised by Katherine Seley and colleagues at the Georgia Institute of Technology, Atlanta.

2.4.2 Other chemical reagents

Alamar Blue reagent was purchased from Trek Diagnostic Systems Ltd. All other chemicals were purchased from Sigma at the highest grade available unless stated otherwise.

2.4.3 Oligonucleotides and molecular biology enzymes

All oligonucleotides were synthesised by MWG Biotech. T4 DNA ligase, *Taq* DNA polymerase, *Pfu* DNA polymerase, dNTPs, and all restriction enzymes were purchased from Promega. Calf intestinal alkaline phosphatase (CIAP) was from Boehringer Mannheim. The pGEM-T Easy Vector system was obtained from Promega.

2.5 Growth and maintenance of parasites

2.5.1 Bloodstream form trypanosomes in vitro

Bloodstream form *T. b. brucei* were maintained in liquid culture using HMI-9 medium plus 20% heat-inactivated foetal calf serum (FCS), and culture conditions of 37 °C and 5% CO₂ (Hirumi & Hirumi, 1989). Cultures were initiated by inoculating 5 ml of HMI-9 medium with a tiny aspiration of the "buffy coat layer" of infected rodent blood (see section 2.8.1). The cultures were then passaged regularly into fresh HMI-9 medium. This method was appropriate for producing a small quantity of parasites, but an *in vivo* route had to be taken to obtain large numbers of bloodstream form parasites.

2.5.2 Bloodstream form trypanosomes in vivo

Adult female Wistar rats were injected intra-peritoneally with *T. b. brucei* EATRO 427 or TREU 927 bloodstream forms (from capillary tube blood stocks in 10.5% DMSO stored in liquid nitrogen). Parasitaemia was monitored by daily examination of blood smears from tail venepuncture. Estimation of total parasite numbers was by a method developed by Herbert & Lumsden (1976) based on number of trypanosomes per microscope field. The blood was collected when peak parasitaemia was reached (between 5×10^8 and 1×10^9 parasites per millilitre of blood).

2.5.3 Procyclic form trypanosomes in vitro

Procyclic form *T. b. brucei* was conveniently maintained at 25 °C in SDM79 medium supplemented with 10% FCS (Brun & Schönenberger, 1979) or purine-free trypanosome medium (PFTM) supplemented with 5% dialysed FCS (De Koning, *et al.*, 2000). Large numbers of procyclics were simple to cultivate by scaling up culture volumes.

2.6 Growth and maintenance of *Saccharomyces cerevisiae*

S. cerevisiae MG887.1 was maintained on solid YPAD medium at 30 °C. It was necessary to streak a fresh plate every 4-5 days. *S. cerevisiae* MG887.1 was made chemically-competent by the method described in section 2.14.13.

2.7 Growth and maintenance of *Escherichia coli*

Non-recombinant *E. coli* JM109 and *E. coli* TOP10 was grown on solid Luria-Bertani (LB) medium or in LB broth at 37 °C overnight.

2.8 Transport assays in trypanosomatids

2.8.1 Collection and purification of bloodstream form *T. b. brucei* from experimental rodents

At peak parasitaemia the blood was removed by cardiac puncture under terminal anaesthesia using a syringe loaded with a small volume of CBSS (Carter's balanced saline solution) containing 100 U/ml heparin. The whole blood was centrifuged at 1,250 x g for 15 minutes to separate the different components. The white, parasite-containing "buffy coat" layer forms at the intersection between the red blood cells and the plasma. This layer was carefully removed using a plastic Pasteur pipette and resuspended in a small volume of PSG (phosphate buffered saline with glucose, pH 8.0). The pre-washed DEAE (DE-52, Whatman) cellulose was poured to a depth of 5 cm into a glass-wool-plugged 50 ml syringe with plunger removed. The cellulose column was equilibrated with 200 ml of PSG. The "buffy coat" suspension was loaded onto the column and ran through with PSG. Blood cell surfaces are negatively charged and these cells remained within the column adsorbed to the cellulose while the less-negatively charged trypanosomes were collected in the flow-through (Lanham, 1968, and Lanham & Godfrey, 1970). The purification was carried out as rapidly as possible since pH 8.0, although necessary for the correct functioning of the column, is quite a hostile environment for the parasites.

2.8.2 Preparation of cells for uptake assay

Bloodstream form trypanosomes collected from the cellulose column were washed twice in the trypanosome assay buffer for 10 minutes at 800 x g, and then suspended at 10^8 cells/ml. The cells were usually left at room temperature for 15-20 minutes before use in the assay.

Procyclic form trypanosomes for transport assays were grown in 100 ml cultures to mid-log stage. The cultures were then harvested and washed in the trypanosome assay buffer as described above for bloodstream forms.

Cell viability and motility were checked under a phase-contrast microscope at the conclusion of each experiment.

2.8.3 Transport assays in trypanosomatids

Uptake of radiolabelled permeants in *T. b. brucei* was determined using a rapid-stop/oil-spin technique previously described by De Koning & Jarvis (1997a). The molar concentration of the radiolabel was adjusted according to the transporter of interest to allow isolation of particular activities. Radiolabel concentrations varied from 15 nM to 1 μ M as appropriate. One hundred microlitres of the trypanosome suspension ($\sim 10^7$ cells) was mixed with 100 μ l assay buffer containing tritiated permeant only or mixed with various concentrations of inhibitor. After a predetermined incubation time at room temperature, uptake was stopped by addition of an ice-cold millimolar solution of unlabelled permeant and centrifugation (30 seconds; 12,000 x g) through an oil layer [7:1 (v/v) mix of di-*n*-butyl phthalate (BDH) and light mineral oil (Sigma)]. The centrifugation step thus separated the parasites from the radiolabel. The microfuge tubes were then flash-frozen in liquid nitrogen and the bottom, containing the cell pellet, cut off and collected in a numbered scintillation vial. The cells were solubilised in 2% SDS (30 minutes; room temperature), mixed with 3 ml Ecoscint scintillation fluid and the accumulated radioactivity measured in the 1450 Microbeta Liquid Scintillation and Luminescence Counter (PerkinElmer Lifesciences).

Some test compounds were used from stock solutions in 100% DMSO. Final DMSO concentrations in the assays never exceeded 1%, which did not affect uptake kinetics.

2.9 Transport assays in human erythrocytes

2.9.1 Preparation of cells for uptake assay

Whole human blood from healthy volunteers was sourced from the Bloodbank. Heparinised blood was stored at 4 °C until needed.

The whole blood was centrifuged at 800 x g for 10 minutes and the red cells were washed twice in erythrocyte assay buffer (see Appendix A) and resuspended at a haematocrit ratio of approximately 25%. The erythrocytes were counted in a haemocytometer; typical densities were $2\text{-}3 \times 10^9$ cells/ml. The integrity of the cells was checked at the conclusion of each experiment.

2.9.2 Transport assays in human erythrocytes

Uptake of [2,8- ^3H] adenine by human erythrocytes was also measured by the oil-stop method, using 100% dibutylphthalate for the oil layer and $2\text{-}3 \times 10^8$ erythrocytes per assay point. The final concentration of radiolabelled adenine in the assay was 1 μM . The uptake was stopped by addition of ice-cold 2 mM papaverine solution (an inhibitor of equilibrative transport). After centrifugation, the oil layer was aspirated and the inside of the tube wiped with absorbent paper to remove traces of radiolabel. Cell pellets were solubilised in 250 μl 1% Triton x100 and the haemoglobin was precipitated with 0.5 ml 5% trichloroacetic acid. Following further centrifugation (10 minutes, 13,000 x g), the supernatant was transferred to scintillation vials, mixed with 3 ml scintillation fluid and counted for radioactivity, as in section 2.8.3.

Some test compounds were used from stock solutions in 100% DMSO. Again, with final DMSO concentrations in the assays never exceeding 1%, uptake kinetics were not significantly affected.

2.10 Transport assays in *Saccharomyces cerevisiae*

2.10.1 Preparation of cells for uptake assay

A yeast starter culture was grown at 30 °C in 5 ml of synthetic complete medium minus uracil (SC-URA) for 6 hours. The starter culture was then used to inoculate a 50 ml overnight culture.

The yeast cells were harvested by centrifugation at 1,800 x g for 5 minutes at 4 °C. The pellet was washed twice in ice-cold yeast assay buffer, before resuspension at $1-2 \times 10^8$ /ml. The cells were allowed to acclimatise to room temperature for 10 minutes before use in the assay.

2.10.2 Transport assays in *Saccharomyces cerevisiae*

Uptake of radiolabelled permeants in *Saccharomyces cerevisiae* MG887.1 transformants was determined using a virtually identical rapid-stop/oil-spin technique to that described for the trypanosome assays (section 2.8.3). One hundred microlitres of the yeast suspension (10^7 cells) was mixed with 100 μ l yeast assay buffer containing tritiated permeant and various concentrations of inhibitor. After a predetermined incubation time, uptake was stopped by addition of an ice-cold millimolar solution of unlabelled permeant and centrifugation through an oil layer [7:1 (v/v) mix of di-*n*-butyl phthalate and light mineral oil]. The microfuge tubes were then flash-frozen in liquid nitrogen and the bottom containing the cell pellet cut off into a numbered scintillation vial. The cells were solubilised in 2% SDS (30 minutes; room temperature), mixed with 3 ml scintillation fluid and the accumulated radioactivity measured in the liquid scintillation counter.

Some test compounds were used from stock solutions in 100% DMSO. Final DMSO concentrations in the assays never exceeded 1%, which did not affect uptake kinetics.

2.11 Transport assays in *Xenopus laevis* oocytes

This work was carried out by Stephen Baldwin's laboratory at the University of Leeds.

2.11.1 Preparation of cells for uptake assay

The oocytes were prepared for uptake as described by Huang, *et al.*, 1993. Briefly, stage VI oocytes were isolated from the ovarian tissue of *Xenopus laevis* and incubated overnight at 18 °C in MBM buffer (88 mM NaCl, 1 mM KCl, 0.33 mM Ca(NO₃)₂, 0.41 mM CaCl₂, 0.82 mM MgSO₄, 2.4 mM NaHCO₃, 2.5 mM sodium pyruvate, 0.05 mg/ml penicillin, 0.1 mg/ml gentamycin sulphate, 10 mM HEPES, pH 7.5). RNA was prepared by transcribing linearised expression vector with T7 polymerase in the presence of m7GpppG cap using the mMESSAGING MACHINE (Ambion) transcription system. The oocytes were injected with 10 ng of the capped, polyA-RNA and then incubated for five days in MBM at 18 °C.

2.11.2 Transport assays in *Xenopus laevis* oocytes

The injected oocytes were placed in transport buffer (100 mM NaCl, 2 mM KCl, 1 mM CaCl₂, 1 mM MgCl₂, 10 mM HEPES, pH 7.5). Uptake of 100 μM [³H] adenine, [³H] adenosine, [³H] uracil or [³H] uridine was assayed at 20 °C over 30 minutes. Transport was stopped by six rapid washes in ice-cold washes in transport buffer. The oocytes were then solubilised in 5% SDS and the accumulated radioactivity was measured by liquid scintillation counting.

2.12 Analysis of data from transport assays

The small amount of radioactivity that was associated with the cell pellet in the presence of saturating concentrations of unlabelled permeant (*i.e.* the component not accounted for by the active transport of the radiolabel) was subtracted from each data point. These corrected counts were converted to transport rates (pmol (10⁷ cells)⁻¹ s⁻¹). The results were plotted by non-linear regression using the FigP or PRISM software packages as appropriate. From the dose-inhibition curves, IC₅₀ values were calculated. Hill slopes were found to be near to -1 supporting the assumption of single-site competitive inhibition. All assays were performed

in triplicate and IC_{50} values were based on a minimum of 8 datapoints over the relevant range. In a few cases, complete inhibition curves could not be obtained due to limited solubility of the test compound. When >50% inhibition was achieved at the maximum test concentration, the IC_{50} value was based on extrapolation, assuming a Hill coefficient of -1 and eventual 100% inhibition, defined as equal to saturating concentrations of unlabelled permeant (or papaverine in case of erythrocytes).

Conversion to K_i was then possible using the Cheng-Prusoff equation:

$$K_i = IC_{50} / [1 + (L + K_m)]$$

where L is the permeant concentration and K_m is the value obtained for this permeant (Cheng & Prusoff, 1973). It is important to note that this equation is only valid for competitive inhibition situations.

Each final K_i value was the the mean $K_i \pm SE$ of at least three independent experiments.

A derivation of the Nernst equation was then used to determine ΔG° values for analogue binding to the transporter:

$$\Delta G^\circ = -RT \ln(K_i)$$

where R is the gas constant and T is the absolute temperature. The ΔG° value gives a measure of the binding energies existing between the transporter and its substrate.

2.13 Alamar Blue assays

The active ingredient of the Alamar Blue reagent is a blue dye called resazurin which is non-fluorescent. In the presence of live cells the resazurin is reduced to resorufin which is pink in colour and is highly fluorescent. The extent of this change in fluorescence and colour is directly proportional to the number of viable cells. The Alamar Blue assay has been used in proliferation/cytotoxicity assays involving many different cells types (O'Brien, *et al.*, 2000).

The *in vitro* trypanocidal activities of the purine analogues were evaluated using the Alamar Blue assay (Räz, *et al.*, 1997). The stock concentration of the drug to be tested was prepared at two times the required highest final concentration in HMI-9 medium. Doubling

dilutions were prepared in 96 well plates in duplicate. A drug-free control was also included. Bloodstream trypanosomes of strain 427 (1×10^4 cells) from preadapted culture in HMI-9 medium, were added to each well and the plates were incubated at 37 °C for 48 hours. Alternatively, 1×10^4 procyclic cells in SDM-79 were added to drug dilutions in the same medium and incubated at 26 °C for 48 hours. Twenty microlitres of Alamar Blue reagent was then added to each well (to give a concentration of 10%) and the plate was subsequently incubated for a further 24 hours. The plates were read for fluorescence using a LS55 Luminescence Spectrometer (Perkin Elmer Instruments) at 530 nm excitation and 590 nm emission wavelengths. Alternatively, the plates were subjected to colorimetric analysis by measuring the absorbance at 600 nm.

2.14 Molecular cloning techniques

2.14.1 Preparation and purification of genomic DNA from *T. b. brucei*

T. b. brucei procyclics were grown in a 500 ml culture for 48 hours. After 48 hours, the cells were harvested by centrifugation at 1,500 x g for 15 minutes at 4 °C. The pellet was resuspended in 450 µl of DNA extraction buffer (see Appendix A). 50 µl of 10% SDS and 25 µl of proteinase K (10 mg/ml in dH₂O) was added. The lysis reaction was allowed to proceed at 37 °C for 2 hours with gentle shaking of the sample on a rocking platform. Five hundred microlitres of liquid phenol (saturated with 10 mM Tris HCl, 1 mM EDTA, pH 8; phenol phase pH 6.7) was added and the sample was vortexed until opaque in appearance. The solution was microfuged at 13,000 x g for 5 minutes, and then the clear top layer was transferred to a fresh sterile tube. To this, 500 µl of phenol:chloroform (1:1) was added, and the sample was mixed thoroughly and microfuged as before. The upper aqueous layer was again removed into a fresh tube, and 500 µl of chloroform was added, followed by vortexing and centrifugation. The upper layer was added to a final clean tube. The DNA was precipitated by adding a 1/10th volume of sodium acetate (3 M, pH 5.2) and 1 ml of ice-cold 100% ethanol. The solution was mixed gently and placed at -20 °C for 30 minutes. Centrifugation at 13,000 x g for 10 minutes to pellet the DNA was followed by a wash in 70% ethanol. The pellet was dried at 37 °C before resuspension in sterile TE

buffer. RNA was removed from the preparation by incubation with 2 μ l RNase A (final concentration of 0.5 μ g/ μ l) at 37 °C for one hour.

2.14.2 Plasmid vectors

Several vectors were employed for different aspects of the project. The vector pTSO-HYG4 (Sommer, *et al.*, 1996) was utilised in the construction of a *T. b. brucei* genomic DNA library for expression in *T. b. brucei*. The plasmid vector pNS328 (supplied by Dr. G. Diallinas of University of Athens) was used to construct a *T. b. brucei* genomic DNA library for expression in *Aspergillus nidulans*. The pGEM-T Easy Vector system from Promega was used to clone PCR products before sub-cloning into other vectors. The plasmid vector pDR195 (Rentsch, *et al.*, 1995) was used to clone genes for expression in *Saccharomyces cerevisiae*. The plasmid vector pGEM-HE was used for production of RNA for expression in *Xenopus laevis* oocytes (Liman, *et al.*, 1992).

The pGEM-T Easy Vector was purchased “ready-to-use” and needed no further preparation before use in ligations. However, the other vectors required to be linearised by restriction enzyme digest and to be treated with calf intestinal alkaline phosphatase (CIAP) to prevent self-ligation.

The choice of restriction enzyme to use for linearisation was dependent on the composition of the multiple cloning site on each vector, and on the source of the insert DNA. The digests were carried out under the conditions described in section 2.14.3, below.

CIAP dephosphorylates the 5' ends of the linearised vector, thus preventing it re-ligating to itself but still allowing it to be ligated with compatible inserts. The CIAP was provided at 1 U/ μ l but had to be diluted in 1x reaction buffer to 0.01 U/ μ l for use. Nineteen microlitres of digested vector was incubated for 1 hour with 5 μ l of 10x reaction buffer, 5 μ l of diluted CIAP and made up to 50 μ l with sterile dH₂O. An extra 5 μ l of diluted CIAP was added half way through the incubation. The enzyme was inactivated by incubation at 65 °C for 10 minutes.

2.14.3 Restriction enzyme digestion of DNA

Restriction enzyme digests were used to prepare vector DNA for ligation, to excise insert DNA for subcloning, to prepare "random" fragments of DNA for library construction and to ensure correct size and orientation of insert DNA.

A typical 20 μ l digest mixture consisted of 1 μ g of DNA, 2 μ l of 10x reaction buffer (provided with enzyme) and 5 units of appropriate enzyme, made up to 20 μ l with dH₂O. The usual incubation conditions were 37 °C for 1 - 2 hours.

Partial restriction digestion of genomic DNA was necessary for the production of "random" fragments of a defined size for the genomic DNA library. The digest protocol was altered to maximise yield of appropriate fragments. A thirty minute digestion of 50 μ g genomic DNA with 5 units of *Sau3A* with a total reaction volume of 200 μ l gave a good yield of DNA molecules in the 2-6 kb range. Following the digestion, the *Sau3A* enzyme was inactivated with 1/100th volume of 0.5 M EDTA to facilitate separation of the DNA/protein complexes. The digest was concentrated by precipitation with 1/25th volume of 5.0 M NaCl and 2 volumes of ethanol. The use of sodium chloride rather than sodium acetate prevented the co-precipitation of SDS. Following an incubation at -20 °C, the DNA was pelleted by centrifugation for 20 minutes at 13,000 x g.

The standardisation of the partial digestion protocol is outlined in Chapter 6. Figure 6.4 shows agarose gel electrophoresis of the resultant genomic DNA fragments.

2.14.4 Agarose electrophoresis of DNA

DNA was separated by molecular size by electrophoresis through a 0.8% agarose gel containing 0.3 μ g/ml ethidium bromide with TBE as the running buffer. The voltage used to run the gel was normally 60 V. The use of lower voltages aided separation of nucleic acid molecules and these were used for isolation of fragments for the genomic DNA library. Gel visualisation was by UV transilluminator (UVP Products).

2.14.5 Purification of DNA from agarose gel

To purify DNA fragments of a defined size, the samples were run in a gel alongside an appropriate standard molecular size ladder. The relevant band was excised using a clean scalpel and transferred into a clean sterile microfuge tube. Exposure to UV was kept to the absolute minimum to prevent damage to the DNA. The agarose was removed using the QIAGEN Gel Extraction Kit following manufacturer's instructions.

2.14.6 Ligation

T4 DNA ligase was provided with the Promega pGEM-T Easy Vector System. The reaction mixture was as follows: 5 μ l of 2x reaction buffer, 1 μ l (50 ng) of pGEM-T Easy Vector, 3 μ l of poly-A tailed PCR product, and 1 μ l (3 units) of T4 DNA ligase.

For ligations not involving pGEM-T Easy Vector, the T4 DNA ligase was provided with 10x reaction buffer and the reaction mixture typically consisted of: 15 ng of vector DNA, 45 ng of insert DNA, 2 μ l of 10x reaction buffer, 1 μ l (3 units) of DNA ligase and dH₂O to final volume of 20 μ l. The vector : insert ratio of 1:3 was usually sufficient for successful ligation reactions.

The ligation mixture was incubated at 4 °C overnight and then the enzyme was heat-inactivated at 65 °C for 10 minutes.

2.14.7 Preparation of chemically-competent Escherichia coli

Initial stocks of JM109 *E. coli* were purchased from Promega. Further stocks were prepared in the laboratory using the rubidium chloride method. An LB agar plate was streaked with *E. coli* JM109 and incubated overnight at 37 °C. A single colony from the plate was inoculated into 2.5 ml of LB broth and this starter culture was incubated overnight at 37 °C with shaking. This was added to 250 ml of LB broth containing 20 mM MgSO₄, which was then incubated at 37 °C with shaking until the OD₆₀₀ reached 0.4-0.6 (around 3 hours). The cells were harvested by centrifugation at 1,250 x g at 4 °C for 5

minutes and resuspended in 80 ml of ice-cold TFB1 solution (see Appendix A). The suspension was incubated on ice for 5 minutes. The cells were pelleted as before and resuspended in 8 ml of ice-cold TFB2 (see Appendix A). The cells were left on ice for 15 - 60 minutes and then gently aliquoted into pre-chilled 1.5 ml microfuge tubes. The tubes were flash-frozen in liquid nitrogen and stored at $-70\text{ }^{\circ}\text{C}$ until required.

The efficiency of the competent cells was tested prior to use and was typically higher than 1×10^7 colony forming units per μg of transformed plasmid DNA.

2.14.8 Preparation of electrocompetent Escherichia coli

Stocks of *E. coli* TOP10 electrocompetent cells were produced “in-house” by the following method. A single colony from a fresh LB plate was inoculated into 5 ml of SLB medium, and this culture was then incubated overnight with shaking at $37\text{ }^{\circ}\text{C}$. The 5 ml “starter” was used to inoculate a 500 ml flask of SLB, which was shaken at $37\text{ }^{\circ}\text{C}$ for approximately 3 hours until the OD was 1.3. The culture was placed on ice for 30 minutes, before centrifugation at $1,500 \times g$ for 15 minutes at $4\text{ }^{\circ}\text{C}$. The pellet was washed twice with 200 ml of ice-cold sterile ultra-pure water and then resuspended in 30 ml of ice-cold 10% glycerol in ultra-pure water. The suspension was subject to a final centrifugation at $1,500 \times g$ for 15 minutes at $4\text{ }^{\circ}\text{C}$. The pellet was resuspended in 2.5 ml of ice-cold 10% glycerol in ultrapure dH_2O and aliquoted into Eppendorf tubes which had been chilled at $-70\text{ }^{\circ}\text{C}$. The aliquots were then stored at $-70\text{ }^{\circ}\text{C}$ until required.

The efficiency of the electrocompetent cells was tested prior to use. As shown in Chapter 6, the efficiency was shown to be sufficiently high at 8.5×10^9 colony forming units per μg of transformed plasmid DNA.

2.14.9 Transformation of E. coli

2.14.9.1 Heat-shock method

The JM109 cells were thawed in an ice-bath, and 50 μl were then added to 2 μl of the ligation mixture and gently mixed. The suspension was placed on ice for 20 minutes before a heat-shock at 42 °C for 45 seconds. The suspension was returned to the ice-bath for 2 minutes, after which 950 μl of room temperature SOC medium was added to the tube. A 1.5 hour incubation at 37 °C with shaking was followed by the spreading of 250 μl of the suspension onto LB plates supplemented with 100 $\mu\text{g/ml}$ of ampicillin. If pGEM-T Easy Vector was being used the plates also contained 0.5 mM isopropylthio- β -D-galactoside (IPTG) and 80 $\mu\text{g/ml}$ 5-bromo-4-chloro-3-indolyl- β -D-galactoside (X-Gal) to facilitate blue-white screening. The plates were incubated at 37 °C overnight.

2.14.9.2 Electroporation

While the heat-shock method using chemically-competent cells was sufficient for obtaining a relatively small number of clones containing a known product, electroporation was used during construction of the libraries to maximise transformation yields.

The TOP10 competent cells were thawed in an ice-bath, then 40 μl were dispensed into chilled microtubes containing 2-3 μl of the ligation mixture. The suspension was carefully transferred to pre-chilled electroporation cuvettes with a gap size of 0.1 cm. The suspension was then electroporated using the Bio-Rad Gene Pulser II with parameters of 25 μF capacitance, 200 Ω resistance, and a voltage of 1.7 kV. After addition of 1 ml of SOC, the cells were transferred to a clean Eppendorf tube and incubated at 37 °C with shaking for an hour. Two hundred and fifty microlitres of the cell suspension was spread onto LB plates supplemented with 100 $\mu\text{g/ml}$ of ampicillin. The plates were incubated at 37 °C overnight.

To harvest colonies for the production of the library, the bacterial colonies were simply washed from the plates using LB broth medium.

2.14.10 Mini-, mid-, and maxi-preps of plasmid DNA

QIAGEN kits were used for the convenient small, mid and large scale purification of plasmid DNA from *E. coli* cultures. Manufacturer's instructions were followed.

2.14.11 Polymerase chain reactions

The proof-reading enzyme *Pfu* DNA polymerase was used for all polymerase chain reactions. PCR mixtures consisted of the following components: 2 μ l *Pfu* 10x buffer; 200 μ M of each of dATP, dCTP, dTTP, dGTP; 2.5 μ M of each primer; 10-20 ng of DNA template; 0.6 units of *Pfu* DNA polymerase; and sterile dH₂O to final 20 μ l volume.

The PTC-200 Peltier Thermal Cycler from MJ Research was used to perform the PCRs. Choice of annealing temperature was dependent on the particular primers. The PCR cycle conditions were as follows: denaturation at 94 °C for 2 minutes; and then a cycle of denaturation at 94 °C for 30 seconds, annealing temperature for 30 seconds, and extension at 72 °C for 2 minutes. This three-step cycle was repeated 30 times, with a final extension step at 72 °C for 10 minutes.

2.14.12 A-tailing of PCR products

Since the pGEM-T Easy Vector is designed with 3'-thymidine overhangs, it was necessary for the PCR product insert to have 5'-deoxyadenosine overhangs for successful ligation. However, PCR fragments produced with *Pfu* polymerase are blunt-ended. In order to facilitate addition of a single deoxyadenosine to each end of the product, it was incubated with *Taq* polymerase which adds deoxyadenosine residues to the end of the DNA in a template independent manner. Typically, 7 μ l of gel-purified *Pfu*-amplified product was mixed with 1 μ l of 10x *Taq* reaction buffer, 0.2 mM dATP, 5 units of *Taq* polymerase and sterile dH₂O to a final volume of 10 μ l. The mixture was then incubated at 72 °C for 30 minutes.

2.14.13 Transformation of chemically-competent *Saccharomyces cerevisiae*

Transformation of *Saccharomyces cerevisiae* was by the method of Gietz & Woods (2002). A 5 ml *Saccharomyces cerevisiae* MG887.1 starter culture was grown in YPAD at 30 °C with shaking overnight and then used to inoculate 50 ml of pre-warmed YPAD. The culture was incubated at 30 °C with shaking for 4-5 hours until the OD at 600 nm was between 1 and 1.5 (equivalent to 2×10^7 cells/ml). The cells were harvested by centrifugation at 1,800 x g for 5 minutes, washed in 25 ml sterile dH₂O and centrifuged as before. The pellet was resuspended in 1 ml of 100 mM lithium acetate and the suspension was then transferred to a 1.5 ml microfuge tube. The cells were pelleted by centrifugation at 13,000 x g for 15 seconds and the lithium acetate was removed. The cells were then resuspended in 100 mM lithium acetate to give a final volume of 500 µl with a cell density of approximately 2×10^9 cells/ml. The suspension was vortexed and 50 µl were pipetted into fresh microfuge tubes for each transformation. The cells were pelleted and the lithium acetate removed with a micropipette. The following components were then added to the cells in the following order: 240 µl PEG (50% w/v in dH₂O), 36 µl 1.0 M lithium acetate, 50 µl SS-DNA (2.0 mg/ml, boiled for 5 minutes prior to use), 0.1-10 µg of plasmid DNA and sterile dH₂O to final volume of 360 µl. Each tube was vortexed vigorously to ensure the complete mixing of the cell pellet. The suspension was incubated at 30 °C for 30 minutes, and then heat-shocked at 42 °C for 30 minutes. The cells were pelleted at 8,000 x g in the microfuge for 15 seconds and the transformation mix was removed. The cells were gently resuspended in 1.0 ml of sterile dH₂O and then 200 µl was plated on SC-URA plates. Sterile glass beads were used to distribute the fluid evenly on the plates. The plates were incubated at 30 °C for 2-4 days to recover transformants.

2.14.14 Growth of *Saccharomyces cerevisiae* in selective media

To select for transformants that had gained the ability to transport purines, several colonies were spread on yeast selective medium plus adenine (1 mg/ml or 7.4 mM) or yeast selective medium plus hypoxanthine (4 mM). Growth of transporter gene transformants was compared with the growth of colonies transformed with pDR195 only.

2.14.15 Preparation and purification of total RNA from *T. b. brucei*

Bloodstream form trypanosomes or procyclic form trypanosomes were grown in culture as described in section 2.5. The cells were harvested by centrifugation at 1,050 x g for 3 minutes at 4 °C. One millilitre of Tri Reagent was added to 10⁷ cells and pipetted up and down to lyse the cells. The suspension was transferred to a sterile Eppendorf tube and incubated at room temperature for 5 minutes, after which 200 µl of chloroform was added. The tube was shaken vigorously for 15 seconds and then incubated at room temperature for two minutes. Cell debris was pelleted by centrifugation at 13,000 x g for 15 minutes at 4 °C, and the supernatant was removed to a fresh sterile tube. An equal volume of isopropanol was mixed with the suspension, and the mixture was incubated at room temperature for 10 minutes. The RNA was pelleted by centrifugation at 13,000 x g for 15 minutes at 4 °C. The pellet was washed in 75% ethanol and the pellet was resuspended by vortexing. A final centrifugation step of 7,500 x g for 5 minutes at 4 °C pelleted the RNA. The pellet was allowed to air-dry, and then resuspended in approximately 30 µl of DEPC-treated water. The RNA suspension was incubated at 55 °C for 10 minutes. RNA concentration was estimated using the GeneQuant II RNA/DNA Calculator (Pharmacia Biotech). The integrity of the RNA was assessed by running a small aliquot on an agarose gel to check for the presence of the three rRNAs (28S, 18S, and 5S) which make up 80% of the total RNA content of the cell. The RNA was stored at -70 °C until required.

2.14.16 Radiolabelling of probes

The labelling of the probe was accomplished using the Stratagene Prime-It II Random Primer Labelling Kit, following manufacturer's instructions.

2.14.17 Northern hybridisation

The extraction of RNA from trypanosomes is outlined in section 2.14.15. A denaturing RNA gel was prepared by mixing 30 ml 2% molten agarose with 30 ml 12% formaldehyde in 2x Northern Gel Buffer (see Appendix A), pouring the resulting mixture into a gel cast and allowing to set. When the gel had cooled, the gel tank was filled with 1x Northern Gel

Buffer/3% formaldehyde and the comb was carefully removed. A magnetic stirring bar was placed in the tank and the tank was set on top of a stirring motor.

The RNA samples were prepared in an RNase-free microfuge tube as follows: 10-20 μg RNA, 1 μl 20x Northern Gel Buffer, 3.5 μl formaldehyde (37%), 10 μl formamide and DEPC-treated dH_2O to a final volume of 20 μl . A tube of RNA markers (Sigma) was also prepared. The samples were heated to 55 $^\circ\text{C}$ for 15 minutes and then chilled on ice. 2 μl of RNA loading buffer (Appendix A) was added to each tube and samples were loaded onto the gel. The electrophoresis was started and once the samples had migrated into the gel a little, the stirring motor was turned on to circulate the buffer. The gel was run at 15 V overnight.

To transfer the RNA from the gel to a nylon support (Hybond N, Amersham), a standard capillary elution blotting apparatus was set up (Sambrook, *et al.*, 1989). The flow of 20x SSC (see Appendix A) up through the gel carries the RNA to be deposited on the nylon membrane. The transfer was allowed to proceed overnight.

The blotting apparatus was dismantled and the nylon membrane was cross-linked by 254 nm ultraviolet irradiation using the Spectrolinker XL-1000 UV Linker (Spectronics Corporation).

To assess RNA transfer, the blot was stained with Blot Stain Blue Reversible Northern Blot Staining Solution (Sigma) for 5 minutes and then washed in dH_2O .

The filter was pre-hybridised for 2 hours at 42 $^\circ\text{C}$ in hybridisation buffer consisting of 50% formamide, 5x SSC, 10x Dendhart's solution, 0.1% SDS, 20 mM NaH_2PO_4 , 5 mM EDTA and 0.2 mg/ml of denatured herring sperm DNA.

The probe was heated to 95 $^\circ\text{C}$ for 5 minutes and then added directly to the hybridisation tube. Hybridisation was allowed to occur overnight at 42 $^\circ\text{C}$ under constant mixing in a Hybaid Shake and Stack hybridisation oven.

The membrane was removed from the hybridisation mixture and washed twice in room temperature wash buffer (0.1x SSC, 0.1% SDS) for 1 minute. This was followed by three washes of 30 minutes each at 55 °C.

The filter was wrapped in Saran wrap and exposed to X-ray film at -70 °C for an appropriate length of time.

2.15 Software and web resources

The Vector NTI Suite 7.0 (InforMax) was used to analyse DNA and protein sequences. Translations of nucleotide sequences were performed, and open reading frames and restriction enzyme sites were located using Vector NTI. AlignX was used to construct alignments of related nucleotide and amino acid sequences.

The following web resources were used:

<http://www.ncbi.nlm.nih.gov/>

<http://www.tigr.org/tdb/>

http://www.sanger.ac.uk/Projects/T_brucei/

<http://www.ebi.ac.uk/parasites/parasite-genome.html>

http://www.ch.embnet.org/software/TMPRED_form.html

<http://www.genedb.org/genedb/tryp/index.jsp>

<http://parsun1.path.cam.ac.uk/>

Chapter Three

**Substrate recognition models for the H2 purine transporter of *T.*
*b. brucei***

3.1 Introduction

The aim of this stage of the project was to gain a greater understanding of how purine nucleobase substrates react with the H2 nucleobase transporter during the binding step of membrane transport. It is necessary for any permeants to reversibly interact with the transporter molecule in the form of non-covalent intermolecular interactions. Since recognition of the substrate by the transporter is central to its subsequent translocation, any potential drugs that would enter through the transporter would presumably have to share essential structural elements that would be able to participate in these intermolecular associations. The hypothesis was that if these constituents, essential for the first step in uptake, could be identified it would be a simpler process to design or select chemotherapeutic agents to be taken up by the H2 transporter.

The administration of purine compounds forms part of the therapeutic intervention in many different disease conditions. Indeed, nucleoside and nucleobase anti-metabolites have a distinguished history as anti-viral and anti-neoplastic agents (Elion, 1989). Among the more well-known examples are the antiviral drug acyclovir, the immunosuppressant azathioprine, the cancer chemotherapeutic 6-mercaptopurine and the anti-parasitic/gout treatment allopurinol. It is interesting to consider that the large bank of existing nucleobase compounds may constitute a possible source of future treatments for African trypanosomiasis. Nucleobase and nucleoside analogues were assayed for *in vitro* trypanocidal activity to establish if interaction of the drugs with the H2 transporter could be correlated to accumulation of toxic concentrations of the analogues.

3.1.1 Why study the H2 transporter?

The concept of exploiting transport systems to deliver chemotherapeutic agents is not a new one. The specific action of many drugs can be attributed to the selective accumulation in target cells and the up- or down-regulation of transporter genes can contribute to an increase or decrease in the target cell sensitivity to anti-metabolites (Lu, *et al.*, 2002). Some of the existing trypanocides are known to enter the trypanosome via the P2 nucleoside transporter (Carter & Fairlamb, 1993; Matovu, *et al.*, 2003), and this fact lends support to the strategy of using the transporters as gateways. Although new drugs could possibly be engineered to enter via this transporter, given that loss of the P2 activity has

been implicated in the development of drug resistance (Carter & Fairlamb, 1993; Matovu, *et al.*, 2003), this may not be the best approach. Other transporters in *T. b. brucei* have merit as potential routes of access for trypanocides (Hasne & Barrett, 2000a), including glucose transporters (Walmsley, *et al.*, 1998), amino acid transporters (Hasne & Barrett, 2000b) and purine transporters other than the P2 activity (De Koning & Jarvis, 1997b; De Koning & Jarvis, 1999). It is widely recognised that uptake of melaminophenyl arsenicals via the P2 transporter is a consequence of the P2 recognition motif present in the melamine ring (De Koning & Jarvis, 1999; Barrett & Fairlamb, 1999). It has been suggested that replacing the melamine ring with an alternative structure designed to direct the arsenic-containing toxophore through other trypanosomal transporters might provide at least a temporary respite from arsenical resistance due to reduced accumulation (De Koning, 2001).

Of the diverse range of transporters involved in purine nucleobase uptake in *T. b. brucei* (described in Chapter 1), the H2 transporter would seem to offer the best chance of providing a viable drug entry system. Obviously, the exploitation of any nucleobase transporters would require their expression in the clinically-relevant life cycle stage. Neither H1 nor H4 activity has been detected in bloodstream forms by biochemical means (De Koning & Jarvis, 1997a), although *TbNBT1* mRNA transcripts (*TbNBT1* is the gene responsible for H4 activity) are present in this life cycle stage (see Chapters 6 and 7; Burchmore, *et al.*, 2003). With the difficulty of studying each individual activity in isolation in its natural environment, the absence of biochemical evidence does not rule out the expression of these transport components in the bloodstream forms. In any case, H2 has a much higher affinity for a wider range of permeants than does H3 (De Koning & Jarvis, 1997b), H1 or H4 (De Koning & Jarvis, 1997a; Burchmore, *et al.*, 2003) and so is preferable as a potential device for drug entry.

3.1.2 Mechanisms of molecular recognition

Various intermolecular forces can contribute to the recognition and binding of substrate to an enzyme or transporter. These forces include hydrogen bonds, electrostatic forces, weak van der Waal's forces, hydrophobic interactions or π bonding (Freitas Jr., 1999). The equilibrium constant for the association of an enzyme with its substrate is typically in the

range of 10^{-2} to 10^{-8} M, with this corresponding to Gibbs free energies of interaction of between 12 and 48 kJ/mol (Stryer, 1995).

Electrostatic bonds form between charged particles, and so may form in protein secondary and tertiary structures between positively-charged amino acids (*e.g.* lysine, and arginine) and negatively-charged amino acids (*e.g.* glutamate and aspartate). These interactions are unlikely to play a major role in recognition of nucleobase or nucleoside permeants, as these molecules are uncharged. However, partial charges may well contribute to interactions with charged groups in the transporter binding pocket.

Van der Waals' forces are weak, transient dipoles which contribute to the attraction between molecules, but while these forces are numerous they are limited in strength and are only important at close distances. Consequently, they may play a role in stabilising transporter-permeant complexes but are not responsible for their formation.

The contribution of hydrophobic forces to binding can be considerable but they are unlikely to be significantly involved given that nucleobase and nucleoside molecules do not possess significant hydrophobic domains. Furthermore these interactions tend not to be very specific and so probably don't play a large role in the recognition of specific molecules (Freitas Jr., 1999).

Pi-pi stacking interactions occur between the delocalised electrons of aromatic ring systems and can contribute as much as an H-bond in terms of binding energy. In the case of purine binding to the H2 transporter, the interaction would occur between the purine ring and aromatic amino acid residues such as phenylalanine, tryptophan or tyrosine. The strength of the π - π stacking interaction depends on the orientation of the rings relative to one another (Hunter, *et al.*, 1991).

The remaining intermolecular attraction is also likely to be the most vital – the hydrogen bond. This bond occurs between a highly electronegative acceptor atom (usually an oxygen or nitrogen atom) and a donor hydrogen atom which is covalently attached to another electronegative atom. The hydrogen bond is characterised by the greater proximity of the acceptor and donor atoms than that which would be anticipated from the van der Waals' radii for the atoms. Figure 3.1 shows the typical geometry of hydrogen bonds and shows

that the hydrogen bond is to some extent flexible in terms of the interatomic distances and angles encountered. There is some disagreement as to the restrictions on these factors. The most generous estimates given for inter-atomic distance in a hydrogen bond given by Kabsch & Sander stipulate that the acceptor-donor distance is no more than 5.2 Å when the alignment is perfect (Kabsch & Sander, 1983). Similarly, Baker & Hubbard specify that the angle between the acceptor and the donor atoms (C=O...H in Figure 3.1) must lie between 90 and 180° (Baker & Hubbard, 1984). Consequently, hydrogen bonds have quite a range of potential energies (between 2 and 20 kJ/mol) (Kubinyi, 2001).

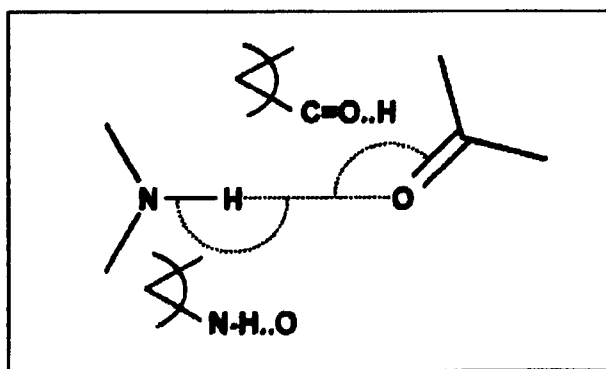


Figure 3.1. The geometry of a hydrogen bond. The typical distance between the electronegative donor group member (N in the figure) and the acceptor ranges from 2.8 to 3.2 Å. The angle N–H...O is usually larger than 150°. Typical angles for C=O...H are between 100 and 180°. (Diagram reproduced from Kubinyi, 2001.)

Obviously, there has to be a degree of complementarity between the binding site of the transporter molecule and at least part of its permeant in terms of shape, however, the ability of the molecules to participate in hydrogen binding with each other would appear to be equally relevant. Certainly, it has been shown with the different modes of binding of dihydrofolate (DHF) and methotrexate (MTX) with the enzyme dihydrofolate reductase (DHFR), that two molecules with structures that at first glance seem very similar can be orientated differently for optimal participation of hydrogen bonds (Kubinyi, 2001) (Figure 3.2).

This dependence on the appropriate formation of hydrogen bonds for efficient transport/transformation may also help to explain why molecules as diverse as adenine, pentamidine and melarsoprol show such high affinities for the P2 transporter (De Koning

& Jarvis, 1999). The P2 substrate recognition unit, $H_2N-CH=N-R$, present in these very different molecules, represent residues with the potential to participate in hydrogen bonding. In addition, these molecules all contain aromatic rings capable of participating in $\pi-\pi$ interactions.

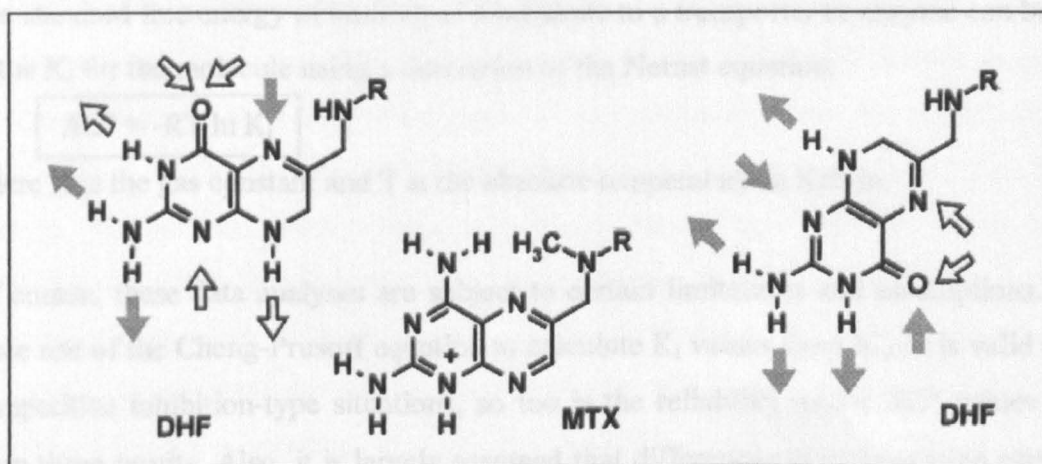


Figure 3.2. Recognition of DHF and MTX by DHFR. This shows how superficially very similar molecules can differ in their recognition by biological molecules. The two alternative orientations for the DHF molecule are shown either side of the binding orientation for MTX. Hydrogen bond donors are indicated by arrows directed away from individual atoms and acceptors are indicated by arrows directed towards atoms. The grey arrows indicate that the acceptor/donor is able to participate in the same interactions as in the MTX molecule, while the white arrows mean that the interactions are no longer possible. In order to maintain the optimal number of H-bond connections the DHF molecule is actually bound by DHFR in a different orientation from that of MTX. (Diagram reproduced from Kubinyi, 2001.)

3.1.3 Recognition models & use of analogues to characterise transporters or enzymes

Analogues of enzyme substrates have been used for a long time in attempts to dissect structure-function relationships. Usually, it is simply the ability of a given analogue to inhibit normal function of the enzyme or transporter that is noted and related to the structural differences (Naguib, *et al.*, 1995). Use of the Cheng-Prusoff equation to calculate K_i values for competitive inhibitors (Cheng & Prusoff, 1973), which can then be compared, is perfectly acceptable but it is useful to be able take the analysis further and actually quantify these differences, and by using changes in ΔG° this can be accomplished.

Gibbs free energy, ΔG , is derived from the combination of the first and second laws of thermodynamics and is essentially the change in energy within a system undergoing a transformation. The standard free energy, ΔG° , is the energy change observed under standard conditions.

The standard free energy of binding of a substrate to a transporter or enzyme can be related to the K_i for the molecule using a derivation of the Nernst equation:

$$\Delta G^\circ = -RT \ln K_i$$

where R is the gas constant and T is the absolute temperature in Kelvin.

Of course, these data analyses are subject to certain limitations and assumptions. Firstly, since use of the Cheng-Prusoff equation to calculate K_i values from IC_{50} 's is valid only for competitive inhibition-type situations, so too is the reliability of the ΔG° values derived from these results. Also, it is largely assumed that differences in translocation rates of the various ligands bound to the transporter molecule will not significantly affect IC_{50} values.

The value of ΔG° can also be affected by necessary conformational changes in the protein molecule during the process of ligand-binding. When portions of the ligand molecule are changed or removed altogether, the normal conformational changes can also be distorted due to the change in entropy, and hence the ΔG° can vary (Jencks, W.P., 1981).

It is also very important to remember that just because a molecule can disrupt the uptake of the natural substrate it does not necessarily follow that said molecule is actually taken up by the transporter.

Yet, when aware of the limitations, quantitative recognition models can identify which positions on the substrate molecules are important for recognition and can give an insight into the nature of the interactions between substrate and enzyme/transporter. This sort of functional characterisation can be particularly beneficial when the structure of the enzyme/transporter has not been elucidated. For integral membrane proteins such as transporters, with up to 14 transmembrane domains, it is still exceedingly difficult to obtain crystals suitable for X-ray diffraction.

Studies into molecular recognition of ligands by protein molecules as diverse as antibodies, streptavidin and HIV protease have taken advantage of the above derivation of the Nernst equation to quantify the strength of protein-ligand interactions (Freire, 1999; Lazaridis, *et al.*, 2002; Akaho, *et al.*, 2001).

This approach has been successfully employed in a study of the P1 and P2 nucleoside transporters in *T. b. brucei* (De Koning & Jarvis, 1999). The H₂N-CH=N-R motif for the recognition of substrates by the P2 transporter, as mentioned above, was identified by these means and also independently by other experimental means by the group of Alan Fairlamb (Barrett & Fairlamb, 1999). Similar methods have been used to derive substrate recognition models in other organisms and systems. Since this work was carried out associated researchers have developed substrate-activity models for the recognition of nucleobase compounds by the *Leishmania major* NBT1 transporter (Al-Salabi, *et al.*, 2003) and for the recognition of nucleobase/nucleosides by the *Toxoplasma gondii* AT2 transporter (De Koning, *et al.*, 2003).

The models can effectively pinpoint areas of the substrate molecule that can be altered, or where toxic components can be coupled, so as not to disrupt initial recognition by the enzyme/transporters. This is of great importance if the analogue has a potential use in chemotherapeutic applications. In *T. b. brucei*, much research has been carried out on the grafting of the P2 recognition motif onto toxic molecules as a way to “piggy-back ligand-bound drugs” into the parasite (Borst & Fairlamb, 1998). Amongst the molecules that have been investigated as potential passengers on such a system have been polyamine analogues and nitric oxide-releasing agents (Tye, *et al.*, 1998; Klenke, *et al.*, 2001; Soulère, *et al.*, 1999).

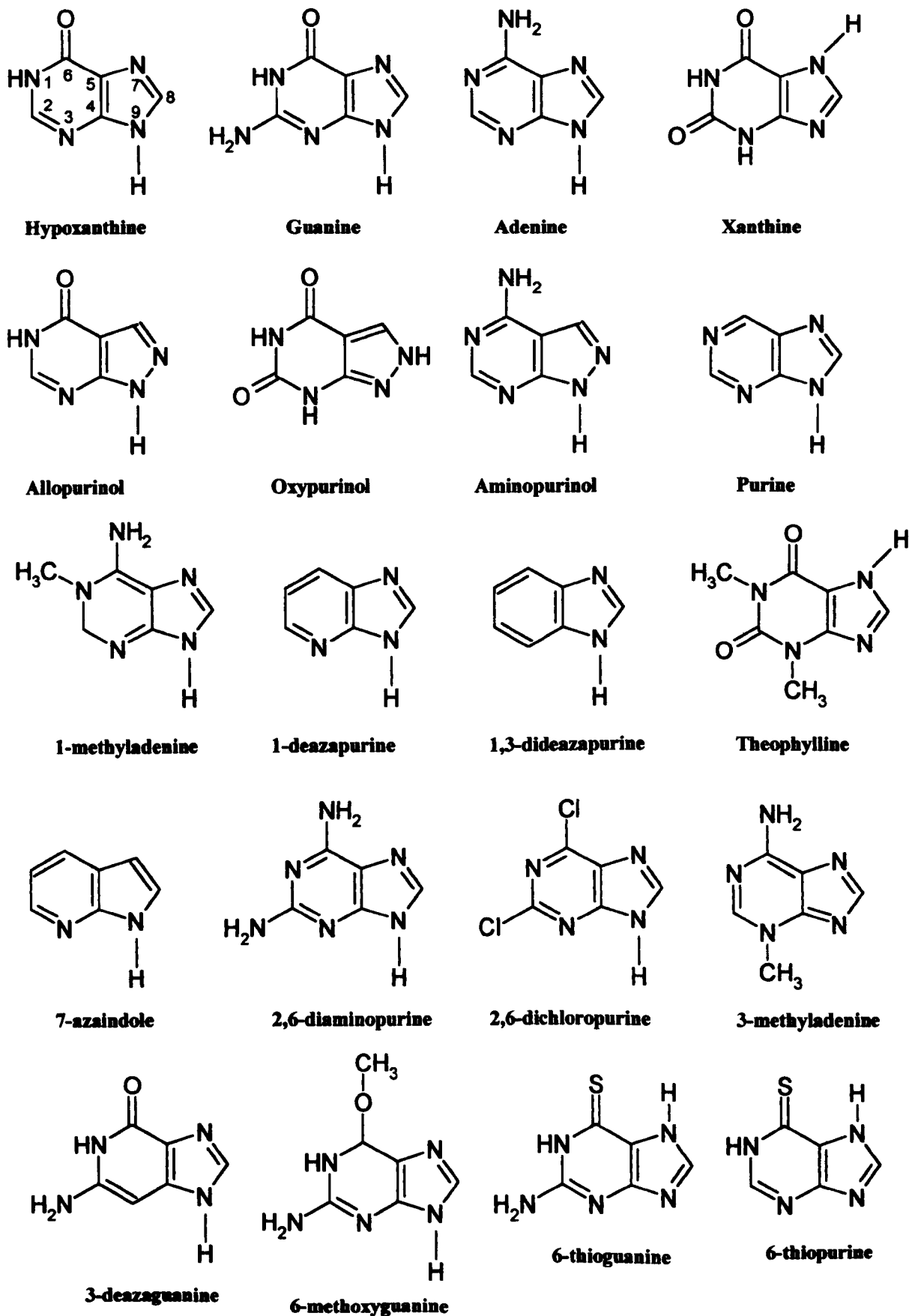


Figure 3.3. Analogues used to characterise substrate recognition by the H2 transporter.
(a) Purines.

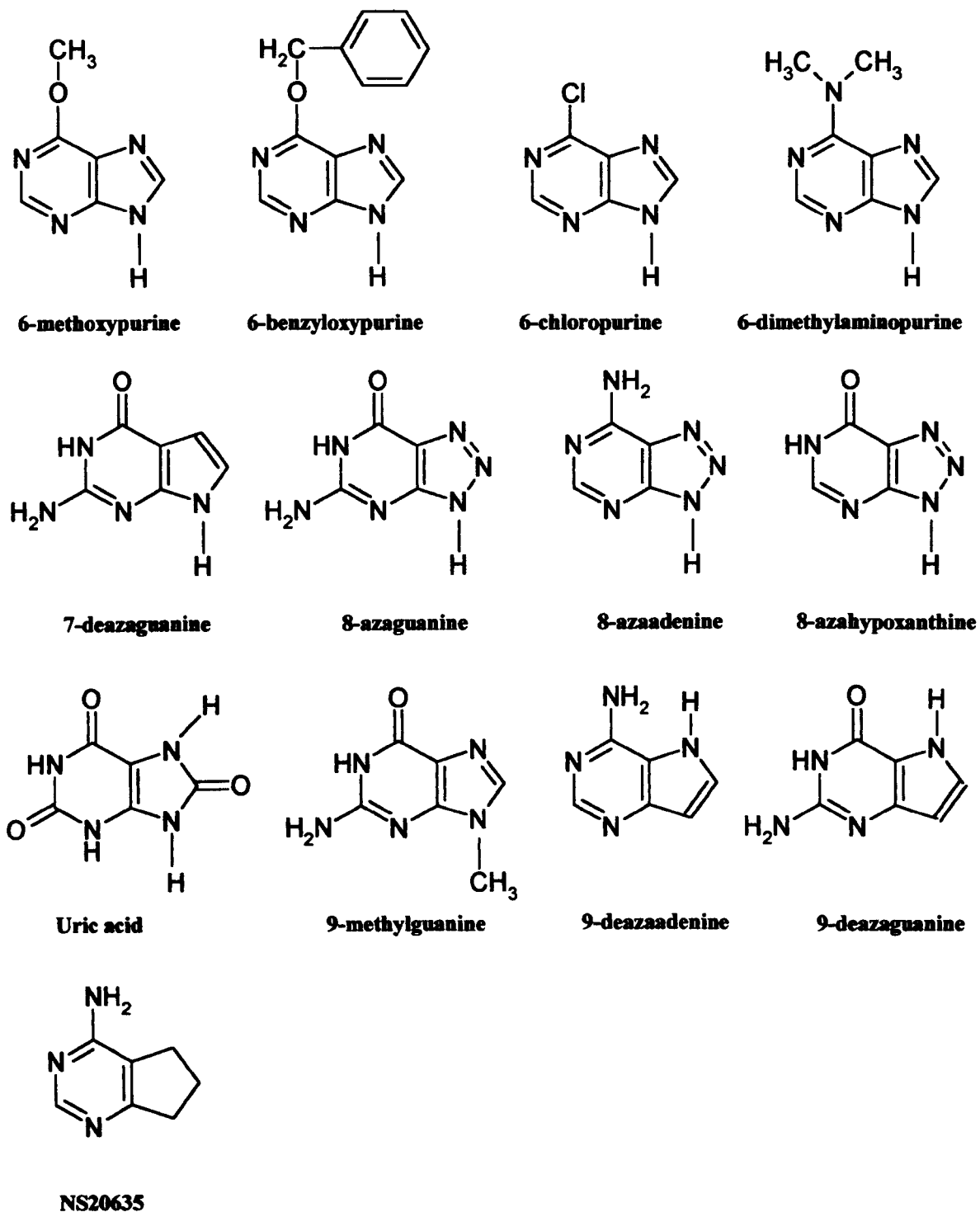


Figure 3.3. Analogues used to characterise substrate recognition by the H2 transporter.
(a) Purines (ctd).

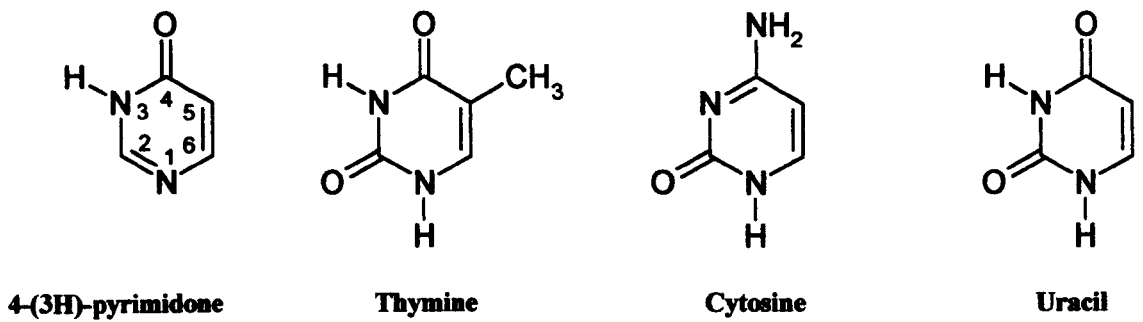


Figure 3.3. Analogues used to characterise substrate recognition by the H2 transporter.
(b) Pyrimidines.

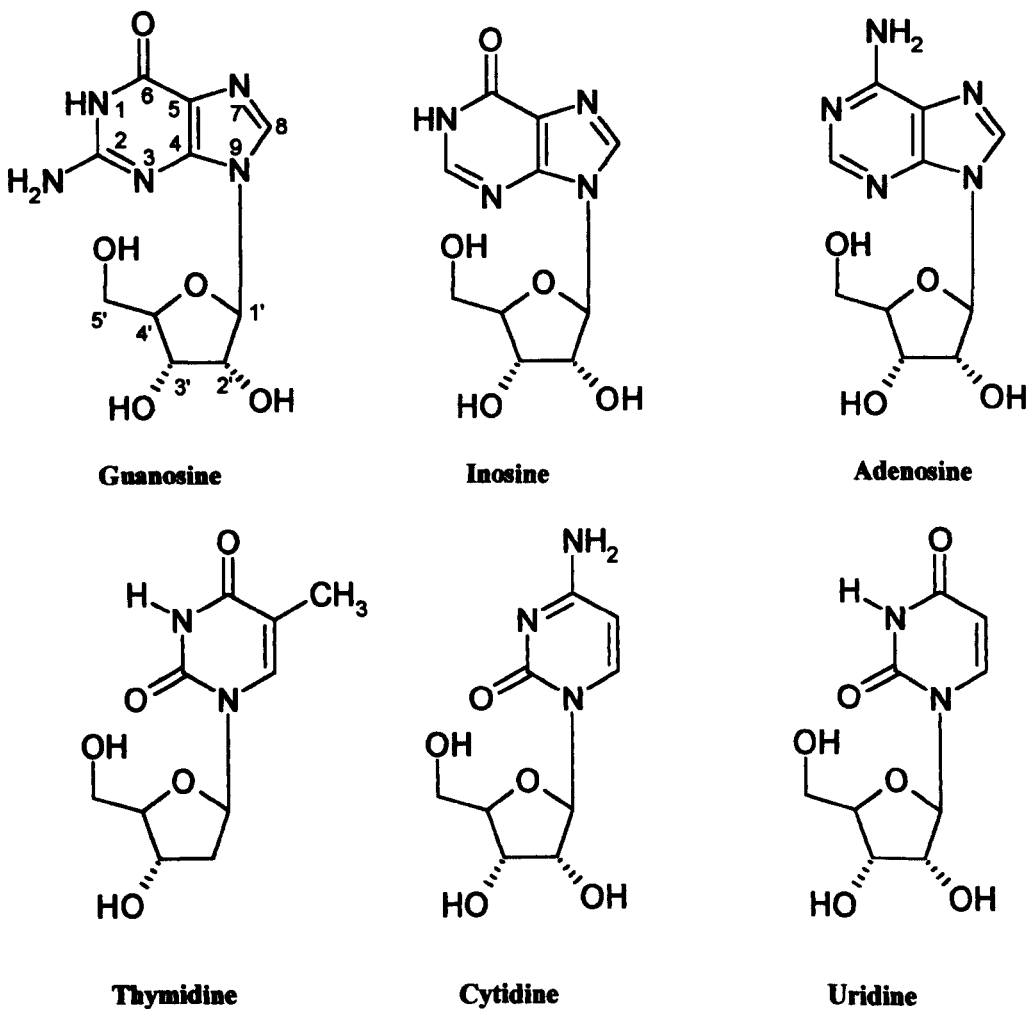


Figure 3.3. Analogues used to characterise substrate recognition by the H2 transporter.
(c) Nucleosides.

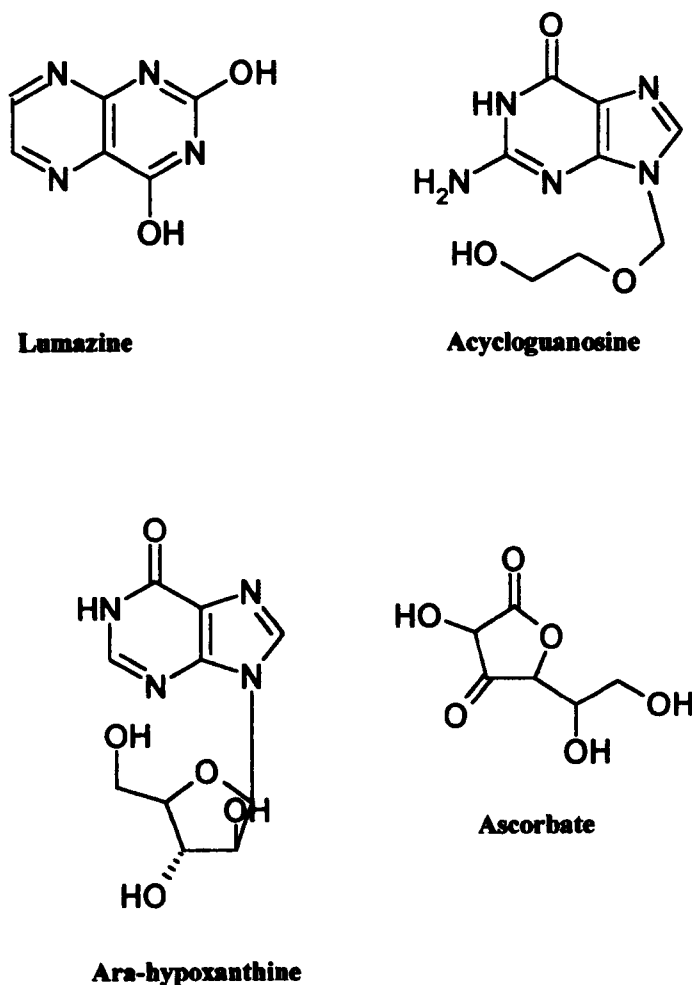


Figure 3.3. Analogues used to characterise substrate recognition by the H2 transporter. (d) Others.

Many of the compounds used to characterise recognition of permeants by the H2 transporter normally occur as a mixture of two or more different tautomeric forms. In most cases, the structures shown in Figure 3.3 have been experimentally shown to be the major components present under physiological conditions.

3.2 Results

3.2.1 Structure-activity relationships

Natural purines, a variety of purine analogues and other related compounds (Figure 3.3) were assayed for their ability to inhibit the *T. b. brucei* 427 H2 hypoxanthine transport activity. At a [³H] hypoxanthine concentration of 0.1 μM, H2 is responsible for over 95% of the hypoxanthine flux (De Koning & Jarvis, 1997b). The K_i values were determined from dose-response curves subject to the assumptions outlined in Chapter 2. Representative examples of the dose-response curves are shown in Figure 3.4. By calculating the binding energies, as Gibbs free energy (ΔG°), involved in the interaction between the transporters and the different molecules, structure-activity relationships were devised. The K_i and the ΔG° values for the different analogues are listed in Table 3.1.

The most obvious observation about substrate recognition by the H2 transporter is that despite being selective for neither oxopurines (hypoxanthine, guanine) or aminopurines (adenine) it does have some preference for 6-oxopurines (see Figure 3.4, panels (a) and (b)). The total ΔG° for the interaction of hypoxanthine with the transporter is greater by 8.1 kJ/mol than that for adenine. This difference is substantial enough to account for the loss of a hydrogen bond. Taken on its own, this could lead to the notion that the keto group at position 6 in oxopurines is involved in a hydrogen bond contributing to substrate recognition. However, the ΔG° values for guanine and 6-thioguanine are virtually identical even though the thio group makes a far less effective acceptor than the keto group (Papageorgiou, *et al.*, unpublished). Therefore, this indicates that the keto group does not significantly contribute to the binding of the substrate by the transporter binding site. Furthermore, the difference in ΔG° between purine and adenine (the only difference being the amino group at position 6), of 4.4 kJ/mol would suggest that this amine is involved in binding interactions, and that an H-bond donor, rather than an H-bond acceptor (such as a keto group) is favoured at position 6 (Figure 3.4, panel (a)). In further support of the idea that 6(NH₂) participates in the binding of adenine, a similar difference in ΔG° value is seen when adenine is compared with 6-chloropurine (4.2 kJ/mol). It is also of note that bulkier substitutions at position 6 of the adenine molecule are detrimental to binding by the

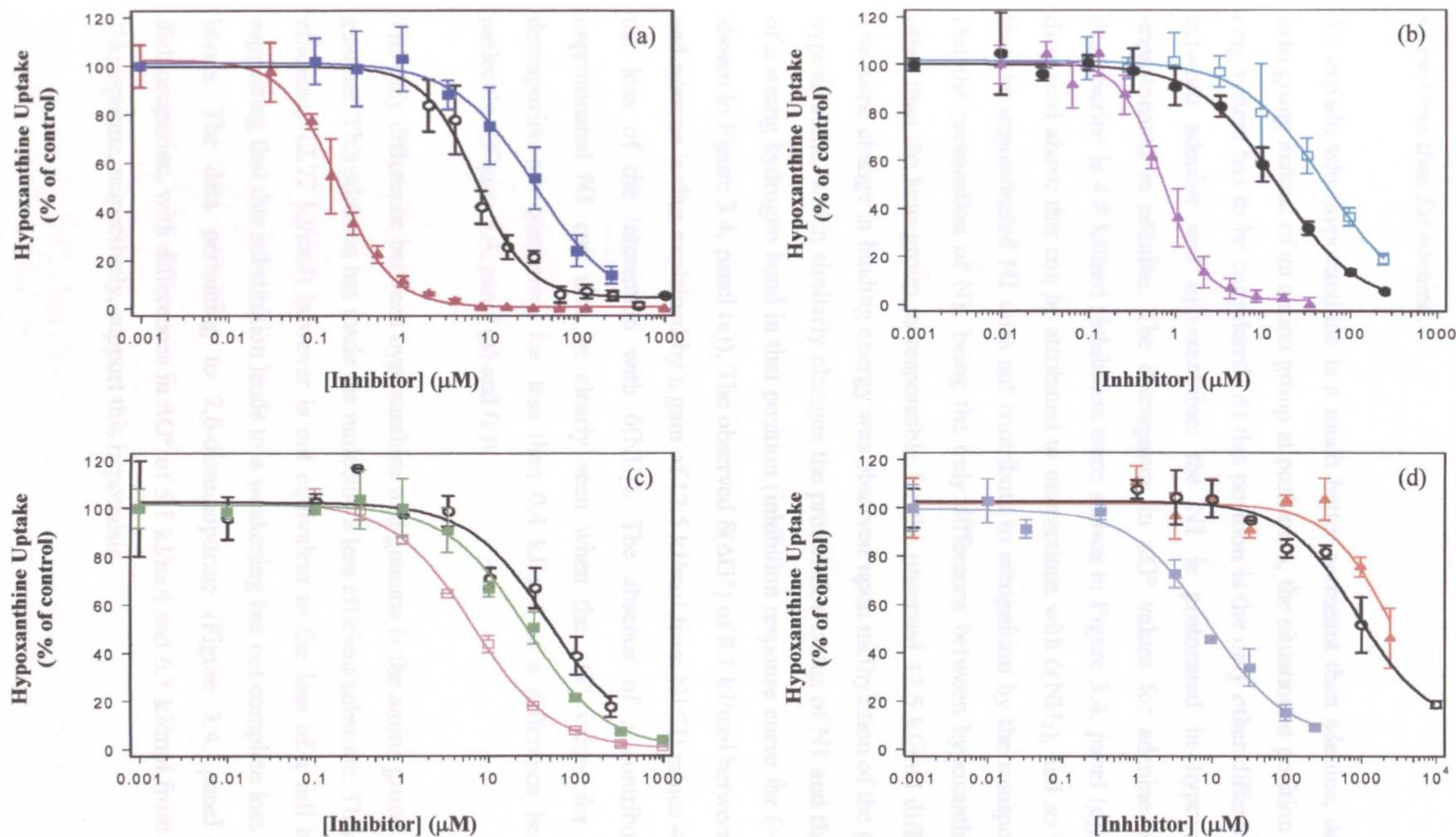


Figure 3.4. Inhibition of H2-mediated [³H] hypoxanthine transport in *T. b. brucei* bloodstream forms by purine analogues. Rates of uptake are expressed as a percentage of control, *i.e.* uptake in the absence of inhibitor. (a) hypoxanthine (▲), adenine (○), and purine (■). (b) 7-deazaguanine (□), 3-deazaguanine (●), and guanine (▲). (c) 6-methoxypurine (□), 2,6-diaminopurine (○), and 1-deazapurine (■). (d) NS20635 (▲), 4-(3H)-pyrimidone (○), and 9-deazaguanine (■). Label concentration in these experiments was 0.1 μM.

transporter: ΔG° for 6-dimethylaminopurine and 6-benzyloxypurine are approximately 10 kJ/mol less than for adenine.

To explain why hypoxanthine is a much better permeant than adenine, despite having a keto group instead of an amino group at position 6, the situation at position 1 of the purine ring system has to be considered. At this position is the only other difference in structure between adenine and hypoxanthine: the N1 is protonated in hypoxanthine but is unprotonated in adenine. The discrepancy in ΔG° values for adenine compared to 1-deazapurine is 4.8 kJ/mol (inhibition trace shown in Figure 3.4, panel (c)) but as already discussed above this can be attributed to interactions with 6(NH₂), and so it can be stated that the unprotonated N1 does not contribute to recognition by the transporter. It follows that the protonation of N1, being the only difference between hypoxanthine and purine other than the keto group, is responsible for the observed 12.5 kJ/mol difference in ΔG° . The same change in binding energy was observed upon methylation of the 6-keto group of hypoxanthine, which similarly changes the protonation status of N1 and the apparent loss of a strong hydrogen bond in that position (inhibition response curve for 6-methoxypurine shown in Figure 3.4, panel (c)). The observed $\delta(\Delta G^\circ)$ of 8.1 kJ/mol between hypoxanthine and adenine is thus explained by a gain of 12.5 kJ/mol from N1(H) minus 4.3 kJ/mol from the loss of the interaction with 6(NH₂). The absence of a contribution from the unprotonated N1 can also be clearly seen when the ΔG° values for purine and 1-deazapurine are compared, *i.e.* less than 0.4 kJ/mol of a difference between the two molecules (Figure 3.4, panel (a) and (c)).

The only difference between hypoxanthine and guanine is the amine group at position 2 in guanine. This addition has made the molecule a less efficient substrate. This drop in uptake efficiency (2.72 kJ/mol) however is not equivalent to the loss of a full hydrogen bond, suggesting that this substitution leads to a weakening but not complete loss of any existing bonds. The data pertaining to 2,6-diaminopurine (Figure 3.4, panel (c)) and 2,6-dichloropurine, with differences in ΔG° of 5.1 kJ/mol and 6.1 kJ/mol from adenine and 6-chloropurine, respectively, support this hypothesis.

Compound	K_i (μM)	ΔG° (kJ mol^{-1})
hypoxanthine	0.12 ± 0.02	-39.5
guanine	0.36 ± 0.18	-36.8
adenine	3.2 ± 1.1	-31.4
xanthine	8.8 ± 3.9	-28.9
allopurinol	4.0 ± 2.2	-30.8
oxypurinol	16 ± 3.5	-27.4
aminopurinol	240 ± 50	-20.7
purine	18 ± 3.7	-27.0
1-methyladenine	84 ± 14	-23.3
1-deazapurine	22 ± 8.2	-26.6
1,3-deazapurine	NE, 1000	
theophylline (1,3-dimethylxanthine)	450 ± 98	-19.1
7-azaindole (1,7-dideazapurine)	NE, 1000	
2,6-diaminopurine	25 ± 5.7	-26.3
2,6-dichloropurine	200 ± 38	-21.1
3-methyladenine	NE, 250	
3-deazaguanine	10 ± 2.0	-28.5
6-methoxyguanine	3.4 ± 0.6	-31.2
6-thioguanine	0.43 ± 0.03	-36.3
6-thiopurine	1.3 ± 0.4	-33.5
6-methoxypurine	6.9 ± 1.9	-29.5
6-benzyloxypurine	150 ± 33	-21.8
6-chloropurine	17 ± 3.3	-27.2
6-dimethylaminopurine	190 ± 36	-21.2
7-deazaguanine	55 ± 12	-24.3
8-azaguanine	7.2 ± 0.9	-29.4
8-azaadenine	110 ± 14	-22.7
8-azahypoxanthine	27 ± 6	-26.0
uric acid (8-hydroxyxanthine)	NE, 250	
9-methylguanine	70 ± 16	-23.7
9-deazaadenine	70 ± 13	-23.7
9-deazaguanine	8.0 ± 1.3	-29.1
NS20635	4100 ± 1800	-13.6
4-(3H)-pyrimidone	900 ± 290	-17.4
thymine	82 ± 25	-23.3
cytosine	>500	
uracil	60 ± 14	-24.1
guanosine	11 ± 1.8	-28.3
inosine	70.2 ± 9.2	-23.7
adenosine	590 ± 180	-18.4
acycloguanosine	62 ± 5	-24.0
ara-hypoxanthine	300 ± 47	-20.1
thymidine	>1000	
cytidine	NE, 1000	
uridine	500	
lumazine	370 ± 28	-19.6
ascorbate	NE, 2500	

Table 3.1. K_i and ΔG° values for the inhibition of hypoxanthine uptake by the *T. b. brucei* H2 nucleobase transporter. Results are shown \pm standard error. All values are the average of three to five independent experiments. NE, no effect at stated concentration.

The loss in binding energy caused by these substitutions at position 2 could be explained to some extent by an associated reduction of the partial negative charge on N3, making this residue a less effective hydrogen bond acceptor. This mechanism was also noted in work relating to the P1 and P2 nucleoside transporters of *T. b. brucei* (De Koning & Jarvis, 1999) and transporters in *Leishmania major* and in *Toxoplasma gondii* (Al-Salabi, *et al.*, 2003, and De Koning, *et al.*, 2003, respectively). Evidence that N3 does act as an H-bond acceptor is provided by the 8.3 kJ/mol energy difference between guanine and 3-deazaguanine (Figure 3.4, panel (b)). Furthermore, methylation of N3 leads to a dramatic loss in affinity, as 250 μ M 3-methyladenine completely failed to inhibit H2-mediated [3 H] hypoxanthine uptake.

Alternatively, these substitutions at position 2 and 3 may physically prevent optimal positioning of the substrate in the binding pocket. It is interesting to note that N3 is unprotonated in all natural purines with the exception of xanthine and uric acid.

The pyrimidine ring thus contributes -20.8 kJ/mol to the total of -39.4 kJ/mol Gibbs free energy for the interactions between the hypoxanthine molecule and the transporter, indicating a similar contribution from the imidazole half of this purine. Consistent with this prediction, 4(3-H)-pyrimidone (Figure 3.4, panel (d)), consisting only of the pyrimidine half of hypoxanthine, displayed a $\delta(\Delta G^\circ)$ of -22.1 kJ/mol compared to hypoxanthine. Similarly, the $\delta(\Delta G^\circ)$ of NS20635 (Figure 3.4, panel (d)), which is equivalent to adenine but with a saturated 5-membered hydrocarbon ring instead of imidazole, compared with adenine was 17.8 kJ/mol.

The involvement of N7 in binding, most probably as a hydrogen bond acceptor, follows most directly from the $\delta(\Delta G^\circ)$ between 7-deazaguanine and guanine of 12.5 kJ/mol (Figure 3.4, panel (b)). In addition, the affinity for allopurinol is significantly reduced compared to hypoxanthine, though its $\delta(\Delta G^\circ)$ of 8.7 kJ/mol suggests that a minor interaction is still possible with the nitrogen residue that has shifted from position 7 to 8. Uric acid had no effect on [3 H] hypoxanthine uptake at 250 μ M, probably due to the protonation of N7 in the dominant tautomeric form of uric acid. An experimental K_i could not be determined for uric acid due to limitations of solubility. The comparatively low affinity of xanthine ($\delta(\Delta G^\circ)$ of 10.7 kJ/mol relative to hypoxanthine) can be explained in part by the

energetically unfavourable substitution at position 2 (see above) and protonation of N3, but mostly because its preferred tautomeric form is N(7)H/N9.

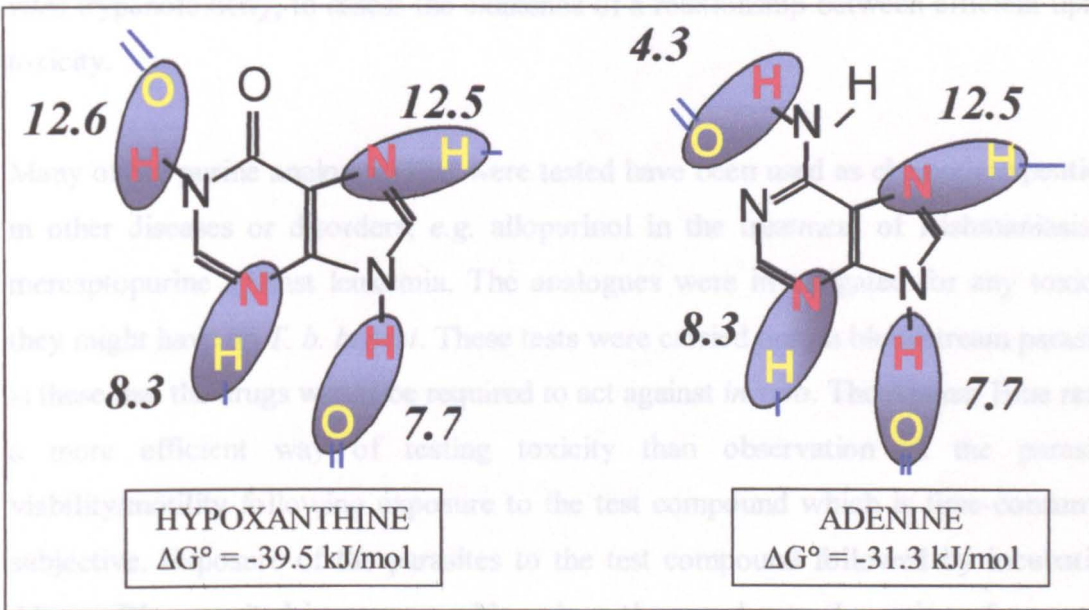


Figure 3.5. Model of the interactions between purines and the *T. b. brucei* H2 transporter. Estimations of the Gibbs free energy of these interactions are given in kJ/mol.

The preference of the H2 transporter for nucleobases over nucleosides suggests that N(9)H may be involved in interactions with the transporter binding pocket. It is possible, however, that rather than preventing a hydrogen bond with N(9)H the bulky ribose moiety interferes with the proper positioning of the purine ring. It is very probable that, for most nucleosides, both factors contribute to the low affinity for the H2 transporter. The $\delta(\Delta G^\circ)$ of both 9-deazaguanine and 9-deazaadenine was 7.7 kJ/mol compared to their respective parent molecules, indicating that N(9)H most likely acts as a hydrogen bond donor. Given the higher difference in ΔG° between most nucleobases and their respective nucleosides (adenine–adenosine 12.9 kJ/mol; hypoxanthine–inosine 15.8 kJ/mol), it is likely that steric factors equally contribute to the low affinity for nucleosides.

The model shown in Figure 3.5 thus describes 4 interactions, probably hydrogen bonds, to bind either oxopurines or aminopurines. The ΔG° values of hypoxanthine (-39.5 kJ/mol) and adenine (-31.3 kJ/mol) are within 5% of the total of the 4 predicted interactions (-41.1 and -32.8 kJ/mol respectively).

3.2.2 Trypanotoxicity of purine analogues

With the substrate recognition models in place, the purine analogues were next tested for *in vitro* trypanotoxicity, to assess the existence of a relationship between efficient uptake and toxicity.

Many of the purine analogues that were tested have been used as chemotherapeutic agents in other diseases or disorders, *e.g.* allopurinol in the treatment of leishmaniasis and 6-mercaptopurine against leukemia. The analogues were investigated for any toxic effects they might have on *T. b. brucei*. These tests were carried out on bloodstream parasites as it is these that the drugs would be required to act against *in vivo*. The Alamar Blue reaction is a more efficient way of testing toxicity than observation of the parasites for viability/motility following exposure to the test compound which is time-consuming and subjective. Exposure of the parasites to the test compound followed by incubation with Alamar Blue resulted in a measurable colour-change, due to the action of an unspecified parasite dehydrogenase. By using a range of drug concentrations dose-response curves could be generated (Figure 3.6). In order to have as sensitive an assay as possible, the bloodstream parasites were resuspended in a nucleobase-free version of HMI-9 medium (with adenosine supplement as purine source). This meant any analogue taken up by the H2 transporter did not have to compete with hypoxanthine when binding to the transporter.

Figure 3.6 shows Alamar Blue assay dose-response curves for the three compounds to consistently show trypanocidal activity *in vitro*, namely aminopurinol, 2,6-dichloropurine and adenine 9- β -D-arabinoside.

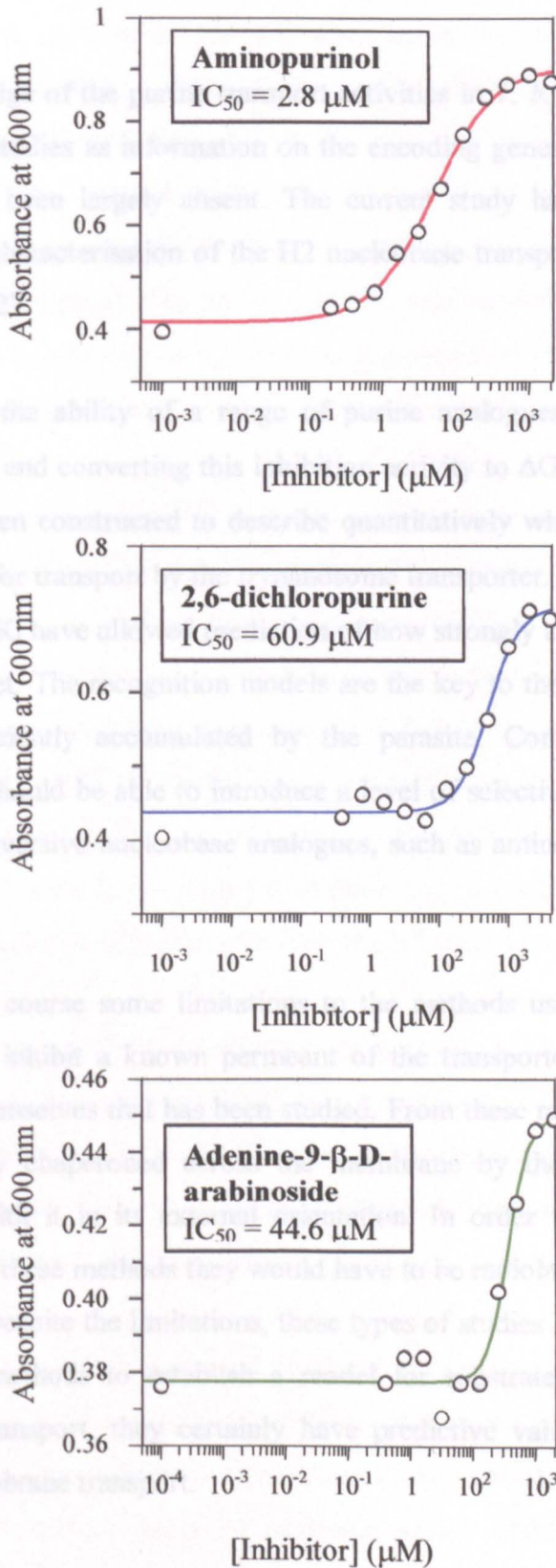


Figure 3.6. Trypanocidal activity of purine analogues. Examples of Alamar Blue assay graphs. These were produced using colorimetric readings.

3.3 Discussion

Most knowledge of the purine transport activities in *T. b. brucei* has been gained through biochemical studies as information on the encoding genes, as well as the structure of the proteins, has been largely absent. The current study has added a further layer to the biochemical characterisation of the H2 nucleobase transporter found in bloodstream form *T. b. brucei* 427.

By assaying the ability of a range of purine analogues to inhibit the uptake of [³H] hypoxanthine and converting this inhibition activity to ΔG° values, a substrate recognition model has been constructed to describe quantitatively which positions of the purine ring are essential for transport by the trypanosome transporter. The ΔG° values calculated from the observed K_i have allowed prediction of how strongly a drug can bind to the transporter binding pocket. The recognition models are the key to the rational design of trypanocides that are efficiently accumulated by the parasite. Comparisons with equivalent host transporters should be able to introduce a level of selectivity. It has been shown here that uptake of subversive nucleobase analogues, such as aminopurinol, is mediated by the H2 transporter.

There are of course some limitations to the methods used here. It is the ability of the analogues to inhibit a known permeant of the transporter and not actual uptake of the analogues themselves that has been studied. From these results it is unclear if an analogue is being fully chaperoned across the membrane by the transporter or if it is simply interacting with it in its external orientation. In order to study actual transport of the analogues by these methods they would have to be radiolabelled individually, which is not practicable. Despite the limitations, these types of studies are in wide useage, and although the current methods to establish a model for substrate-transporter interactions do not depend on transport, they certainly have predictive value for the substrate recognition phase of membrane transport.

Still, it is conceivable that such factors could distort individual estimates of K_i , and hence, ΔG° . The speed at which the transporter-permeant complex transverses the membrane and the speed of release of the permeant into the interior of the cell can vary for different

molecules, and may increase or decrease the observed K_i , as this value is ultimately derived from the amount of radiolabel taken up by the cell. A prolonged occupancy of the transporter by an inhibitor could theoretically reduce this significantly, in addition to its effects as competitive inhibitor. During the construction of the substrate recognition model, it was ensured that more than one analogue contributed to the final designated value for each interaction, and that the individual estimates were generally in good agreement. The model was also supported by the fact that the total sum of the ΔG° values [$\Sigma(\Delta G^\circ)_{\text{obs}}$] for the separate H-bonds, calculated from the apparent K_i values, is within 5% of the total ΔG° calculated from the actual K_m of the natural substrate.

The H2 transporter appears to recognise several residues on both the pyrimidine part and the imidazole half of the purine ring system. This appears to leave relatively little room for the modifications and substitutions for binding antimetabolites. Certainly, the recognition motif for the P2 transporter is mostly confined to the pyrimidine part of the purine ring, allowing for coupling of toxic moieties to or in place of the imidazole ring. However, the H2 model may still be useful as a starting point for designing or deploying new trypanocides. Substitutions are possible at positions 2, 6, and 8, and the “allopurinol shift” in position N7 could be combined with other changes. Chapter 5 describes the recognition of some novel purine-like compounds by the H2 transporter.

Of course, a high-affinity interaction with transporter does not necessarily mean good trypanocidal activity. An analogue may not actually be taken up by the transporter. In many cases, selective uptake alone may be insufficient for trypanocidal action. It will be necessary to investigate the structure-activity relationships of enzymes involved in purine metabolism as a next step in the rational design of purine antimetabolites.

The Alamar Blue assay was used to assess the potential therapeutic value of selectively transported reagents in an *in vitro* situation. Alamar Blue assay works very well for known trypanocides giving results comparable to those obtained by other means (Räz, *et al.*, 1997). In this work, a range of nucleobases and related compounds were assayed for trypanocidal activity. Alamar Blue assays and other toxicity assays fail to address which transporter(s) are actually involved in the uptake of any drugs – the constitution of media can be changed to favour certain transporters but uptake by other transporters can only be effectively prevented by utilising transporter gene knock-outs or RNA_i knock-downs.

Although some compounds did show some activity, it is prudent to note that this research was preliminary – introducing the approach and validating it as a way of identifying possible lead compounds for the development of new trypanocidal regimes. The list of compounds assayed for trypanocidal activity was by no means comprehensive. Existing purine-related compounds are in use in other disease conditions and given that researchers in these other areas also strive to improve existing chemotherapy it is inevitable that new compounds will continue to be developed by chemists and drug companies. It is to be anticipated that compounds may have to be optimised for appropriate recognition by trypanosome transporters and also for active toxic side groups. Nevertheless, the Alamar Blue results obtained raised some interesting points.

Allopurinol is the only purine compound currently in use against a species of Trypanosomatidae (*Leishmania spp.*) but is usually only used in conjunction with other drugs (Das, *et al.*, 2001). The selective action of allopurinol is due to the different metabolic pathways in trypanosomatids as opposed to mammalian tissues. In *Leishmania* the allopurinol is metabolised to the toxic 4-aminopyrazolopyrimidine-5'-monophosphate (APPR-MP) which is further phosphorylated to APPR-DP and APPR-TP which is then incorporated into the cellular RNA (Marr, 1983). In mammalian cells the same molecule is metabolised to oxipurinol and other by-products and harmlessly excreted from the cell. As seen in this study, allopurinol is taken up by the H2 transporter with a relatively high apparent K_i of 4.0 μM . However, in the Alamar Blue assay, allopurinol is not very effective *in vitro* against bloodstream form *T. b. brucei* 427 at the concentrations assayed. The adenine analogue, aminopurinol, conversely shows little affinity for the H2 transporter (K_i of 240 μM) but in the Alamar Blue assay displays an *in vitro* IC_{50} of 2.8 μM . An adenosine analogue, adenine-9- β -D-arabinoside, also performed relatively well in the Alamar Blue (IC_{50} of 44.6 μM) while poorly inhibiting H2 activity in the transport assays. This apparent paradox can almost certainly be explained by the uptake of these compounds by the P2 transport activity - both molecules possess the P2 recognition motif. It is uncertain how these analogues would affect the mammalian cell – they may be rapidly metabolised and excreted as happens for allopurinol but it may be that these amino analogues are more palatable to the metabolic enzymes of man.

Chapter Four

Substrate recognition models for the equilibrative nucleobase transporter of human erythrocytes

4.1 Introduction

In the previous chapter, it was established that the H2 nucleobase transporter of the protozoan parasite *T. b. brucei* has the potential to act as a conduit for the delivery of novel trypanocides to the interior of the organism where such molecules could interfere with trypanosomal metabolic pathways. However, it is also of paramount importance to examine how any new drugs would affect the mammalian tissues that they would inevitably come into contact with. With regards to the exploitation of transporters to conduct drugs across membranes, the ideal drug molecule would be efficiently conveyed across the parasite membrane while being excluded by the mammalian transport systems. Uptake of nucleobases by human erythrocytes was characterised in terms of substrate recognition motifs in the same way as for the trypanosome H2 transporter.

Understanding the substrate recognition pattern for the facilitative nucleobase transporter (hFNT1) can add a further dimension to the design of new trypanocides, optimising for selectivity alongside efficacy, to at least one major host nucleobase transporter.

4.1.1 The human erythrocyte as experimental model

There are several reasons why the human erythrocyte has been chosen as the model in this study. The plasma membrane of the red blood cell has long been a paradigm for studies of membrane structure and function (Stryer, 1995). This is partly due to the ease with which material can be obtained – although blood is a bonafide tissue in its own right, its fluid nature allows easy extraction and separation of the different components. The simplicity of the cell structure is also advantageous – with a lack of membrane-bound organelles the only erythrocyte membrane system is the plasmalemma. Glycophorin A, a major constituent of the erythrocyte membrane, was the first integral membrane protein to have its amino acid sequence elucidated, and membrane-associated systems such as the cytoskeleton were initially studied in the erythrocyte (Marchesi, 1985).

The main function of the circulatory system is of course the transport of various chemicals around the body. The bloodstream provides oxygen and nutrients to all the tissues and is responsible for the removal of waste materials from these same tissues. It is also the

primary vehicle for hormone delivery and immune system components. Many drugs are administered via the bloodstream, allowing dissemination to many distant sites, and essentially co-opting this transport network, much as researchers want to exploit the transport activities of individual cells.

It is therefore relevant to study nucleobase uptake by erythrocytes as a model human tissue. Moreover, effective salvage of anti-parasitic drugs by the erythrocytes would probably not only poison these vital cells, but also quickly deplete the free drug concentration in the bloodstream.

4.1.2 The facilitative nucleobase transporter

As discussed in Chapter One, humans possess several different nucleobase and nucleoside transport activities. These range from concentrative transporters that usually reside in highly specialised tissues, such as placenta and kidney, to the more ubiquitous equilibrative transporter found in many different cell types (Plagemann, *et al.*, 1988; Griffith & Jarvis, 1996).

The human facilitative nucleobase transporter (hFNT1) is the only nucleobase transporter present in human erythrocytes (Domin, *et al.*, 1988) but it, or transport proteins closely-related in function, have also been described in various other tissues and have been shown to be involved in the uptake of several chemotherapeutic purine analogues including allopurinol (Razavi, *et al.*, 1993), acyclovir (Mahony, *et al.*, 1988), and 2',3'-dideoxyguanosine (Gati, *et al.*, 1992). In the range of different cell-types it has been described in, the K_m or K_i values obtained have been similar to those derived in experiments using the erythrocyte.

It was determined that adenine, guanine, and hypoxanthine are taken up by the erythrocyte facilitative nucleobase transporter with K_m 's of 13, 37 and 180 μM , respectively (Domin, *et al.*, 1988). Carrier mobility studies by Kraupp and colleagues (1991) confirmed that the three permeants were each carried by the same transporter.

Even though mammalian cells are generally considered to be able to manufacture the purine ring, in fact not all cell types, including erythrocytes, are capable of this synthesis.

These cells, like the bloodstream trypanosome, must salvage free purines from the blood. Some purines will be obtained through the diet, but other tissues must synthesise and release sufficient quantities of nucleobase/nucleosides into the bloodstream. This follows most directly from the observation that man and other mammals can be maintained indefinitely on purine-free diets (Murray, 1971).

4.2 Results

4.2.1 Confirmation of basic kinetics of hFNT1 in human erythrocytes

Transport of tritiated permeants by the hFNT1 was determined using the rapid-stop oil-spin technique very similar to that used to study uptake by the parasite transporter. Transport was effectively terminated using ice-cold papaverine (a non-competitive inhibitor of hFNT1 – Kraupp, *et al.*, 1994) rather than unlabelled permeant, and it was necessary to extract the accumulated radioactivity in the acid-soluble fraction of the cell pellets as haemoglobin would cause severe quenching during liquid scintillation counting. Transport of 1 μM [^3H] adenine by human erythrocytes was rapid, and linear over 20 s with a rate of $0.056 \pm 0.004 \text{ pmol } (10^7 \text{ cells})^{-1} \text{ s}^{-1}$ (Figure 4.1). The transport activity was saturable as shown by the 92% reduction in uptake rate in the presence of 1 mM unlabelled permeant. In the subsequent inhibition studies [^3H] adenine uptake was apparently monophasic, with a Hill slope close to -1 , consistent with a single transport system for the transport of adenine (data shown in next section). This was in keeping with previous studies of nucleobase uptake by human erythrocytes (Domin, *et al.*, 1988). Figure 4.2 shows a Michaelis-Menten plot for adenine uptake.

The apparent K_m was $16.2 \pm 4.5 \mu\text{M}$ and the V_{max} was $1.92 \pm 0.89 \text{ pmol } (10^7 \text{ cells})^{-1} \text{ s}^{-1}$ ($n=3$). Subsequent inhibition experiments were conducted using a [^3H] adenine concentration of 1 μM and an incubation time of 3-5 s, which produced highly reproducible results.

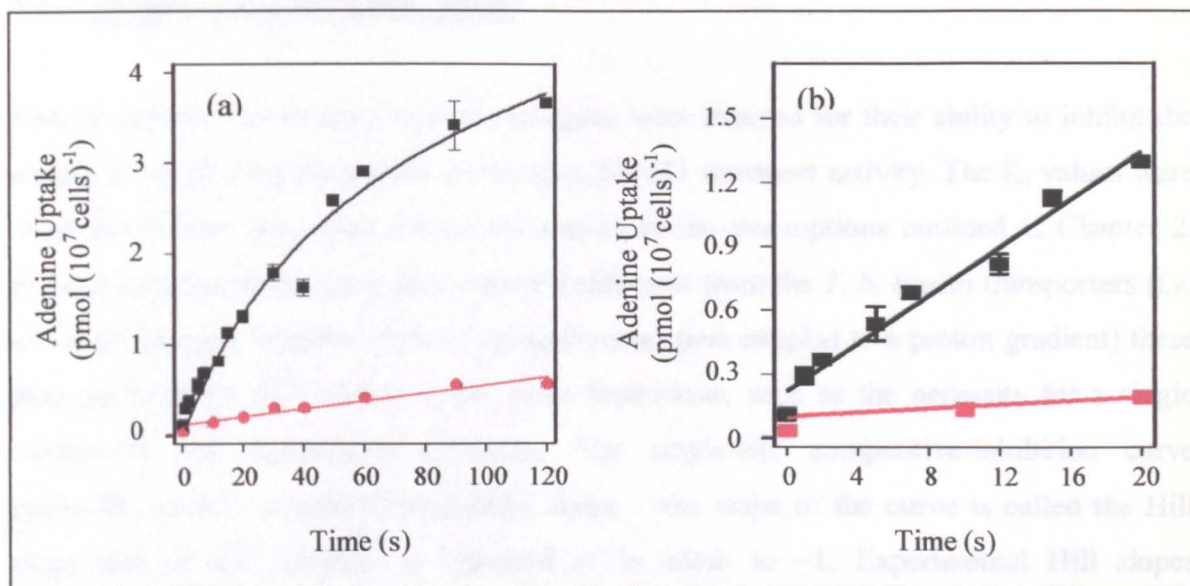


Figure 4.1. Uptake of [³H] adenine by human erythrocytes as a function of time. Uptake of 1 μM [³H] adenine in the absence (■) or presence (■) of 1 mM unlabelled adenine. (a) Uptake over 120 s. (b) Linear phase of uptake over 20 s ($r^2 = 0.97$ by linear regression) with a rate of 0.056 ± 0.004 pmol (10⁷ cells)⁻¹ s⁻¹. Uptake in the presence of 1 mM unlabelled permeant was taken as the rate of diffusion: 0.0044 ± 0.0005 pmol (10⁷ cells)⁻¹ s⁻¹ over 120 s.

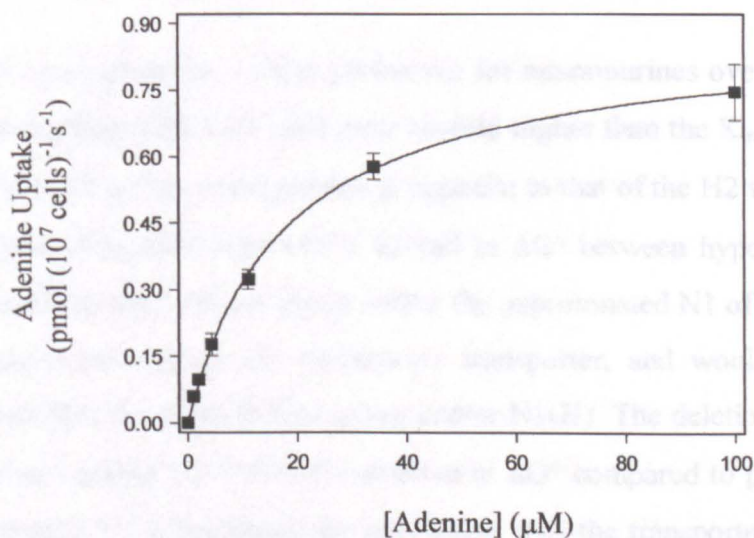


Figure 4.2. Michaelis-Menten plot for transport of 1 μM [³H] adenine by human erythrocytes. Michaelis-Menten plot showing a K_m of 16.7 ± 2.1 μM and a V_{max} of 0.84 ± 0.07 pmol (10⁷ cells)⁻¹ s⁻¹ for this experiment.

4.2.2 Structure-activity relationships

Natural purines and selected purine analogues were assayed for their ability to inhibit the uptake of adenine by the human erythrocyte hFNT1 transport activity. The K_i values were determined from dose-response curves subject to the assumptions outlined in Chapter 2. Even though the mechanism of transport is different from the *T. b. brucei* transporters (*i.e.* a facilitative-type transport rather than active-transport coupled to a proton-gradient) these data analyses are still subject to the same limitations, such as the necessity for a single transporter and competitive-inhibition. The single-site competitive-inhibition curve generally exhibits a standard sigmoidal shape – the slope of the curve is called the Hill slope and in this scenario is expected to be close to -1 . Experimental Hill slopes approximating -1 were routinely observed, consistent with competitive inhibition of a single transporter and the literature as discussed above. Representative examples of the dose-response curves are shown in Figure 4.3. By calculating the binding energies, as Gibbs free energy (ΔG°), involved in the interaction between the transporter and the different molecules, structure-activity relationships were devised. The K_i and the ΔG° values for the different analogues are listed in Table 4.1.

The hFNT1 transporter has a clear preference for aminopurines over oxopurines, with the K_i for hypoxanthine ($288 \pm 21 \mu\text{M}$) over 10-fold higher than the K_m for adenine ($16 \pm 4.5 \mu\text{M}$). This specificity for aminopurines is opposite to that of the H2 which has a preference for oxopurines. The difference of 7.1 kJ/mol in ΔG° between hypoxanthine and adenine could indicate that the 6-amino group and/or the unprotonated N1 of adenine is involved in the recognition process by the erythrocyte transporter, and would appear to limit the potential contribution of the 6-keto group and/or N1(H). The deletion of the N1 residue in 1-deazapurine leads to a 5.1 kJ/mol reduction in ΔG° compared to purine, confirming that the unprotonated N1 is important for interaction with the transporter. Adenine and purine differ only in the presence or absence of the 6-amino group and the $\delta(\Delta G^\circ)$ of 4.1 kJ/mol implies that this component is also necessary for the optimal interaction of adenine and the transporter recognition site. The combined ΔG° for interactions at position 1 and 6 of the adenine molecule is therefore 9.2 kJ/mol, but the $\delta(\Delta G^\circ)$ between adenine and hypoxanthine is only 7.1 kJ/mol, suggesting that hypoxanthine is perhaps capable of making alternative, albeit weaker, arrangements. If the 6-keto group is involved, it would

be predicted that 6-thioguanine would make a less effective substrate than guanine due to the 6-thione group being less capable of participating in H-bonds. Indeed, this is exactly what is observed with a ΔG° discrepancy of 3.1 kJ/mol. The difference of 3 kJ/mol in binding energy between purine and hypoxanthine confirms that the H-bond with N1 is stronger than with 6-keto. It also reinforces the assertion that the N1(H) does not participate in recognition. The ΔG° for molecules such as 6-chloropurine, in which N1 is unprotonated, do not differ significantly from that for purine ($p > 0.05$ in Student t test) (Figure 4.3, panel (a)).

Elsewhere in the pyrimidine half of the purine ring system, the participation of substitutions at position 2 and the unprotonated N3 is indicated. The participation of substitutions at position 2 during substrate recognition can be deduced from the $\delta(\Delta G^\circ)$ of 5.8 kJ/mol between guanine and hypoxanthine. The involvement of N3 is inferred from the $\delta(\Delta G^\circ)$ of 7.3 kJ/mol between guanine and 3-deazaguanine, and the 8.6 kJ/mol difference between adenine and 3-methyladenine (Figure 4.3, panel (a) and (b)). The inability of xanthine and uric acid to inhibit [^3H] adenine uptake at the limit of their solubility is consistent with the requirement for an H-bond donor at position 2 and an H-bond acceptor at position 3.

The pyrimidine ring of adenine thus contributes -16.5 kJ/mol to the total of -27.3 kJ/mol Gibbs free energy for the interactions between the adenine molecule and the hFNT1 transporter, indicating a contribution of ~ 10 kJ/mol from the imidazole half of the purine ring system.

Consistent with this assertion, the total sum of the binding energy values calculated for the interactions of the pyrimidine halves of hypoxanthine and guanine are -8.9 kJ/mol and -16.2 kJ/mol, respectively; again these apparent ΔG° values are ~ 10 kJ/mol less than the observed ΔG° for the entire molecules.

The imidazole half of the purine ring system somehow contributes ~ 10 kJ/mol in binding energy to recognition by the transporter binding pocket. The participation of the imidazole ring, however, is not mediated by hydrogen-bonding at position N7(H) or N9 since the transporter actually exhibits slightly higher affinity for 7-deazaguanine, 9-deazaguanine

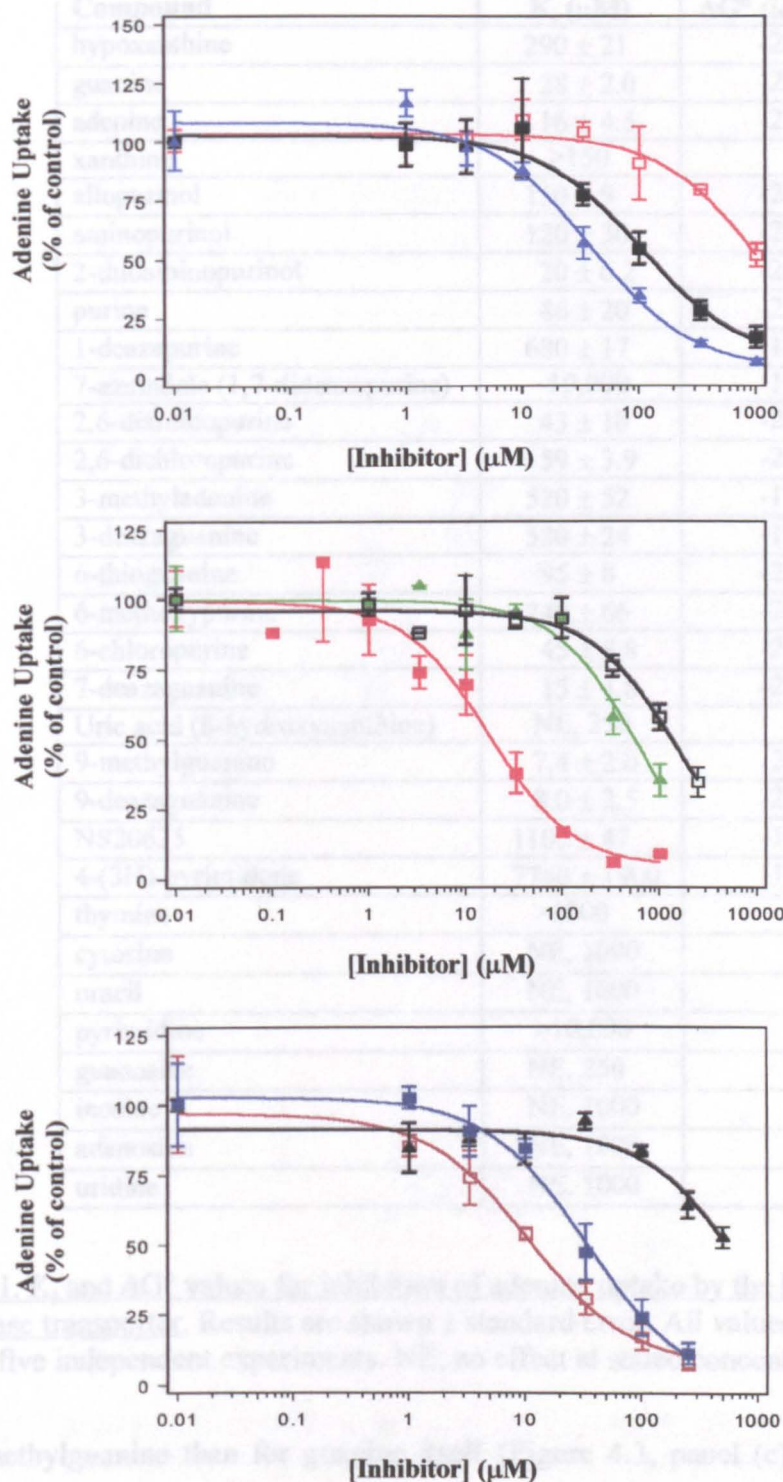


Figure 4.3. Inhibition of FNT1-mediated $[^3\text{H}]$ adenine transport in human erythrocytes by purine analogues. Rates of uptake are expressed as a percentage of control, *i.e.* uptake in the absence of inhibitor. (a) 1-deazapurine (\square), purine (\blacksquare), and 6-chloropurine (\blacktriangle). (b) adenine (\blacksquare), 3-methyladenine (\blacktriangle), and NS20635 (\square). (c) 9-methylguanine (\square), 3-deazaguanine (\blacktriangle), and 7-deazaguanine (\blacksquare). Label concentration in these experiments was 1 μM .

Compound	K_i (μM)	ΔG° (kJ mol^{-1})
hypoxanthine	290 ± 21	-20.2
guanine	28 ± 2.0	-26.0
adenine	16 ± 4.5	-27.3
xanthine	>150	
allopurinol	150 ± 9	-21.8
aminopurinol	120 ± 30	-22.4
2-thioaminopurinol	20 ± 6.2	-26.8
purine	86 ± 20	-23.2
1-deazapurine	680 ± 17	-18.1
7-azaindole (1,7-dideazapurine)	$\sim 10,000$	-11.4
2,6-diaminopurine	43 ± 10	-24.9
2,6-dichloropurine	59 ± 3.9	-24.1
3-methyladenine	520 ± 52	-18.7
3-deazaguanine	520 ± 24	-18.7
6-thioguanine	95 ± 8	-23.0
6-methoxypurine	240 ± 66	-20.6
6-chloropurine	45 ± 5.8	-24.8
7-deazaguanine	15 ± 4.8	-27.6
Uric acid (8-hydroxyxanthine)	NE, 250	
9-methylguanine	7.4 ± 2.0	-29.3
9-deazaguanine	8.0 ± 2.5	-29.1
NS20635	1100 ± 47	-16.9
4-(3H)-pyrimidone	7740 ± 1900	-12.1
thymine	>1000	
cytosine	NE, 1000	
uracil	NE, 1000	
pyrimidine	>10,000	
guanosine	NE, 250	
inosine	NE, 1000	
adenosine	NE, 1000	
uridine	NE, 1000	

Table 4.1. K_i and ΔG° values for inhibition of adenine uptake by the human facilitative nucleobase transporter. Results are shown \pm standard error. All values are the average of three to five independent experiments. NE, no effect at stated concentration.

and 9-methylguanine than for guanine itself (Figure 4.3, panel (c)). The $\delta(\Delta G^\circ)$ of 8.6 kJ/mol between 4-(3H)-pyrimidone and hypoxanthine emphasises that the presence of the imidazole ring is required for proper recognition by the transporter even though the interaction cannot be correlated to a particular position or group. The compound NS20635 possesses a double ring system consisting of a 6-member ring corresponding to the pyrimidine ring of adenine, and a 5-member ring lacking nitrogen atoms and π -orbitals.

This compound was also recognised with very low affinity by the transporter molecule (Figure 4.3, panel (b)).

The above data are all consistent with attributing the surplus binding energy to interactions between π -orbitals of the imidazole member of the purine ring with the π -orbitals of aromatic residues in the hFNT1 binding pocket, rather than H-bonds to N7 or N9.

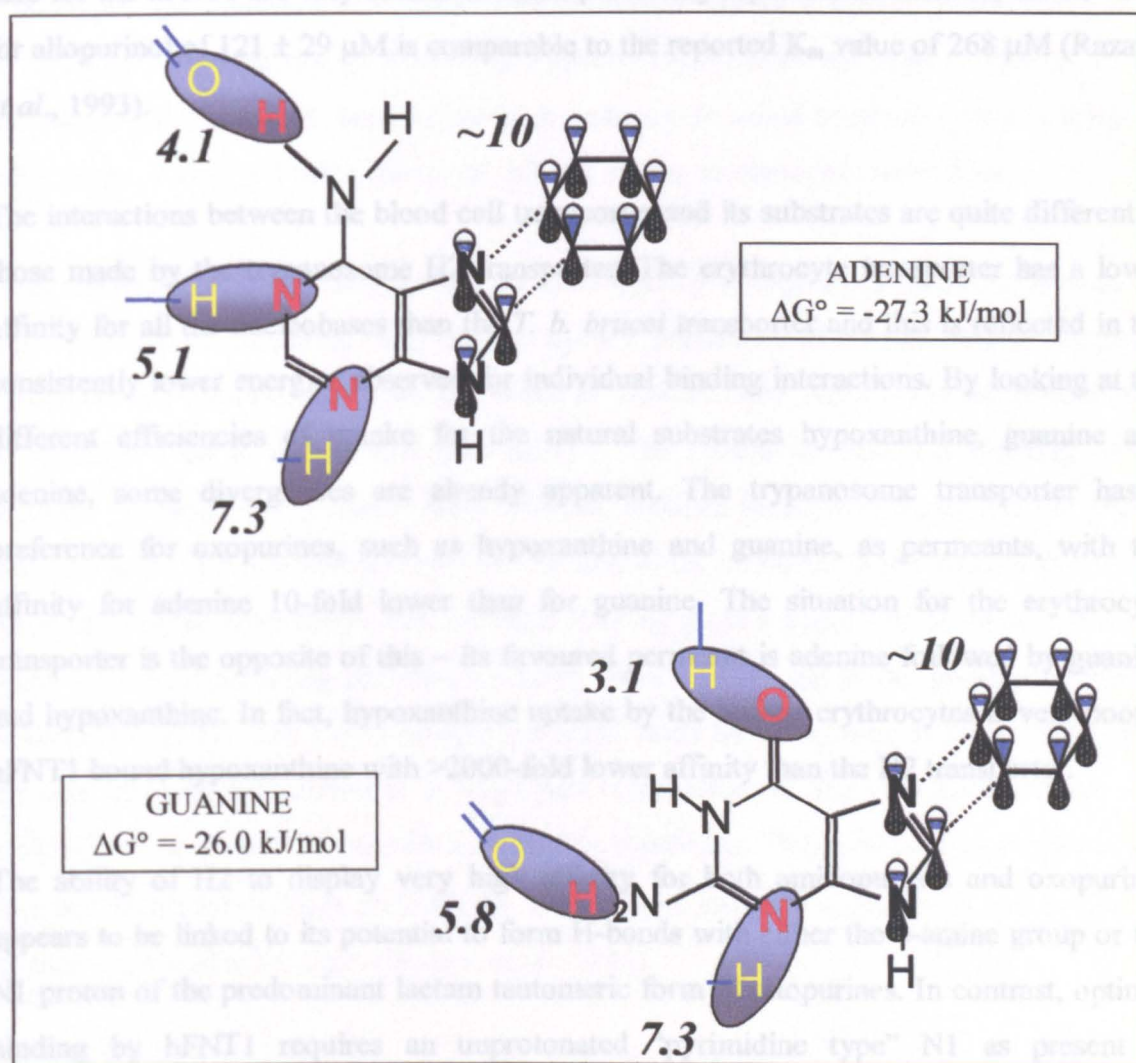


Figure 4.4. Model of the interactions between purines and the hFNT1 transporter. Estimations of the Gibbs free energy of these interactions are given in kJ/mol.

The model shown in Figure 4.4 thus describes 3 interactions, probably hydrogen bonds, to recognise the pyrimidine subunit of the purine ring system and a further interaction through the π -orbitals of the imidazole ring atoms. The ΔG° values of adenine (-27.3 kJ/mol) and guanine (-26.0 kJ/mol) are in close agreement of the total of the 4 predicted interactions (-26.5 and -26.2 kJ/mol respectively).

4.3 Discussion

The Michaelis-Menten constants and limited substrate specificity details for hFNT1 of human erythrocytes have been published previously (Plagemann, *et al.*, 1987; Domin, *et al.*, 1988; Kraupp, *et al.*, 1991), and the current findings are in close agreement with these earlier studies. The K_m and K_i values for adenine, guanine, and hypoxanthine, reported here for the hFNT1 are very similar to those previously reported. In addition, the K_i value for allopurinol of $121 \pm 29 \mu\text{M}$ is comparable to the reported K_m value of $268 \mu\text{M}$ (Razavi, *et al.*, 1993).

The interactions between the blood cell transporter and its substrates are quite different to those made by the trypanosome H2 transporter. The erythrocyte transporter has a lower affinity for all the nucleobases than the *T. b. brucei* transporter and this is reflected in the consistently lower energies observed for individual binding interactions. By looking at the different efficiencies of uptake for the natural substrates hypoxanthine, guanine and adenine, some divergences are already apparent. The trypanosome transporter has a preference for oxopurines, such as hypoxanthine and guanine, as permeants, with the affinity for adenine 10-fold lower than for guanine. The situation for the erythrocyte transporter is the opposite of this – its favoured permeant is adenine followed by guanine and hypoxanthine. In fact, hypoxanthine uptake by the human erythrocytes is very poor – hFNT1 bound hypoxanthine with >2000-fold lower affinity than the H2 transporter.

The ability of H2 to display very high affinity for both aminopurines and oxopurines appears to be linked to its potential to form H-bonds with either the 6-amine group or the N1 proton of the predominant lactam tautomeric form of oxopurines. In contrast, optimal binding by hFNT1 requires an unprotonated “pyrimidine type” N1 as present in aminopurines. Yet, hFNT1 displays relatively high affinity for guanine due to a weak hydrogen bond to the 6-keto group and a stronger one to the amine at position two. These interactions appear to be absent in the H2 binding pocket, and this transporter displays 3-fold lower affinity for guanine than for hypoxanthine, presumably for steric reasons.

The one feature shared by the two base transporters is a strong interaction, presumably by H-bonding, with N3, which is unprotonated in all natural purines except xanthine and uric acid. This is consistent with the $\delta(\Delta G^\circ)$ value of 10.6 kJ/mol for xanthine compared with

hypoxanthine binding by H2, which consists of the loss of the N3 H-bond (8.3 kJ/mol) and the steric effect of the substitution at position 2. For hFNT1 the affinity of xanthine would also be expected to be lower than for hypoxanthine, particularly because an H-bond donor such as an amine appears to be favored in position 2, but it was not possible to establish a K_i value due to limitations of solubility. Similarly, the hFNT1 transporter was not inhibited by up to 250 μM uric acid, but H2 also failed to bind this purine, in which N7 is protonated. The total lack of affinity of these transporters for uric acid, which exists at up to 400 μM in human plasma (Wung & Howell, 1980), is an essential adaptation to the bloodstream environment, because the high urate levels would compete with low levels of other purine bases, and urate cannot be utilised for the synthesis of nucleotides.

Both transporters derive roughly half of their binding energy from interactions with the imidazole part of the purine ring, explaining their preference of purines over pyrimidines. However, whereas H2 forms strong H-bonds with N7 and N(9)H, neither residue was directly involved in interactions with hFNT1. The conclusion that π - π stacking of the aromatic purine ring and one or more aromatic residues in the transporter binding pocket plays an important role in stabilizing the binding of the permeant is not without precedent. Structural studies have shown that π -orbital stacking plays a major role in the active site of many purine-metabolizing enzymes (Somoza, *et al.*, 1996) and in the stability of nucleic acids (Kool, 2001). The P1/P2 recognition motif study by De Koning & Jarvis (1999) also showed that this mechanism is in large part responsible for the very high affinity with which the *T. b. brucei* P2 transporter binds its substrates. The combined electrostatic and Van der Waals interactions between the π -orbitals of aromatic amino acids can exceed 10 kJ/mol at optimal orientation (Hunter, *et al.*, 1991).

The models for the substrate recognition motif for H2 described in Chapter Three and presented here for hFNT1 show that there is ample scope for selective uptake of purine analogues by either transporter. Table 4.2 shows specificity ratios for interaction of various compounds with the different transporter molecules. Higher levels of selectivity could be achieved with rationally designed hypoxanthine analogues, because these display the greatest differential affinity between the two carriers.

Compound	K_i (H2) (μ M)	K_i (hRBC) (μ M)	K_i (hRBC) / K_i (H2)
hypoxanthine	0.12	288	2404
6-thioguanine	0.43	95.3	222
2-aminopurine	3.5	686	195
3-deazaguanine	10	519	52
6-methoxypurine	6.9	242	35
1-deazapurine	22.1	676	31
guanine	0.36	28	10
adenine	3.2	16	5.1
purine	18	86	4.7
6-chloropurine	17	45	2.7
2,6-diaminopurine	25	43	1.7
7-deazaguanine	55.2	14.8	0.27
9-methylguanine	70	7.4	0.11

Table 4.2. Specificity ratio table.

Although the hFNT1 transporter, or closely related members of the same transporter family, appears to be the most ubiquitous human nucleobase transporter and the only one characterised in blood cells, other nucleobase transporters have been characterised in specialised cells of the kidney, intestine, choroid plexus, and placenta (De Koning & Diallinas, 2000). These sodium-dependent nucleobase transporters usually display high affinity for their substrates and seem to be expressed at the interface of the bloodstream with other environments. The importance of this class of transporters for the distribution, side effects, and pharmacokinetics of therapeutic nucleobase analogues would argue for intensified efforts for their cloning and characterisation.

It is interesting to note that while hFNT1 and the H2 recognise and transport hypoxanthine with very different affinities, thus suggesting that hypoxanthine analogues might be worthy of pursuit, a note of caution is necessary, since many of the sodium-dependent active transporters in the mammalian system are capable of transporting hypoxanthine with very high affinity (De Koning & Diallinas, 2000).

Chapter Five

Recognition of unusual potential trypanocides by the purine transporters of *T. b. brucei*

5.1 Introduction

The elucidation of the substrate recognition motifs for the trypanosome H2 transporter and the hFNT1 were described in Chapter 3 and 4, respectively. Substrate recognition models for the trypanosome P1 and P2 nucleoside transporters were described previously by De Koning & Jarvis (1999). In this chapter, the substrate recognition of a range of unusual purine analogues was assessed for both trypanosome and human purine transporters. Since preliminary studies suggested that these molecules may have trypanocidal activity, the compounds were also assayed for *in vitro* trypanotoxicity using the Alamar Blue assay.

5.1.1 Tricyclic purine compounds - origins

Tricyclic purine analogues were pioneered by Leonard and colleagues in the 1970's with the production of extended adenine analogues containing a benzene spacer ring between the imidazole and pyrimidine components. These new molecules could assume different configurations (*lin-*, *dist-*, *prox-*) depending on where the purine components linked to the benzene bridge (Leonard, *et al.*, 1975). Figure 5.1 shows these original tricyclic molecules.



Figure 5.1. Original benzo-adenine compounds.

The rationale behind the design of these molecules was to enable their usage as “bioprobes” to investigate the recognition of substrates by enzyme active sites and to explore the physical limitations of these binding sites (Leonard & Hiremath, 1986). The numerous other nucleobase and nucleoside derivatives that were subsequently designed and synthesised often displayed significant biological effects both in enzyme activation and inhibition. Many of the analogues were fluorescent and this aided in the localisation and elucidation of intermolecular interactions (Seley, *et al.*, 2002).

Although the analogues differ from the parent molecule in size and shape, they still contain all the necessary purine ring components for molecular recognition – *i.e.* all the residues present on the purine scaffold that are able to participate in hydrogen-bonding are still intact. The original benzoadenine molecules were also flat, conjugated π -systems, hence they were still able to participate in π - π stacking.

5.1.2 Thieno-separated tricyclic and fleximer purine analogues

Katherine L. Seley and colleagues at the Georgia Institute of Technology have designed and synthesised a range of extended purines descended from the original benzo-analogues as investigational tools and as potential chemotherapeutic agents (Seley, *et al.*, 2000; Seley, *et al.*, 2001; Seley, *et al.*, 2002).

In collaboration with Seley and colleagues the ability of various analogues to inhibit trypanosome and human transporters was investigated and their trypanotoxicity was evaluated. Thieno-separated tricyclic purines have a sulphur containing 5-membered ring in place of the original benzene spacer (Seley, *et al.*, 2000). The inclusion of the third ring separates the purine subunits by a distance of 1.5 and 2.9 Å (see Fig 5.2). In addition, the properties of a small number of fleximer purine nucleosides in which the spacer was a single 1.5 Å C-C bond between the two subunits of the purine framework were examined (Seley, *et al.*, 2001; Seley, *et al.*, 2002). The thieno-separated tricyclic molecules still maintain the rigidity of a joined-ring geometry while the fleximer connection allows the planes of the rings to rotate relative to each other.

The thieno-separated nucleosides that were made available were the adenosine (TRI-001), inosine (TRI-002), guanosine (TRI-003), 6-thiomethylpurine nucleoside (TRI-004) and the purine nucleoside (TRI-005) analogues (as shown in Figure 5.2). The nucleobase counterparts of these thieno-separated molecules were also provided (Figure 5.3). The fleximer nucleosides that were supplied were the adenosine (FLX-001), inosine (FLX-002) and guanosine (FLX-003) analogues (Figure 5.4).

It is important to note that with the addition of the thieno-spacer ring, the tricyclic purine derivatives are no longer conjugated π -systems. Although the pyrimidine component is

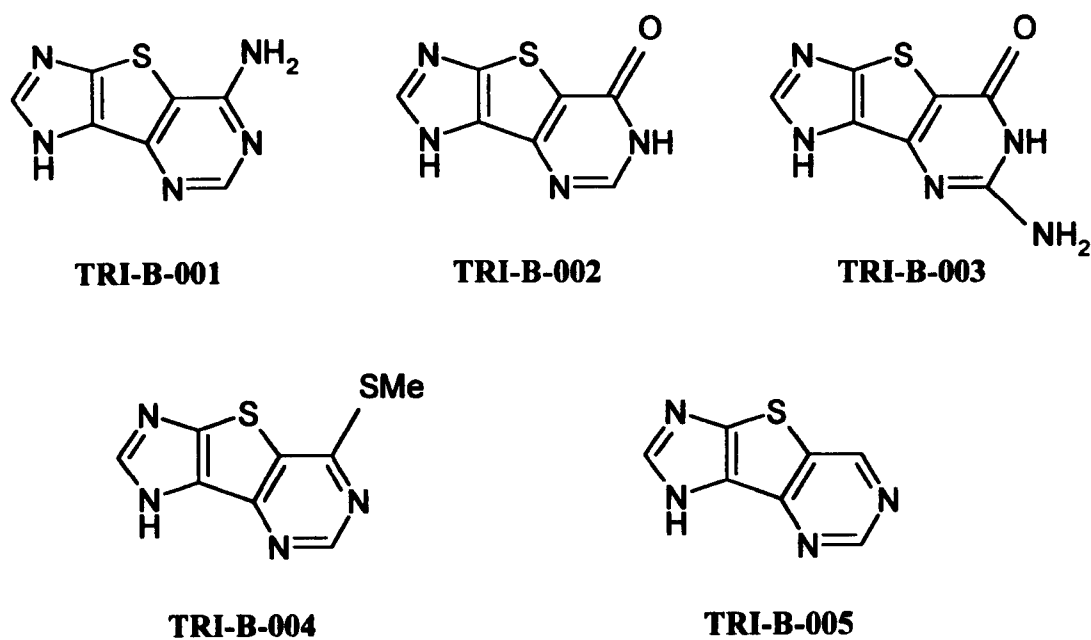


Figure 5.3. Tricyclic analogues of purine nucleobases.

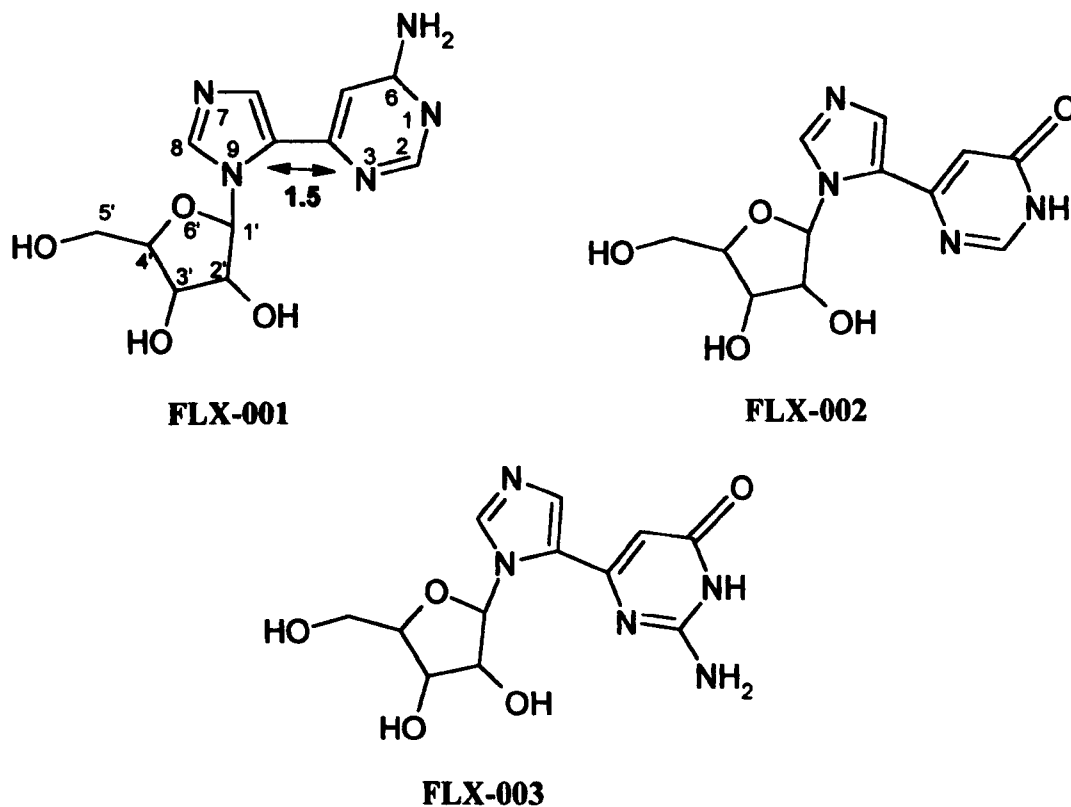


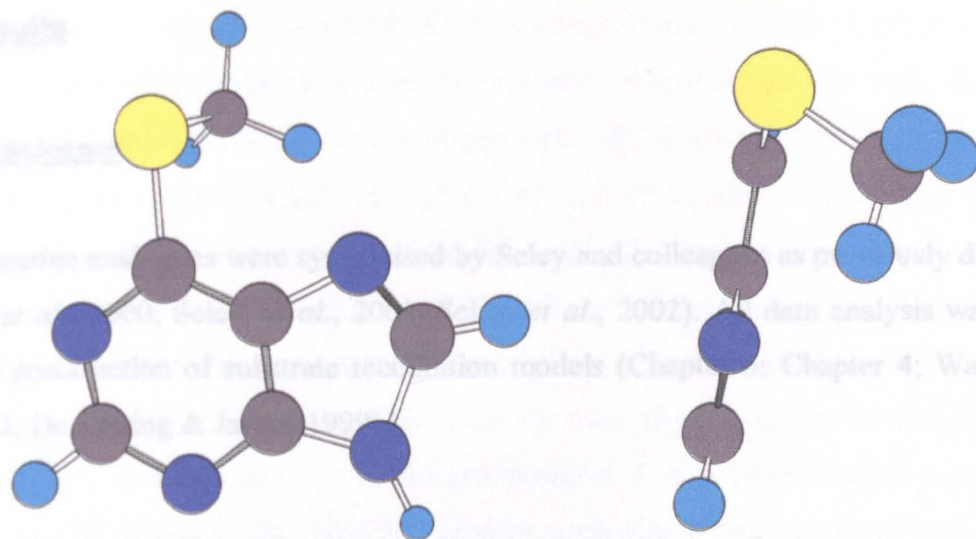
Figure 5.4. Fleximer analogues of purine nucleosides. The distances between the pyrimidine and imidazole ring of the fleximer purine system are shown for FLX-001.

5.2 Results

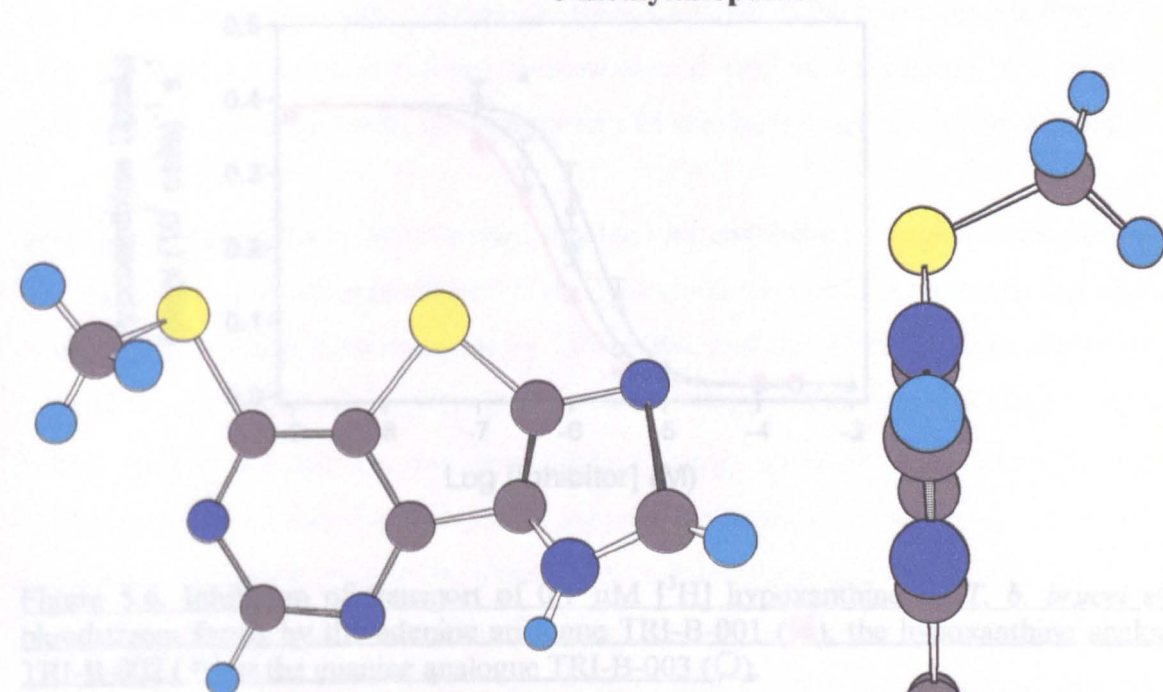
5.2.1 Substrate

All the kinetic studies were carried out by Selley and colleagues as previously described (Selley *et al.*, 2002; Selley *et al.*, 2003; Selley *et al.*, 2002). The data analysis was as for original recognition of substrate recognition models (Chapter 3; Chapter 4; Wallace, *et al.*, 2002; Ingleton & Selley, 2002).

5.2.2 Inhibition of H2 activity by thieno-separated purine nucleobases



6-methylthiopurine



TRI-B-004

Representative examples of the dose-response curves for the inhibition of H_2 activity by the purine analogues are shown in Figure 5.6. The K_i and ΔG° values obtained for the thieno-separated nucleobase compounds are shown in Table 5.1. The table also shows the $\Delta(\Delta G^\circ)$ for the analogue compared with the relevant parent molecule.

Figure 5.5. The 3-dimensional structure of TRI-B-004 compared to the parent molecule 6-methylthiopurine. With the addition of interspersing thieno-ring the molecule is no longer planar. (Yellow is sulphur, light blue is hydrogen, dark blue is nitrogen, grey is carbon.)

5.2 Results

5.2.1 Analogues

All the purine analogues were synthesised by Seley and colleagues as previously described (Seley, *et al.*, 2000; Seley, *et al.*, 2001; Seley, *et al.*, 2002). All data analysis was as for original construction of substrate recognition models (Chapter 3; Chapter 4; Wallace, *et al.*, 2002; De Koning & Jarvis, 1999).

5.2.2 Inhibition of H2 activity by thieno-separated purine nucleobases

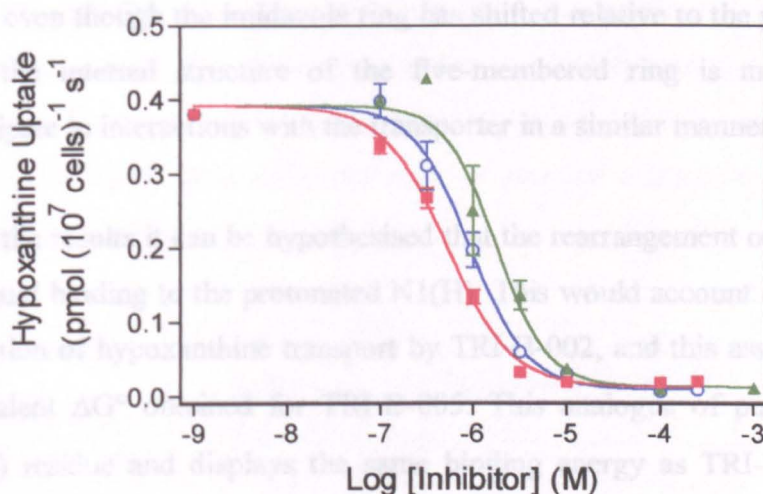


Figure 5.6. Inhibition of transport of $0.1 \mu\text{M}$ [^3H] hypoxanthine by *T. b. brucei* s427 bloodstream forms by the adenine analogue TRI-B-001 (■), the hypoxanthine analogue TRI-B-002 (▲) or the guanine analogue TRI-B-003 (○).

Representative examples of the dose-response curves for the inhibition of H2 activity by the purine analogues are shown in Figure 5.6. The K_i and ΔG° values obtained for the thieno-separated nucleobase compounds are shown in Table 5.1. The table also shows the $\delta(\Delta G^\circ)$ for the analogue compared with the relevant parent molecule.

All the thieno-separated nucleobase analogues showed reasonable inhibitory effects on the uptake of $0.1 \mu\text{M}$ hypoxanthine by the H2 transporter. Surprisingly, the substrate specificity spectrum for the thieno-separated analogues is the opposite of the normal spectrum

(hypoxanthine > guanine > adenine) for the parent molecules (De Koning & Jarvis, 1997b). The adenine analogue displayed the best inhibition of H2 activity with a K_i of $0.38 \pm 0.04 \mu\text{M}$, followed by the guanine analogue with a K_i of $0.7 \pm 0.24 \mu\text{M}$, and finally the hypoxanthine analogue with a K_i of $1.87 \pm 0.45 \mu\text{M}$. If the pyrimidine ring is bound as normal, the energy associated with shifting the imidazole ring to a new position in the H2 binding pocket would be expected to be similar for all the analogues, relative to their bicyclic natural parent bases, because all interactions to the imidazole unit are essentially the same for the parent molecules. This is not the case, suggesting that instead the shared imidazole ring mostly maintains its normal position. The adenine analogue is a better inhibitor of H2 than adenine itself; the guanine analogue is slightly worse than guanine itself; and the hypoxanthine analogue is a much worse substrate than hypoxanthine itself. Thus, even though the imidazole ring has shifted relative to the pyrimidine moiety (Figure 5.5), the internal structure of the five-membered ring is maintained and is able to participate in interactions with the transporter in a similar manner as the parent purine.

From the results it can be hypothesised that the rearrangement of rings is unfavourable for the usual binding to the protonated N1(H). This would account for the much less efficient inhibition of hypoxanthine transport by TRI-B-002, and this assertion is supported by the equivalent ΔG° obtained for TRI-B-005. This analogue of purine lacks the protonated N1(H) residue and displays the same binding energy as TRI-B-002. When the $\delta(\Delta G^\circ)$ values for the hypoxanthine and purine analogues compared to the parent molecules are considered it is apparent that the absence of an interaction to the N1(H) is not the only discrepancy in analogue recognition. Despite a lack of participatory groups at position N1 and C6, the TRI-B-005 purine analogue is still a significantly better inhibitor than purine itself (by -5.6 kJ/mol). If our assumption that the imidazole ring maintains its normal positioning is correct, this would implicate a strengthening of the bond to N3. This change at N3 would also explain why the interaction of the hypoxanthine analogue differs from hypoxanthine by only 6.8 kJ/mol despite involving the loss of a bond with an energy of 12.6 kJ/mol . The ΔG° values for each analogue suggests that the normal -7.3 kJ/mol interaction at N3 has increased to 12.9 kJ/mol for the analogue. This increase in bond strength is likely to have resulted from the participating amino acid residues of the binding site being brought into a more favourable orientation and/or proximity to the substrate.

Given that the guanine analogue is a better inhibitor than the hypoxanthine analogue it seems that the 2-amino group of guanine is not disadvantageous in the analogue as it is in the parent molecule. Based on the ΔG° value obtained for the TRI-B-003 molecule it seems that the 2-amino group contributes around 2.0 kJ/mol to the interaction of the analogue with the transporter. It is unclear whether this is the result of a very weak H-bond to 2-NH₂ however, as the energy gain is perhaps a little low. Alternatively, an indirect contribution through the further strengthening of the N3 bond could be envisaged.

These results confirm that the analogues are, at the very least, capable of preventing binding by the radiolabelled substrate to the H2 transporter binding site showing that the binding pocket will allow interactions with substantially larger molecules than its original substrate and this does not necessarily involve a concurrent loss of binding energy. A preliminary model for recognition of the tricyclic compounds by the H2 transporter is shown in Figure 5.7. More analogues including 1-deaza- and 3-deaza- tricyclics are currently being synthesised by our collaborators and assay of these will help to support or refute these postulations.

Analogue	K _i (μ M)	n	ΔG° (kJ/mol)	$\delta(\Delta G^\circ)$ (kJ/mol)	Parent molecule
KLS-TRI-B-001	0.38 \pm 0.04	3	-36.6	-5.3	Adenine
KLS-TRI-B-002	1.87 \pm 0.45	4	-32.7	6.8	Hypoxanthine
KLS-TRI-B-003	0.70 \pm 0.24	3	-35.1	1.6	Guanine
KLS-TRI-B-004	18.5 \pm 1.6	3	-27.0	0.2	6-thiomethylpurine
KLS-TRI-B-005	1.93 \pm 0.27	2	-32.6	-5.6	Purine

Table 5.1. Inhibition of *T. b. brucei* nucleobase uptake by thieno-separated tricyclic purine nucleobases. K_i and ΔG° values for the *T. b. brucei* H2 nucleobase transporter. Results are shown \pm standard error.

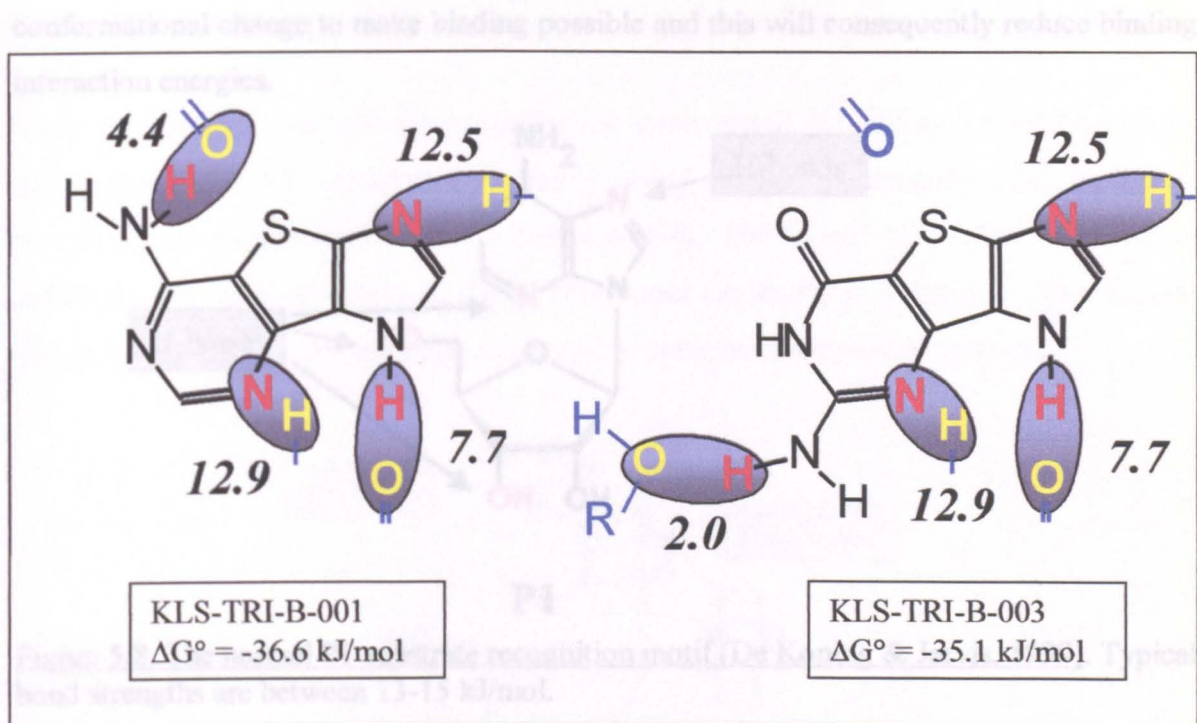


Figure 5.7. Model of the interactions between tricyclic purines and the *T. b. brucei* H2 transporter. Estimations of the Gibbs free energy of these interactions are given in kJ/mol. Hypothetical groups from the H2 binding pockets (blue/yellow) were retained in their positions from the original model as depicted in Wallace, *et al.* (2002) and Chapter 3.

5.2.3 Inhibition of P1 activity by thieno-separated and fleximer purine analogues

Only the nucleoside analogues were assayed for their ability to inhibit uptake of adenosine by the P1 transporter since this transporter is specific for nucleosides and has little affinity for nucleobases. The K_i and ΔG° values obtained for inhibition of adenosine uptake by the P1 transporter are shown in Table 5.2. The table also shows the $\delta(\Delta G^\circ)$ for the analogue compared with the relevant parent molecule.

All the analogues tested showed a worse inhibitory effect on P1 activity than their purine parent molecules. Overall, the fleximer compounds were poorer inhibitors than the tricyclic compounds. This was not totally unexpected since the fleximer molecule is capable of assuming a variety of conformations due to the flexible nature of the link between the ring constituent of the purine system. The entropy of the analogue differs from that of the parent molecule and a certain amount of energy may be required for the

conformational change to make binding possible and this will consequently reduce binding interaction energies.

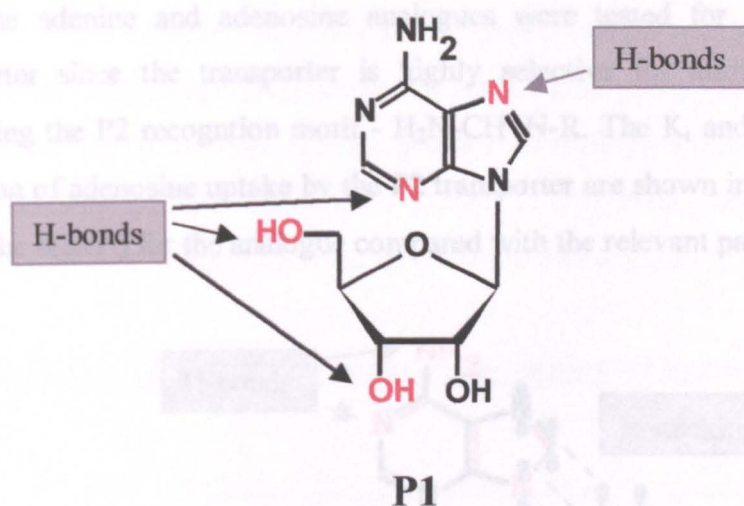


Figure 5.8. The normal P1 substrate recognition motif (De Koning & Jarvis, 1999). Typical bond strengths are between 13-15 kJ/mol.

It is difficult to adequately explain the ΔG° values obtained for the tricyclic analogues in terms of the current recognition model for the P1 transporter (Figure 5.8). All the analogues still possess the residues necessary for recognition, and it would be expected that these residues have shifted by the same degree for all the analogues. The introduction of the thieno-separator seems to have given the 6-aminopurine tricyclic TRI-001 a distinct advantage over tricyclic purines with other groups at position 6 (TRI-002, TRI-003, TRI-004 and TRI-005). It is impossible to construct a viable model for recognition of these purine analogues by the P1 transporter based on these preliminary studies.

Analogue	K_i (μM)	n	ΔG° (kJ/mol)	$\delta(\Delta G^\circ)$ (kJ/mol)	Parent Molecule
KLS-TRI-001	0.98 ± 0.19	3	-34.3	2.5	Adenosine
KLS-TRI-002	26.4 ± 5.0	3	-26.1	10.2	Inosine
KLS-TRI-003	21.1 ± 3.2	3	-26.7	6.1	Guanosine
KLS-TRI-004	748 ± 262	3	-17.8	18.9	6-methylthiopurine nucleoside
KLS-TRI-005	3.9 ± 1.4	3	-27.2	9.6	Purine nucleoside
KLS-FLX-001	95.3 ± 44.5	3	-22.9	13.8	Adenosine
KLS-FLX-002	461 ± 72	3	-19.0	17.2	Inosine
KLS-FLX-003	244 ± 73	3	-20.6	12.1	Guanosine

Table 5.2. Inhibition of *T. b. brucei* P1- transport activity by fleximer and tricyclic nucleoside analogues. K_i and ΔG° values for the inhibition of adenine-insensitive adenosine uptake. Results are shown \pm standard error.

5.2.4 Inhibition of P2 activity by thieno-separated and fleximer purine analogues

Only the adenine and adenosine analogues were tested for ability to inhibit the P2 transporter since the transporter is highly selective for aminopurines and molecules containing the P2 recognition motif - H₂N-CH=N-R. The K_i and ΔG° values obtained for inhibition of adenosine uptake by the P2 transporter are shown in Table 5.3. The table also shows the δ(ΔG°) for the analogue compared with the relevant parent molecule.

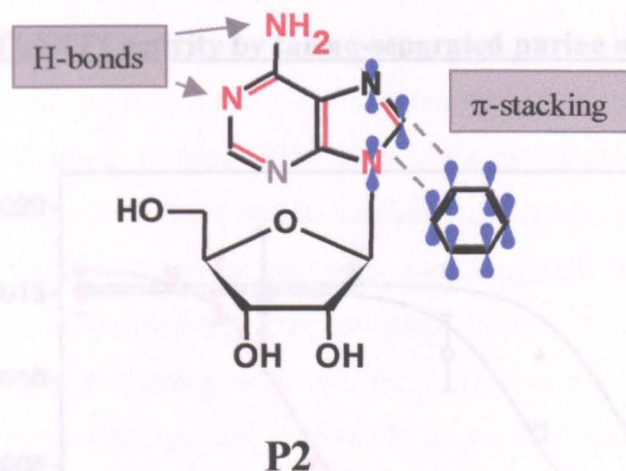


Figure 5.9. The normal P2 substrate recognition motif (De Koning & Jarvis, 1999).

Analogue	K _i (μM)	n	ΔG° (kJ/mol)	δ(ΔG°) (kJ/mol)	Parent Molecule
KLS-TRI-001	16.2 ± 6.8	3	-27.3	7.1	Adenosine
KLS-FLX-001	37.7 ± 3.0	2	-25.2	9.2	Adenosine
KLS-TRI-B-001	9.7 ± 2.3	3	-28.6	8.7	Adenine

Table 5.3. Inhibition of *T. b. brucei* P2- transport activity by fleximer and tricyclic purine analogues. K_i and ΔG° values for the inhibition of inosine-insensitive adenosine uptake. Results are shown ± standard error.

The three relevant molecules were poorer ligands than their parent molecules, despite all the analogues possessing an intact P2 motif. When it is considered that the P2 transporter is involved in the uptake of comparatively large melamine-linked drug molecules it seems less likely that the analogues higher K_i values are due to steric interference. Interestingly, the ΔG° values obtained for the analogues were comparable to the ΔG° obtained for 2-aminopyridine (De Koning & Jarvis, 1999) which consists of the pyrimidine subunit of

adenine. This suggests the difference in ΔG° values are due to some change occurring in the interaction of the imidazole subunit of the purine ring system and the transporter binding site. π - π stacking involving the imidazole subunit has been previously implicated in the recognition of purine molecules by the P2 transporter (De Koning & Jarvis, 1999). The introduction of the third ring in the tricyclic analogues can indeed cause a disruption of π - π stacking as discussed earlier (Seley, *et al.*, 2000), and so this seems a likely explanation for the observed results for the purine analogues.

5.2.5 Inhibition of hFNT1 activity by thieno-separated purine nucleobases

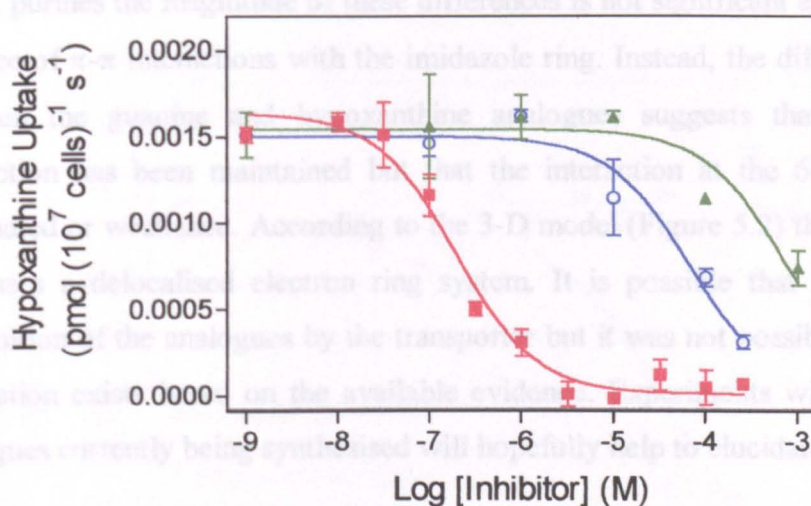


Figure 5.10. Inhibition of transport of 1 μM [^3H] adenine by human erythrocytes by the adenine analogue TRI-B-001 (■), the hypoxanthine analogue TRI-B-002 (▲) or the guanine analogue TRI-B-003 (○).

Representative examples of the dose-response curves for the inhibition of hFNT1 activity by the purine analogues are shown in Figure 5.10. The K_i and ΔG° values obtained for the thieno-separated nucleobase compounds are shown in Table 5.4. The table also shows the $\delta(\Delta G^\circ)$ for the analogue compared with the relevant parent molecule.

The substrate preference for interaction with the hFNT1 is the same for the analogues as for the parent molecules, *i.e.* adenine > guanine \gg hypoxanthine. Uptake of 1 μM adenine was strongly inhibited by the tricyclic adenine analogue with a K_i of 0.47 μM . Intriguingly, this K_i is the highest affinity yet reported for the hFNT1 and is almost 35 times the usual K_m of 16.2 μM for the adenine parent. Meanwhile, the guanine analogue, TRI-B-003, is

slightly less active than guanine itself, with a $\delta(\Delta G^\circ)$ of 2.1 kJ/mol. With a K_i of 290 μM hypoxanthine itself is a poor inhibitor of hFNT1 activity but its tricyclic analogue is even poorer with a K_i of 2440 μM .

It has proven difficult to reconcile these results with the recognition model constructed in Chapter 4. The most significant discrepancy is the very high affinity for the TRI-B-001 adenine analogue. According to the 3-D model of the tricyclic compounds the imidazole ring is no longer able to participate in π - π stacking and so it would have been expected that all analogues would exhibit concordantly worse inhibition of hFNT1. Even though the inhibition of hFNT1 by the guanine and the hypoxanthine analogues is worse than for the parent purines the magnitude of these differences is not significant enough to be due to the absence of π - π interactions with the imidazole ring. Instead, the differences in ΔG° value between the guanine and hypoxanthine analogues suggests that the 2-amino group interaction has been maintained but that the interaction at the 6-keto group has been eliminated or weakened. According to the 3-D model (Figure 5.2) the pyrimidine ring still possesses a delocalised electron ring system. It is possible that this is significant for recognition of the analogues by the transporter but it was not possible to determine if this interaction exists based on the available evidence. Experiments with additional tricyclic analogues currently being synthesised will hopefully help to elucidate this issue.

If it is assumed that steric effects allow equal access to N3 for all the analogues, it follows that the much improved affinity for the TRI-B-001 compared to adenine must be at least partly due to a strengthening of the interactions with the unprotonated N1 and/or 6-amino groups.

Analogue	K_i (μM)	n	ΔG° (kJ/mol)	$\delta(\Delta G^\circ)$ (kJ/mol)	Parent Molecule
KLS-TRI-B-001	0.47 ± 0.21	3	-36.1	-8.8	Adenine
KLS-TRI-B-002	2440 ± 1200	3	-14.9	5.3	Hypoxanthine
KLS-TRI-B-003	64 ± 11	3	-23.9	2.1	Guanine
KLS-TRI-B-004	>1000	3			6-methylthiopurine

Table 5.4. Inhibition of hFNT1- transport activity by tricyclic purine nucleobase analogues. K_i and ΔG° values for the human erythrocyte nucleobase transporter. Results are shown \pm standard error.

5.2.6 Trypanotoxicity of thieno-separated and fleximer purine analogues

The thieno-separated purine analogues and the fleximer purine nucleosides were tested for trypanocidal activity against *T. b. brucei* bloodstream forms *in vitro* in the same way as described in Chapter 3. The Alamar Blue assays were performed with *T. b. brucei* s427 bloodstream forms and *T. b. brucei* TbAT1 knockout bloodstream forms.

Figure 5.11 shows Alamar Blue assay dose-response curves for TRI-B-004 as compared to trypanocidal activity of allopurinol and aminopurinol. Table 5.5 show the EC₅₀ values obtained in Alamar Blue assays for the two parasite lines.

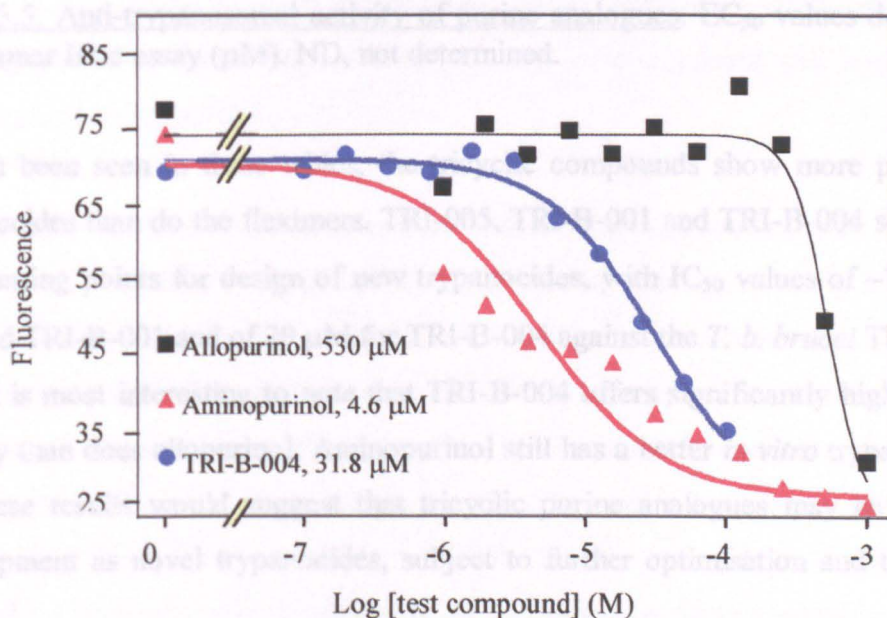


Figure 5.11. Example of Alamar Blue assay graph. Trypanotoxicity of TRI-B-004 compared with aminopurinol and allopurinol. *T. b. brucei* TbAT1 KO. The fluorescence was measured using 530 nm excitation, 590 nm emission parameters. This graph was constructed using the data produced from one of two identical experiments which gave comparable results.

Analogue	<i>T. b. brucei</i> s427 EC ₅₀ (μM)	n	<i>T. b. brucei</i> TbAT1 KO EC ₅₀ (μM)	n
KLS-TRI-001	>100	2	>100	1
KLS-TRI-002	595 ± 35	2	>100	1
KLS-TRI-003	652 ± 19	2	>100	1
KLS-TRI-004	>100	2	>100	2
KLS-TRI-005	69.2 ± 14.8	2	66 ± 16	3
KLS-FLX-001	1660 ± 71	2	ND	
KLS-FLX-002	1205 ± 60	2	ND	
KLS-FLX-003	868 ± 0.35	2	ND	
KLS-TRI-B-001	155 ± 1	2	71 ± 12	3
KLS-TRI-B-002	450 ± 7	2	>100	3
KLS-TRI-B-003	243 ± 1	2	>100	3
KLS-TRI-B-004	69.1 ± 6	3	29 ± 4	3
KLS-TRI-B-005	>100	2	>100	3

Table 5.5. Anti-trypanosomal activity of purine analogues. EC₅₀ values determined using the Alamar Blue assay (μM). ND, not determined.

As can be seen in these tables, the tricyclic compounds show more potential as lead trypanocides than do the fleximers. TRI-005, TRI-B-001 and TRI-B-004 seem to offer the best starting points for design of new trypanocides, with IC₅₀ values of ~70 μM for TRI-005 and TRI-B-001 and of 29 μM for TRI-B-004 against the *T. b. brucei* TbAT1 knock out line. It is most interesting to note that TRI-B-004 offers significantly higher trypanocidal activity than does allopurinol. Aminopurinol still has a better *in vitro* trypanocidal activity but these results would suggest that tricyclic purine analogues may have potential for development as novel trypanocides, subject to further optimisation and their therapeutic index.

5.3 Discussion

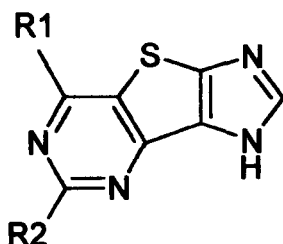
The study detailed in this chapter has demonstrated how specially-constructed purine analogues can be used both as investigational tools and as potential trypanocides. A number of the purine analogues showed encouraging trypanocidal activity which can hopefully be optimised with further molecular engineering. The use of the analogues have also contributed to our knowledge of how purines are recognised by the various purine transporters, and have also given insight into the physical dimensions of the transporter binding pocket.

The results detailed here are preliminary and have been limited by the small number and quantities of compounds available. More compounds are currently being synthesised and 1-deaza- and 3-deaza-tricyclics in particular should augment the preliminary understandings detailed here. The availability of a larger range of compounds will enable some of the findings here to be verified.

Despite these recognised limitations some initial inferences can be made. The affinity with which the analogues are recognised by the H2 transporter are certainly lower than for the parent molecules but the K_i values derived for the compounds are still in the low or sub-micromolar range. This study has shown that even tricyclic purines are efficiently and selectively recognised by the transporter. We have not proven that the analogues are actually internalised by the parasites but the fact that at least some of them do have a degree of *in vitro* efficacy is highly suggestive that they are able to be taken up by one or more of the transport systems present in the trypanosomal plasma membrane.

As noted earlier, any speculation about the interaction of the analogues with the H2 transporter are dependent on the assumption that the position and binding interactions of the imidazole ring really is unchanged. Although the hypoxanthine analogue shows less affinity for the H2 transporter than the adenine analogue the selectivity index for the recognition of TRI-B-002 by the H2 transporter as compared to the recognition by hFNT1 is around 1300. This would appear to reinforce the suggestion from earlier chapters that hypoxanthine analogues are likely to be the most interesting lead compounds from the selective targeting perspective. Table 5.6 shows the selectivity indices for the recognition

of the thieno-separated tricyclic nucleobases for the parasite H2 transporter as compared to hFNT1.



Compound	R ₁	R ₂	S.I FNT1/H2
TRI-B-001	NH ₂	H	1.24
TRI-B-002	O	H	1304
TRI-B-003	O	NH ₂	91.5
TRI-B-004	SCH ₃	H	>50
TRI-B-005	H	H	N.D

Table 5.6. The selectivity indices of thieno-separated tricyclic purine nucleobases for uptake by the H2 transporter and hFNT1.

Matters are somewhat complicated by the fact that although the adenine analogue shows very high affinity for both H2 and hFNT1, and so relatively low selectivity for the parasite, this analogue seems to offer a higher trypanocidal potential, based on the evaluation of the *in vitro* effects.

Although the trypanocidal activity of the analogues clearly needs optimisation, most of the analogues tested (with the notable exception of the fleximers) have comparable or better trypanocidal activity than allopurinol. Indeed, the action of TRI-B-004 is already 10-fold better against bloodstream form trypanosomes *in vitro* than allopurinol.

Purine nucleobase analogues may be more amenable to use as trypanocides since nucleosides are rapidly hydrolysed following acquisition by the parasite. The nucleobase on the other hand is just one enzyme step from the nucleotide pool through phosphoribosylation. One obvious mode of action for purine antimetabolites is their incorporation into RNA and DNA and so nucleobase analogues are that much closer to the end "target". In addition, as noted in previous chapters, nucleobase-specific transporters have the attraction of not having been implicated in the development of resistance and so

drugs entering through these transporters are less likely to show cross-resistance to existing drugs such as the arsenicals. The complicating issue in this argument is that the transporter that has been definitively shown to play a role in the development of drug resistance (but that is not the only contributory factor) is the P2 transporter which has a very high affinity for adenine (Carter & Fairlamb, 1993). With the compounds that have been tested in this study the absence of a conjugated π -system has meant that the affinity of the analogues for the P2 is much reduced. The analogue which showed the most promising *in vitro* activity, in spite of showing only moderate interaction with the H2 transporter, was TRI-B-004. Based on its structure, this compound is unlikely to be an efficient substrate for the P1 or P2 transporter.

In the case of the fleximers there was a correlation in that poor recognition by the transporters was paired with concurrent poor trypanocidal effects. The correlation was not straightforward however. While the affinity of the P1 and P2 transporter for FLX-001 was the highest of all the fleximers, the *in vitro* effect of this analogue showed the worst IC_{50} .

Another intriguing aspect thrown up by the study was that several of the analogues were more toxic to the TbAT1 KO cells than the WT cells. In a paired Student's T-test these groups are not significantly different, partly because of the limited amount of data available. However, it raises the possibility that there is an upregulation of other transporter(s) in the absence of a functional P2 system. This could mean that drug-resistant strains could actually be more vulnerable to the effects of purine nucleobase drugs. While this possibility is highly intriguing, it is at the moment also highly speculative and will require further investigation.

It should be interesting to test what effect these unique compounds have on the parasite phosphoribosyltransferases and the other enzymes of purine metabolism and to study any incorporation into nucleotides. If the compounds strongly or even irreversibly inhibit the action of the parasite PRTases another chemotherapeutic option could be to administer a combination of the tricyclic purines so as to impede incorporation of natural purines by the PRTases with different substrate specificities (adenine PRTase, hypoxanthine/guanine PRTase and xanthine PRTase). Any effects on the parasite would have to be very potent since the trypanosome is able to survive if even low amounts of purine are able to be salvaged. Also this would again very much depend on any effect on the mammalian

systems. The thieno-separated tricyclic adenine and guanine analogues used in this study have previously been shown to have biological activity against colorectal tumour cells (Seley, *et al.*, 2000), with the adenine analogue inhibiting growth of these cells by up to 50% over 72 hours. Ideally, molecular recognition models should be worked out for concentrative transporters of mammalian systems and also for the various purine-metabolising enzymes.

Many other tricyclic purine analogues have been constructed and it may be interesting to test some of these other compounds on trypanosomes. As well as utilising different spacer rings, additional rings can also be added to the periphery of the natural ring system to give alternative tricyclic structures (Seley, 2002).

As discussed in Chapter 3 it is the ability of substrates to form interactions with the enzyme that leads to “recognition”. It therefore makes sense that analogues which possess the abilities necessary to maintain these elements but have an extended ring system and so are shaped differently can tell us a lot about the nature of enzyme-substrate recognition. In terms of chemotherapy, hopefully, these shape-modified molecules will be sufficiently well recognised by the parasite transporters and enzymes but will be disruptive when incorporated into nucleotide systems such as RNA, DNA, and ATP, or possibly disrupt metabolic, signalling or other pathways dependent on purines as substrates or co-factors.

With further work, the selectivity for the trypanosomal transporters and the anti-trypanosomal action of these compounds could be increased by modifications to the tricyclic purine structure.

Chapter Six

Functional complementation strategy for cloning of nucleobase transporter genes from *T. b. brucei*

6.1 Introduction

The availability of gene clones is an invaluable tool in the characterisation of transporters and other proteins. The identification of a gene can allow further characterisation of the function and kinetic parameters of the resulting protein in a suitable heterologous system. The amino acid sequence will allow first predictions about protein secondary structure. Residues important for the function of the protein can be identified using site-directed mutagenesis leading to models for the structure of the active/binding sites. Furthermore, elucidation of the gene sequence allows comparisons with homologues in other organisms and the mapping of evolutionary relationships as well as in-depth studies of regulation of gene expression and localisation studies using antibodies or fusion proteins.

Until relatively recently studies of nucleoside and nucleobase transport in trypanosomatids relied almost exclusively on biochemical methodologies with little or no input from molecular approaches. This was largely due to the absence of gene information. When the work detailed in this chapter was undertaken, this situation was beginning to change with the cloning of nucleoside transporter genes from *T. b. brucei* (Sanchez, *et al.*, 1999; Mäser, *et al.*, 1999; Sanchez, *et al.*, 2002) and *Leishmania donovani* (Vasudevan, *et al.*, 1998; Carter, *et al.*, 2000). Some of the nucleoside transporters cloned by these groups were shown to mediate transport of nucleobase molecules in addition to nucleosides but usually with lower affinity than for the corresponding nucleoside and none of these genes were responsible for the high-affinity dedicated nucleobase transport activities seen in *T. b. brucei*. The aim of the work described in the next chapters was to clone and characterise nucleobase transporter genes from *T. b. brucei*.

Several approaches were taken towards the identification of the nucleobase transporter genes. The initial strategy was to construct genomic DNA libraries for functional complementation studies in *T. b. brucei* itself and also in the ascomycete *Aspergillus nidulans*. It was anticipated that the cloning of one transporter gene sequence would facilitate the identification of other related transporter genes from the trypanosome genome database.

6.1.1 Functional complementation in *T. b. brucei*

Functional complementation is a reliable method for cloning of genes in *Leishmania spp* (Clayton, 1999). The first trypanosomatid purine transporter genes to be cloned were the *Leishmania donovani* nucleoside transporters *LdNT1.1* and *LdNT1.2* (Vasudevan, *et al.*, 1998). These were isolated following functional complementation of a parasite line resistant to the nucleoside analogue drug tubercidin. The *LdNT2* nucleoside transporter gene was also identified by functional complementation of a parasite line resistant to the nucleoside analogue formycin B (Carter, *et al.*, 2000).

Sommer, *et al.* (1996) showed that functional complementation was a valid method of gene cloning in *T. b. brucei*. In this study, transfection of a *T. b. brucei* genomic library into the ornithine decarboxylase (ODC) double-knockout cell line complemented the deficiency and allowed the isolation of plasmids containing the ODC gene. In order to accomplish the cloning of a nucleobase transporter gene by functional complementation in *T. b. brucei*, a genomic DNA library in a suitable vector had to be constructed and a nucleobase transport-deficient background had to be established.

Introduction of exogenous genes into *T. b. brucei* is possible using homologous recombinatory events (Lee & Van der Ploeg, 1990) but the transformation frequencies obtained are relatively low and unlikely to be suitable for use in functional complementation studies. In the method pioneered by Sommer and colleagues (1996) an episomal self-replicating plasmid was constructed and it was this vector that was used for construction of the genomic DNA library. The pTSO-HYG4 vector contains an origin of replication (*ori*) isolated from a mitochondrial kinetoplastid minicircle (Metzenberg & Agabian, 1994) which allows autonomous replication of the plasmid. To ensure expression of inserted gene sequences the vector also possesses the PARP (procyclic acidic repetitive protein) promoter. This promoter is routinely used in *T. b. brucei* vectors and normally controls the expression of procyclin which is constitutively expressed in procyclic parasites. To ensure the proper post-transcriptional processing of mRNA from introduced genes the vector also contains splice sites in the multi-cloning site to allow for the addition of the splice leader sequence typically appended to all *T. b. brucei* mRNA molecules.

The use of procyclics rather than bloodstream forms for the selection model was preferred due to several important practical considerations. Firstly, procyclics had the advantage of being simple to handle, easy to grow up in bulk and transformation protocols for procyclics were also more straightforward and featured higher transformation efficiencies than for bloodstream form parasites. In addition, at the time this strategy was devised the only purine nucleobase transport component known to exist in procyclics was the H1 activity (De Koning & Jarvis, 1997a). By exposing cell cultures of procyclic *T. b. brucei* S427 parasites to increasing concentrations of the toxic purine nucleobase analogue allopurinol it was hoped that a nucleobase transport-deficient cell line would be generated through an induced loss of the transporter responsible for the H1 activity.

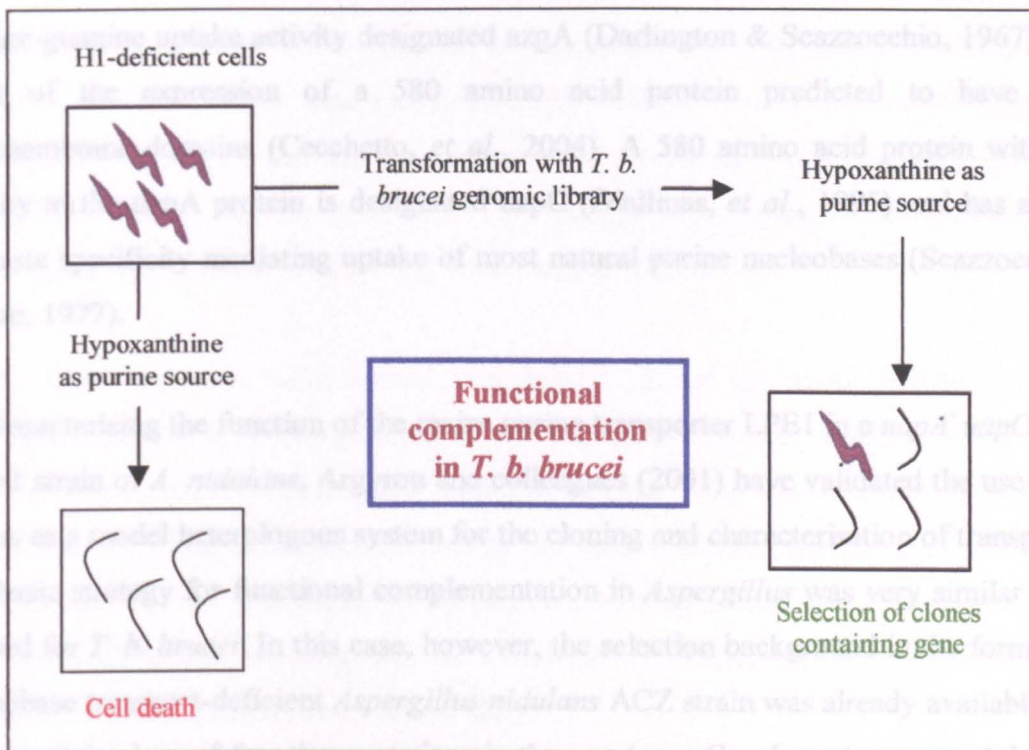


Figure 6.1. Functional complementation strategy in *T. b. brucei*.

The complementation strategy is represented diagrammatically in Figure 6.1. A procyclic *T. b. brucei* S427 line deficient in H1 activity due to drug pressure should be unable to grow on medium containing hypoxanthine as the sole purine source. Transformation of this newly transporter-deficient line with the *T. b. brucei* DNA library would allow the isolation of clones able to grow in the selective medium. The plasmid responsible for the

restoration of transport could then be extracted from the *T. b. brucei* cells and the gene sequenced.

6.1.2 Functional complementation in *Aspergillus nidulans*

Purine metabolism and uptake in *Aspergillus nidulans* has been extensively researched and the genes for the nucleobase transporters have been cloned and characterised. The *uapA* gene encodes a 595 amino acid protein predicted to have 12-14 membrane-spanning regions (Diallinas & Scazzocchio, 1989; Gorfinkiel, *et al.*, 1993) and is responsible for uptake of uric acid and xanthine (Darlington & Scazzocchio, 1967). A hypoxanthine-adenine-guanine uptake activity designated *azgA* (Darlington & Scazzocchio, 1967) is the result of the expression of a 580 amino acid protein predicted to have 10-12 transmembrane domains (Cecchetto, *et al.*, 2004). A 580 amino acid protein with 58% identity to the *uapA* protein is designated *uapC* (Diallinas, *et al.*, 1995) and has a broad substrate specificity mediating uptake of most natural purine nucleobases (Scazzocchio & Gorton, 1977).

By characterising the function of the maize purine transporter LPE1 in a *uapA⁻ uapC⁻ azgA⁻* mutant strain of *A. nidulans*, Argyrou and colleagues (2001) have validated the use of this fungus as a model heterologous system for the cloning and characterisation of transporters. The basic strategy for functional complementation in *Aspergillus* was very similar to that devised for *T. b. brucei*. In this case, however, the selection background in the form of the nucleobase transport-deficient *Aspergillus nidulans* ACZ strain was already available. This strain contains loss-of-function mutations in the *uapA*, *uapC* and *azgA* genes and therefore lacks endogenous purine transport systems. Functional complementation in *A. nidulans* was carried out in collaboration with Dr. G. Diallinas and colleagues at the University of Athens. A second DNA library had to be constructed in an *Aspergillus* expression vector.

The pNS328 vector used for construction of the DNA library for transformation of *Aspergillus* was derived from pAN519. Regulatory sequences which usually control expression of the *uapA* gene surround the *Bam*HI cloning site and should drive the transcription of introduced sequences. The vector integrates into the *A. nidulans* genome by heterologous recombination.

6.2 Results

6.2.1 *T. b. brucei* genomic DNA libraries

Both libraries were constructed: one for expression in *T. b. brucei* and the other for expression in *Aspergillus nidulans*. The appropriate plasmids, pTSO-HYG4 (Figure 6.2) and pNS328 (Figure 6.3), were amplified in *E. coli*, then linearised by *Bam*HI digestion and the ends were de-phosphorylated with calf intestinal alkaline phosphatase (CIAP) as described in Chapter 2. After this treatment, the plasmids were gel-purified to minimise contamination with any uncut plasmid. Genomic DNA extracted from *T. b. brucei* S427 procyclics was partially-digested with the enzyme *Sau*3A to generate a “random” collection of fragments. This enzyme is commonly used to generate DNA library fragments. It has the four base recognition site ↓GATC and in a complete digest cuts roughly every 256 bp. It also has the advantage of generating 5' overhangs compatible for cloning into *Bam*HI, *Bcl*I or *Bgl*II sites. This reaction was run out on an agarose gel and fragments of the required size (2-6 kb) were excised (Figure 6.4).

The purified fragments were ligated into *Bam*HI site of the multi-cloning site of the appropriate linearised, de-phosphorylated vector (Figure 6.5). The resulting products were used to transform electrocompetent *E. coli* TOP10 cells. Selection of transformed colonies was by the ampicillin-resistance encoded by the vector. Random screening of the resulting colonies was carried out to check for the presence of integrated genomic fragments (Figure 6.6). The basis of the screening was the *Hind*III restriction digest of miniprep colony plasmids to evaluate insert presence and size.

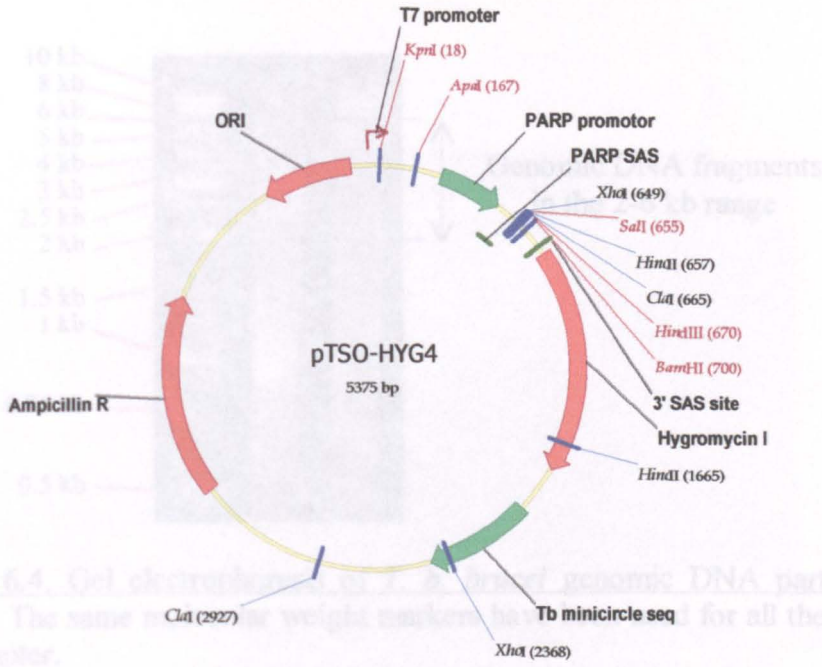


Figure 6.4. Gel electrophoresis of genomic DNA partially-digested using *Sma*IA. The same weight markers have been used for all the gels documented in that chapter.

Figure 6.2. Plasmid vector pTSO-HYG4 (Sommer, et al., 1996).

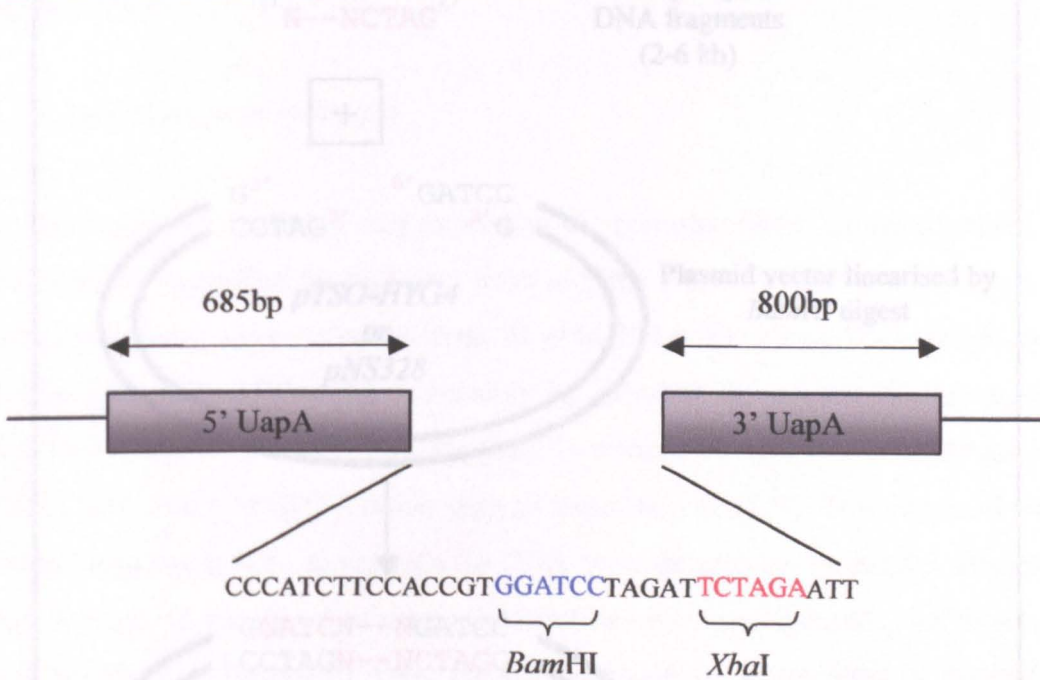


Figure 6.3. The UapA transcriptional cassette of plasmid vector pNS328.

Figure 6.5. Location of *Sma*IA fragments and plasmid vector

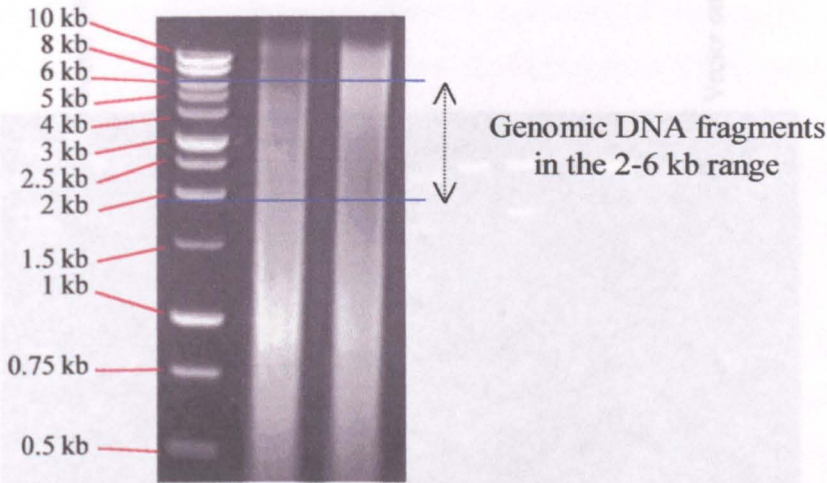


Figure 6.4. Gel electrophoresis of *T. b. brucei* genomic DNA partially-digested using *Sau3A*. The same molecular weight markers have been used for all the gels documented in this chapter.

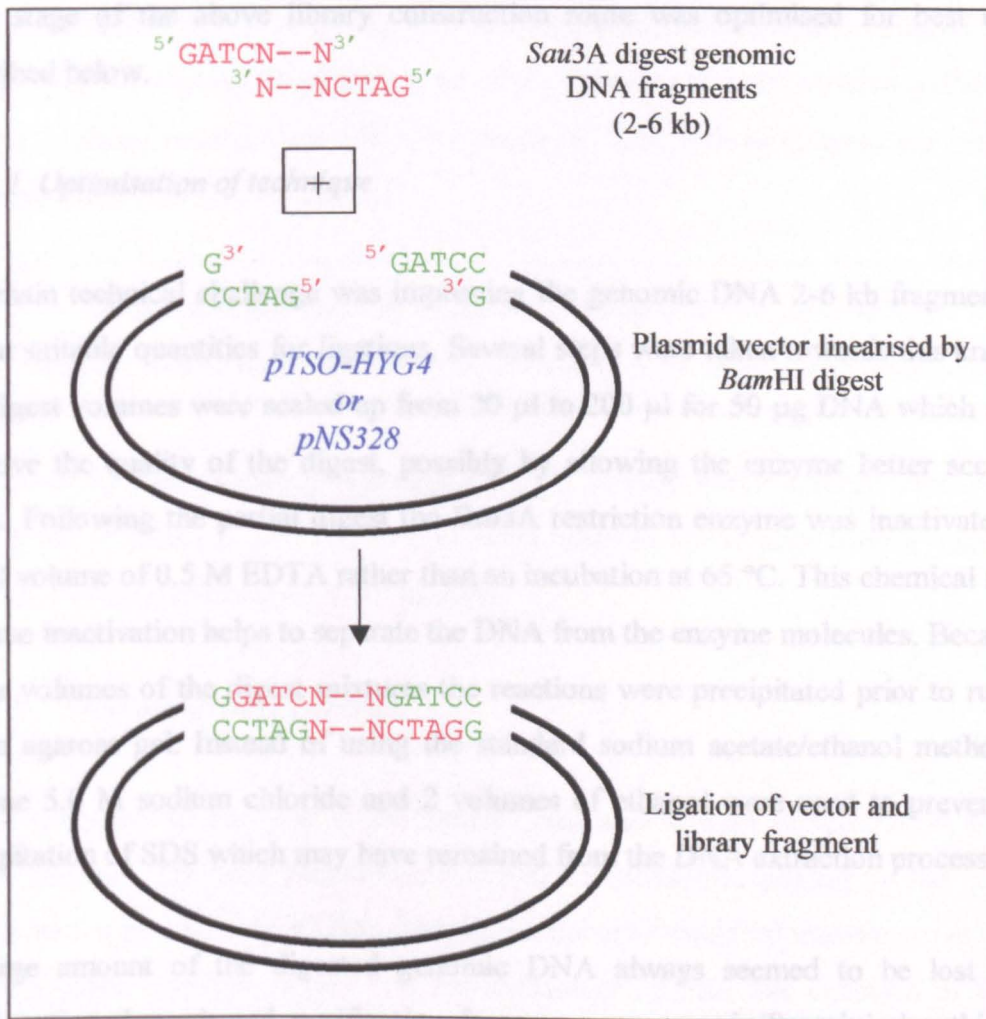


Figure 6.5. Ligation of *Sau3A* fragments and plasmid vector.



Figure 6.6. Nine random library colony minipreps digested with *HindIII*. The clones show a good range of different insert lengths and compositions (2 to 5 kb).

Each stage of the above library construction route was optimised for best results, as described below.

6.2.1.1 Optimisation of technique

The main technical challenge was improving the genomic DNA 2-6 kb fragment yield to obtain suitable quantities for ligations. Several steps were taken towards this end. First of all, digest volumes were scaled up from 20 μ l to 200 μ l for 50 μ g DNA which seemed to improve the quality of the digest, possibly by allowing the enzyme better access to the DNA. Following the partial digest the *Sau3A* restriction enzyme was inactivated using a 1/100 volume of 0.5 M EDTA rather than an incubation at 65 $^{\circ}$ C. This chemical method of enzyme inactivation helps to separate the DNA from the enzyme molecules. Because of the larger volumes of the digest mixtures the reactions were precipitated prior to running out on an agarose gel. Instead of using the standard sodium acetate/ethanol method, a 1/25 volume 5.0 M sodium chloride and 2 volumes of ethanol were used to prevent any co-precipitation of SDS which may have remained from the DNA extraction process.

A large amount of the digested genomic DNA always seemed to be lost following fractionation through and purification from an agarose gel. To minimise this loss the partially-digested DNA was run slowly (20V for up to 6 hours) to aid separation in a

“trench” rather than in individual lanes – this limited the time taken to excise the appropriate gel portion under damaging UV and reduced the amount of agarose associated with the DNA. When using the QIAGEN Gel Extraction Kit to purify the DNA from the agarose the maximum weight of agarose used in separation columns was 50-100 mg. According to the manufacturer’s instructions each column can handle up to 400 mg of agarose but using more than 100 mg drastically reduced the DNA yield.

The results of several transformation procedures were not satisfactory because contamination by small quantities of circular plasmid due to either incomplete linearisation or incomplete dephosphorylation by CIAP resulted in large numbers of colonies containing empty vector. This problem was corrected by adjusting the quantities of DNA and enzyme used in the linearisation and CIAP treatment, to allow complete reactions.

It was verified that the *E. coli* TOP10 cells used for electroporation were of suitably high transformation efficiency by setting up a control transformation with 0.01 ng of the control plasmid pUC18. Plating 10 µl from 1 ml of the transformed cells resulted in the formation of 852 separate colonies on LB solid medium. The following equation was used to calculate transformation efficiency:

$$\text{Transformation efficiency (colony forming units per } \mu\text{g of DNA)} = \\ (\text{cfu on control plate/ng of control DNA}) \times (1 \times 10^3 \text{ ng}/\mu\text{g}) \times \text{dilution plated}$$

The transformation efficiency was thus 8.5×10^9 cfu/µg, which is more than adequate for these types of cells (*E. coli* TOP10 purchased ready to use usually boast a transformation efficiency of approximately 1×10^9 cfu/µg).

6.2.1.2 Validation of DNA libraries

It was necessary to establish if the libraries constructed were representative of the *T. b. brucei* genome. The total number of bacterial transformants making up the *T. b. brucei* library was approximately 92,000. The total number of bacterial transformants making up the *Aspergillus nidulans* library was approximately 50,000. The equation of Clarke and Carbon (1976) allows the calculation of the minimum number of transformation events

required in a screening for a particular DNA sequence to be present within a randomly produced library with 99% probability (*i.e.* $P = 0.99$).

$$N = \ln(1-P) / \ln[1 - (1/n)]$$

where N = number of events to be screened (*i.e.* number of colonies required)
 P = probability of obtaining a particular fragment
 n = size of haploid genome (kb) / size of fragment used (kb)

In *T. b. brucei* the haploid genome size is 3.7×10^4 kb. The libraries were produced using DNA fragments in the range 2-6 kb. If it is assumed the average insert size is 4 kb, the minimum number of transformants for 99% coverage is ~43,000. Both libraries meet this minimum criterion. The number of transformants obtained for the pTSO-HYG4 library was more than double this so the coverage of the library is more than satisfactory. This level of coverage represents almost ten haploid genome equivalents.

The pTSO-HYG4 library was also validated by the amplification of known gene sequences by polymerase chain reaction. The sequences chosen for this validation were all well-studied genes, and included known or putative purine transporter genes and the enzyme phosphogluconate dehydrogenase (PGND). The PCR primers for PGND and AT1 did not span the entire reading frames and so only fragments were produced. It is especially relevant that the TbAT1 gene was successfully amplified from the library since this gene is known to be a single copy gene. The PCR using the primers for NTX produced at least two products and this fits the profile of this putative transporter belonging to a family of closely-related genes.

Primer	Sequence	Annealing temp.
PGND – F	5' -GACTGGATCCATGTCAATGGATGTCGGTGTT-3'	60 °C
PGND – R	5' -GACTAAGCTTCCAATCTTCAAGAACGGCAGC-3'	'
NTX – R	5' -AAAGTGGTGTAGTGAGAGGC-3'	55 °C
NTX – F	5' -TTAACTGAATTGCATCGCTGG-3'	'
AT1 – F	5' -GACTGGATCCATGCTCGGGTTTGACTCAGCC-3'	55 °C
AT1 – R	5' -GACTAAGCTTTCATCGCCTCCGTGGGGGTCA-3'	'

Table 6.1. Primers used for polymerase chain reactions using DNA library as template.

Figure 6.7 shows gel electrophoresis of the PCR products resulting from use of the library DNA as reaction template.

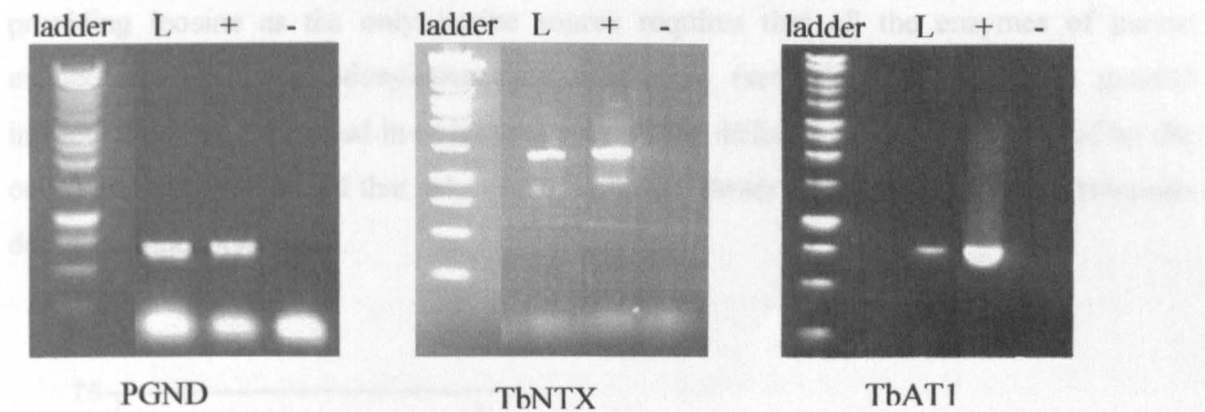


Figure 6.7. PCR reactions using library as template. The template for the positive controls was 20 ng genomic DNA. The negative controls contained no DNA template at all.

The range of sequences amplified was obviously limited but the presence of known DNA sequences in the library was encouraging. These results are by no means proof that the library represents the whole genome but it gives an indication that the quality of the library could be sufficiently representative.

6.2.2 Growth of *T. brucei* procyclics in allopurinol in attempt to obtain H1-deficient line

A *T. b. brucei* S427 line lacking purine nucleobase transporters was to be developed through exposure to increasing levels of allopurinol as described in the introduction to this chapter. It was an experimental concern that resistance to allopurinol could also be induced by changes in purine metabolism rather than loss of the H1 transporter. Loss of the adenylosuccinate synthetase enzyme responsible for conversion of the allopurinol ribonucleotide to the active adenosine ribonucleotide analogue would also render allopurinol ineffective. To prevent this alternative metabolic change taking place and to minimise allopurinol having to compete for access to the H1 transporter with hypoxanthine in the medium, the *T. b. brucei* S427 procyclics were grown in purine-free trypanosome medium (PFTM) (De Koning, *et al.*, 2000) supplemented with inosine. Inosine is taken up by the P1 nucleoside transporter expressed in the procyclic life-cycle stage and is

converted into inosine nucleotides by the action of purine nucleoside hydrolase and hypoxanthine-guanine phosphoribosyltransferase. Growth on inosine as the sole purine source should not be affected by the loss of the hypoxanthine transporter. However, providing inosine as the only purine source requires that all the enzymes of purine metabolism, including adenylosuccinate synthetase (see Figure 1.12 in the general introduction), are functional in order to supply all the different nucleosides required by the cell. This strategy ensured that selection of resistant clones would be based on a transport-deficient phenotype only.

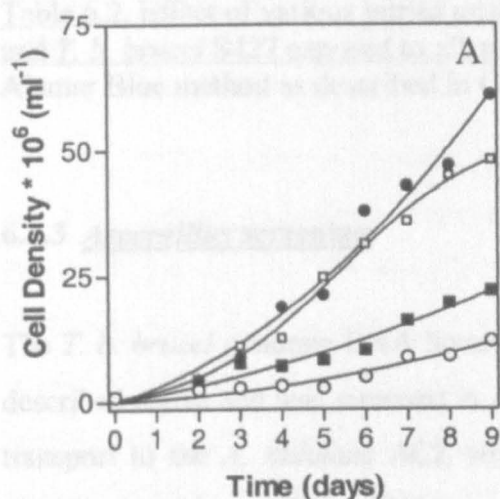


Figure 6.8. Effect of allopurinol on growth of *T. b. brucei* S427 procyclics. Trypanosomes were seeded at 10^6 cells/ml in PFTM with 200 μ M of inosine as sole purine source and grown at 25 °C in the presence of 2 mM (○), 1 mM (■), 15 μ M (□) or no allopurinol (●).

The presence of allopurinol in the culture medium affected procyclic growth in a dose-dependent manner (Figure 6.8) but some growth continued to occur even in the highest concentration of allopurinol tested (2 mM). *T. b. brucei* S427 procyclic cells were continually maintained in PFTM [+inosine] with 2 mM allopurinol for an extended period of time (>12 months). Growth rates were consistently lower than those observed for *T. b. brucei* S427 procyclics grown under the same media conditions minus the allopurinol. No resistance to allopurinol occurred. When the effect of various experimental compounds on survival of the allopurinol exposed cells was compared to their effect on *T. b. brucei* S427 WT cells it was observed that the results were not significantly different for the two types of cells (Table 6.2).

Compound	Control		Allopurinol exposed	
	ED ₅₀ (μM)	n	ED ₅₀ (μM)	n
Adenine-9-β-D-arabinofuranoside	90 ± 22	4	127 ± 46	3
Allopurinol	380 ± 101	5	315 ± 72	3
Aminopurinol	12 ± 2	3	11 ± 5	3
6-chloropurine	850 ± 260	3	680 ± 20	3
Thiopurinol	300 ± 68	5	280 ± 60	3
2,6-dichloropurine	290 ± 56	5	310 ± 76	3
Pentamidine	0.35 ± 0.04	4	0.41 ± 0.11	3
Melarsen oxide	0.46 ± 0.12	4	0.58 ± 0.23	3

Table 6.2. Effect of various purine analogues and trypanocides on *T. b. brucei* S427 WT and *T. b. brucei* S427 exposed to allopurinol. ED₅₀ values were determined using the Alamar Blue method as described in Chapter 2.

6.2.3 *Aspergillus* screening

The *T. b. brucei* genomic DNA library for expression in this organism was constructed as described above and was screened in Athens for fragments capable of restoring nucleobase transport to the *A. nidulans* ACZ strain and allowing survival on hypoxanthine as sole nitrogen source. The library was transformed into the transport-deficient (Δ uapA/ Δ uapC/ Δ azgA) mutant strain but there was no success in identifying rescued cells.

6.3 Discussion

The functional complementation approach to cloning of transporter genes from *T. b. brucei* undertaken relied on the availability of both the genomic libraries and the appropriate selection backgrounds.

Construction of the genomic DNA libraries was ostensibly a straight-forward process but in practice the optimisation of the individual steps proved to be quite challenging and required a great deal of perseverance. However, satisfactory libraries of good quality were eventually produced and validated using the Carbon-Clarke equation and a small series of PCRs.

The attempt to produce a nucleobase transport-deficient parasite line relied on H1 being the only purine nucleobase transporter present in procyclics. Previous research had intimated that this was the situation in *T. b. brucei* S427 (De Koning & Jarvis, 1997a). Following the failure to induce allopurinol resistance by exposing cultures to allopurinol, uptake of [³H] allopurinol by procyclics was studied in the laboratory by M.Sc. student Manal Natto. This work showed that 1 μM [³H] allopurinol was rapidly taken up *T. brucei brucei* S427 procyclics with a rate of 0.48 ± 0.02 pmol (10⁷ cells)⁻¹ min⁻¹, compared with a initial uptake rate of 1.6 ± 0.1 pmol (10⁷ cells)⁻¹ min⁻¹ in *L. major* promastigotes (Al-Salabi, *et al.*, 2003). It was also shown that uptake of allopurinol radiolabel by the procyclics trypanosome could be completely inhibited by high concentrations of either unlabelled hypoxanthine or allopurinol. However, the uptake activity was only partially inhibited by uracil. This suggested that, contrary to the earlier studies, there were possibly two nucleobase transport activities present in *T. b. brucei* procyclics.

Further work in our lab by Mohammed Al-Salabi led to the characterisation of this second activity which was designated H4 (characterisation described in Burchmore, *et al.*, 2003).

When the hypoxanthine uptake activities by H1 and H4 in the allopurinol exposed cells were compared with that in control cells (Table 6.3), no significant differences were observed, though V_{\max} values were somewhat lower in the exposed cells. The K_i values for the inhibition of uptake of [³H] hypoxanthine by allopurinol for the two transporters were

found to be $5.0 \pm 0.9 \mu\text{M}$ and $2.5 \pm 0.4 \mu\text{M}$ for H1 and H4, respectively. The failure to induce the loss of the procyclic nucleobase transport activity must be attributed in large part to the presence of two separate transporters equally able to mediate allopurinol uptake. An additional factor may have been that allopurinol is not sufficiently toxic at low concentrations to apply strong selective pressure. Since uptake of allopurinol by *T. b. brucei* procyclics was shown to be reasonably efficient, this insufficient *in vitro* toxicity compared to the leishmanicidal activity of allopurinol, is likely to be due to differences in the metabolism of allopurinol in the different trypanosomatids.

	H1			H4		
	K_m (μM)	V_{max} ($\text{pmol}/10^7 \text{ cells/s}$)	n	K_m (μM)	V_{max} ($\text{pmol}/10^7 \text{ cells/s}$)	n
Control	15.2 ± 2.3	2.4 ± 0.7	7	0.55 ± 0.07	0.27 ± 0.08	7
Exposed cells	19.5 ± 7.0	1.2 ± 0.6	8	0.49 ± 0.14	0.09 ± 0.02	8

Table 6.3. Kinetic parameters of procyclic hypoxanthine transporters in control and long-term allopurinol exposed cells. Experiments carried out by Mohammed Al-Salabi at the University of Glasgow.

The failure of the functional complementation of *Aspergillus* mutants to identify nucleobase transporter sequences from the *T. b. brucei* library was disappointing. It is possible that the *Aspergillus* cellular machinery is not compatible with the expression, processing and targeting of the *T. b. brucei* transporter gene product. There has also been the suggestion that multiple integration events into the *Aspergillus* genome can be toxic and that the resulting over-expression of genes (even those normally found in *Aspergillus*) can lead to significant decreases in cell growth (Argyrou, *et al.*, 2001). Yeast studies have suggested that over-expression of endogenous and/or introduced transporter gene may lead to over-crowding during formation of membrane proteins in the ER or Golgi (Loayza *et al.*, 1998) and thus to degradation of the protein or the formation of inclusion bodies. Other attempts to express a known *T. b. brucei* purine transporter gene in *A. nidulans* were also unsuccessful (De Koning, unpublished).

The functional complementation attempted in our laboratory did not lead to the identification of novel transporter sequences but I believe the approach in *T. b. brucei* is still a valid concern if the appropriate background could be established. With the advent of

novel molecular techniques, such as RNA interference (LaCount, *et al.*, 2000), there are new options for the construction of deficient backgrounds for the cloning of genes.

Chapter Seven

**Characterisation of a novel ENT family member as the first
protozoan nucleobase transporter**

7.1 Introduction

Another approach to the cloning of the *T. b. brucei* nucleobase transporter genes, carried out in parallel to attempts at functional complementation, was the regular interrogation of the burgeoning *T. b. brucei* genome database with the aim of identifying sequences with homology to known nucleobase transporter genes.

7.1.1 Identification of sequence in *T. b. brucei* genome database with homology to TbAT1

The first steps towards the sequencing of the entire *T. b. brucei* 927 genome were taken in 1994. The majority of the actual sequencing has been undertaken by researchers at The Sanger Institute in the UK and The Institute for Genomic Research (TIGR) in the USA. The expected completion date was in 2005 but as of writing the first release of the entire sequence of the eleven megabase chromosomes is now available.

Based on comparison of sequence identities there are at least three families of nucleobase transporter genes – the nucleobase/ascorbate transporters (NAT), the purine-related transporters (PRT) and the plant purine-related transporters (PUP) (De Koning & Diallinas, 2000). Known nucleobase transporter gene sequences were used as search tools to interrogate the genome database. Using the amino acid sequence of NAT, PRT and PUP family members as query sequences in TBLASTN searches produced no significant hits to any sequences in the *T. b. brucei* genome database.

At the start of the project, substantial knowledge was available on the range of different transport activities that are present in *T. b. brucei*. For several nucleoside transport components in *T. b. brucei* sequence information was also available. These sequences have identified TbAT1 and TbNT2-7 as members of the equilibrative nucleoside transporter family. Some of the ENT family members characterised to date, including some of the *T. b. brucei* transporters, have been shown to also transport nucleobases but usually with much lower affinity than for the corresponding nucleoside, e.g. TbNT5 has affinity for hypoxanthine of 50 μM and of <5 μM for adenosine/inosine (Sanchez, *et al.*, 2002). One

possible exception to this “nucleobase uptake as low-affinity secondary activity only” assertion is the TbAT1 transporter.

Although TbAT1 is most often described as a nucleoside transporter its substrate profile suggests that nucleoside/nucleobase transporter is more accurate. TbAT1 from *T. brucei* actually displays higher affinity for adenine than for adenosine but the entire functional characterisation of TbAT1 was conducted using adenosine as the substrate. It is for this reason that the *T. b. brucei* genome database was probed with *TbAT1* rather than any of the *NT2-7* sequences.

A TBLASTN search of the available *T. b. brucei* sequence information using the predicted protein sequence of TbAT1 conducted by Richard Burchmore identified a novel 1308 nucleotide open reading frame coding for a protein with 33% identity (53% similarity) to the query sequence (Figure 7.1). The 435 amino acid protein was predicted to have 11 transmembrane domains. This secondary structure and the fact that the protein has such high similarity to a known transporter is consistent with a protein that resides in the membrane and that has a transport function. The presence of 11 putative transmembrane regions was also significant since other members of the ENT family have been shown or predicted to possess 11 membrane-spanning domains (Griffiths, *et al.*, 1997; Hyde, *et al.*, 2001).

The novel putative transporter gene was amplified by PCR and cloned into pGEM-T Easy vector by Richard Burchmore. Sequencing verified the complete open reading frame composition (nucleotide sequence and amino acid translation shown in Figure 7.2).

Due to the substrate preference ambiguity of TbAT1 it was hypothesised that this novel sequence might code for a nucleobase transporter. To investigate substrate preference, it was necessary to express the gene in an appropriate heterologous system, as *T. b. brucei* expresses a multitude of purine transporters with overlapping substrate specificity (Carter & Fairlamb, 1993; De Koning & Jarvis, 1997a; De Koning & Jarvis, 1997b; De Koning, *et al.*, 1998).

The heterologous system chosen for the characterisation was expression in an *fcy2*-null *Saccharomyces cerevisiae* cell line. The lack of the FCY2 permease resulted in cells

deficient in purine nucleobase and cytosine uptake (see later). A limited series of experiments involving the transient expression of introduced mRNA in *Xenopus laevis* oocytes was also conducted.

TbAT1: 2	LGFDSENEFIVYVTFLEFFGMSVVVVTNSIFSMPPFFIEYYKYAQGKPDAPKPEDPKFWKHM	61
	LGF SA E +Y T + G+S+++ N++ S P F ++YYKY GK D++P P FWK++	
AT-like:3	LGFSAGEVYMYATCILLGVSLMLPLNALVSAPRFMVDYKYVSGKEDSEPNLPFFWKNI	62
TbAT1: 62	FTYYSIAAFLVELVLASIMLTPIGRRISVTVRLGVGLVIPIVLVFSVMMVTIVTTTETGA	121
	FT+Y++ + ++ +LT RR+ ++VR + + + + VF V+M+ ++ +T A	
AT-like:63	FTFYNVVSLASQVTAGPTVLTRAARRLPLSVRFALSITLMMSEVFFVLMMPVIKVPQTV	122
TbAT1: 122	KVTIMLIAIANGVAMTLCDAGNAALIAPFPFKFYSSVVWGVIAVCGVVTSSFFSIVIKASMG	181
	V + L+ I G+ + +A L+A P+KF S+V++G+++CGV+TS +IKASM	
AT-like:123	IVLLCLVTIFAGIGKSYHEATCYVLVASMPSKFMASVMFGVSLCGVITSTLQCI IKASME	182
TbAT1: 182	GGYHNMLIQSRIYFGLVMFMQVISCALLVLRKNPYAQKYAAEFY--AARKGIDDKGAD	239
	Y ++L QS IYF L + + + A+ + LR N YAQ++ AE+R +G+D + +	
AT-like:183	DTYESVLTSQSYIYFSLGLLIMAGTLAMALCLRYNSYAQEHVAEYRMLKLQEQGVDAE-SQ	241
TbAT1: 240	GDEGNGAAKGPADQDDDPHGDDTDKGNVMTATVDPDTMKDMDQVENITTSQQMLMARVW	299
	DE A+G + G+ +G + TA E +T + M +AR+	
AT-like:242	NDENEPVAEGKGE-----GEGKSEGAMTTA-----EQLTATAVMPVARI-	280
TbAT1: 300	NVFWRVWPMFLFACFMVFFTFFLVYPVYFAIKADTGDGWYLTIAAALFNLGDFLSRLCLQ	359
	+ ML F FF T ++P++ I D W+ TIA L+N GD + R	
AT-like:281	-----IRMMLVTVFCGFFLTLFIFPSLIPI--DRDHNWFATIAILLYNCGDAIGRFSTS	333
TbAT1: 360	FKALHVSPRWVLIGTFARMLLIPLVLCVRSIITGPWLPYILVHAWGFTYGYGGISQIY	419
	FK + R +L TFAR + ++P +LC+ I G PYI G T G +S +Y	
AT-like:334	FKCVWPPRRALLYATFARFIFVLPFMLCIYQYIPGHVGPYIFSFLGLT-NCVGMASMVY	392
TbAT1: 420	APRTGSLTTAGERSLAANWTIISLLGGIFVGMFALAVNEGLP	462
	P T L TAG++ +A ISLL GI ++ A+ V LP	
AT-like:393	GPITPGLTAGQKLMAGQLMGISLLSGIAAASVLMIVVVFLP	435

Figure 7.1. Alignment comparing predicted amino acid sequences of *TbAT1* and AT-like gene. The two sequences share 33% identity (53% similarity).

7.1.2 Yeast expression systems

The availability of appropriate plasmid vectors and the progress in transformation protocols for yeast cells at the end of the 1970's allowed the isolation of the yeast arginine permease gene in the first yeast complementation study (Broach, *et al.*, 1979). Studies involving complementation of yeast mutants by expression of genes from a variety of other organisms quickly followed on from the original experiments. Since then yeast complementation has presented a robust system for both identification of novel genes and

1	M A L G F S S A G E V Y M Y A T C ATGGCTCTTGGATTTTCTCTGCGGGGGAAGTGTACATGTACGCAACATG
51	I L L G V S L L M P L N A L V S CATCCTTCTTGGAGTGCCTTCTAATGCCCTTAACGCTCTCGTTTCGG A P R F M V D Y Y K Y V S G K E D
101	CACCGCGCTTTATGGTGGACTACTACAAGTACGTATCTGGTAAAGAGGAT S E P N L P F F W K N I F T F Y N
151	TCCGAACCGAACCTTCCCTTTTTCTGGAAGAATATTTTCACGTTCTACAA V V S L A S Q V T A G P T V L T
201	TGTTGTATCGCTTGGTGCAGGTGACTGCTGGACCGACCGTTCTAACTC R A A R R L P L S V R F A L S I T
251	GTGCAGCCCGTGCAGCTTCCATTATCTGTGCGCTTTGCCCTTCCATCAGG L M M S E V F V V L M M P V I K V
301	TTGATGATGTCGGAGGTATTTGTAGTTCATGATGCCTGTGATCAAGGT P Q T V A I V L L C L V T I F A
351	ACCTCAAACAGTTGCCATTGTTCTTCTGCTGTGACAATATTTGCAG G I G K S Y H E A T C Y V L V A S
401	GTATTGGGAAATCATAACCATGAGGCGCGTCTACGTTCTGGTGGCGTCCG M P S K F M S A V M F G V S L C G
451	ATGCCATCTAAGTTCATGTCTGCTGTTATGTTGGAGTGTCACTATGCGG V I T S T L Q C I I K A S M E D
501	TGTAATAACGTCCACATTACAGTGCATCATCAAGGCATCAATGGAAGATA T Y E S V L T Q S Y I Y F S L G L
551	CCTATGAGTCCGTGCTGACGCAGTCATACATTTATTTTCACTGGTCTA L I M A G T L A M A L C L R Y N S
601	CTGATAATGGCGGTACACTTGCATGGCTCTCTGTCTACGATATAATTC Y A Q E H V A E Y R M L K L Q E
651	CTACGCGCAGGACACGTTGCTGAGTACCGTATGCTCAAATACAAGAAC Q G V D A E S Q N D E N E P V A E
701	AAGGAGTAGATGCTGAGTCTCAAATGATGAGAATGAACCCGTGGCTGAA G K G E G E G K S E G A M T T A E
751	GGTAAAGGTGAAGGTGAAGGTAAGAGTGAGGGTGCCATGACGACAGCAGA Q L T A T A V M P V A R I I R M
801	GCAACTGACGGCAACTGCTGTTATGCCCGTAGCGAGGATAATCCGATGA M L V T V F C G F F L T L F I F P
851	TGTTAGTGACAGTCTTCTGCGGCTTCTTCTCACCTTATTTATCTTCCCC S L I I P I D R D H N W F A T I A
901	AGTCTTATTATTTCCCATCGATCGTGACCACAATTGGTTTGGCAATTCG I L L Y N C G D A I G R F S T S
951	CATTCTGCTATACAACTGTGGGGATGCTATGGACGTTTCTCCACCTCGT F K C G V M P R R A L L Y A T F A
1001	TCAAGTGCCTTTGGCCGCCCGCCGTGCTGCTGTACGCCACCTTCGCC R F I F V L P F M L C I Y Q Y I P
1051	CGTTCATTTTTGTCTGCCCTTTCATGTTATGCATTTACCAATACATCCC G H V G P Y I F S F L L G L T N
1101	TGGCCATGTGGTCCGTATATCTTCTCGTTTCTCCTTGGCCTGACCAACT C V G A M S M V Y G P I T P G L E
1151	GTGTGGGTGCCATGTCGATGGTGTATGGCCAATAACCCCTGGTCTTGAG T A G Q K L M A G Q L M G I S L L
1201	ACTGCGGGTCAGAAATTGATGGCTGGACAGTTGATGGGGATTCGCTGCT S G I A A A S V L A M I V V V F
1251	TTCTGGAATTGCCGTCGATCTGTGCTTGGCATGATTGTGGTTGTCTTCC L P *
1301	TACCATGA

Figure 7.2. Nucleotide and amino acid sequence of AT-like sequence. The highlighted sequence is the *SalI* restriction site. The predicted transmembrane domains are shown in red.

functional characterisation of genes discovered by other means (Frommer & Ninnemann, 1995).

Uptake of purines and pyrimidines in *Saccharomyces cerevisiae* is mediated by three main transport components. FUR4 represents a high-affinity, highly specific uracil uptake activity. The substrate preference for this transporter is very particular – the system has no affinity for any other pyrimidine substrates such as cytosine and thymine (Jund, *et al.*, 1977; Chevallier, 1982). The FUI1 permease exhibits high selectivity for its uridine substrate and does not seem to contribute significantly to the uptake of any other nucleosides or nucleobases (Grenson, 1969; Vickers, *et al.*, 2000). The 533 amino acid purine-cytosine permease FCY2 is a broad specificity purine transporter which also has a significant cytosine uptake capacity. This transporter has no affinity for uracil or thymine (Polak & Grenson, 1973; Schmidt, *et al.*, 1984; Weber, *et al.*, 1990).

Saccharomyces cerevisiae MG887.1 is a *fcy2* mutant effectively deficient in purine nucleobase and cytosine uptake (Gillissen, *et al.*, 2000). As *Saccharomyces cerevisiae* does not have a plasma membrane transporter for purine nucleosides or nucleotides, this strain is completely deficient in mediated purine uptake. The strain has also been engineered to have a truncated copy of the *ura3* gene making it auxotrophic for uracil. This uracil auxotrophy is a useful means of selecting cells transformed with plasmids containing the full-length *ura3*. Cells not in possession of the plasmid will not grow on media lacking in uracil while successful transformants will prosper.

The pDR195 plasmid is one such plasmid and was used by Rentsch and colleagues (1995) to characterise the function of the NTR1 oligopeptide transporter from *Arabidopsis thaliana* in *Saccharomyces cerevisiae*. Gillissen subsequently used this vector for functional expression of the *A. thaliana* purine transporter AtPUP1 in *Saccharomyces cerevisiae* MG887.1 (Gillissen, *et al.*, 2000).

The pDR195 vector is shown in Figure 7.4. It contains the ADH expression cassette and also contains the PMA1 (yeast plasma membrane ATPase) promoter to increase expression levels of the introduced permease. As noted above, the vector also contains a functional full-length *ura3* to allow for selection of transformants on uracil drop-out medium.

7.1.3 *Xenopus laevis* oocyte expression systems

Pioneered by Gurdon and colleagues (1971, 1983), the technique of transiently expressing foreign genes in *Xenopus laevis* oocytes has made an important contribution to functional characterisation of myriad gene products. In particular, expression of transport proteins in oocytes has become a dependable method for elucidating transporter properties (Frommer & Ninnemann, 1995). Parasite transporters characterised in *Xenopus* oocytes include several classes of *Plasmodium falciparum* transporters (Penny, *et al.*, 1998), other *Trypanosoma brucei* purine transporters (Sanchez, *et al.*, 1999; Sanchez, *et al.*, 2002) and *Leishmania major* purine transporters (Sanchez, *et al.*, 2004).

Figure 7.3 shows a diagrammatic representation of the methodology used to establish the expression of exogenous permeases in the *Xenopus* oocyte system.

The vector used for the production of mRNA for expression of the putative AT-like transporter in the oocytes was the pGEM-3Z-based pGEM-HE (Liman, *et al.*, 1992). This plasmid is 3019 bp in size and the multi-cloning site is surrounded by the 5' and 3' UTRs of the *Xenopus* β -globin gene (Figure 7.7).

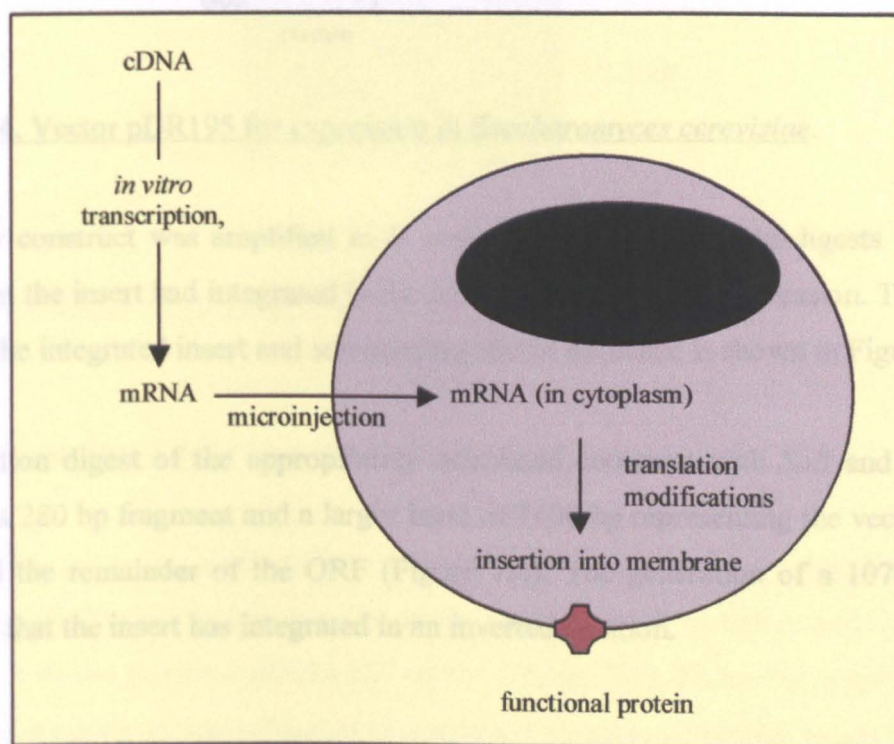


Figure 7.3. Transient expression of exogenous permease genes in *Xenopus laevis* oocytes. Adapted from Miller & Zhou, 2000.

7.2 Results

7.2.1 Sub-cloning of AT-like putative transporter gene into pDR195

The cloned AT-like gene was provided by Richard Burchmore as a pGEM-T Easy construct. The complete open reading frame was excised from the vector using the *NotI* restriction enzyme to give a 1.35 kb insert. The digestion was electrophoresed and the fragment was purified from the agarose. The AT-like fragment was ligated into the *NotI* site of the linearised, de-phosphorylated pDR195 vector (Figure 7.4).

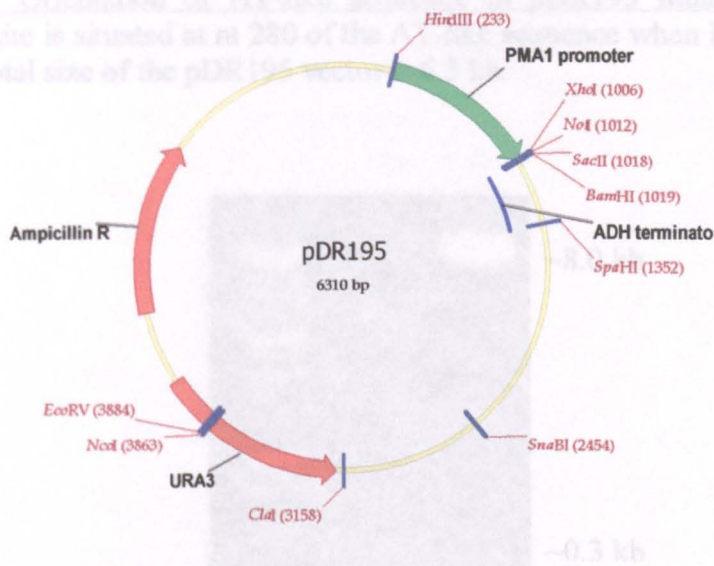


Figure 7.4. Vector pDR195 for expression in *Saccharomyces cerevisiae*.

This new construct was amplified in *E. coli* JM109 and restriction digests were used to verify that the insert had integrated in the correct orientation for expression. The restriction map for the integrated insert and surrounding vector sequence is shown in Figure 7.5.

A restriction digest of the appropriately orientated construct with *SalI* and *XhoI* should produce a 280 bp fragment and a larger band of 7400 bp representing the vector (6.3 kb in size) and the remainder of the ORF (Figure 7.6). The generation of a 1070 bp product indicates that the insert has integrated in an inverted position.

As before and ligated into the *EcoRI* site of the prepared pGEM-T vector (Figure 7.7). Following amplification in *E. coli* the new construct was subjected to restriction digest to determine which way the insert had integrated into the vector. For this construct the appropriate digest was a *SalI-XhoI*

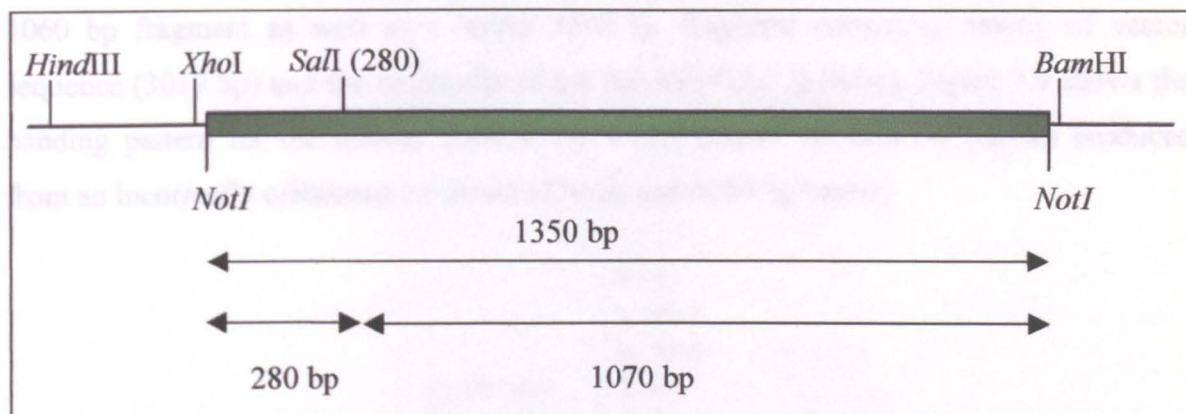


Figure 7.5. Orientation of AT-like sequence in pDR195 multicloning site. The *SalI* restriction site is situated at nt 280 of the AT-like sequence when it is ligated in the correct way. The total size of the pDR195 vector is 6.3 kb.

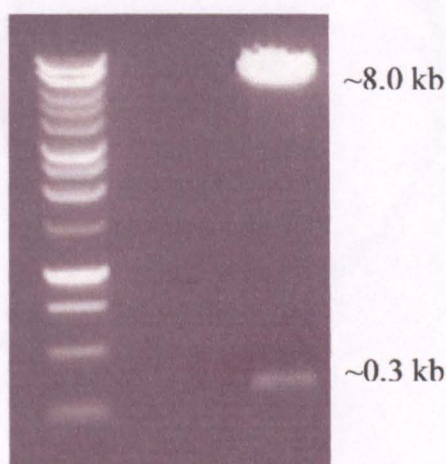


Figure 7.6. Orientation of the AT-like insert in pDR195.

7.2.2 Sub-cloning of AT-like putative transporter gene into pGEM-HE

The AT-like insert was excised from the pGEM-T Easy construct using *EcoRI* to give a 1.33 kb insert. The insert was purified from the agarose gel as before and ligated into the *EcoRI* site of the prepared pGEM-HE vector (Figure 7.7). Following amplification in *E. coli* the new construct was subjected to restriction digest to determine which way the insert had integrated into the vector. For this construct the appropriate digest was a *SalI-XbaI*

double digest (restriction map shown in Figure 7.8) with the correct assembly generating a 1060 bp fragment as well as a larger 3290 bp fragment consisting mostly of vector sequence (3019 bp) and the remainder of the AT-like ORF (270 bp). Figure 7.9 shows the banding pattern for the desired construct and also shows the banding pattern produced from an incorrectly orientated construct (270 bp and 4080 bp bands).

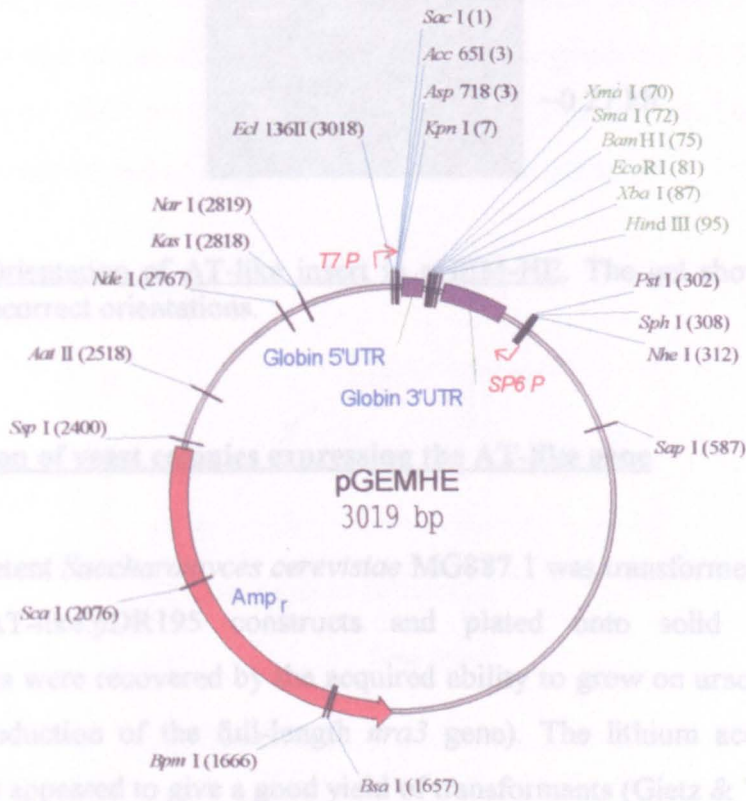


Figure 7.7. *Xenopus* oocyte vector pGEM-HE.

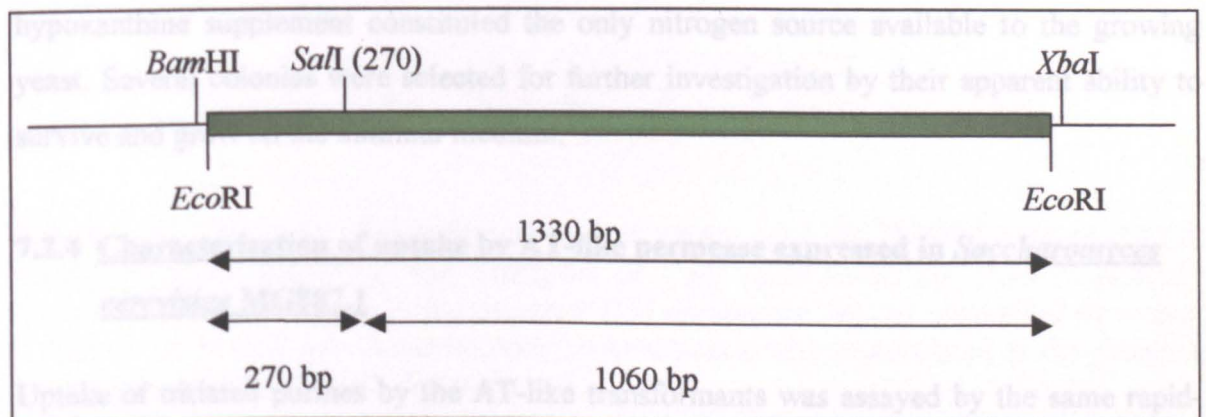


Figure 7.8. Orientation of AT-like sequence in pGEM-HE. For this construct, the *SalI* restriction site is situated at nt 270 of the AT-like sequence when it is ligated in the correct way. The total size of the pGEM-HE vector is 3019 bp.

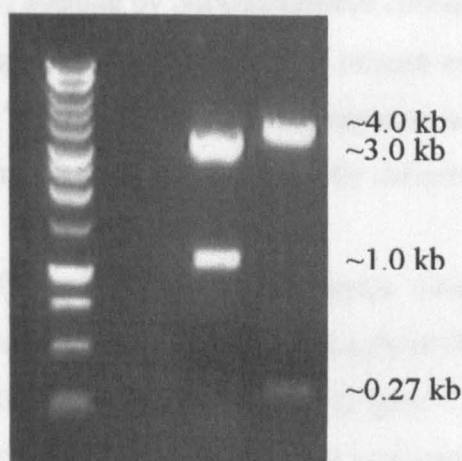


Figure 7.9. Orientation of AT-like insert in pGEM-HE. The gel shows band pattern for correct and incorrect orientations.

7.2.3 Selection of yeast colonies expressing the AT-like gene

Electrocompetent *Saccharomyces cerevisiae* MG887.1 was transformed with the correctly-orientated AT-like:pDR195 constructs and plated onto solid SC-URA medium. Transformants were recovered by the acquired ability to grow on uracil-minus plates (due to the reintroduction of the full-length *ura3* gene). The lithium acetate transformation protocol used appeared to give a good yield of transformants (Gietz & Woods, 2002).

Colonies from the SC-URA plates were transferred onto yeast selective medium plus hypoxanthine (4 mM) plates. This medium contained very few nutrients and the hypoxanthine supplement constituted the only nitrogen source available to the growing yeast. Several colonies were selected for further investigation by their apparent ability to survive and grow on the minimal medium.

7.2.4 Characterisation of uptake by AT-like permease expressed in *Saccharomyces cerevisiae* MG887.1

Uptake of tritiated purines by the AT-like transformants was assayed by the same rapid-stop oil-spin technique used to study uptake in *T. b. brucei*. Throughout, there was no significant accumulation of any of the radiolabelled permeants by control transformants which received only the empty pDR195 vector.

Accumulation of $0.1 \mu\text{M}$ [^3H] adenine by *Saccharomyces cerevisiae* MG887.1 transformed with the AT-like gene was rapid, and linear for over a minute with a rate of $0.0216 \pm 0.001 \text{ pmol} (10^7 \text{ cells})^{-1} \text{ s}^{-1}$ (Figure 7.10). The transport activity was saturable and in the presence of 1 mM unlabelled adenine uptake was not significantly different from zero.

The uptake of $0.1 \mu\text{M}$ [^3H] hypoxanthine by the yeast transformants was even more voracious than that of adenine with a linear phase throughout the 5 minute timecourse and an uptake rate of $0.048 \pm 0.006 \text{ pmol} (10^7 \text{ cells})^{-1} \text{ s}^{-1}$ (Figure 7.10). Again transport could be completely suppressed in the presence of unlabelled permeant.

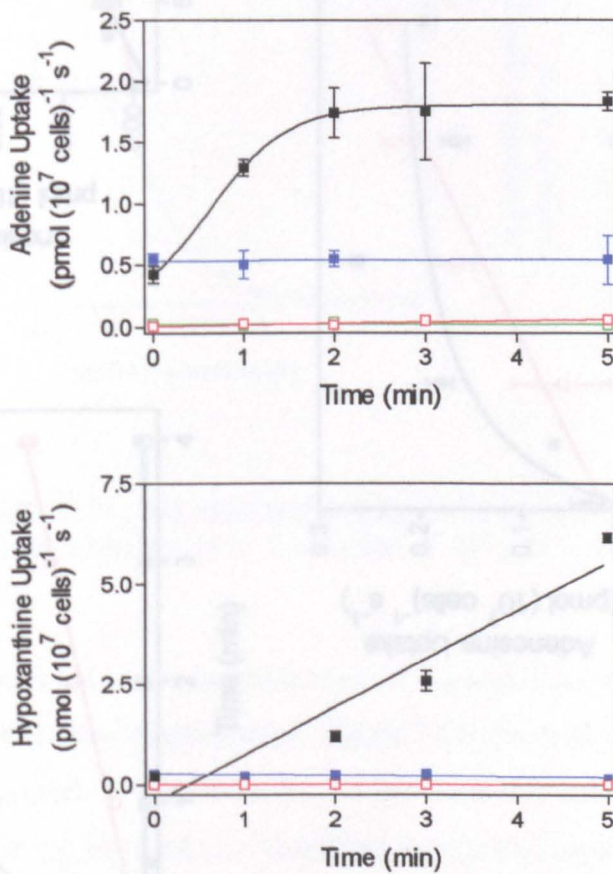


Figure 7.10. Uptake of [^3H] purine permeants versus time for *TbNBT1* expressed in *S. cerevisiae* strain MG887-1. (a) Transport of [^3H] nucleobases by *TbNBT1*:pDR195 transformants was assayed in the presence (\square) or absence (\blacksquare) of unlabelled permeant. Transport by control transformants with pDR195 was similarly measured in the presence (\square) or absence (\blacksquare) of unlabelled permeant.

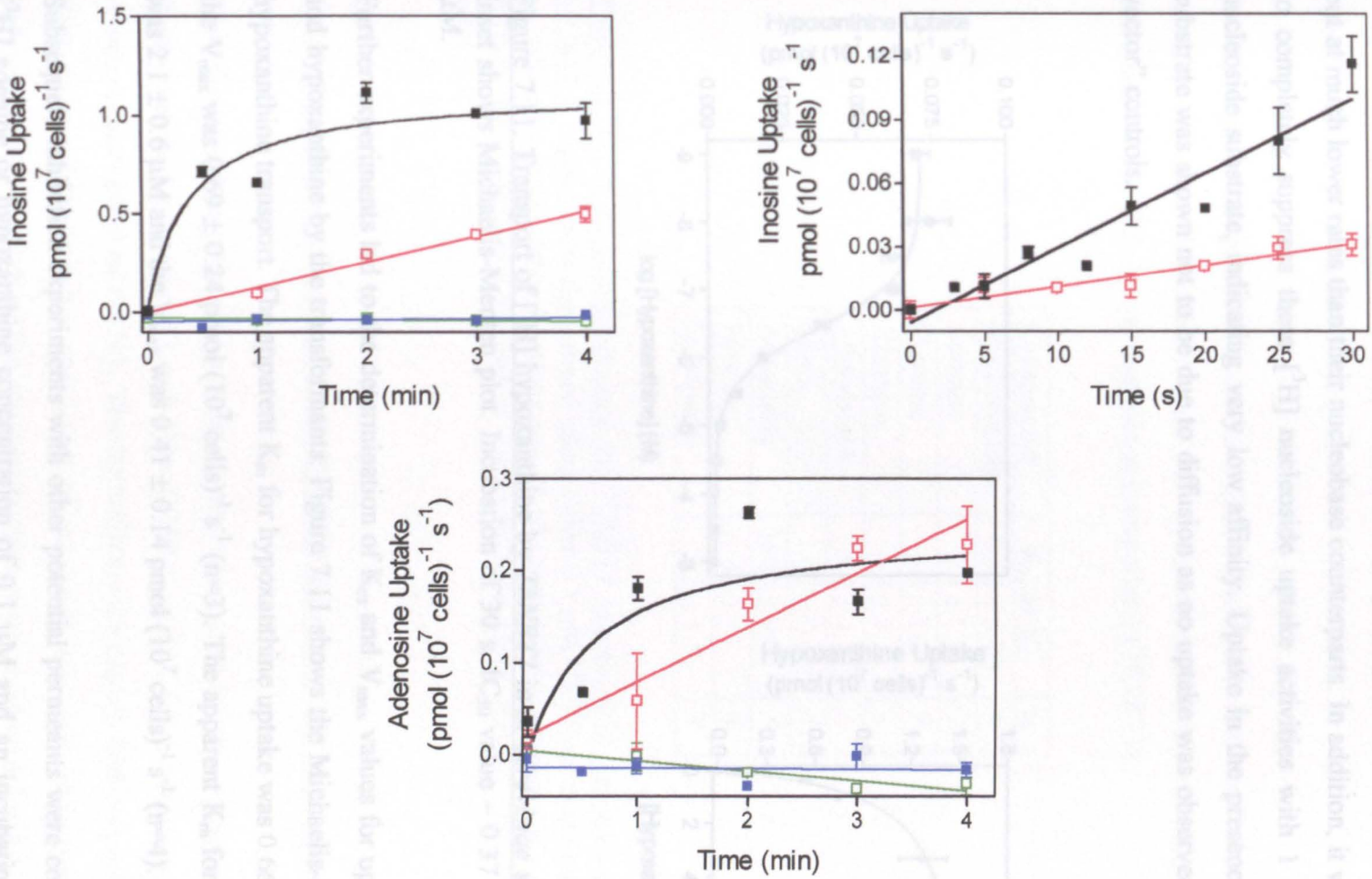


Figure 7.10 (ctd). Uptake of [³H] purine permeants versus time for *TbNBT1* expressed in *S. cerevisiae* strain MG887-1. (b) Transport of [³H] nucleosides by *TbNBT1*:pDR195 transformants was assayed in the presence (□) or absence (■) of unlabelled permeant. Transport by control transformants with pDR195 was similarly measured in the presence (□) or absence (■) of unlabelled permeant.

The nucleosides of adenine and hypoxanthine (adenosine and inosine, respectively) were also assayed at this stage to determine if the transporter had any preference for nucleobases over nucleosides. The nucleosides were taken up by the yeast transformants (Figure 7.10) but at much lower rates than their nucleobase counterparts. In addition, it was not possible to completely suppress these [^3H] nucleoside uptake activities with 1 mM unlabelled nucleoside substrate, indicating very low affinity. Uptake in the presence of unlabelled substrate was shown not to be due to diffusion as no uptake was observed in the “empty vector” controls.

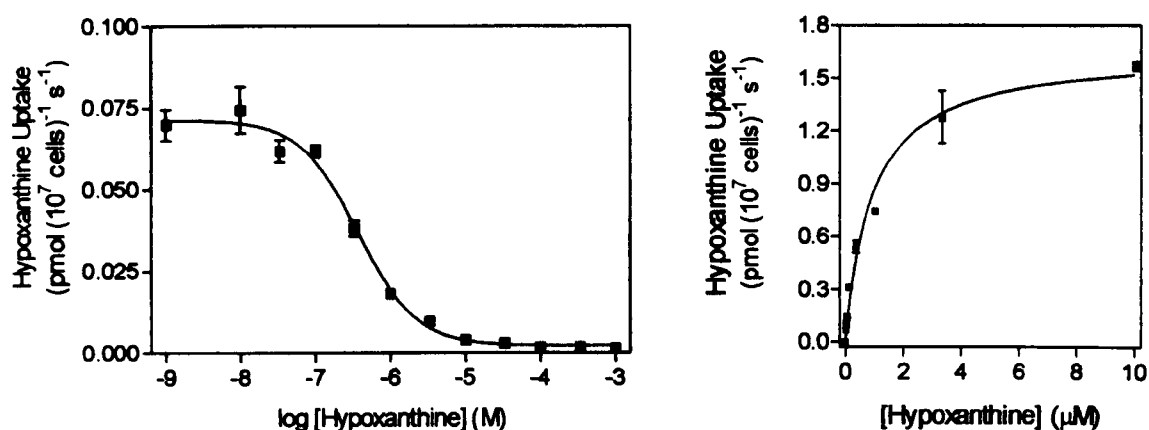


Figure 7.11. Transport of [^3H] hypoxanthine by *TbNBT1* in *S. cerevisiae* strain MG887-1. Inset shows Michaelis-Menten plot. Incubation of 30 s. IC_{50} value $-0.37 \mu\text{M}$; $K_m - 0.93 \mu\text{M}$.

Further experiments led to the determination of K_m and V_{\max} values for uptake of adenine and hypoxanthine by the transformants. Figure 7.11 shows the Michaelis-Menten plot for hypoxanthine transport. The apparent K_m for hypoxanthine uptake was $0.66 \pm 0.22 \mu\text{M}$ and the V_{\max} was $0.69 \pm 0.24 \text{ pmol } (10^7 \text{ cells})^{-1} \text{ s}^{-1}$ ($n=3$). The apparent K_m for adenine uptake was $2.1 \pm 0.6 \mu\text{M}$ and the V_{\max} was $0.41 \pm 0.14 \text{ pmol } (10^7 \text{ cells})^{-1} \text{ s}^{-1}$ ($n=4$).

Subsequent inhibition experiments with other potential permeants were conducted using a [^3H] adenine or hypoxanthine concentration of $0.1 \mu\text{M}$ and an incubation time of 30 s, which produced highly reproducible results. Table 7.1 shows the K_m and K_i values obtained for uptake by the AT-like transporter expressed in *Saccharomyces cerevisiae* MG887.1. The permease mediated uptake of all the purine nucleobases with high affinity.

Nucleosides were also able to inhibit uptake of radiolabelled permeant but all of the nucleosides demonstrated considerably lower affinities than the nucleobases. Even the reasonably high-affinity interaction exhibited by guanosine of 5.3 μM was significantly less than for its nucleobase counterpart.

At this stage, it was possible to conclude that, based on the functional characterisation, the AT-like sequence did indeed code for a nucleobase transporter and the gene was designated as the *T. b. brucei* nucleobase transporter 1 (*TbNBT1*).

Compound	K_m or K_i	n
Hypoxanthine	0.66 ± 0.22	4
Adenine	2.1 ± 0.6	3
Guanine	1.4 ± 0.3	3
Xanthine	4.3 ± 1.1	3
Allopurinol	5.4 ± 1.1	3
Uracil	68 ± 6.5	4
Adenosine	1900 ± 980	3
Inosine	47 ± 17	4
Guanosine	5.3 ± 1.5	3

Table 7.1. K_m or K_i values obtained for *TbNBT1* expressed in *Saccharomyces cerevisiae* MG887.1. Values were determined using either 0.1 μM [^3H] hypoxanthine or [^3H] adenine as radiolabel for K_i determinations and 25 nM radiolabel to measure K_m values. K_m were derived from Michaelis-Menten or Eadie-Hofstee plots. Results are shown \pm standard error.

7.2.5 Characterisation of uptake by TbNBT1 expressed in *Xenopus laevis* oocytes

The *Xenopus* oocyte transport assays were conducted by the group of Prof. Stephen Baldwin at the University of Leeds. The *TbNBT1*:pGEM-HE constructs were used for the *in vitro* transcription of mRNA. The transcripts were capped and polyA-tailed to prevent degradation of the message and 10 ng of transcript was injected into the cytoplasm of isolated stage VI oocytes. The injected oocytes were incubated for 4-5 days with daily medium changes before transport assays were performed. The oocytes were assayed for uptake of 100 μM radiolabelled adenine, adenosine, uracil and uridine over a 30 minute timecourse. The level of transport activity was expressed as a percentage of the amount of

uptake seen over the same time-course in oocytes from the same batch of cells when injected with DEPC-treated dH₂O only. The transport values shown were the result of the simultaneous assay of 10-12 oocytes. Figure 7.12 shows the uptake recorded for oocytes injected with *TbNBT1* and *hENT1* mRNAs. As the positive control, *hENT1*-injected oocytes accumulated uridine and adenosine, but not adenine or uracil, in keeping with previous studies (Griffith, *et al.*, 1997).

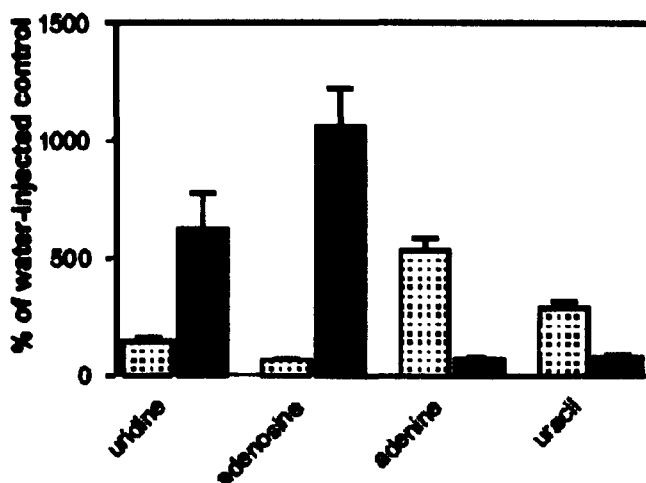


Figure 7.12. Purine and pyrimidine transport in *Xenopus* oocytes injected with RNA transcripts encoding protozoan and mammalian members of the ENT family. *TbNBT1* – open bars; *hENT1* – filled bars. Transport is expressed as a percentage of the rates of uptake in control oocytes injected with water alone. Uptake was measured at pH 7.5.

These oocyte system results served to reiterate what had been determined with the yeast expression system. The newly-named *TbNBT1* transporter was specific for adenine and, to a lesser extent uracil, over adenosine and uridine.

7.2.6 Reconciliation of heterologous system results with transport activities *in situ*

The fact that the substrate specificity and kinetic profile for *TbNBT1* expressed in yeast was very similar to that observed for the H4 uptake activity in procyclics (see Table 6.3) was strongly suggestive that the *TbNBT1* gene codes for the H4 transporter. A series of elegant experiments by Mohammed Al-Salabi using the RNAi approach further corroborated this assertion (Burchmore, *et al.*, 2003).

7.3 Discussion

The *TbNBT1* (*T. b. brucei* nucleobase transporter 1) gene described here is the first dedicated nucleobase transporter gene to be characterised not only from *T. b. brucei* but from any protozoan. The level of sequence identity with members of the equilibrative nucleoside transporter family suggests that *TbNBT1* is a new relative. As noted earlier in the chapter, other ENTs have been shown to mediate uptake of nucleobases but only in addition to nucleosides. The most significant examples of this situation are *hENT2* (Yao, *et al.*, 2002), *TbAT1* (Mäser, *et al.*, 1999) and *TbNT5* (and to a much lesser extent *TbNT6* and *TbNT7*) (Sanchez, *et al.*, 2002).

The 435 residue TbNBT1 protein is predicted to form 11 membrane-spanning helices with a large cytosolic loop between TMS 6 and 7, and this is particularly significant since this topology is a feature of most ENT family members (Griffiths, *et al.*, 1997; Hyde, *et al.*, 2001). It should be considered, however, that predictions of TMDs are speculative at best and ideally topology should be determined experimentally (Sundaram, *et al.*, 2001). Several permeases that are clearly defined as ENT members in terms of sequence identity and substrate specificity are predicted to possess a variable number of TMDs. LdNT2 is predicted to possess only 9 TMDs (Carter, *et al.*, 2000), and TbAT1 was initially predicted to possess only 10 helices (Mäser, *et al.*, 1999).

It was necessary to express the transporter in a heterologous system in order to study its function unimpeded by interference from other endogenous *T. b. brucei* transport activities. The two systems used here are both long-established techniques for study of gene expression and both are also associated with the cloning and characterisation of many different transporters (Frommer & Ninnemann, 1995).

Expression in the yeast system demonstrated that *TbNBT1* encoded a permease capable of uptake of adenine and hypoxanthine and that the transporter displayed high affinity for these substrates. Other nucleobases were also able to interact with the transporter with high affinity. Nucleosides were able to inhibit uptake of radiolabelled adenine and hypoxanthine but to a much lesser degree. Even the relatively low K_i value for guanosine was almost five times higher than that obtained for guanine (5.3 μM compared with 1.4 μM). Guanosine is

a special case with several of the *T. b. brucei* and *L. major* nucleobase transport activities showing surprisingly high affinity for this nucleoside only. An internal H-bond between the 5'-hydroxyl group and the 2-amino group stabilises the molecule in the advantageous *syn* conformation, whereas all other natural nucleosides are in the *anti* conformation (Al-Salabi, *et al.*, 2003).

The yeast system also offered robust controls in the form of empty vector transformants. The uptake of labelled nucleosides even in the presence of 1 mM unlabelled nucleosides could not be explained by endogenous uptake systems or diffusion as there was no apparent uptake by these control pDR195 transformants.

The results in *Saccharomyces cerevisiae* were corroborated by the limited characterisation of TbNBT1 in *Xenopus laevis* oocytes. The same general trends were observed, namely that the TbNBT1 transporter was specific for nucleobases and had much less preference for nucleoside permeants. It also showed that although the transporter was very much specific for purines it did have some ability to transport the pyrimidine nucleobase uracil (K_i of 68 μM in yeast assays).

Saccharomyces cerevisiae (or other yeast species) may be the expression system of choice for *T. b. brucei* transporter genes since it also utilises the proton-motive force for energisation of the transport process, whereas energy-dependent transport in *Xenopus* oocytes is known to use the Na^+ -gradient (Shayeghi, *et al.*, 1999). However, this does not necessarily mean that the *Xenopus* oocyte is an unsuitable system for proton symporters since it does maintain a substantial proton-motive force across its membrane.

It is necessary to verify results obtained from expression in any heterologous system since proteins can behave differently in "alien" environments particularly if other cofactors or proteins necessary for proper function are absent.

The kinetic profile of TbNBT1 expressed in *Saccharomyces cerevisiae* was very similar to that elucidated for the H4 transport activity in *T. b. brucei* procyclics (Burchmore, *et al.*, 2003; see Chapter 6). In fact, none of the K_m or K_i values derived for TbNBT1 in yeast and for H4 *in situ* were significantly different ($p > 0.05$).

In a series of elegant RNAi experiments by Mohammed Al-Salabi, expression of the *TbNBT1* gene in procyclic parasites was “knocked-down” to confirm the assertion that *TbNBT1* encodes the gene for H4. In the “knock-down” cells the *TbNBT1* mRNA transcript was reduced by ~80% and the H4 hypoxanthine transport activity was concurrently very much reduced (V_{\max} fell from 3.2 pmol (10⁷ cells)⁻¹ s⁻¹ in normal cells to 0.20 pmol (10⁷ cells)⁻¹ s⁻¹ in RNAi cells).

The fact that the results in the yeast system could be corroborated by the results obtained in *T. b. brucei* was significant because it validated the use of this particular yeast expression system for the study of trypanosome transporter genes.

It is somewhat ironic that the *TbNBT1* gene belongs to the equilibrative nucleoside transporter family considering that it is primarily a nucleobase transporter and is likely to be an active transporter reliant on the proton gradient for function (De Koning & Jarvis, 1997a; De Koning, *et al.*, 1998). The family name was based on the characterisation of the definitive member (*hENT1*), and many other family members do not quite conform to the profile inferred by the name either. It is possible that ENT family members are also responsible for the nucleobase-specific high-affinity transport activities characterised in a range of other organisms, including humans, though this remains to be proven.

Many issues remain to be resolved regarding nucleobase uptake in *T. b. brucei*. Although *TbNBT1* belongs to the ENT family this does not preclude the presence of nucleobase transporter genes in *T. b. brucei* that are not connected to this family. Also there is the continuing uncertainty of whether each characterised activity is the result of only one gene product or the result of the expression of a combination of similar genes, leading to closely-related transporters that are not easily distinguished using kinetic profiles.

There are at least 3 sequences in the *T. b. brucei* genome databases that are very similar (>95%) to *TbNBT1*. One of these sequences which differs at only 3 amino acid positions has been cloned and characterised as *TbNT8.1* by other researchers (Henriques, *et al.*, 2003). Although both *TbNBT1* and *TbNT8.1* both mediate high-affinity uptake of nucleobase compounds the substrate profiles do not completely concur. Initial characterisation of *NT8.1* showed that it had little affinity for either guanosine or uracil even at concentrations as high as 400 μM but *NBT1* activity is affected by guanosine with

a K_i of 5.3 μM and by uracil with a K_i of 68 μM . Of course, these kinetic parameters were obtained in different heterologous expression systems and may reflect either this or other variations in methodology. Recently, a nucleobase transporter of the ENT family that mediates uptake of hypoxanthine, guanine, adenine and xanthine has also been cloned and characterised for the related parasite *Leishmania major* (Sanchez, *et al.*, 2004).

Until very recently, the only information about the nucleoside and nucleobase transporters in *T. b. brucei* had been gleaned solely by biochemical means. With this work and the cloning of several nucleoside transporters from trypanosomes in the past few years, there is now an unprecedented opportunity to dissect the vital role the purine transporters play, both in terms of purine salvage and chemotherapy. One example of the latter is the construction of a genetic knock-out for *TbATI* and the subsequent full elucidation of the role of the resulting P2 transport activity in drug transport (Matovu, *et al.*, 2003).

The initial discovery, cloning, functional characterisation of the gene/gene product and identification of H4 as the *in situ* transport activity corresponding to *TbNBT1* expression is described in our paper (Burchmore, *et al.*, 2003).

Chapter Eight

Cloning and characterisation of AT-like transporter genes

8.1 Introduction

The previous chapter discussed how the *TbNBT1* gene was cloned, characterised and determined to be responsible for the H4 transport activity. This was a significant accomplishment since it marks the first time a gene has been identified for any protozoan nucleobase transporter. However, there are still at least three other purine nucleobase transport components in *T. b. brucei* for which a genetic basis remains to be identified, in addition to at least two pyrimidine nucleobase transporters. As well as three sequences with very high sequence homology to *TbNBT1* (>95% identity at amino acid level), which included the TbNT8.1 characterised by Henriques and colleagues (2003), several other AT-like sequences were recovered following interrogation of the *T. b. brucei* genome database with the TbAT1 protein sequence. The predicted primary amino acid sequences for three of these putative purine transporters, designated AT-like A, AT-like B and AT-like D, shared between 54% and 58% identity with the TbAT1 protein sequence.

This chapter describes the cloning and preliminary characterisation of these AT-like permeases. It also provides a comprehensive overview of the known and other predicted ENT family members that appear in the *T. b. brucei* genome, as of March 2004.

8.2 Results

8.2.1 Polymerase chain reactions and cloning of AT-like sequences

PCR primers were designed for the AT-like sequences A, B and D (Figure 8.1). The primer sequences lay outwith the predicted open-reading frame so as to amplify the entire putative gene. Products of the expected sizes were obtained for all three putative gene sequences following PCR using the proof-reading enzyme *Pfu*, as described in Chapter 2 (see Figure 8.2 for the results of the AT-like D PCR). The annealing temperature for the amplification of AT-like A and AT-like B was 56 °C while the annealing temperature for the amplification of AT-like D was 52 °C. The positive control utilised primers which amplified a fragment of NBT1. The gel-purified products were A-tailed by incubation with

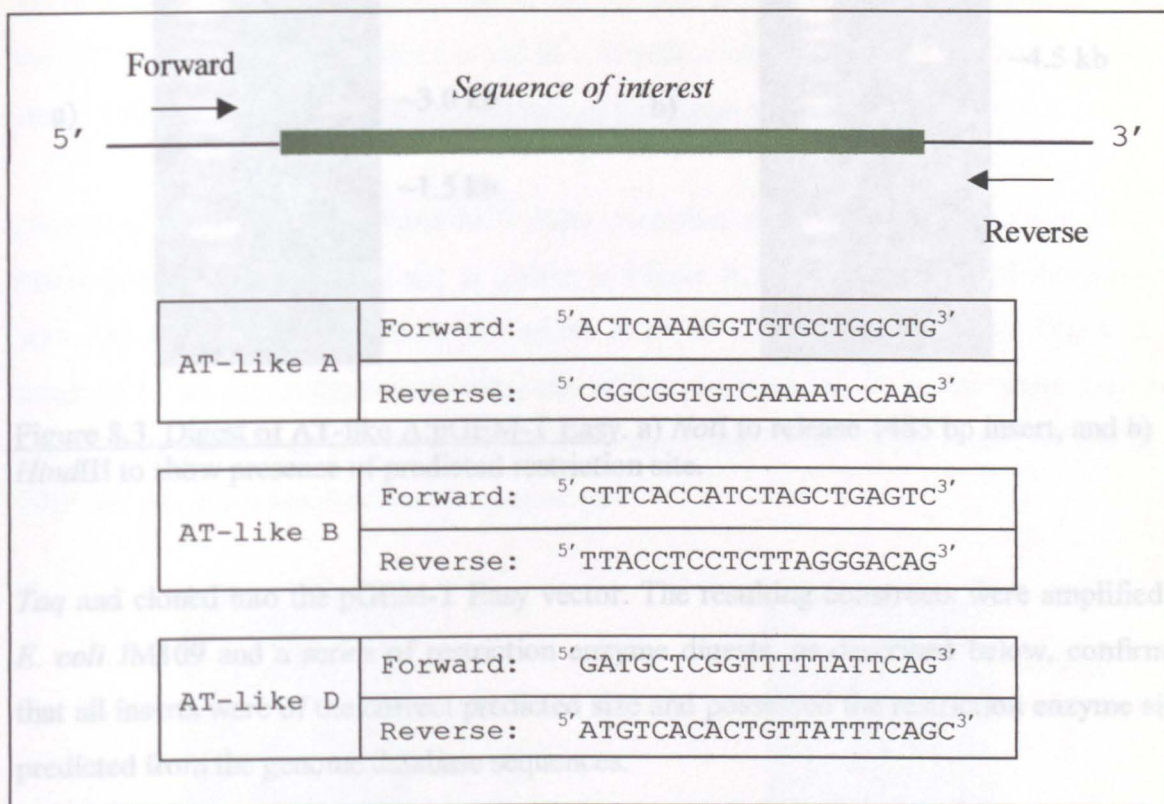


Figure 8.1. Primers used for amplification of AT-like sequences from total *T. b. brucei* genomic DNA.

PCR +

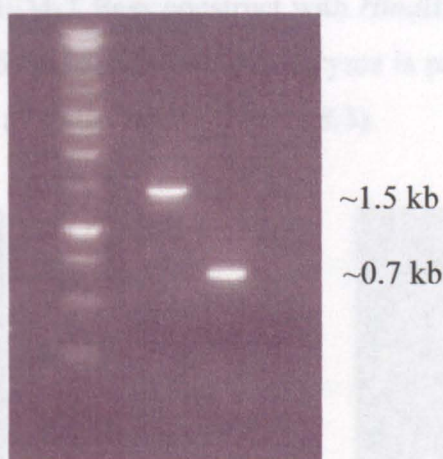


Figure 8.2. Polymerase chain reaction. AT-like D amplified from *T. b. brucei* using PCR primers detailed above. A positive control was included and consisted of primers designed to amplify a fragment of *TbNBT1*. The molecular weight markers are the same as those used in Chapter Six and Seven.

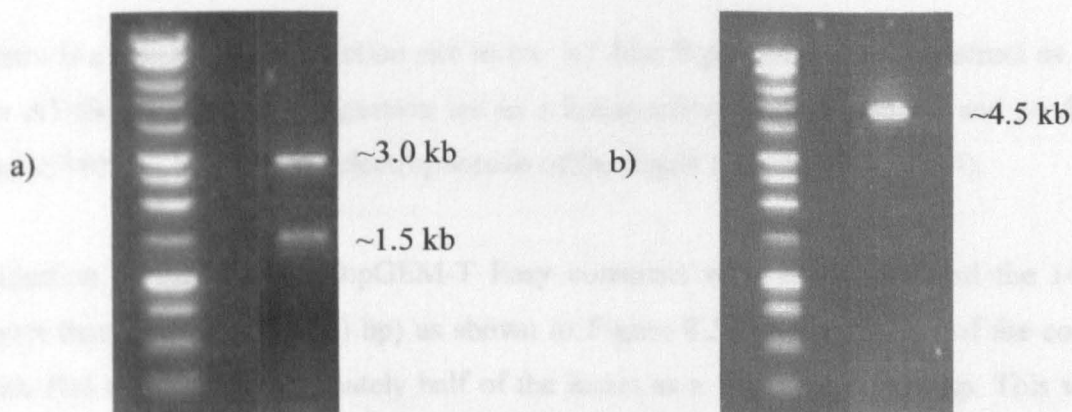


Figure 8.3. Digest of AT-like A:pGEM-T Easy. a) *NotI* to release 1483 bp insert, and b) *HindIII* to show presence of predicted restriction site.

Taq and cloned into the pGEM-T Easy vector. The resulting constructs were amplified in *E. coli* JM109 and a series of restriction enzyme digests, as described below, confirmed that all inserts were of the correct predicted size and possessed the restriction enzyme sites predicted from the genome database sequences.

NotI digestion of the AT-like A:pGEM-T Easy and AT-like B:pGEM-T Easy constructs generated the vector as a 3.0 kb fragment and the AT-like A or AT-like B fragments of the appropriate size (Figure 8.3 and Figure 8.4).

Digestion of the AT-like A:pGEM-T Easy construct with *HindIII* led to linearisation of the whole construct (a single 4465 bp band) since this enzyme is predicted to cut once in the AT-like A sequence but not at all in the vector (Figure 8.3).

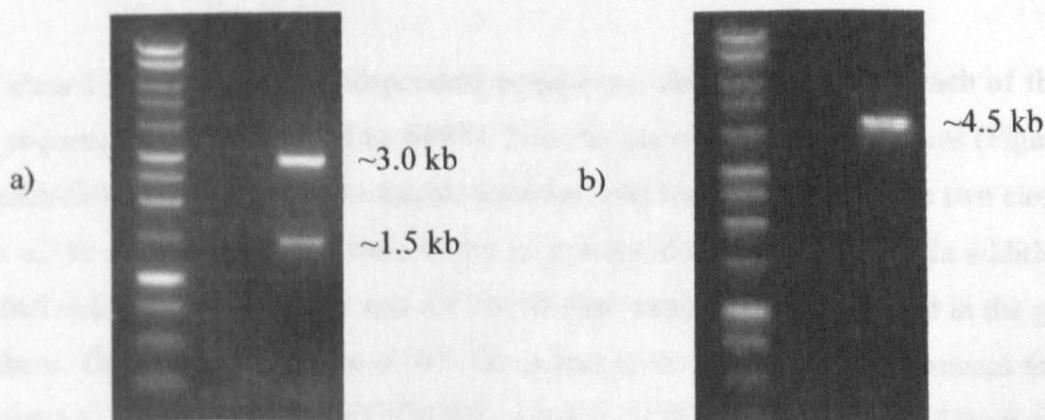


Figure 8.4. Digest of AT-like B:pGEM-T Easy. a) *NotI* to release 1420 bp insert, and b) *XhoI* to show presence of predicted restriction site.

There is a single *XhoI* restriction site in the AT-like B:pGEM-T Easy construct as part of the AT-like B sequence. Digestion led to a linearisation of the construct and produced a single 4405 bp fragment on electrophoresis of the digest mixture (Figure 8.4).

Digestion of the AT-like D:pGEM-T Easy construct with *EcoRI* released the 1410 bp insert from the vector (3000 bp) as shown in Figure 8.5. Another digest of the construct with *PstI* released approximately half of the insert as a fragment of 680 bp. This was the result of a *PstI* site in the multicloning site of the vector and a site in the insert sequence. This *PstI* digest also gives a fragment of 90 bp as a consequence of a second *PstI* site in the ORF but this is not resolved on the agarose gel.

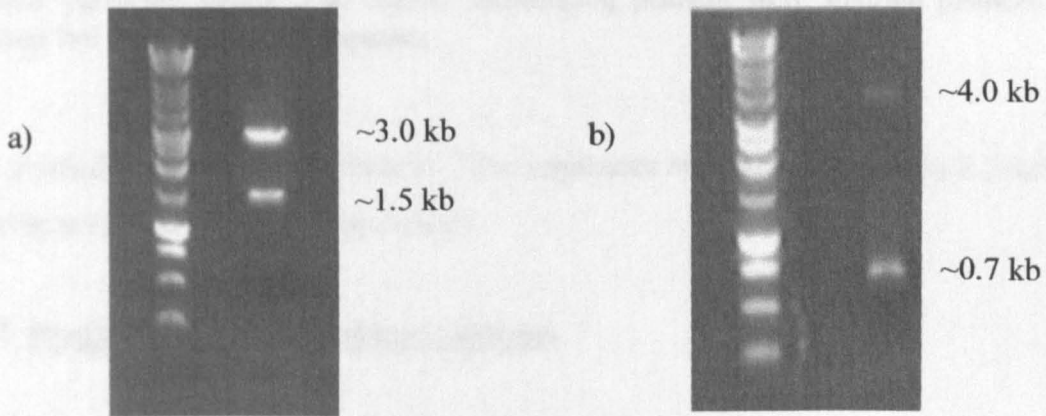


Figure 8.5. Digest of AT-like D:pGEM-T Easy. a) *EcoRI* to release 1410 bp insert, and b) *PstI* to show presence of predicted restriction site.

8.2.2 Sequencing

The cloned products of two independent polymerase chain reactions for each of the AT-like sequences were sequenced by MWG. Four separate sequencing reactions (Figure 8.6) for each clone led to a complete double-stranded read for each sample. The two clones for each of the AT-like products were found to possess identical sequences. In addition, the verified sequence of AT-like B and AT-like D were identical to those found in the genome database. The verified sequence of AT-like A had several single base differences from the sequence in the database (C369T; G436T; A501G; T1332C) but only one of these changes led to a change in the amino acid sequence (G436T changed a glycine residue to a serine residue).

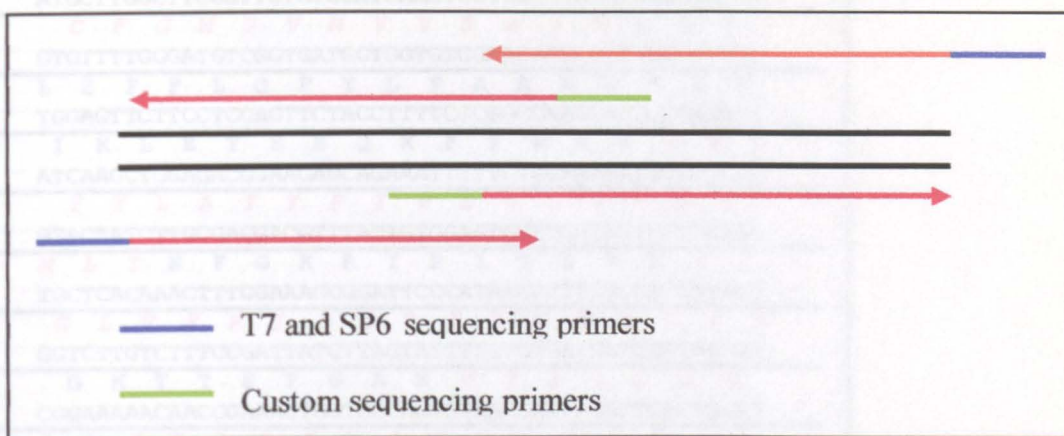


Figure 8.6. Sequencing. Reactions required to elucidate nucleotide sequence of entire putative permease genes. The custom sequencing primers were internal primers which allowed full coverage of the sequence.

The verified sequences of all three AT-like sequences are shown in Figures 8.7-8.9 along with the predicted amino-acid sequences.

8.2.3 Prediction of transmembrane domains

The presence of putative membrane-spanning domains in a protein can be detected by subjecting the primary amino acid sequence to hydropathy analysis (Stryer, L., 1995). By investigating the likelihood of certain hydrophobic α -helical regions of the protein showing a preference for the non-polar environment of the membrane interior it is possible to make predictions regarding the structural organisation of transmembrane proteins. The TMpred program (http://www.ch.embnet.org/software/TMPRED_form.html) was used to determine the incidence of putative transmembrane domains in the AT-like A, B and D secondary structures. All three amino acid sequences exhibited an apparent secondary structure consistent with a membrane location and a transport function. The transmembrane helix length was set between 14 and 23 amino acids and with these parameters all three AT-like sequences were predicted to have 11 transmembrane regions with the N-terminal on the cytosolic side of the membrane (Figure 8.10). Other ENT family members have been shown or predicted to have 11 transmembrane domains. The

	M L G F G S V H E L L A Y I T F M
1	ATGCTTGGCTTCGGTCTGTGCATGAACTCCTTGCCTATATCACCTTCAT
	C F G M S V M V V S N T V L S F
51	GTGTTTTGGGATGTCGGTGTGGTGGTGTGCAACACGGTCTTGTTCGTTCC
	L E F F L Q F Y L F A A K D G E N
101	TGGAGTTCCTCCTCCAGTTCCTACCTTTTCGCGCCAAGGATGGCGAGAAC
	I K L E T E E Q K F F W K N V F T
151	ATCAAGCTGGAGACGGAAGAGCAGAAAATTTTTCTGGAAAAATGTCTTCAC
	Y Y L A T T F I V E C L V V S L
201	GTACTATCTTGCACGACGTTTATTGTGGAGTGTGGTGTAGTGTCACTGA
	M L T N F G K R I P I T L R L Y I
251	TGCTCACAACTTTGGAAAGCGGATTCCCATAACCTTCGCCTCTATATT
	G L V F P I I L V F S V M M V T I
301	GGTCTTGTCTTCCGATTATCTTAGTATTTTTCTGTGATGATGGTTACCAT
	G K T T E T G A R V T I I L I G
351	CGGAAAAACAACGGAACTGGTGCCAGGGTAACCATATACTGATTGGTT
	L I N G A S T A L C S S S A V A L
401	TGATAACCGAGCTTCCACTGCACCTTTCAGCTCCTGTGCCGTTGCACCT
	A G P F P T K F L S A Y V W G V S
451	GCCGGTCCCTTCCAACGAAGTTTTTGAGTGCCTACGTGTGGGGTGTTC
	V C G V I T S T F A I V I K A S
501	GGTGTGTGGTGTATCACGTCGACGTTTGCATTGTATTAAAGCTTCCA
	T E S N F K R T E D R V A S R L T
551	CGGAGAGTAACCTCAAGCGTACAGAAGACCGCGTCGCGAGTAGGCTCACT
	Q S R I Y F G L V M I M Q S I S C
601	CAGTCACGCATATACTTTGGGTTGGTCATGATTATGCAGTCGATTTCTTG
	G L L L L L R K N P Y A M K Y T
651	TGGTCTTCGCTGCTGCTGAGGAAGAACCCTTACGCCATGAAGTATACAG
	A D F R Y A A R K G N A V E G D D
701	CAGACTTTCGTTACGCGGAGGAAAGGGAATGCTGTGAAGGTGATGAC
	A G D D N E P S S L G K G P A D Q
751	GCTGGAGATGATAATGAACCGAGTAGCTTAGGAAAGGGTCCGGCCGACCA
	D D D L K A D C N A G K S N V M
801	GGATGACGATTTGAAAGCGGATTGCAACGCGGGCAAGAGCAACGTGATGA
	T S T V D P D T M R D T D Q V E N
851	CTTCCACTGTAGACCCTGACACGATGAGGGACACGGACCAGGTTGAGAAT
	I T N S Q Q M L K A S A L S V F R
901	ATCAGCAACTCGCAACAGATGTTGAAGGCGAGTCGTTGTCTGTGTTTCAG
	R V W P M L A V C F I A F F T A
951	GCGTGTGGCCCATGTTAGCCGTGTGCTTTATTGCGTTCTTTACCGCCT
	F L I Y P G V F F A V K L G P D D
1001	TCCTCATCTACCCTGGTGTATTCTTTGCTGTCAAACCTGGGGCCGGATGAC
	N G W Y M V I I P M M F N L G D F
1051	AACGGCTGGTATATGGTGTATTCCTGATGATGTTAACTTGGGAGATT
	V A R L F V Q F K T L H A S P L
1101	TGTGGCGCGCCTTTTCGTTCAAGTTCAGTTCAGCTGACGCATCACCGTCT
	F V V I G T F A R L L L V I P I V
1151	TTGTGGTGATTGGGACGTTTGCCTGTTGTTGCTCGTCATTCCAATTGTG
	L C A Y S V I K G T T F P Y I L C
1201	CTTTGCGCATAAGTGTGATTAAGGGCAGACATCCCTTATATCTTTG
	F L W S L T Y G Y V G G L A G V
1251	CTTCTCTGGTGCCTCACGTATGGCTACGTGGGGGTCTAGCGGGAGTCT
	Y A P R T G S L T T A G E R S L A
1301	ACGCGCCGCTACTGGTTCGCTGACGACCGCCGGCGAACGTTCTCTAGCA
	A N W A V S S L L F G I F A G C M
1351	GCCAACTGGGCCGTTAGTTCAGTCTGTTGGTATCTTTGCTGGATGAT
	C A L G V N S A L P K D E S Q *
1401	GTGTGCCCTGGGTGTCAATTCCGCTCTCCCGAAAGATGAGTCACAGTAA

Figure 8.7. Nucleotide and amino acid sequence of AT-like A. The sequence highlighted in blue is the *Hind*III restriction site. The predicted transmembrane domains are shown in red.

1	M L G F E S F S E F V V Y V T F I ATGCTCGGGTTT GAGTCGTTTTCTGAGTTCGTCGTCTATGTCACCTTCAT
	F F G M S V M M V T N A I Y S I
51	CTTTTTTGGGATGTCGGTGATGATGGTGACAAATGCCATTTACTCCATAC
	P A F F T E Y Y K Y A Q G S S D A
101	CAGCTTCTTTACGGAATACTACAAGTATGCACAAGGCAGCTCGGACGCT
	Q T E N E N F W N N I L T Y Y N A
151	CAAACAGAGAATGAGAATTTCTGGAACAACATACTCACGTACTACAACGC
	A V F S A Q V L L E T F M L T N
201	CGCAGTGTTTAGTGCTCAGGTGCTTCTGGAACTTTTATGCTGACGAATG
	V G R R I P I R I R L I F G L T I
251	TTGGAAGGCGAATCCCATCCGGATCCGGCTTATCTTTGGCCTCACTATT
	P L V E L I A L I L I T V C H T S
301	CCTCTTGTAGAACTTATTGCGCTTATACTTATCACCGTGTGCCATACCAG
	E A G A K A T I I I I A L V G G
351	TGAAGCAGGGCGCAAAGCAACTATTATAATTATTGCTTTGGTTGGTGGTG
	V S K T L C D S S N A A L V G P F
401	TTTCCAAAACACTTGCAGCTCGAGTAATGCGGCACCTGGTAGGACCGTTT
	P T R F Y G A I V W G L G V S G L
451	CCAACGAGGTTTATAGGGGCTATTGTGTGGGGTCTTGGTGTTCGGGGCT
	I T S L M S I I I K A S M D D S
501	CATTACTTCCCTCATGTCTATCATTATTAAGCTTCGATGGATGATAGCT
	F E S M L T Q S R I Y F G I V I F
551	TCGAGAGCATGTTAACTCAGTCGAGGATATACTTTGGTATGTCATATTT
	I Q V I A C V L L A L L T K N P Y
601	ATTCAGGTGATCGCCTGTGTTCTTTGGCTCTGCTAACGAAGAATCCTTA
	A I K Y A A E F R H A A A K E S
651	TGCGATAAAATACGCCGCTGAGTTTAGGCATGCTGCAGCGAAAGAGAGCG
	A V E S N E P V Q E T I T D Q E A
701	CAGTGGAAAGTAACGAACCTGTTCAAGAGACCATTACAGACCAAGAAGCT
	N A G E E G E R V E K S T S K M N
751	AATGCCGGAGAGGAGGCGAACGGGTGGAGAAGTCAACTTCCAAGATGAA
	V L N V S E D P D K M K D T D Q
801	TGTCCTGAACGTCAGCGAAGATCCGGACAAGATGAAGGATACCGATCAGG
	V D G T T N A Q Q M L D A N L W F
851	TTGATGGCACCACCAACGCACAACAAATGCTCGATGCTAATTTGTGGTTT
	V V K R I W P M L V S C F F V F F
901	GTGGTGAAGCGCATTTGGCCCATGTTGGTCTCGTGTTCCTTCGTATTTTT
	A T L L V F P G V F F A V E V K
951	TGCTACCCTCCTCGTCTTCCCGGTGTATTTTTCGCCGTTGAAGTGAAG
	D G W Y I T L T A A M F N F G D F
1001	ATGGATGGTACATAACTCTCACCGCCGCTATGTTAACTTCGGTGACTTT
	L S R L V L Q F K Q L R P S P I V
1051	CTCTCCCGCTCGTACTTCAGTTCAGCAGCTGCGCCCATCGCCCATCGT
	V L I G T F F A R L L I I P L L V
1101	GGTCCTTATCGGAACGTTTCGCTCGTTTGTGATCATTCCACTGCTTGTGT
	L C V R G I I P G S A L P Y I L C
1151	TGTGCGTGCGCGGCATCATTCCCGGTCCGCACTCCCTTATATTCTTTGT
	L L W G L T N G Y F G G M S M I Y
1201	CTTCTTTGGGGTCTCACAATGGTTATTTTGGTGGTATGTCTATGATTTA
	A P R T G S L T T A G Q R S L A
1251	TGCGCCACGTACCGGCTCTTTAACAACGCGGGTCAACGCTCCCTTGCCG
	A I C G N L A L L L G L F A G S M
1301	CCATTTGTGGGAATTTGGCCCTTTACTCGGCCTCTTTGCCGGCTCCATG
	L A L A V M T A L P E S *
1351	TTGGCTTTGGCGGTTATGACGGCTCTTCCAGAATCATAA

Figure 8.8. The nucleotide and amino acid sequence of AT-like B. The sequence highlighted in blue is the *Hind*III restriction site and the sequence highlighted in pink is the *Xho*I restriction site. The predicted transmembrane domains are shown in red.

1	M L G F Y S V P E F V V Y V T F I 17
	ATGCTCGGTTTTTATTTCAGTACCTGAATTTGTCGTTTACGTCACCTTCAT
51	F F G M S V M N V T N A I Y S I 33
	CTTTTTTGGGATGTCGGTGTGAATGTGACGAATGCCATCTATTTCGATAC
101	P F F F K E Y Y K F A Q G D A D V 50
	CATTTTCTTTAAGGAGTACTACAAGTTTGCTCAGGGGGACGCTGATGTA
151	Q P K D E G F W K H M F T Y Y N V 67
	CAGCCGAAGGACGAAGGCTTTTGGAAAGCACATGTTACGCTACTACAATGT
201	V V Y T M Q V L L E A F M L T P 83
	CGTTGTGTACACTATGCAGGTGCTTTTGGAGGCCTTCATGCTTACGCCAC
251	L G R R F P I R W R L T F G L A V 100
	TGGGAAGAAGGTTTCCAATACGCTGGCGGCTCACCTTTGGTCTGGCGGTT
301	P I V E I I V I L V I P V V R T S 117
	CCTATCGTGGAGATCATTGTGATTTTAGTGATCCCTGTGGTCCGCACAAG
351	E D A A K A A M M M I A F I G G 133
	CGAGGACCGGGCAAAGGCGGCTATGATGATGATCGCCTTCATTGGTGGTG
401	V S K T L C D S G N A A L V G P F 150
	TTTCAAGACATTGTGTGACTCTGGTAATGCCGCACTTGTAGGGCCGTTT
451	P T K F Y Y G A V V W G L G I S G L 167
	CCCACCAAGTCTACGGTGCCGTCGTTTGGGGTCTCGGTATATCCGGGCT
501	L T S F M S I I I K V S M D D S 183
	TCTCACCTCATTTCATGTCTATTATCATCAAGGTATCTATGGACGATAGCT
551	F S S L L T Q S R I Y F G L I M L 200
	TTTCCAGCTTGCTTACACAGTCGCGGATATACTTTGGACTAATTATGCTT
601	L Q V I A C I L L V L L R K N P Y 217
	CTTCAGGTGATCGCGTGCATTCTTCTAGTTTTACTGAGGAAGAACCCTA
651	A M R Y A A E L R F D A K K S G 233
	CGCCATGAGGTATGCTGCAGAGTTAAGGTTTGCAGCAAAGAAGAGTGGTA
701	T K D S N G L V D V A D A R G T G 250
	CAAAGGACTCCAACGGTTTAGTCGACGTAGCCGATGCGAGAGGAAGTGGT
751	P A D E E C E R E A D E R S D I N 267
	CCTGCAGACGAGGAATGCGAACGTGAGCGGATGAAAGGTCTGACATAAA
801	V M N A T T D P D T M R D T D Q 283
	TGTGATGAATGCCACGACAGATCCAGATACAATGAGAGATACCGACCAGT
851	L E N M T N A K Q M L D A S V M V 300
	TGGAAAATATGACTAACGCAAAACAAATGTTGGACGCGAGTGTATGGTT
901	V A K R I W P M L V S C F F V F F 317
	GTGGCAAAGCGTATTTGGCCCATGCTTGTTCCTGTTTCTTTGTGTTCTT
951	A T L L V F P G V F F A V K T D 333
	TGCAACACTTCTCGTCTTCCCTGGTGTGTTCTTTGCTGTCAAGACGGATG
1001	V P S G W Y F T I V A A M Y N L G 350
	TTCCCAGTGGGTGGTATTTACCATCGTCGCTGCGATGTACAACCTGGGT
1051	D F L S R L V L Q F K R L H P S P 367
	GACTTCTTATGCTTGCCTTGTCTCAGTCAAGCGGTTGCACCCTTCGCC
1101	R G V V I G T F S R L L V I P L 383
	ACGTGGCGTTGTGATCGGAACCTTTTCGCGTTTGTGGTTATTCCACTGC
1151	L A L C V Y D V I S G P W V P Y V 400
	TTGCACTTTGCGTGTACGATGTTATTAGTGGCCCGTGGGTCCCTTATGTT
1201	L C L I W G L T N G Y F G G M S M 417
	CTTTGCCTTATTTGGGCCTTACGAATGGCTACTTTGGCGGCATGTCGAT
1251	I Y G P R T G S L T T A G Q R S 433
	GATTTATGGACCGGTACGGATCCCTTACAACAGCGGGCCAGAGGTCCC
1301	L A A I C I N L A L L L G L F G G 450
	TTGCTGCCATTTGCATTAATTTGGCCCTTCTTCTGGCCTCTTCGGTGGT
1351	A M S A M A V I K A L P H *
	GCCATGTCTGCCATGGCGGTTATAAAAGCTCTTCCGCATTAA

Figure 8.9. The nucleotide and amino acid sequence of AT-like D. The sequence highlighted in green is the *Bam*HI restriction site and the sequences highlighted in yellow are the *Pst*I restriction sites. The predicted transmembrane domains are shown in red.

predictions for the AT-like sequences are also ENT-like in that they have a large intracellular loop between transmembrane domain 6 and 7. It is prudent to note that useful though these predictions are, they are speculative only. The number of transmembrane domains may be over-estimated or under-estimated since soluble proteins can contain areas of hydrophobicity and transmembrane segments can contain amphipathic regions that would not be flagged as potential membrane spanning regions (Stryer, L., 1995). The results from TMpred were accompanied by the disclaimer that caution must be exercised in the interpretation of any predictions.

8.2.4 Sub-cloning of AT-like sequences into pDR195

The three AT-like sequences were subcloned into the *NotI* site of the pDR195 yeast expression vector as described for *TbNBT1* in Chapter Seven.

The orientation of the insert for each AT-like sequence:pDR195 construct was verified using an appropriate series of restriction enzyme digests as described below.

Figure 8.11 shows the restriction map for the AT-like A:pDR195. A *HindIII-BamHI* double digest of the construct generates three bands on an agarose gel. The correct orientation of the gene produces bands of 1400, 920 and 5460 bp, while the incorrect orientation gives bands of 560, 1760, and 5460 bp. Figure 8.12 shows examples of both banding patterns.

To verify the correct orientation of AT-like B in the pDR195 vector (Figure 8.13) the construct was digested with the *XhoI* enzyme. The correct orientation gave 2 bands of 440 and 7280 bp while the incorrect orientation yielded fragments of 980 and 6740 bp. Figure 8.14 shows these band variations but there were other banding patterns observed, also shown in the figure. These alternative digest products were consistent with more than one insert being incorporated in tandem during ligation events.

Figure 8.11. Restriction map for AT-like A:pDR195. The transmembrane domains are numbered 1-XI.

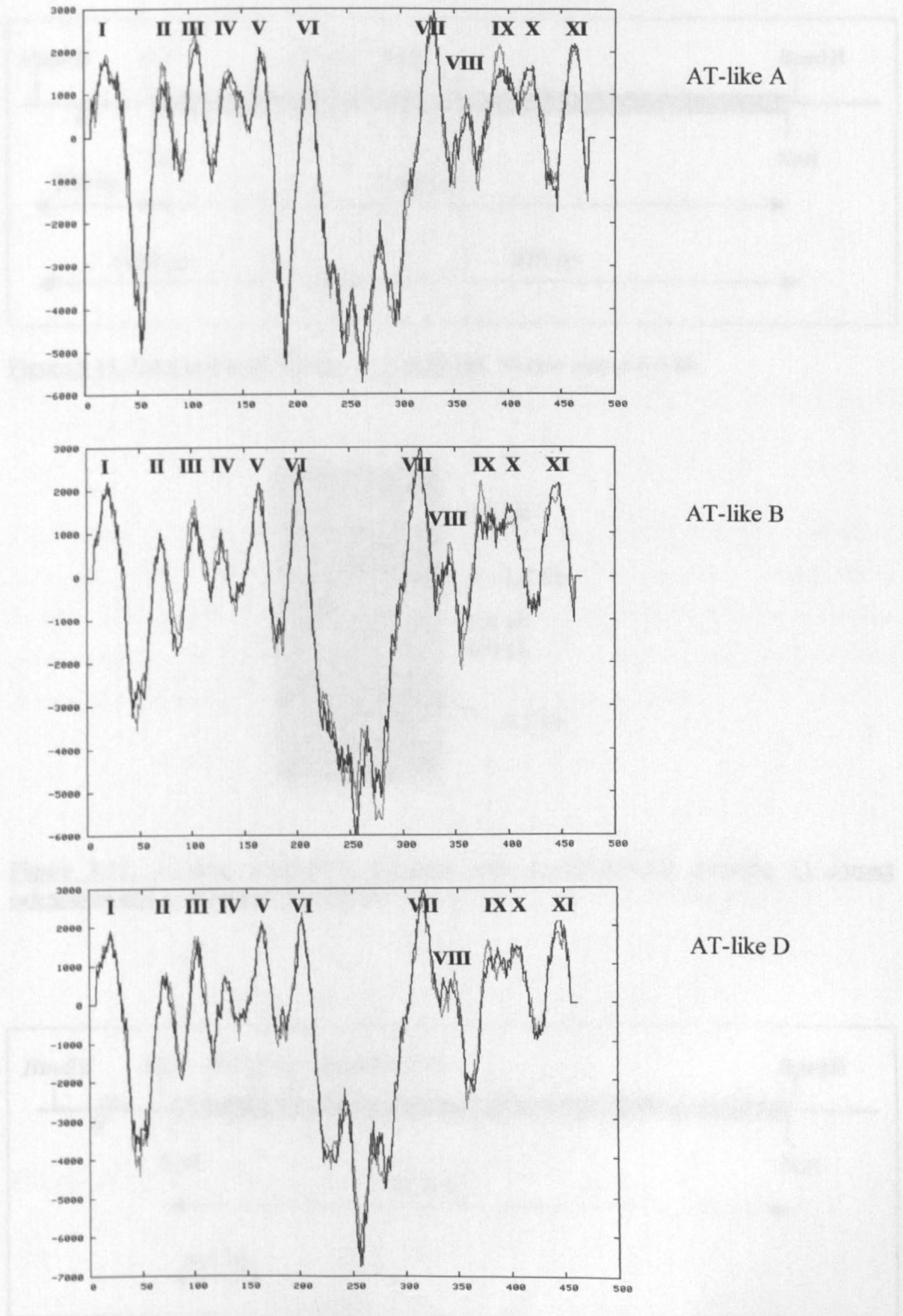


Figure 8.10. Hydropathy plots for AT-like amino acid sequences. The transmembrane domains are numbered I-XI.

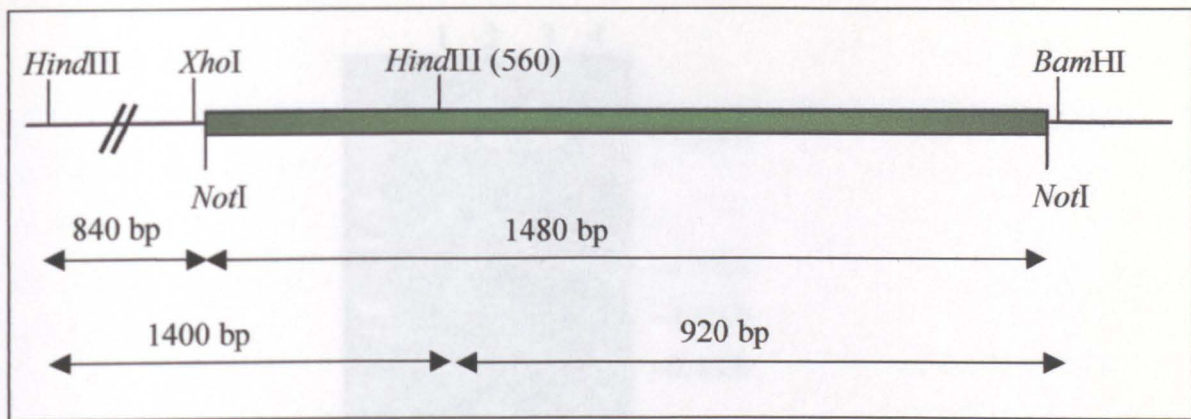


Figure 8.11. Orientation of AT-like A in pDR195. Vector size is 6.3 kb.

Figure 8.14. AT-like B in pDR195. The BamHI sites in the vector are 136 bp apart. The BamHI sites in the construct are 136 bp apart. The BamHI sites in the construct are 136 bp apart. The BamHI sites in the construct are 136 bp apart.

The BamHI sites in the vector are 136 bp apart. The BamHI sites in the construct are 136 bp apart. The BamHI sites in the construct are 136 bp apart. The BamHI sites in the construct are 136 bp apart.

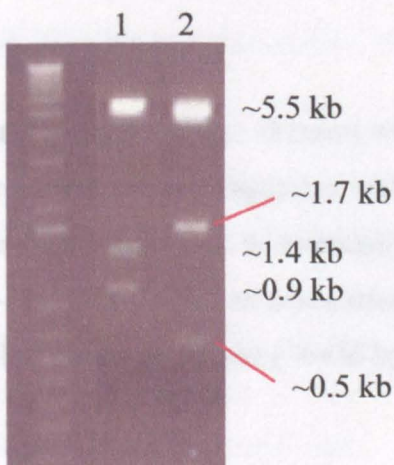


Figure 8.12. AT-like A:pDR195 digested with BamHI/HindIII showing 1) correct orientation and 2) incorrect orientation.

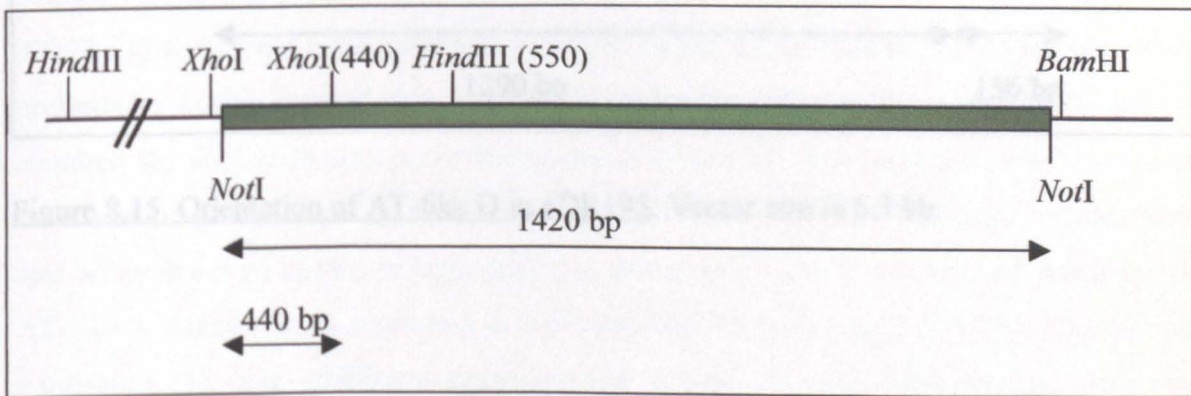


Figure 8.13. Orientation of AT-like B in pDR195. Vector size is 6.3 kb.

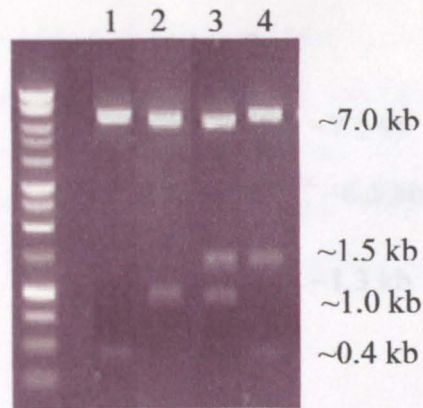


Figure 8.14. AT-like B:pDR195 digested with *XhoI* showing 1) correct orientation and 2-4) incorrect orientation.

The *Bam*HI sites in the vector and the AT-like D insert were situated quite close together if the orientation in the construct was correct. Digestion with *Bam*HI produces a small 136 bp fragment and the remainder of the construct is essentially linearised and shows up on the gel as a large fragment of ~ 7590 bp. Incorrect orientation effectively leads to the excision of most of the insert (1290 bp) out of the vector (~6436 bp) on digestion.

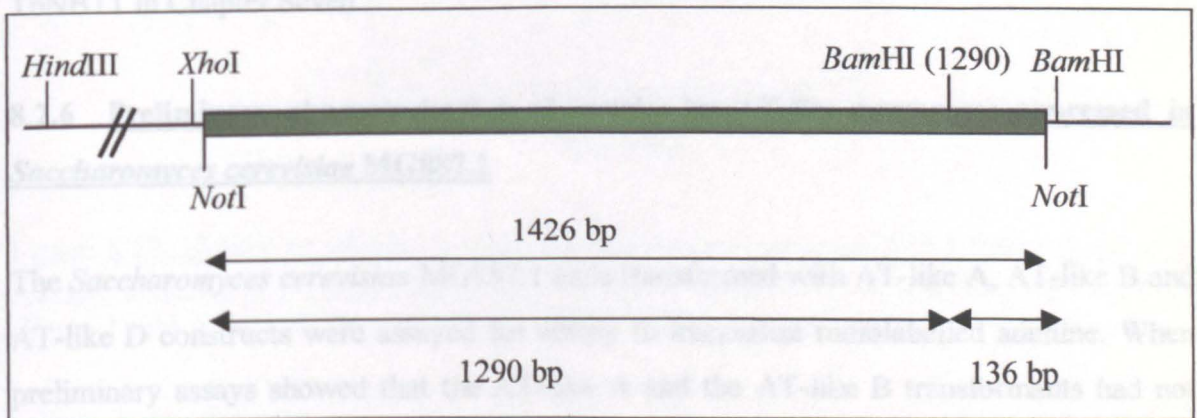


Figure 8.15. Orientation of AT-like D in pDR195. Vector size is 6.3 kb.

As shown in Figure 8.17 the cells transformed with the AT-like A and B constructs did not internalise adenine. The uptake was not affected by the presence of unlabelled adenine. The cells transformed with the AT-like D construct showed a high affinity for this substrate and the uptake was not affected by the presence of unlabelled adenine. As no uptake was observed for the AT-like A and B constructs, it seems to be unlikely that they are able to transport adenine. The AT-like D transporter seems to be able to transport adenine and the uptake was linear over the time range tested (0-10 min). The uptake was saturable with a K_m of 10^{-5} mol/L and a V_{max} of 1.5×10^{-4} mol/L cell/h. The results indicate that the AT-like D transporter is able to transport adenine.

The AT-like D transporter seems to be able to transport adenine and the uptake was linear over the time range tested (0-10 min). The uptake was saturable with a K_m of 10^{-5} mol/L and a V_{max} of 1.5×10^{-4} mol/L cell/h. The results indicate that the AT-like D transporter is able to transport adenine.

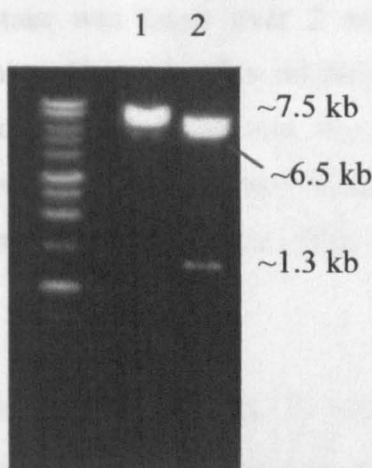


Figure 8.16. AT-like D:pDR195 digested with *Bam*HI showing 1) correct orientation and 2) wrong orientation.

8.2.5 Selection of yeast colonies expressing the AT-like A, B or D gene

The transformation of the pDR195/AT-like constructs into the *S. cerevisiae* strain MG887.1 and the selection of transformants on first SC-URA and then minimal media supplemented with 1 mg/ml (7.4 mM) adenine plates was carried out as described for TbNBT1 in Chapter Seven.

8.2.6 Preliminary characterisation of uptake by AT-like permeases expressed in *Saccharomyces cerevisiae* MG887.1

The *Saccharomyces cerevisiae* MG887.1 cells transformed with AT-like A, AT-like B and AT-like D constructs were assayed for ability to internalise radiolabelled adenine. When preliminary assays showed that the AT-like A and the AT-like B transformants had not acquired the facility to transport adenine, these cells were then presented with a range of radiolabelled potential purine permeants. As well as an absence of adenine uptake, there was no evidence of uptake of hypoxanthine, adenosine, inosine, cytosine, or uracil by the AT-like A transformants compared to cells transformed with empty pDR195. Due to time constraints the only additional radiolabel the AT-like B cells were assayed with was hypoxanthine – again, no transport activity was detected.

As shown in Figure 8.17 the cells transformed with AT-like D construct were able to internalise adenine. The uptake was linear over 2 minutes and was inhibited by the presence of unlabelled adenine. However, this inhibition was not total suggesting low affinity for this substrate and that perhaps adenine was not the primary substrate for the introduced permease. As noted above, the empty vector transformants did not seem to accumulate adenine and there was no significant difference in the presence or absence of unlabelled permeant.

The AT-like D transformants were shown to take up 0.015 μM adenosine rapidly and the uptake was linear over the entire 4 minute timecourse with a rate of 0.024 ± 0.002 pmol $(10^7 \text{ cells})^{-1} \text{ min}^{-1}$ (see Figure 8.18). Transport was saturable as shown by the capacity for unlabelled adenosine to completely suppress uptake of the radiolabel. Adenine could also inhibit the transport of the adenosine radiolabel but this was only partial inhibition again indicating that adenine has a relatively low affinity for this transporter.

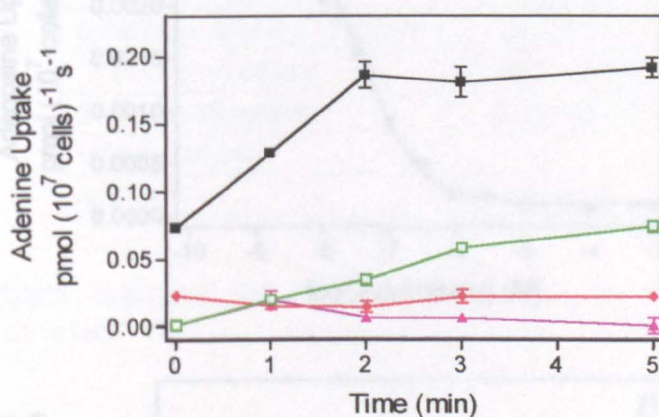


Figure 8.17. Uptake of adenine by *Saccharomyces cerevisiae* MG887.1 transformed with AT-like D:pDR195 or empty pDR195. AT-like D:pDR195 - 0.1 μM [^3H] adenine only (■), + 1 mM adenine (□); pDR195 - 0.1 μM [^3H] adenine only (◆), + 1 mM adenine (▲).

Figure 8.19 shows the substrate saturation curve for inhibition of the transport of 15 nM tritiated adenosine by various concentrations of unlabelled adenosine for a fixed time course. The IC_{50} for inhibition of radiolabelled adenosine by unlabelled adenosine is 0.042 μM . The data from Figure 8.19 was used to construct the Michaelis-Menten plot for adenosine uptake by the AT-like D transporter expressed in *Saccharomyces cerevisiae*

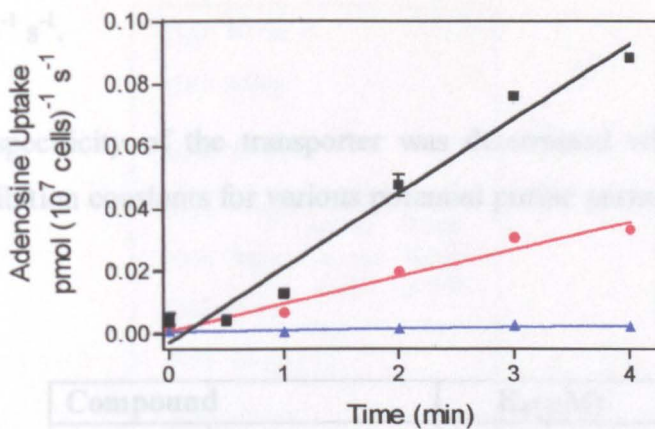


Figure 8.18. Uptake of 15 nM [^3H] adenosine by *Saccharomyces cerevisiae* MG887.1 transformed with AT-like D:pDR195. Label only (■), + 1 mM adenine (●), or + 1 mM adenosine (▲).

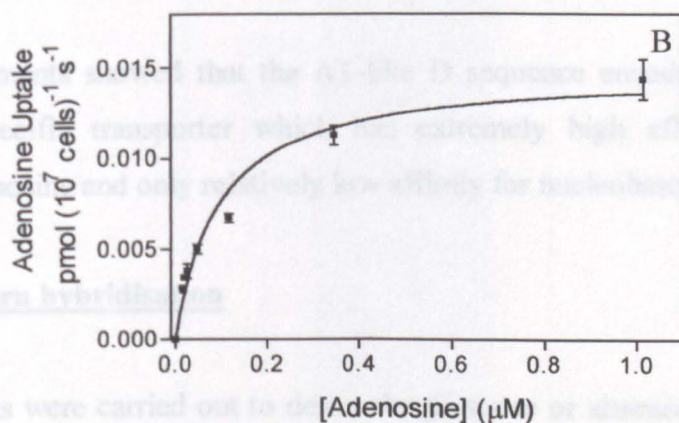
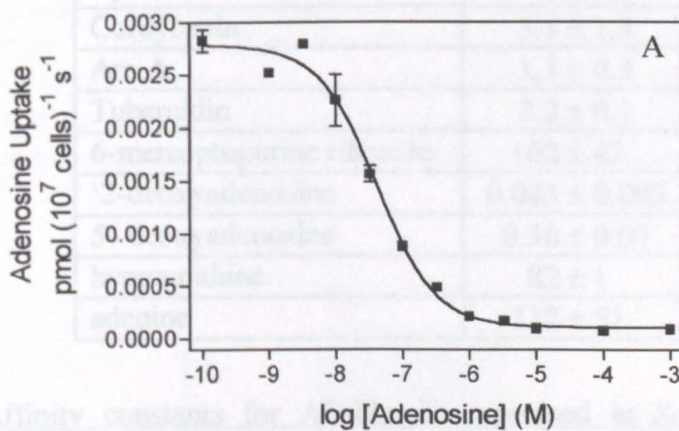


Figure 8.19. (A) Inhibition of 15 nM [^3H] adenosine uptake by *Saccharomyces cerevisiae* MG887.1 transformed with AT-like D:pDR195. K_i value is 0.042 μM . (B) Michaelis-Menten plot of adenosine uptake in *Saccharomyces cerevisiae* MG887.1 transformed with AT-like D:pDR195. V_{max} of 0.015 $\text{pmol} (10^7 \text{ cells})^{-1} \text{ s}^{-1}$. K_m of 0.093 μM .

MG887.1 (Figure 8.20). The apparent K_m was $0.093 \mu\text{M}$ and the apparent V_{max} was $0.015 \text{ pmol} (10^7 \text{ cells})^{-1} \text{ s}^{-1}$.

The substrate specificity of the transporter was determined with a series of transport assays. The inhibition constants for various potential purine permeants are shown in Table 8.1.

Compound	$K_i (\mu\text{M})$	n
Adenosine ¹	0.058 ± 0.012	4
Inosine	4.3 ± 1.5	4
Guanosine	5.7 ± 0.6	3
Uridine	219 ± 37	3
Thymidine	471 ± 32	3
Cytidine	86 ± 30	3
Cordycepin	5.5 ± 1.3	3
Ara A	1.3 ± 0.3	3
Tubercidin	2.2 ± 0.1	2
6-mercaptapurine riboside	102 ± 42	3
'2-deoxyadenosine	0.043 ± 0.005	3
5'-deoxyadenosine	0.30 ± 0.07	3
hypoxanthine	82 ± 1	2
adenine	112 ± 51	3

Table 8.1. Affinity constants for AT-like D expressed in *Saccharomyces cerevisiae* MG887.1. ¹ K_m value.

These experiments showed that the AT-like D sequence encodes a high-affinity purine nucleoside-specific transporter which has extremely high affinity for the definitive substrate adenosine and only relatively low affinity for nucleobases.

8.2.7 Northern hybridisation

Northern blots were carried out to detect the presence or absence of AT-like A, B and D transcripts in both bloodstream and procyclic form *T. b. brucei* 927. Figure 8.21 shows the RNA markers and ribosomal RNAs successfully transferred to the membrane. The membrane was probed with DNA probes consisting of the entire gene sequences. The AT-like B probe hybridised to the region between 3638 and 4981 kb in the bloodstream RNA

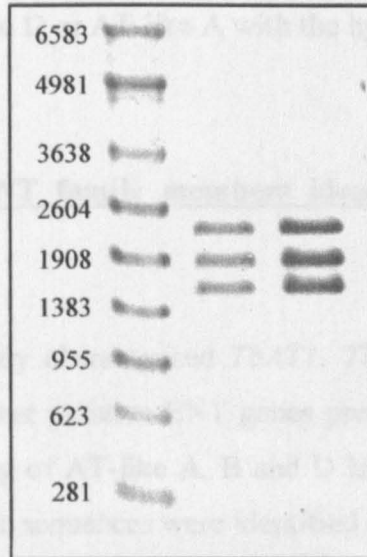


Figure 8.21. Transfer of RNA to membrane for Northern analysis. Following overnight blotting the Hybond membrane was stained with Blot Stain Blue Reversible Northern Blot Staining Solution (Sigma). There are three size categories of ribosomal RNA in *Trypanosoma brucei* accounting for up to 80% of the total RNA present in the cell. The presence of the three rRNAs on the membrane (2.3 kb, 1.9 kb and 1.5 kb) confirmed that transfer had been accomplished and also controlled for differences in RNA loading.

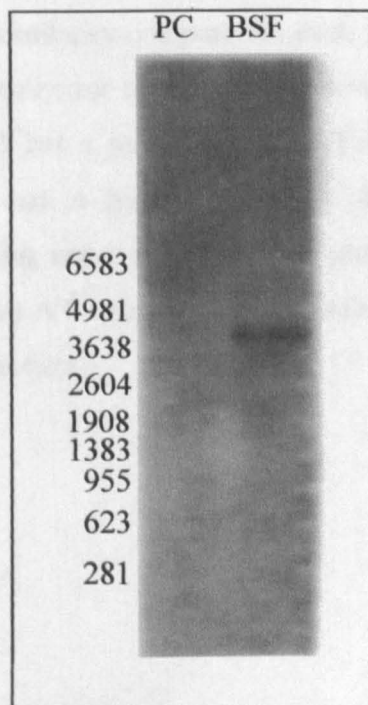


Figure 8.22. Northern hybridisation using the full-length AT-like B ORF as probe.

lane but not in the procyclic sample. (Figure 8.22). There was no apparent hybridisation to the membrane for AT-like D or AT-like A with the hybridisation conditions used.

8.2.8 Overview of ENT family members identified in the *T. b. brucei* genome database

As well as the previously characterised *TbAT1*, *TbNT2-7*, *TbNBT1* and *TbNT8.1* there appears to be several other putative ENT genes present in the *T. b. brucei* genome. The identification and cloning of AT-like A, B and D have been described in this chapter. In addition 5 more ENT-like sequences were identified *in silico* which have sequence identity to the genes listed above. These sequences have been designated AT-like E-I.

All the known sequences were used to construct a multiple alignment (Figure 8.23). The sequence comparisons resolved three distinct groups. TbAT-like A, E and G aligned most closely with the *TbAT1* sequence; TbAT-like F and H associated with *TbNBT1* and *TbNT8.1*; and, finally, TbAT-like B, D and I aligned with the *TbNT2-7* sequences. Figure 8.24 shows the tree constructed as a result of the multiple alignment. Table 8.2 shows how the sequence identity and similarity compare for each pair of sequences. TbAT-like F and H differ from *TbNT8.1* at only one amino acid position (AT-like F has an alanine residue at position 51 while *NT8.1* has a serine residue; AT-like H has an asparagine residue at position 245 and *NT8.1* has a lysine residue at the same position). Whether these differences reflect sequencing errors or perhaps the presence of different alleles is unclear. AT-like G only differs from AT-like A at three positions but also possesses a putative 12 amino acid N-terminal extension.

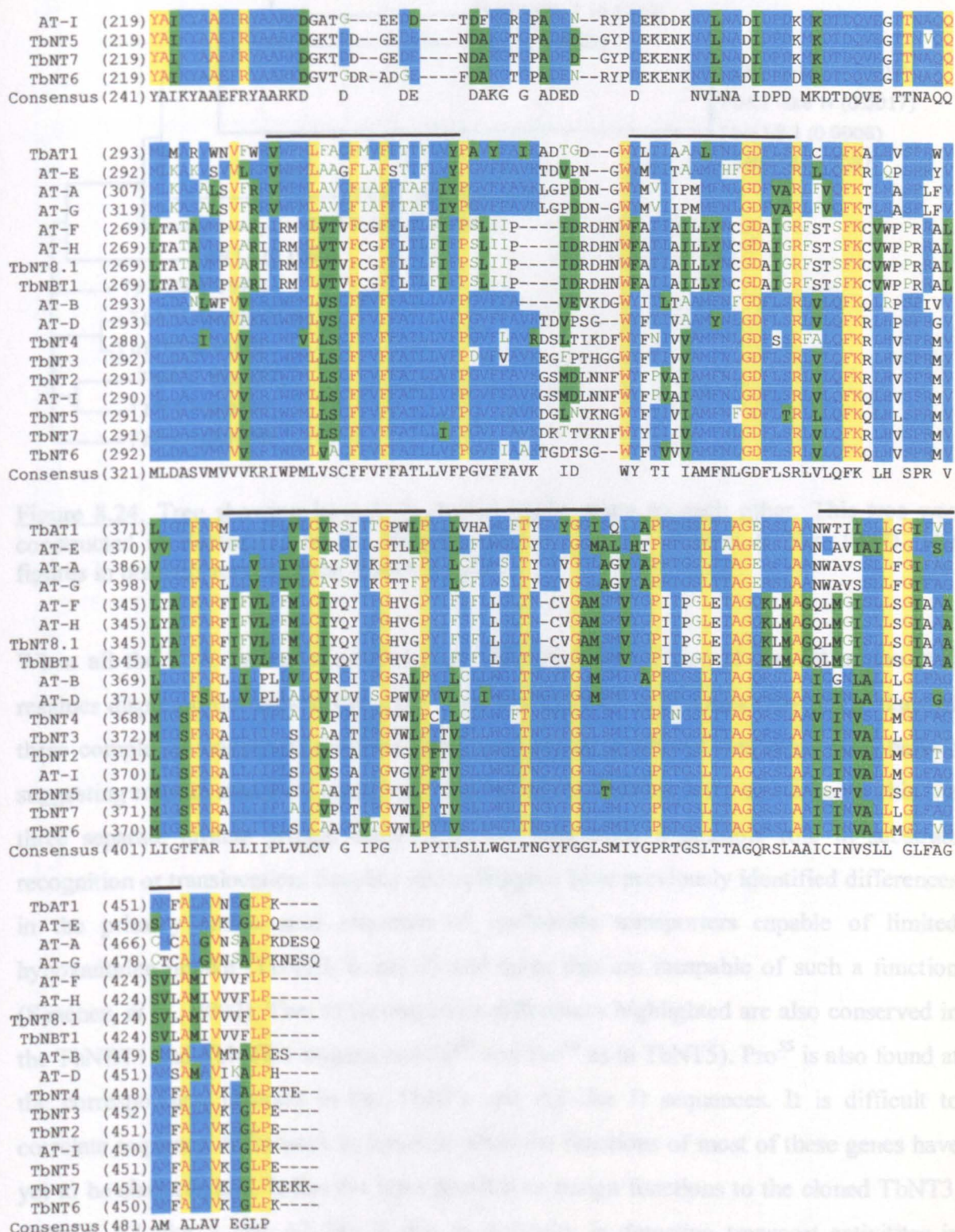


Figure 8.23. Multiple alignment of ENT gene family members in *T. b. brucei*. The transmembrane domains as they appear in TbAT1 are represented as bold lines above the sequences.

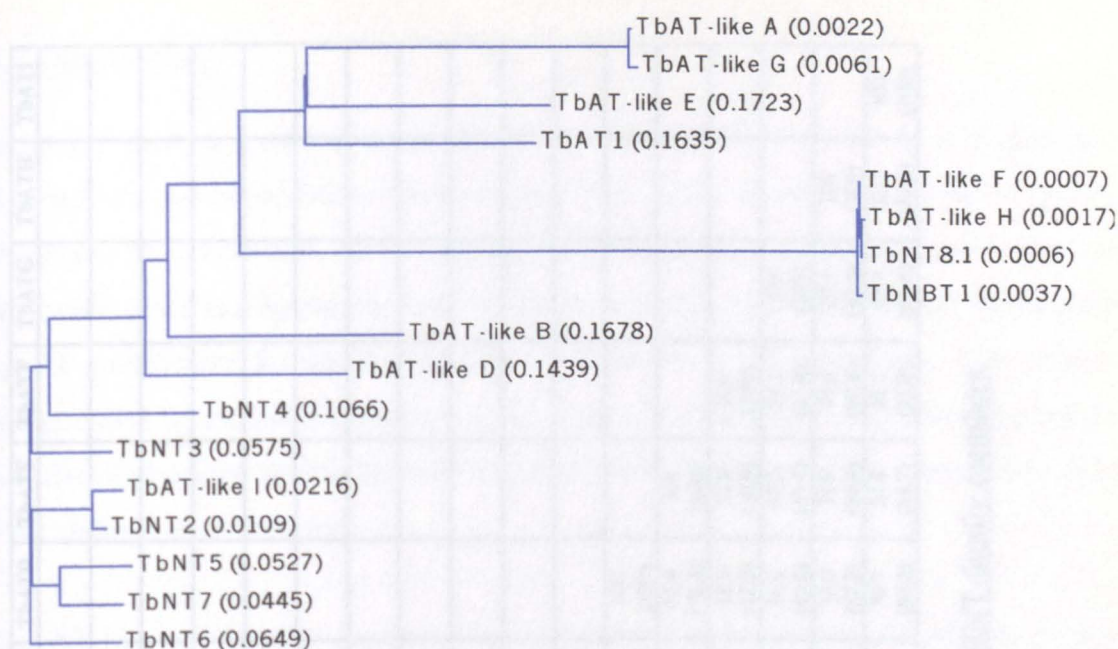


Figure 8.24. Tree showing how *T. b. brucei* ENTs relate to each other. This tree was constructed in VectorNTI by the Neighbor-Joining method (Saitou & Nei, 1987). The figures in brackets represent the branch length.

When all the *T. b. brucei* sequences were aligned it was observed that 74 amino acid residues dispersed throughout the proteins were conserved in all cases (15-17%). Many of these completely conserved residues were found in the predicted transmembrane helices suggesting roles in structural integrity. Other groups of residues were conserved within the three separate protein groups outlined above, suggesting a possible role in substrate recognition or translocation. Sanchez and colleagues have previously identified differences in the primary amino acid sequence of nucleoside transporters capable of limited hypoxanthine uptake (TbNT5, 6 and 7) and those that are incapable of such a function (Sanchez, *et al.*, 2002). Two of the sequence differences highlighted are also conserved in the TbNBT1 and TbNT8.1 sequences (Val⁴⁷ and Pro⁵⁵ as in TbNT5). Pro⁵⁵ is also found at the corresponding position in the TbAT1 and AT-like D sequences. It is difficult to correlate sequence differences to function when the functions of most of these genes have yet to be characterised. It has not been possible to assign functions to the cloned TbNT3, TbNT4, AT-like A and AT-like B due to difficulty in detecting transport activities in heterologous systems. AT-like E, AT-like F, AT-like G, AT-like H and AT-like I have not yet been cloned. It will be necessary to elucidate the functions of these genes in a heterologous system, and the relative importance of distinct residues or groups of residues can be probed using site-directed mutagenesis.

	TbAT1	TbNT2	TbNT3	TbNT4	TbNT5	TbNT6	TbNT7	TbNT8.1	TbNBT1	TbATA	TbATB	TbATD	TbATE	TbATF	TbATG	TbATH	TbATI
TbAT1	100 (100)																
TbNT2	57.2 (71.5)	100 (100)															
TbNT3	57.9 (71.4)	88.8 (92.5)	100 (100)														
TbNT4	54.0 (66.8)	80.5 (86.3)	82.0 (86.1)	100 (100)													
TbNT5	56.7 (71.5)	87.3 (92.0)	86.9 (91.4)	77.0 (83.7)	100 (100)												
TbNT6	57.0 (71.0)	86.6 (90.3)	87.1 (90.8)	79.7 (85.2)	86.9 (90.9)	100 (100)											
TbNT7	56.4 (71.1)	88.4 (92.3)	86.5 (90.1)	79.4 (85.4)	89.7 (94.4)	85.2 (89.9)	100 (100)										
TbNT8.1	32.3 (51.9)	32.4 (52.3)	32.5 (51.3)	31.4 (50.4)	33.7 (51.8)	32.7 (51.9)	32.0 (51.3)	100 (100)									
TbNBT1	32.1 (51.5)	32.0 (52.7)	32.4 (51.9)	31.4 (50.2)	33.5 (52.5)	32.5 (51.5)	31.6 (51.7)	99.3 (99.3)	100 (100)								
TbATA	57.9 (71.0)	47.8 (62.9)	49.2 (63.0)	47.9 (60.5)	48.5 (61.6)	49.4 (63.6)	48.5 (62.9)	29.6 (48.7)	30.0 (48.9)	100 (100)							
TbATB	55.2 (70.5)	65.6 (76.7)	64.6 (75.3)	62.3 (73.8)	64.3 (75.6)	64.2 (75.3)	64.9 (75.5)	31.7 (51.6)	32.0 (51.6)	47.9 (63.9)	100 (100)						
TbATD	56.5 (74.1)	70.4 (80.1)	69.9 (79.5)	66.0 (76.4)	67.9 (78.4)	70.5 (80.4)	68.7 (79.4)	33.0 (52.2)	33.2 (52.2)	48.1 (64.7)	67.7 (79.1)	100 (100)					
TbATE	65.8 (77.0)	55.3 (70.5)	56.0 (69.7)	52.6 (66.9)	54.6 (68.8)	54.4 (68.9)	54.9 (69.2)	31.8 (50.9)	32.0 (50.9)	57.0 (69.2)	57.4 (74.2)	55.6 (72.4)	100 (100)				
TbATF	32.5 (51.9)	32.8 (52.5)	33.2 (51.7)	31.6 (50.4)	34.3 (52.3)	32.9 (51.9)	32.2 (51.5)	99.8 (100)	99.1 (99.3)	29.6 (48.7)	32.0 (51.6)	33.0 (52.2)	32.0 (50.9)	100 (100)			
TbATG	56.1 (69.0)	46.9 (61.6)	48.2 (61.7)	47.0 (59.3)	47.5 (60.4)	47.8 (62.6)	47.5 (61.4)	28.9 (47.4)	29.4 (47.6)	96.8 (96.8)	46.2 (61.7)	46.6 (63.0)	55.2 (67.1)	29.1 (47.8)	100 (100)		
TbATH	32.3 (51.9)	31.8 (52.7)	32.2 (51.9)	31.2 (50.2)	33.3 (52.5)	32.3 (51.5)	31.4 (51.7)	99.8 (99.8)	99.5 (99.5)	29.8 (48.9)	31.7 (51.6)	33.0 (52.2)	31.8 (50.9)	99.5 (99.8)	29.1 (47.6)	100 (100)	
TbATI	57.2 (71.5)	96.5 (97.0)	86.2 (90.3)	80.4 (86.5)	84.9 (90.1)	86.2 (90.9)	86.3 (90.6)	32.3 (52.6)	32.3 (52.4)	47.8 (63.1)	66.5 (77.1)	70.7 (80.5)	54.8 (69.7)	32.7 (52.8)	46.7 (61.6)	32.3 (52.6)	100 (100)

Table 8.2. Amino acid sequence similarities and identities (%) shared between *T. b. brucei* ENT-family members.

8.3 Discussion

Evidently there are several putative ENT family members in the *T. b. brucei* genome database for which activities have yet to be assigned. In addition to the new AT-like sequences described here, these transporters of unknown function include several of the NT genes described by Sanchez and colleagues (2002). Conversely, there are nucleobase uptake components for which a genetic basis has yet to be determined. This situation is compounded by the indefinite nature of biochemical elucidation of uptake components – it is difficult given the multitude and overlap of the different activities to conclude that they have all been accounted for.

The AT-like A, B and D sequences were encountered in the same BLAST searches that uncovered the TbNBT1 gene. They showed better sequence homology to TbAT1 than did the TbNBT1 sequence and, in fact, AT-like B and D were more akin to the TbNT2-7 than to any of the other genes. Although prediction of function based on such relationships are far from infallible it seemed reasonable to speculate that AT-like B and D might code for transport proteins leaning more towards nucleosides as preferred permeants. TbAT-like A seemed quite unique in that it had a reasonably high amount of shared sequence identity with all of the known purine transporter genes sharing only slightly higher levels of homology with TbAT1 than with the others.

With the successful expression of TbNBT1 in *Saccharomyces cerevisiae* MG877.1 this heterologous system was validated as a route for elucidation of *T. b. brucei* purine transporters and so it seemed plausible that the same system would allow the characterisation of the other three AT-like sequences that had been cloned. Although colonies of MG887.1 transformed with each of the sequences could be isolated on adenine-selective plates only colonies possessing the AT-like D gene were shown to have acquired the ability to internalise purines.

Given the identification of the AT-like D activity as a high affinity nucleoside uptake system with relatively low affinity for nucleobase molecules it may seem curious that its presence in yeast could allow selective growth on adenine as the sole source of nitrogen. This is an indication of the sensitivity of the yeast system for allowing selection even on secondary substrates of introduced permeases. The NTR1 gene cloned and characterised by

Rentsch and colleagues (1995) in *Saccharomyces cerevisiae* was originally selected for its ability to complement a histidine-uptake deficient strain but further characterisation showed that the encoded permease was actually an oligo-peptide transporter and has comparatively low affinity for histidine itself. Considering this sensitivity and the flexibility with which yeast strains can utilise purines and pyrimidines as nitrogen sources this approach has the potential to identify many transporters with widely varying substrate specificity (Gillissen, *et al.*, 2000).

The AT-like D transport component characterised in the yeast heterologous system exhibited a P1-like substrate specificity and the AT-like D gene also aligned most closely with the P1-type NT permeases previously characterised by Sanchez, *et al.* (2002). Despite this relationship there was a more significant degree of identity within the previously characterised NT sequences than there was between AT-like D and any individual NT sequence. It is noteworthy that AT-like D displays higher affinity for adenosine by at least an order of magnitude than any of the other *T. b. brucei* ENT family members yet characterised.

Northern analysis was undertaken to try to determine the lifecycle stage in which the AT-like A, AT-like B and AT-like D genes are transcribed. Under the hybridisation conditions used only AT-like B mRNA was detected and this was only present in the bloodstream form parasites. Given that the AT-like D has been characterised as a transporter operating at very low adenosine concentrations (at least in the heterologous system which may not reflect the actual activity of AT-like D *in situ*) and given that AT-like D mRNA could not be detected in either procyclics or bloodstream forms it was speculated that AT-like D may be expressed in the lifecycle stage exposed to the lowest endogenous purine levels (*e.g.* in the metacyclic stages). Due to time constraints it was not possible to investigate this hypothesis any further.

Regulation of gene expression in *T. b. brucei* seems quite complex as the Northern analysis has shown previously that the TbAT1 mRNA transcript is present in both bloodstream form and procyclic parasites although the P2 transport component is not biochemically detectable in insect-stage parasites (De Koning, *et al.*, 1998). Conversely, the initial characterisation of the P1-type TbNT2 (Sanchez, *et al.*, 1999) showed that mRNA was only found in bloodstream stage parasites in the strain used (EATRO 110) although P1

activity is present in both life-cycle stages. Further studies in reference strain *T. b. brucei* 927 showed that in this strain the TbNT2 gene (distinct from gene in EATRO 110) was expressed in both bloodstream forms and procyclics (Sanchez, *et al.*, 2002). The TbNBT1 gene is also transcribed in both bloodstream form and procyclic parasites as determined by Northern analysis but the biochemical activity has only been studied in procyclic forms and it is unclear if it is present in bsf. Many questions remain regarding the mechanisms present in trypanosomes for the regulation of gene expression. There is the possibility that *T. b. brucei* genes and the subsequent proteins can be regulated at several different levels including post-transcriptionally or post-translationally.

The current situation with AT-A, AT-B, TbNT3 and TbNT4, *i.e.* not knowing exactly what role they fulfil, highlights major problems with identifying functions for the enormous number of genes that are being generated by genome projects. If a function can be putatively assigned either by results in heterologous systems or by homology with proteins of known function techniques such as RNAi should prove very useful for reconciling genetic information with biochemical profiles *in situ*.

Considering the phylogenetic distance and the clear functional differences between the protozoan and mammalian ENTs it is not so surprising that there is a great deal of diversity between the transporters at the amino acid level. Even so there are some residues and putative motifs that seem to bridge the gap.

There is a good deal of sequence homology shared between the ENTs identified in *T. b. brucei* to date although it has been challenging to link structure and function given the gaps in our knowledge. Although some residues have been conserved across the phylogenetic distance between trypanosomes and mammals there is a large amount of sequence divergence (Carter, *et al.*, 2001). Gly²⁰ (as appears in TbAT1) is completely conserved in more than thirty ENTs from organism as diverse as *C. elegans* and *A. thaliana* analysed by Acimovic & Coe (2002). Glycines are also completely conserved at positions 161 and 166 of TbAT1 (within TMS 5). A conserved proline at position 151 falls in the intracytoplasmic loop between TMS 4 and 5. A NXXDXXGR motif or very similar is found in the TMS 8 of most of the ENTs analysed - there is some speculation that these residues are involved in recognition of substrates or inhibitors. A putative motif of unknown functional significance, S/TNGY has been observed in TMD 10. Interestingly, in

the nucleobase transporter sequences only the threonine and asparagine residues are conserved in this region.

Found throughout the ENT family, the conserved residues most likely play some role in structural integrity, substrate recognition and/or translocation. Some of the sequence variations found for the various taxonomic groups will determine the functional differences observed for the different transporters such as sensitivity to inhibitors, the higher affinities with which the parasite transporters recognise their substrates, and the differences in energy-dependency.

The relatively recent explosion in sequence data available has obviously provided a veritable goldmine for gene discovery. Certainly, nucleobase and nucleoside transport in protozoan parasites has proved to be much more complicated at the molecular level than had been anticipated from biochemical investigations. Clearly, with a multitude of potential transporters still to characterise functionally and transport activities still to characterise genetically there remains much to explore and clarify in the elucidation of nucleobase and nucleoside transport in *T. b. brucei*.

Chapter Nine

General Discussion

9. General Discussion

The main aim of project was to further our understanding of the purine transporters of the parasitic protozoan *Trypanosoma brucei* at the biochemical and molecular level, with an emphasis on advancing the current knowledge regarding purine nucleobase uptake.

The study of selectivity and substrate recognition is particularly challenging for transporters, yet is of obvious pharmacological relevance given the importance of drug uptake by target cells. Particular difficulties include obtaining genetic information through functional cloning, considering the problems with (over)expressing membrane proteins, not to mention purifying them in an active configuration. Even when the gene encoding a particular transport activity is known, obtaining structural data through crystallisation is extremely difficult. We have therefore opted to study substrate-transporter interactions using kinetic approaches using intact cells to characterise transporters *in situ*.

Using these techniques it has been possible to identify and quantify the components necessary for the recognition of purine substrates by the H2 transporter of *T. b. brucei* and by the hFNT1 transporter of human erythrocytes. As well as identifying differences in the host and parasite transporters these experiments have allowed the prediction of which analogues are most likely to be efficiently accumulated by the parasite. The relevance of the models and the implication for possible rational uptake of trypanocides becomes even more evident when it is considered that models constructed for the *Leishmania major* NBT1 transporter (Figure 9.1) show that this transporter appears to recognise its substrates in a very similar manner to H2. This raises the possibility of a broad-spectrum trypanocide/leishmanicide, although caution is warranted since the LmNBT1 model has been constructed using data obtained from experiments with promastigotes rather than from the amastigotes that cause human disease. In addition, even if the same activity is evident in the clinically relevant life-cycle stage, the situation is further complicated by the intracellular status of *Leishmania* amastigotes, which introduces further barriers between a drug in the bloodstream and the parasite.

As an alternative to using the free energy calculations used for a large portion of this thesis, a recent study (Chang, *et al.*, 2004) used computational methods to define the

different pharmacologically relevant components of the substrate and combined this information with inhibition data to determine the molecular requirements for substrates/inhibitors of some of the human nucleoside transporters.

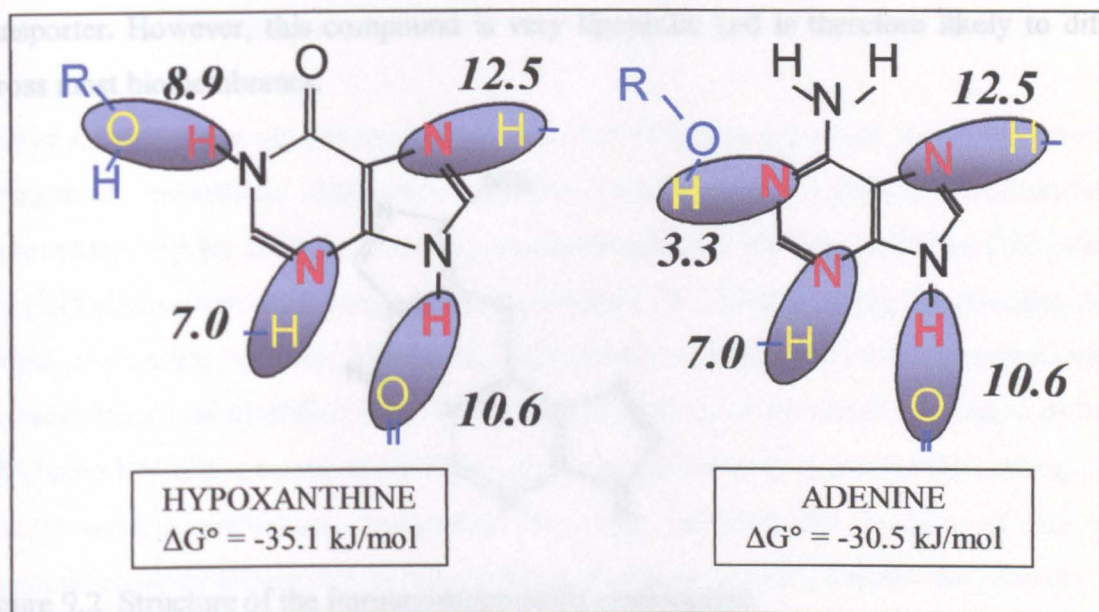


Figure 9.1. Model of the interactions between purines and the *L. major* NBT1 transporter. Estimations of the Gibbs free energy of these interactions are given in kJ/mol. This model is reproduced from Al-Salabi, *et al.* (2003).

The aim of the study in Chapter 3 was not so much to identify purine antimetabolites with strong trypanocidal activity. Rather, the intention was to prove the principle, that selective accumulation by the parasite is possible and such purines can be designed or selected based on our substrate-recognition models. The list of purine analogues tested for this study was therefore not exhaustive and there remains a large number of molecules that could still be tested both for uptake by the various *T. b. brucei* transporters and for trypanocidal activity *in vitro* and *in vivo*. One potentially interesting purine-like molecule of interest is the immunosuppressant azathioprine, which has been administered to mouse models of late stage trypanosomiasis to modulate the severe post-treatment reactive encephalopathy (PTRE) that develops following non-curative berenil treatment (Hunter, *et al.*, 1992; Kennedy, 1999). This substance is a purine analogue (Figure 9.2) and it would be interesting to determine if it has any anti-trypanosomal activity and if this activity is related to the prevention of PTRE or if the anti-inflammatory effect of the drug is an

immunological one only. The use of azathioprine in a recent case of HAT misdiagnosed as systemic lupus erythematosus in a Western hospital did not lead to an improvement in the patient's condition although the treatment schedules used may not have been ideal to determine any effect on the parasites (Kirstetter, *et al.*, 2004). The H2 transporter is not fond of bulky substitutions so it is unclear if azathioprine would be taken up by this transporter. However, this compound is very lipophilic and is therefore likely to diffuse across most biomembranes.

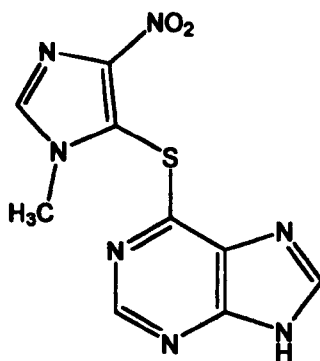


Figure 9.2. Structure of the immunosuppressant azathioprine.

Chapter 6 details the attempts to design tools for functional complementation as a means of gene identification in *T. b. brucei*. It was intended to induce a null background for purine nucleobase transport by gradually increasing exposure to a toxic purine nucleobase, allopurinol. The growth conditions, on inosine as sole purine source, were designed to select for transporter-related allopurinol resistance. This mechanism is widely held to be the main cause of drug resistance in African trypanosomes (De Koning, 2001; Mäser, *et al.*, 2003). A clonal population of nucleobase transport-deficient trypanosomes would be an ideal expression system for a genomic expression library following selection on hypoxanthine as sole purine source. A similar strategy has worked very well for the cloning of the first protozoan nucleoside transporters, from *Leishmania donovani*, where LdNT1 and LdNT2 were identified after complementing strains resistant to tubercidin and formycin B, respectively (Vasudevan, *et al.*, 1998; Carter, *et al.*, 2000). However we found allopurinol resistance impossible to induce by stepwise increasing exposure and that this was due to the fact that allopurinol uptake in *T. b. brucei* is mediated by two sets of transporters (Natto, *et al.*, submitted), in contrast to the situation for tubercidin (Aronow, *et al.*, 1987), formycin B (Aronow, *et al.*, 1987) or allopurinol in *Leishmania* promastigotes

(Al-Salabi, *et al.*, 2003). Functional complementation of *T. b. brucei* transporters in yeast is certainly possible, as demonstrated by the cloning of *TbAT1* (Mäser, *et al.*, 1999) and an expression library of genomic fragments was constructed and validated. However, the availability of increasing amounts of genomic information that were becoming available at the time meant that direct cloning by PCR of novel *T. b. brucei* nucleoside/nucleobase transport genes was becoming possible.

One of the genes we cloned in this fashion, *TbNBT1*, and expressed in purine transport-deficient *S. cerevisiae*, displayed excellent activity as a nucleobase transporter as demonstrated by its ability to mediate accumulation of [³H] hypoxanthine, [³H] adenine and [³H] allopurinol. Similar results were obtained for *TbNBT1* using the *Xenopus laevis* oocyte expression system. Moreover, a nucleobase transporter with identical kinetic characteristics was identified in *T. b. brucei* procyclics and its activity knocked down by 90% using RNAi fragments of *TbNBT1*. These results not only represent the cloning of the first protozoan nucleobase transporter they also establish the validity of the yeast expression system chosen. Since the publication of these results, another very similar gene from *T. b. brucei* and a related gene from *L. major* have also been shown to encode nucleobase transporters (Henriques, *et al.*, 2003; Sanchez, *et al.*, 2004), indicating that *TbNBT1* is likely to be the first of a subfamily of nucleobase transporters within the ENT family.

We have now cloned and characterised several additional ENT-family genes from *T. b. brucei* (Chapter 8) and are aiming to further investigate the molecular requirements that determine substrate specificity. Such studies will employ the construction of chimeric transporters to identify sequences determining recognition of nucleosides over nucleobases (and vice versa) and site directed mutagenesis based on our detailed kinetic analysis coupled with multiple-gene alignments. The dataset of well-characterised ENT transporters in *T. b. brucei* is highly suited to this purpose, and the yeast expression system allows positive and negative selection based on growth phenotype. It is possible that some of the ENT transporter genes may not encode purine transporters but one of the *T. b. brucei* pyrimidine transport activities (De Koning and Jarvis, 1998; De Koning, unpublished), or one of the pentamidine transport activities, HAPT1 and LAPT1 (De Koning, 2001b; Matovu, *et al.*, 2003). The cloning of the first protozoan pyrimidine transporter is one of the important next challenges.

The presence of up to 17 ENT family genes in the *T. b. brucei* genome clearly poses some interesting questions. There are at least 6 genes encoding functional P1-type transporters alone. Kinetically, the P1 activities in procyclics (De Koning, *et al.*, 1998) and long-slender bloodstream forms (De Koning & Jarvis, 1999) are indistinguishable. In short-stumpy bloodstream forms, a P1-type adenosine transport activity is also present (De Koning, unpublished), but is less well characterised, partially due to the difficulty in obtaining large numbers of these cells. Recently, Sanchez and colleagues (2004) presented evidence that “TbNT10”, which is AT-like B in our annotation, is expressed exclusively in short-stumpy forms, but the evidence rested entirely on the presence of mRNA, rather than transport assays with short-stumpy trypanosomes. Still, it is possible that the numerous different life-cycle stages express subtly different purine nucleoside transporters. Certainly this seems to be true for nucleobase transporters of procyclics (De Koning & Jarvis, 1997a) and long-slender bloodstream forms (De Koning & Jarvis, 1997b) and a P2-type activity is not expressed in short-stumpy forms (De Koning, unpublished) or procyclics (De Koning, *et al.*, 1998). Furthermore, it is possible that some nucleoside transporters are located in organellar membranes, such as the mitochondrial membrane, rather than in the plasma membrane.

Dissecting the individual physiological roles of this confusing array of similar but non-identical transporters is a major challenge. RNAi can be part of the overall strategy but in some cases the transporter genes are too similar for this approach and targeted gene deletion would be necessary. Nor is it likely that sufficiently specific antibodies could be raised to each individual transporter, but epitope tagging of particular genes should be possible. Such strategies may also aid in the elucidation of any functional role for ENT transporters that so far have not shown any ability to transport purine or pyrimidines in heterologous systems, including TbNT3, TbNT4 and AT-like A.

In this new century, African trypanosomiasis continues to be a major health threat both to humans and, through their livestock, their livelihood. The ultimate driving force behind many research studies involving *T. brucei spp.* is the very real need for novel therapeutics. The quest for new drugs is not inexpensive or straightforward, requiring expertise drawn from several disciplines. Beyond the discovery of any new drugs are problems of

production and distribution. And yet still the search for these life-saving compounds goes on.

References

A

Acimovic, Y. & Coe, I. R. (2002) Molecular evolution of the equilibrative nucleoside transporter family: identification of novel family members in prokaryotes and eukaryotes.

Akaho, E., Morris, G., Goodsell, D., Wong, D., & Olson, A. (2001) A study on docking mode of HIV protease and their inhibitors. *Journal of Chemical Software* 7: 103-114.

Aksoy, S., Maudlin, I., Dale, C., Robinson, A. S., & O'Neill, S. L. (2001) Prospects for control of African trypanosomiasis by tsetse vector manipulation. *Trends in Parasitology* 17: 29-35.

Allen, T. E. & Ullman, B. (1993) Cloning and expression of the hypoxanthine-guanine phosphoribosyltransferase gene from *Trypanosoma brucei*. *Nucleic Acids Research* 21: 5431-5438.

Allsop, R. (2001) Options for vector control against trypanosomiasis in Africa. *Trends in Parasitology* 17: 15-19.

Al-Salabi, M. I., Wallace, L. J. M., & De Koning, H. P. (2003) A *Leishmania major* nucleobase transporter responsible for allopurinol uptake is a functional homolog of the *Trypanosoma brucei* H2 transporter. *Molecular Pharmacology* 63: 814-820.

Anene, B. M., Onah, D. N., & Nawa, Y. (2001) Drug resistance in pathogenic African trypanosomes: what hopes for the future? *Veterinary Parasitology* 96: 83-100.

Argyrou, E., Sophianopoulou, V., Schultes, N., & Diallinas, G. (2001) Functional characterisation of a maize purine transporter by expression in *Aspergillus nidulans*. *The Plant Cell* 13: 953-964.

Aronow, B., Kaur, K., McCartan, K., & Ullman, B. (1987) Two high affinity nucleoside transporters in *Leishmania donovani*. *Molecular and Biochemical Parasitology* 22: 29-37.

Atouguia, J. & Costa, J. (1999) Therapy of human African trypanosomiasis: current situation. *Memorias do Instituto Oswaldo Cruz* 94: 221-224.

B

Bacchi, C. J., Garofalo, J., Mockenhaupt, D., McCann, P. P., Diekema, K. A., Pegg, A. E., Nathan, H. C., Mullaney, E. A., Chunosoff, L., Sjoerdsma, A., & Hutner, S. H. (1983) *In vivo* effects of alpha-DL-difluoromethylornithine on the metabolism and morphology of *Trypanosoma brucei brucei*. *Molecular and Biochemical Parasitology* 7: 209-225.

Bacchi, C. J. (1993) Resistance to clinical drugs in African trypanosomes. *Parasitology Today* 9: 190-193.

Baker, E. & Hubbard, R. (1984) Hydrogen bonding in globular proteins. *Progress in Biophysics and Molecular Biology* 44: 97-179.

Barrett, M. P., Zhang, Z. Q., Denise, H., Giroud, C., & Baltz, T. (1995) A diamidine-resistant *Trypanosoma equiperdum* clone contains a P2 purine transporter with reduced substrate affinity. *Molecular and Biochemical Parasitology* 73: 223-229.

Barrett, M. P. (1999) The fall and rise of sleeping sickness. *Lancet* 353: 1113-1114.

Barrett, M. P. & Fairlamb, A. H. (1999) The biochemical basis of arsenical-diamidine crossresistance in African trypanosomes. *Parasitology Today* 15: 136-140.

Barrett, S. V. & Barrett, M. P. (2000) Anti-sleeping sickness drugs and cancer chemotherapy. *Parasitology Today* 16: 7-9.

Barrett, M. P. (2000) Problems for the chemotherapy of human African trypanosomiasis. *Current Opinion in Infectious Diseases* 13: 647-651.

Barrett, M. P., Burchmore, R. J., Stich, A., Lazzari, J. O., Frasch, A. C., Cazzulo, J. J., & Krishna, S. (2003) The trypanosomiases. *Lancet* 362: 1469-1480.

Barry, J. D. & McCulloch, R. (2001) Antigenic variation in trypanosomes: enhanced phenotypic variation in a eukaryotic parasite. *Advances in Parasitology* 49: 1-70.

Benne, R. (1994) RNA editing in trypanosomes. *European Journal of Biochemistry* 221: 9-23.

- Berger, B. J., Carter, N. S., & Fairlamb, A. H. (1995) Characterisation of pentamidine-resistant *Trypanosoma brucei brucei*. *Molecular and Biochemical Parasitology* 69: 289-298.
- Bitonti, A. J., Bacchi, C. J., McCann, P. P., & Sjoerdsma, A. (1986) Uptake of alpha-difluoromethylornithine by *Trypanosoma brucei brucei*. *Biochemical Pharmacology* 35: 351-354.
- Borst, P. & Fairlamb, A. H. (1998) Surface receptors and transporters of *Trypanosoma brucei*. *Annual Review of Microbiology* 52: 745-778.
- Broach, J. R., Strathern, J. N., & Hicks, J. B. (1979) Transformation in yeast: development of a hybrid cloning vector and isolation of the CAN1 gene. *Gene* 8: 121-133.
- Brown, H. W. & Neva, F. A. (1993) *Basic Clinical Parasitology*. 5th Edition. Prentice-Hall International.
- Brun, R. & Schönenberger, M. (1979) Cultivation and *in vitro* cloning of procyclic culture forms of *Trypanosoma brucei* in a semi-defined medium. *Acta Tropica* 36: 289-292.
- Brun, R., Schumacher, R., Schmid, C., Kunz, C., & Burri, C. (2001) The phenomenon of treatment failures in Human African Trypanosomiasis. *Tropical Medicine and International Health* 6: 906-914.
- Burchmore, R., Wallace, L. J. M., Candlish, D., Al-Salabi, M. I., Beal, P., Barrett, M. P., Baldwin, S. A., & De Koning, H. P. (2003) Cloning, heterologous expression and *in situ* characterization of the first high affinity nucleobase transporter from a protozoan. *Journal of Biological Chemistry* 278: 23502-23507.
- Burri, C., Nkunku, S., Merolle, A., Smith, T., Blum, J., & Brun, R. (2000) Efficacy of new, concise schedule for melarsoprol in treatment of sleeping sickness caused by *Trypanosoma brucei gambiense*: a randomised trial. *Lancet* 355: 1419-1425.

C

- Carter, N. S. & Fairlamb, A. H. (1993) Arsenical-resistant trypanosomes lack an unusual adenosine transporter. *Nature* 361: 173-176.

- Carter, N. S., Berger, B. J., & Fairlamb, A. H. (1995) Uptake of diamidine drugs by the P2 nucleoside transporter in melarsen-sensitive and -resistant *Trypanosoma brucei brucei*. *Journal of Biological Chemistry* 270: 28153-28157.
- Carter, N. S., Drew, M. E., Sanchez, M., Vasudevan, G., Landfear, S. M., & Ullman, B. (2000) Cloning of a novel inosine-guanosine transporter gene from *Leishmania donovani* by functional rescue of a transport-deficient mutant. *Journal of Biological Chemistry* 275: 20935-20941.
- Cattand, P., Jannin, J., & Lucas, P. (2001) Sleeping sickness surveillance: an essential step towards elimination. *Tropical Medicine and International Health* 6: 348-361.
- Cecchetto, G., Amillis, S., Diallinas, G., Scazzocchio, C., & Drevet, C. (2004) The AzgA purine transporter of *Aspergillus nidulans*: Characterisation of a protein belonging to a new phylogenetic cluster. *Journal of Biological Chemistry* 279: 3132-3141.
- Chang, C., Swaan, P. W., Ngo, L. Y., Lum, P. Y., Patil, S. D., & Unadkat, J. D. (2004) Molecular requirements of the human nucleoside transporters hCNT1, hCNT2, and hENT1. *Molecular Pharmacology* 65: 558-570.
- Cheng, Y-C. & Prusoff, W. H. (1973) Relationship between the inhibition constant (K_i) and the concentration of inhibitor which causes 50 per cent inhibition (IC_{50}) of an enzymatic reaction. *Biochemical Pharmacology* 22: 3099-3108.
- Chevallier, M. R. (1982) Cloning and transcriptional control of a eucaryotic permease gene. *Molecular and Cellular Biology* 2: 977-984.
- Clarke, L. & Carbon, J. (1976) A colony bank containing synthetic ColE1 hybrids representative of the entire *Escherichia coli* genome. *Cell* 9: 91-99.
- Clayton, C. E. (1999) Genetic manipulation of kinetoplastida. *Parasitology Today* 15: 372-378.
- Clayton, C. E. (2002) Life without transcriptional control? From fly to man and back again. *EMBO Journal* 21: 1881-1888.
- Cowan, G. O. & Heap, B. J. (1993) *Clinical Tropical Medicine*. Chapman & Hall (London).

D

Darlington, A. J. & Scazzocchio, C. (1967) Use of analogues and the substrate specificity of mutants in analysis of purine uptake and breakdown in *Aspergillus nidulans*. *Journal of Bacteriology* 93: 937-940.

Das, V. N., Ranjan, A., Sinha, A. N., Verma, N., Lal, C. S., Gupta, A. K., Siddiqui, N.A., & Kar, S. K. (2001) A randomized clinical trial of low dosage combination of pentamidine and allopurinol in the treatment of antimony unresponsive cases of visceral leishmaniasis. *Journal of the Association of Physicians India* 49: 609-613.

De Greef, C., Chimfwembe, E., Kihang'a Wabacha, J., Bajyana Songa, E., & Hamers, R. (1992) Only the serum-resistant bloodstream forms of *Trypanosoma brucei rhodesiense* express the serum resistance associated (SRA) protein. *Annales de la Societe Belge de Medecine Tropicale* 72 Suppl 1: 13-21.

De Koning, H. P. & Jarvis, S. M. (1997a) Hypoxanthine uptake through a purine-selective nucleobase transporter in *Trypanosoma brucei brucei* procyclic cells is driven by protonmotive force. *European Journal of Biochemistry* 247: 1102-1110.

De Koning, H. P. & Jarvis, S. M. (1997b) Purine nucleobase transport in bloodstream forms of *Trypanosoma brucei brucei* is mediated by two novel transporters. *Molecular and Biochemical Parasitology* 89: 245-258.

De Koning, H. P. & Jarvis, S. M. (1998) A highly selective, high-affinity transporter for uracil in *Trypanosoma brucei brucei*: evidence for proton-dependent transport. *Biochemistry and Cell Biology* 76: 853-858.

De Koning, H. P., Watson, C. J., & Jarvis, S. M. (1998) Characterization of a nucleoside/proton symporter in procyclic *Trypanosoma brucei brucei*. *Journal of Biological Chemistry* 273: 9486-9494.

De Koning, H. P. & Jarvis, S. M. (1999) Adenosine transporters in bloodstream forms of *Trypanosoma brucei brucei*: substrate recognition motifs and affinity for trypanocidal drugs. *Molecular Pharmacology* 56: 1162-1170.

De Koning, H. P., Watson, C. J., Sutcliffe, L., & Jarvis, S. M. (2000) Differential regulation of nucleoside and nucleobase transporters in *Crithidia fasciculata* and *Trypanosoma brucei brucei*. *Molecular and Biochemical Parasitology* 106: 93-107.

- De Koning, H. P. & Diallinas, G. (2000) Nucleobase transporters (Review). *Molecular Membrane Biology* 72: 75-94.
- De Koning, H. P. (2001a) Transporters in African trypanosomes: role in drug action and resistance. *International Journal of Parasitology* 31: 512-522.
- De Koning, H.P. (2001b) Uptake of pentamidine in *Trypanosoma brucei brucei* is mediated by three distinct transporters: implications for cross-resistance with arsenicals. *Molecular Pharmacology* 59: 586-592.
- De Koning, H. P., Al-Salabi, M. I., Cohen, A., Coombs, G. H., & Wastling, J. M. (2003) Identification and characterisation of high affinity purine nucleoside and nucleobase transporters in *Toxoplasma gondii*. *International Journal of Parasitology* 33: 821-831.
- De Koning, H. P., Anderson, L. F., Stewart, M., Burchmore, R. J., Wallace, L. J., Barrett, M. P. (2004) The trypanocide diminazene aceturate is accumulated predominantly through the TbAT1 purine transporter: additional insights on diamidine resistance in african trypanosomes. *Antimicrobial Agents and Chemotherapy* 48: 1515-1519.
- Denise, H., Giroud, C., Barrett, M. P., & Baltz, T. (1999) Affinity chromatography using trypanocidal arsenical drugs identifies a specific interaction between glycerol-3-phosphate dehydrogenase from *Trypanosoma brucei* and Cymelarsan. *European Journal of Biochemistry* 259: 339-346.
- Diallinas, G. & Scazzocchio, C. (1989) A gene coding for the uric acid-xanthine permease of *Aspergillus nidulans*: inactivational cloning, characterisation and sequence of a *cis*-acting mutation. *Genetics* 122: 341-350.
- Diallinas, G., Gorfinkiel, L., Arst, H. N., Jr., Cecchetto, G., & Scazzocchio, C. (1995) Genetic and molecular characterisation of a gene encoding a wide specificity purine permease of *Aspergillus nidulans* reveals a novel family of transporters conserved in prokaryotes and eukaryotes. *Journal of Biological Chemistry* 270: 8610-8622.
- Domin, B. A., Mahony, W. B., & Zimmerman, T. P. (1988) Purine nucleobase transport in human erythrocytes. Reinvestigation with a novel "inhibitor stop" assay. *Journal of Biological Chemistry* 263: 9276-9284.
- Donelson, J.E. & Rice-Ficht, A. C. (1985) Molecular biology of trypanosome antigenic variation. *Microbiol Reviews* 49: 107-125.

E

Ekwanzala, M., Pépin, J., Khonde, N., Molisho, S., Bruneel, H., & De Wals, P. (1996) In the heart of darkness: sleeping sickness in Zaire. *Lancet* 348: 1427-1430.

Elion, G. B. (1989) The purine path to chemotherapy. *Bioscience Reports* 9: 509-529.

El Kouni, M. H. (2003) Potential chemotherapeutic targets in the purine metabolism of parasites. *Pharmacology and Therapeutics* 99: 283-309.

El Sayed, N. M., Hegde, P., Quackenbush, J., Melville, S. E., & Donelson, J. E. (2000) The African trypanosome genome. *International Journal of Parasitology* 30: 329-345.

Enanga, B., Burchmore, R. J., Stewart, M. L., & Barrett, M. P. (2002) Sleeping sickness and the brain. *Cellular and Molecular Life Science* 59: 845-858.

Ersfeld, K., Melville, S. E., & Gull, K. (1999) Nuclear and genome organization of *Trypanosoma brucei*. *Parasitology Today* 15: 58-63.

F

Fairlamb, A. H., Henderson, G. B. & Cerami, A. (1989) Trypanothione is the primary target for arsenical drugs against African trypanosomes. *Proceedings of the National Academy of Sciences USA* 86: 2607-2611.

Fairlamb, A. H. (1989) Novel biochemical pathways in parasitic protozoa. *Parasitology* 99 Suppl: S93-112.

Fairlamb, A. H. (1990) Future prospects for the chemotherapy of human trypanosomiasis. 1. Novel approaches to the chemotherapy of trypanosomiasis. *Transactions of the Royal Society of Tropical Medicine and Hygiene* 84: 613-617.

Fairlamb, A. H., Carter, N. S., Cunningham, M., & Smith, K. (1992) Characterisation of melarsen-resistant *Trypanosoma brucei brucei* with respect to cross-resistance to other drugs and trypanothione metabolism. *Molecular and Biochemical Parasitology* 53: 213-222.

Fish, W. R., Looker, D. L., Marr, J. J., & Berens, R. L. (1982) Purine metabolism in the bloodstream forms of *Trypanosoma gambiense* and *Trypanosoma rhodesiense*. *Biochimica et Biophysica Acta* 719: 223-231.

Freire, E. (1999) The propagation of binding interactions to remote sites in proteins: analysis of the binding of the monoclonal antibody D1.3 to lysozyme. *Proceedings of the National Academy of Sciences USA* 96: 10118-10122.

Freitas, R. A., Jr. (1999) *Nanomedicine, Volume I: Basic Capabilities*. Landes Bioscience, Georgetown, TX. <http://www.nanomedicine.com/NMI.htm>

Frommel, T. O. & Balber, A. E. (1987) Flow cytometric analysis of drug accumulation by multidrug-resistant *Trypanosoma brucei brucei* and *T. b. rhodesiense*. *Molecular and Biochemical Parasitology* 26: 183-191.

Frommer, W. B. & Ninnemann, O. (1995) Heterologous expression of genes in bacterial, fungal, animal, and plant cells. *Annual Review of Plant Physiology and Plant Molecular Biology* 46: 419-444.

G

Gati, W. P., Paterson, A. R., Tyrrell, D. L., Cass, C. E., Moravek, J., & Robins, M. J. (1992) Nucleobase transporter-mediated permeation of 2',3'-dideoxyguanosine in human erythrocytes and human T-lymphoblastoid CCRF-CEM cells. *Journal of Biological Chemistry* 267: 22272-22276.

Ghoda, L., Phillips, M. A., Bass, K. E., Wang, C. C., & Coffino, P. (1990) Trypanosome ornithine decarboxylase is stable because it lacks sequences found in the carboxyl terminus of the mouse enzyme which target the latter for intracellular degradation. *Journal of Biological Chemistry* 265: 11823-11826.

Gibson, W. (2002) Will the real *Trypanosoma brucei rhodesiense* please step forward? *Trends in Parasitology* 18: 486-490.

Gietz, R. D. & Woods, R. A. (2002) Transformation of yeast by lithium acetate/single-stranded carrier DNA/polyethylene glycol method. *Methods in Enzymology* 350: 87-96.

Gillissen, B., Bürkle, L., André, B., Kühn, C., Rentsch, D., Brandl, B., & Frommer, W. B. (2000) A new family of high-affinity transporters for adenine, cytosine, and purine derivatives in *Arabidopsis*. *The Plant Cell* 12: 291-300.

- Goldberg, B., Yarlett, N., Sufrin, J., Lloyd, D., & Bacchi, C. J. (1997) A unique transporter of S-adenosylmethionine in African trypanosomes. *FASEB Journal* 11: 256-260.
- Gorfinkiel, L., Diallinas, G., & Scazzocchio, C. (1993) Sequence and regulation of the *uapA* gene encoding a uric acid-xanthine permease in the fungus *Aspergillus nidulans*. *Journal of Biological Chemistry* 268: 23376-23381.
- Grant, I. F. (2001) Insecticides for tsetse and trypanosomiasis control: is the environmental risk acceptable? *Trends of Parasitology* 17: 10-14.
- Grenson, M. (1969). The utilization of exogenous pyrimidines and the recycling of the uridine-5'-phosphate derivatives in *Saccharomyces cerevisiae*, as studied by means of mutants affected in pyrimidine uptake and metabolism. *European Journal of Biochemistry* 11: 249-260.
- Griffith, D. A & Jarvis, S. M. (1996) Nucleoside and nucleobase transport systems of mammalian cells. *Biochimica et Biophysica Acta* 1286: 153-181.
- Griffiths, M., Beaumont, N., Yao, S. Y. M., Sundaram, M., Boumah, C. E., Davies, A., Kwong, F. Y. P., Coe, I., Cass, C. E., Young, J. D., & Baldwin, S. A. (1997) Cloning of a human nucleoside transporter implicated in the cellular uptake of adenosine and chemotherapeutic drugs. *Nature Medicine* 3: 89-93.
- Gurdon, J. B., Lane, C. D., Woodland, H. R., & Marbaix, G. (1971) Use of frogs and oocytes for the study of messenger RNA and its translation in living cells. *Nature* 233: 177-182.
- Gurdon, J. B. & Wickens, M. P. (1983) The use of *Xenopus* oocytes for the expression of cloned genes. *Methods in Enzymology* 101: 370-386.
- Gutteridge, W. E. & Coombs, G. H. (1977). *Biochemistry of Parasitic Protozoa*. MacMillan Press Ltd. (London).

H

- Hammond, D. J. & Gutteridge, W. E. (1984) Purine and pyrimidine metabolism in the Trypanosomatidae. *Molecular and Biochemical Parasitology* 13: 243-261.

- Hassan, H. F. & Coombs, G. H. (1988) Purine and pyrimidine metabolism in parasitic protozoa. *FEMS Microbiology Reviews* 54: 47-83.
- Hasne, M-P. & Barrett, M. P. (2000a) Drug uptake via nutrient transporters in *Trypanosoma brucei*. *Journal of Applied Microbiology* 89: 697-701.
- Hasne, M-P. & Barrett, M. P. (2000b) Transport of methionine in *Trypanosoma brucei brucei*. *Molecular and Biochemical Parasitology* 111: 299-307.
- Henriques, C., Sanchez, M. A., Tryon, R., & Landfear, S. M. (2003) Molecular and functional characterization of the first nucleobase transporter gene from African trypanosomes. *Molecular and Biochemical Parasitology* 130: 101-110.
- Herbert, W. J. & Lumsden, W. H. R. (1976) *Trypanosoma brucei*: a rapid "matching" method for estimating the host's parasitemia. *Experimental Parasitology* 40: 427-431.
- Hirumi, H. & Hirumi, K. (1989) Continuous cultivation of *Trypanosoma brucei* blood stream forms in a medium containing a low concentration of serum protein without feeder cell layers. *Journal of Parasitology* 75: 985-989.
- Hoare, C. A. (1972) *The trypanosomes of mammals. A Zoological Monograph.* Blackwell Scientific Publications, Oxford, U.K.
- Horak, J. (1997) Yeast nutrient transporters. *Biochimica et Biophysica Acta* 1331: 41-79.
- Huang, Q. Q., Harvey, C. M., Paterson, A. R., Cass, C. E., & Young, J. D. (1993) Functional expression of Na(+)-dependent nucleoside transport systems of rat intestine in isolated oocytes of *Xenopus laevis*. Demonstration that rat jejunum expresses the purine-selective system N1 (cif) and a second, novel system N3 having broad specificity for purine and pyrimidine nucleosides. *Journal of Biological Chemistry* 268: 20613-20619.
- Hunter, C. A., Singh, J., & Thornton, J. M. (1991) π - π interactions: the geometry and energetics of phenylalanine-phenylalanine interactions in proteins. *Journal of Molecular Biology* 218: 837-846.
- Hunter, C. A., Jennings, F. W., Adams, J. H., Murray, M., & Kennedy, P. G. (1992) Subcurative chemotherapy and fatal post-treatment reactive encephalopathies in African trypanosomiasis. *Lancet* 339: 956-958.

Hutchinson, O. C., Fèvre, E. M., Carrington, M., & Welburn, S. C. (2003) Lessons learned from the emergence of a new *Trypanosoma brucei rhodesiense* sleeping sickness focus in Uganda. *Lancet Infectious Diseases* 3: 42-45.

Hyde, R. J., Cass, C. E., Young, J. D., & Baldwin, S. A. (2001) The ENT family of eukaryote nucleoside and nucleobase transporters: recent advances in the investigation of structure/function relationships and the identification of novel isoforms. *Molecular Membrane Biology* 18: 53-63.

I

Iten, M., Mett, H., Evans, A., Enyaru, J. C., Brun, R., & Kaminsky, R. (1997) Alterations in ornithine decarboxylase characteristics account for tolerance of *Trypanosoma brucei rhodesiense* to D,L-alpha-difluoromethylornithine. *Antimicrobial Agents and Chemotherapy* 41: 1922-1925.

J

James, D. M. & Born, G. V. (1980) Uptake of purine bases and nucleosides in African trypanosomes. *Parasitology* 81: 383-393.

Jencks, W. P. (1981) On the attributions and additivity of binding energies. *Proceedings of the National Academy of Sciences USA* 7: 4046-4050.

Jund, R., Chevallier, M. R., & Lacroute, F. (1977) Uracil transport in *Saccharomyces cerevisiae*. *Journal of Membrane Biology* 36: 233-251.

K

Kabsch, W. & Sander, C. (1983) Dictionary of protein secondary structure: pattern recognition of hydrogen-bonded and geometrical features. *Biopolymers* 22: 2577-2637.

Kaminsky, R. & P. Maser. (2000) Drug resistance in African trypanosomes. *Current Opinion in Anti-infective Investigational Drugs* 2: 76-82.

Keiser, J., Ericsson, O., & Burri, C. (2000) Investigations of the metabolites of the trypanocidal drug melarsoprol. *Clinical Pharmacology and Therapeutics* 67: 478-488.

- Keiser, J., Stich, A., & Burri, C. (2001) New drugs for the treatment of human African trypanosomiasis: research and development. *Trends in Parasitology* 17: 42-49.
- Kennedy, P. G. (1999) The pathogenesis and modulation of the post-treatment reactive encephalopathy in a mouse model of Human African Trypanosomiasis. *Journal of Neuroimmunology* 100: 36-41.
- Kennedy, P.G. (2004) Human African trypanosomiasis of the CNS: current issues and challenges. *Journal of Clinical Investigation* 113: 496-504.
- Kirchhoff, L. V., Bacchi, C. J., Wittner, M., & Tanowitz, H. B. (2000) African Trypanosomiasis (Sleeping Sickness). *Current Treatment Options in Infectious Diseases* 2: 66-69.
- Kirrstetter, M., Lerin-Lozano, C., Heintz, H., Manegold, C., Gross, W. L., & Lamprecht, P. (2004) Trypanosomiasis in a woman from Cameroon mimicking systemic lupus erythematosus. (Article in German) *Deutsche Medizinische Wochenschrift* 129: 1315-1317.
- Klenke, B., Stewart, M., Barrett, M. P., Brun, R., & Gilbert, I. H. (2001) Synthesis and biological evaluation of s-triazine substituted polyamines as potential new anti-trypanosomal drugs. *Journal of Medicinal Chemistry* 44: 3440-3452.
- Kool, E. T. (2001) Hydrogen-bonding, base stacking, and steric effects in DNA replication. *Annual Review of Biophysics and Biomolecular Structure* 30: 1-22.
- Kraupp, M., Marz, R., Prager, G., Kommer, W., Razavi, M., Baghestanian, M., & Chiba, P. (1991) Adenine and hypoxanthine transport in human erythrocytes: distinct substrate effects on carrier mobility. *Biochimica et Biophysica Acta* 1070: 157-162.
- Kraupp, M., Paskutti, B., Schon, C., & Marz, R. (1994) Inhibition of purine nucleobase transport in human erythrocytes and cell lines by papaverine. Investigation of structure-activity relationship. *Biochemical Pharmacology* 48: 41-47.
- Kreier, J. P. & Baker, J. R. (1987) *Parasitic protozoa*. Allen and Unwin, Boston, MA.
- Kubinyi, H. (2001) Hydrogen bonding: the last mystery in drug design? In *Pharmacokinetic Optimization in Drug Research: Biological, Physicochemical, and Computational Strategies*. Edited by Testa, B., van de Waterbeemd, H., Folkers, G., and Guy, R.

Kuzoe, F. A. S. (1993) Current situation of African trypanosomiasis. *Acta Tropica* 54: 153-162.

L

LaCount, D. J., Bruse, S., Hill, K. L., & Donelson, J. E. (2000) Double-stranded RNA interference in *Trypanosoma brucei* using head-to-head promoters. *Molecular and Biochemical Parasitology* 111: 67-76.

Landfear, S. M. (2001) Molecular genetics of nucleoside transporters in *Leishmania* and African trypanosomes. *Biochemical Pharmacology* 62: 149-155.

Landfear, S. M., Ullman, B., Carter, N. S., & Sanchez, M. A. (2004) Nucleoside and nucleobase transporters in parasitic protozoa. *Eukaryotic Cell* 3: 245-254.

Lanham, S. M. (1968) Separation of trypanosomes from the blood of infected rats and mice by anion-exchangers. *Nature* 218: 1273-1274.

Lanham, S. M. & Godfrey, D. G. (1970) Isolation of salivarian trypanosomes from man and other mammals using DEAE-cellulose. *Experimental Parasitology* 28: 521-534.

Lazaridis, T., Masunov, A., & Gandolfo, F. (2002) Contributions to the binding free energy of ligands to avidin and streptavidin. *Proteins: Structure, Function and Genetics* 47: 194-208.

Lee, M. G. & Van der Ploeg, L. H. (1990) Homologous recombination and stable transfection in the parasitic protozoan *Trypanosoma brucei*. *Science* 250: 1583-1587.

Legros, D., Ollivier, G., Gastellu-Etchegorry, M., Paquet, C., Burri, C., Jannin, J., & Buscher, P. (2002) Treatment of human African trypanosomiasis - present situation and needs for research and development. *Lancet Infectious Diseases* 2: 437-440.

Leonard, N. J., Morrice, A. G., & Sprecker, M. A. (1975) Linear benzoadenine. A stretched-out analogue of adenine. *Journal of Organic Chemistry* 40: 356-366.

Leonard, N. J. & Hiremath, S. P. (1986) Dimensional probes of binding and activity. *Tetrahedron* 42: 1917-1961.

Liman, E. R., Tytgat, J., & Hess, P. (1992) Subunit stoichiometry of a mammalian K⁺ channel determined by construction of multimeric cDNAs. *Neuron* 9: 861-871.

Loayza, D., Tam, A., Schmidt, W. K., & Micaelis, S. (1998) Step6p mutants defective in exit from the endoplasmic reticulum (ER) reveal aspects of an ER quality control pathway in *Saccharomyces cerevisiae*. *Molecular & Cellular Biology* 10: 2767.

Lu, X., Gong, S., Monks, A., Zaharevitz, D., & Moscow, J. A. (2002) Correlation of nucleoside and nucleobase transporter gene expression with antimetabolite drug cytotoxicity. *Journal of Experimental Therapeutics and Oncology* 2: 200-212.

Lukeš, J., Guilbride, D. L., Votypka, J., Zikova, A., Benne, R., & Englund, P. T. (2002) Kinetoplast DNA network: evolution of an improbable structure. *Eukaryotic Cell* 1: 495-502.

M

MacLeod, A., Tweedie, A., Welburn, S. C., Maudlin, I., Turner, C. M., & Tait, A. (2000) Minisatellite marker analysis of *Trypanosoma brucei*: reconciliation of clonal, panmictic, and epidemic population genetic structures. *Proceedings of the National Academy of Sciences USA* 97: 13442-13447.

Mahony, W. B., Domin, B. A., McConnell, R. T., & Zimmerman, T. P. (1988) Acyclovir transport into human erythrocytes. *Journal of Biological Chemistry* 263: 9285-9291.

Mahony, W. B., Domin, B. A., Daluge, S. M., Miller, W. H., & Zimmerman, T. P. (1992) Enantiomeric selectivity of carbosvir transport. *Journal of Biological Chemistry* 267: 19792-19797.

Marchesi, V. T. (1985) The cytoskeletal system of red blood cells. *Hospital Practice* 20: 113-131.

Marr, J. J. (1983) Pyrazolopyrimidine metabolism in *Leishmania* and trypanosomes: significant differences between host and parasite. *Journal of Cellular Biochemistry* 22: 187-196.

Mäser, P., Sutterlin, C., Kralli, A., & Kaminsky, R. (1999) A nucleoside transporter from *Trypanosoma brucei* involved in drug resistance. *Science* 285: 242-244.

- Mäser, P., Luscher, A., & Kaminsky, R. (2003) Drug transport and drug resistance in African trypanosomes. *Drug Resistance Update* 6: 281-290.
- Matovu, E., Geiser, F., Schneider, V., Maser, P., Enyaru, J. C., Kaminsky, R., Gallati, S., & Seebeck, T. (2001) Genetic variants of the TbAT1 adenosine transporter from African trypanosomes in relapse infections following melarsoprol therapy. *Molecular and Biochemical Parasitology* 117: 73-81.
- Matovu, E., Stewart, M. L., Geiser, F., Brun, R., Mäser, P., Wallace, L. J. M., Burchmore, R. J., Enyaru, J. C., Barrett, M. P., Kaminsky, R., Seebeck, T. and De Koning, H. P. (2003) The mechanisms of arsenical and diamidine uptake and resistance in *Trypanosoma brucei*. *Eukaryotic Cell* 2: 1003-1008.
- Matthews, K. R. (1999) Developments in the differentiation of *Trypanosoma brucei*. *Parasitology Today* 15: 76-80.
- Mehlitz, D., Zillmann, U., Scott, C. M., & Godfrey, D. G. (1982) Epidemiological studies on the animal reservoir of Gambiense sleeping sickness. Part III. Characterization of trypanozoon stocks by isoenzymes and sensitivity to human serum. *Tropenmedizin und Parasitologie* 33: 113-118.
- Metzenberg, S. & Agabian, N. (1994) Mitochondrial minicircle DNA supports plasmid replication and maintenance in nuclei of *Trypanosoma brucei*. *Proceedings of the National Academy of Sciences USA* 91: 5962-5966.
- Miller, A. J. & Zhou, J. J. (2000) *Xenopus* oocytes as an expression system for plant transporters. *Biochimica et Biophysica Acta* 1465: 343-358.
- Milner, J. D. & Hajduk, S. L. (1999) Expression and localization of serum resistance associated protein in *Trypanosoma brucei rhodesiense*. *Molecular and Biochemical Parasitology* 104: 271-283.
- Mulligan, H. W. (1970) *The African trypanosomiases*. George Allen & Unwin (London).
- Murray, A. W. (1971) The biological significance of purine salvage. *Annual Review of Biochemistry* 40: 811-826.

N

Naguib, F. N. M., Iltzsch, M. H., El Kouni, M. M., Panzica, R. P., & El Kouni, M. H. (1995) Structure-activity relationships for the binding of ligands to xanthine or guanine phosphoribosyltransferase from *Toxoplasma gondii*. *Biochemical Pharmacology* 50: 1685-1693.

Natto, M. J., Wallace, L. J. M., Candlish, D., Al-Salabi, M. I., Coutts, S. E., & De Koning, H. P. Characterisation of allopurinol transport in *Trypanosoma brucei*: implications for resistance to purine antimetabolites. In submission.

Navarro, M. & Gull, K. (2001) A pol I transcriptional body associated with VSG mono-allelic expression in *Trypanosoma brucei*. *Nature* 414: 759-763.

Saitou, N. & Nei, M. (1987) The neighbor-joining method: a new method for reconstructing phylogenetic trees. *Molecular Biology & Evolution* 4: 406-25.

Njiru, Z. K., Ndung'u, K., Matete, G., Ndungu, J. M., & Gibson, W. C. (2004) Detection of *Trypanosoma brucei rhodesiense* in animals from sleeping sickness foci in East Africa using the serum resistance associated (SRA) gene. *Acta Tropica* 90: 249-254.

O

O'Brien, J., Wilson, I., Orton, T., & Pognan, F. (2000) Investigation of the Alamar Blue (resazurin) fluorescent dye for the assessment of mammalian cell cytotoxicity. *European Journal of Biochemistry* 267: 5421-5426.

Opperdoes, F. R., Baudhuin, P., Coppens, I., De Roe, C., Edwards, S. W., Weijers, P. J., & Misset, O. (1984) Purification, morphometric analysis, and characterization of the glycosomes (microbodies) of the protozoan hemoflagellate *Trypanosoma brucei*. *Journal of Cell Biology* 98: 1178-1184.

Opperdoes, F. R. & Michels, P. A. (1993) The glycosomes of the Kinetoplastida. *Biochimie* 75: 231-234.

P

Papageorgiou, I. G., Yakob, L., Diallinas, G., Soteriadou., K. P., & De Koning, H. P. Manuscript. Uracil transporters in the kinetoplastida: Analysis of substrate-transporter

interactions in *L. major* and *T. brucei* provides a rationale for their high affinity and exceptional specificity. Unpublished.

Penny, J. I., Hall, S. T., Woodrow, C. J., Cowan, G. M., Gero, A. M. & Krishna, S. (1998) Expression of substrate-specific transporters encoded by *Plasmodium falciparum* in *Xenopus laevis* oocytes. *Molecular & Biochemical Parasitology* 93: 81-89.

Pépin, J. & Milord, F. (1994) The treatment of Human African Trypanosomiasis. *Advances in Parasitology* 33: 1-47.

Pépin, J., Khonde, N., Maiso, F., Doua, F., Jaffar, S., Ngampo, S., Mpia, B., Mbulamberi, D., & Kuzoe, F. (2000) Short-course eflornithine in Gambian trypanosomiasis: a multicentre randomized controlled trial. *Bulletin of the World Health Organization* 78: 1284-1295.

Peregrine, A. S. & Mamman, M. (1993) Pharmacology of diminazene: a review. *Acta Tropica* 54: 185-203.

Pfefferkorn, E. R., Bzik, D. J., & Honsinger, C. P. (2001) *Toxoplasma gondii*: mechanism of the parasitostatic action of 6-thioxanthine. *Experimental Parasitology* 99: 235-243.

Phillips, M. A., Coffino, P., & Wang, C. C. (1987) Cloning and sequencing of the ornithine decarboxylase gene from *Trypanosoma brucei*. Implications for enzyme turnover and selective difluoromethylornithine inhibition. *Journal of Biological Chemistry* 262: 8721-8727.

Plagemann, P. G. W., Woffendin, C., Puziss, M. B., & Wohlhueter, R. M. (1987) Purine and pyrimidine transport and permeation in human erythrocytes. *Biochimica et Biophysica Acta* 905: 17-29.

Plagemann, P. G., Wohlhueter, R. M., & Woffendin, C. (1988) Nucleoside and nucleobase transport in animal cells. *Biochimica et Biophysica Acta* 947: 405-443.

Polak, A. & Gresson, M. (1973) Evidence for a common transport system for cytosine, adenine and hypoxanthine in *Saccharomyces cerevisiae* and *Candida albicans*. *European Journal of Biochemistry* 32: 276-282.

Pokera, A. A. (1985) Pathology of human African trypanosomiasis with reference to experimental African trypanosomiasis and infections of the central nervous system. *British Medical Bulletin* 41: 169-174.

R

Raper, J., Molina Portela, M. P., Lugli, E., Frevert, U., & Tomlinson, S. (2001) Trypanosome lytic factors: novel mediators of human innate immunity. *Current Opinion in Microbiology* 4: 402-408.

Ráz, B., Iten, M., Kaminsky, R., Kaminsky, R., & Brun, R. (1997) The Alamar Blue® assay to determine drug sensitivity of African trypanosomes (*T. b. rhodesiense* and *T. b. gambiense*) *in vitro*. *Acta Tropica* 68: 139-147.

Razavi, M., Kraupp, M., & Marz, R. (1993) Allopurinol transport in human erythrocytes. *Biochemical Pharmacology* 45: 893-897.

Rentsch, D., Laloi, M., Rouhara, I., Schmelzer, E., Delrot, S., & Frommer, W. B. (1995) NTR1 encodes a high affinity oligopeptide transporter in *Arabidopsis*. *FEBS Letters* 370: 264-268.

Roditi, I., Furger, A., Ruepp, S., Schurch, N., & Butikofer, P. (1998) Unravelling the procyclin coat of *Trypanosoma brucei*. *Molecular and Biochemical Parasitology* 91: 117-130.

Rogers, D. J. & Randolph, S. E. (2002) A response to the aim of eradicating tsetse from Africa. *Trends in Parasitology* 18: 534-536.

Ruiz, J. A., Simarro, P. P., & Josenando, T. (2002) Control of human African trypanosomiasis in the Quicama focus, Angola. *Bulletin of the World Health Organization* 80: 738-745.

S

Sambrook, J., Fritsch, E. F., & Maniatis, T. (1989) *Molecular Cloning: A Laboratory Manual*, 2nd Edition, Cold Spring Harbor Laboratory, Cold Spring Harbor, NY.

Sanchez, G., Knight, S., & Strickler, J. (1976) Nucleotide transport in African trypanosomes. *Comparative Biochemistry and Physiology B - Biochemistry and Molecular Biology* 53: 419-421.

Sanchez, M. A., Ullman, B., Landfear, S. M., & Carter, N. S. (1999) Cloning and functional expression of a gene encoding a P1 type nucleoside transporter from *Trypanosoma brucei*. *Journal of Biological Chemistry* 274: 30244-30249.

Sanchez, M. A., Tryon, R., Green, J., Boor, I., & Landfear, S. M. (2002) Six related nucleoside/nucleobase transporters from *Trypanosoma brucei* exhibit distinct biochemical functions. *Journal of Biological Chemistry* 277: 21499-21504.

Sanchez, M. A., Tryon, R., Pierce, S., Vasudevan, G., & Landfear, S. M. (2004) Functional expression and characterization of a purine nucleobase transporter gene from *Leishmania major*. *Molecular Membrane Biology* 21: 11-18.

Sanchez, M. A., Drutman, S., Van Ampting, M., Matthews, K., & Landfear, S. M. (2004) A novel purine nucleoside transporter whose expression is up-regulated in the short stumpy form of the *Trypanosoma brucei* life cycle. *Molecular and Biochemical Parasitology* 136: 265-272.

Scazzocchio, C. & Gorton, D. J. (1977) The regulation of purine breakdown. In Smith, J. E. & Pateman, J. A. (eds), *Genetics and Physiology of Aspergillus*. Academic Press, NY pp. 255-265.

Schmidt, R., Manolson, M. F., Angelides, K. J., & Poole, R. J. (1984) 8-azidoadenine: a photoaffinity label for the purine transport system of *Saccharomyces cerevisiae*. *FEBS Letters* 129: 305-308.

Schofield, C.J. & Maudlin, I. (2001) Trypanosomiasis control. *International Journal of Parasitology* 31: 614-619.

The Scientist. (May 13, 2002) Fighting the 10/90 gap. By Ricki Lewis.

Seed, J. R. (2000) Current status of African trypanosomiasis. *ASM News* 66: 395-402.

Seley, K. L., Januszcyk, P., Hagos, A., Zhang, L., & Dransfield, D. T. (2000) Synthesis and antitumor activity of thieno-separated tricyclic purines. *Journal of Medicinal Chemistry* 43: 4877-4883.

Seley, K. L., Zhang, L., & Hagos, A. (2001) "Fleximers." Design and synthesis of two novel split nucleosides. *Organic Letters* 3: 3209-3210.

Seley, K. L., Zhang, L., Hagos, A., & Quirk, S. (2002) "Fleximers". Design and synthesis of a new class of novel shape-modified nucleosides. *Journal of Organic Chemistry* 67: 3365- 3373.

Shayeghi, M., Akerman, R., & Jarvis, S. M. (1999) Nucleobase transport in opossum kidney epithelial cells and *Xenopus laevis* oocytes: the characterisation, structure-activity relationship of uracil analogues and oocyte expression studies of sodium-dependent and -independent hypoxanthine uptake. *Biochimica et Biophysica Acta – Biomembranes* 1416: 109-118.

Sloof, P. & Benne, R. (1997) RNA editing in kinetoplastid parasites: what to do with U. *Trends in Microbiology* 5: 189-195.

Smith, D. H., Pépin, J., & Stich, A. H. R. (1998) Human African trypanosomiasis: an emerging public health crisis. *British Medical Bulletin* 54: 341-355.

Sommer, J. M., Hua, S.-, Li, F., Gottesdiener, K. M., & Wang, C. C. (1996) Cloning by functional complementation in *Trypanosoma brucei*. *Molecular and Biochemical Parasitology* 76: 83-89.

Somoza, J. R., Chin, M. S., Focia, P. J., Wang, C. C., & Fletterick, R.J. (1996) Crystal structure of the hypoxanthine-guanine-xanthine phosphoribosyltransferase from the protozoan parasite *Tritrichomonas foetus*. *Biochemistry* 35: 7032-7040.

Somoza, J. R., Skillman, A. G., Jr., Munagala, N. R., Oshiro, C. M., Knegtel, R. M., Mpoke, S., Fletterick, R. J., Kuntz, I. D., & Wang, C. C. (1998) Rational design of novel antimicrobials: blocking purine salvage in a parasitic protozoan. *Biochemistry* 37: 5344-5348.

Soulère, L., Hoffmann, P., Bringaud, F., & Périé, J. (1999) Uptake of NO-releasing drugs by the P2 nucleoside transporter in trypanosomes. *Brazilian Journal of Medical and Biological Research* 32: 1447-1452.

Stevens, J. R., Noyes, H. A., Dover, G. A, & Gibson, W. C. (1999) The ancient and divergent origins of the human pathogenic trypanosomes, *Trypanosoma brucei* and *T. cruzi*. *Parasitology* 118: 107-116.

Stevens, J. R., Noyes, H. A., Schofield, C. J., & Gibson, W. (2001) The molecular evolution of Trypanosomatidae. *Advances in Parasitology* 48: 1-56.

Stich, A., Barrett, M. P., & Krishna, S. (2003) Waking up to sleeping sickness. *Trends in Parasitology* 19: 195-197.

Stryer, L. (1995) *Biochemistry* (4th Edition) W.H. Freeman & Company, New York.

Sundaram, M., Yao, S. Y. M., Ingram, J. C., Berry, Z. A., Abidi, F., Cass, C. E., Baldwin, S. A., & Young, J. D. (2001) Topology of a human equilibrative, nitrobenzylthioinosine (NBMPR)-sensitive nucleoside transporter (hENT1) implicated in cellular uptake of adenosine and anti-cancer drugs. *Journal of Biological Chemistry* 276: 45270-45275.

I

Tait, A., Babiker, E. A., & Le Ray, D. (1984) Enzyme variation in *Trypanosoma brucei* spp. I. Evidence for the sub-speciation of *Trypanosoma brucei gambiense*. *Parasitology* 89: 311-326.

Tait, A., Barry, J. D., Wink, R., Sanderson, A., & Crowe, J. S. Enzyme variation in *T. brucei* spp. II. (1985) Evidence for *T. b. rhodesiense* being a set of variants of *T. b. brucei*. *Parasitology* 90: 89-100.

Turner, C. M. & Barry, J. D. (1989) High frequency of antigenic variation in *Trypanosoma brucei rhodesiense* infections. *Parasitology* 99: 67-75.

Turner, C. M. (1999) Antigenic variation in *Trypanosoma brucei* infections: an holistic view. *Journal of Cell Science* 112: 3187-3192.

Tye, C-K., Kasinathan, G., Barrett, M. P., Brun, R., Doyle, V. E., Fairlamb, A. H., Weaver, R., & Gilbert, I. H. (1998) An approach to use an unusual adenosine transporter to selectively deliver polyamine analogues to trypanosomes. *Bioorganic and Medicinal Chemistry Letters* 8: 811-816.

V

Van Schaftingen, E., Opperdoes, F. R., & Hers, H. G. (1987) Effects of various metabolic conditions and of the trivalent arsenical melarsen oxide on the intracellular levels of fructose 2,6-bisphosphate and of glycolytic intermediates in *Trypanosoma brucei*. *European Journal of Biochemistry* 166: 653-661.

- Vansterkenburg, E. L., Coppens, I., Wilting, J., Bos, O. J., Fischer, M. J., Janssen, L. H., & Opperdoes, F. R. (1993) The uptake of the trypanocidal drug suramin in combination with low-density lipoproteins by *Trypanosoma brucei* and its possible mode of action. *Acta Tropica* 54: 237-250.
- Van Xong, H., Vanhamme, L., Chamekh, M., Chimfwembe, C. E., Van Den Abbeele, J., Pays, A., Van Meirvenne, N., Hamers, R., De Baetselier, P., & Pays, E. (1998) A VSG expression site-associated gene confers resistance to human serum in *Trypanosoma rhodesiense*. *Cell* 95: 839-846.
- Vasudevan, G., Carter, N. S., Drew, M. E., Beverley, S. M., Sanchez, M. A., Seyfang, A., Ullman, B., & Landfear, S. M. (1998) Cloning of *Leishmania* nucleoside transporter genes by rescue of a transport-deficient mutant. *Proceedings of the National Academy of Sciences USA* 95: 9873-9878.
- Veeken, H. & Pécoul, B. (2000) Drugs for 'neglected diseases': a bitter pill. *Tropical Medicine and International Health* 5: 309-311.
- Vickerman, K. (1985) Developmental cycles and biology of pathogenic trypanosomes. *British Medical Bulletin* 41: 105-114.
- Vickerman, K., Tetley, L., Hendry, K. A., & Turner, C. M. (1988) Biology of African trypanosomes in the tsetse fly. *Biology of the Cell* 64: 109-119.
- Vickerman, K. (1997) Landmarks in trypanosome research. In *Trypanosomiasis and Leishmaniasis*. Eds Hide, G., Mottram, J. C., Coombs, G. H., & Holmes, P. H. CAB International.
- Vickers, M. F., Yao, S. Y. M., Baldwin, S. A., Young, J. D., & Cass, C. E. (2000) Nucleoside transporter proteins of *Saccharomyces cerevisiae*. Demonstration of a transporter (FUI1) with high uridine selectivity in plasma membranes and a transporter (FUN26) with broad nucleoside selectivity in intracellular membranes. *Journal of Biological Chemistry* 275: 25931-25938.
- Vreysen, M. J., Saleh, K. M., Ali, M. Y., Abdulla, A. M., Zhu, Z. R., Juma, K. G., Dyck, V. A., Msangi, A. R., Mkonyi, P. A., & Feldmann, H. U. (2000) *Glossina austeni* (Diptera: Glossinidae) eradicated on the island of Unguja, Zanzibar, using the sterile insect technique. *Journal of Economic Entomology* 93: 123-135.

W

Wallace, L. J. M., Candlish, D., & De Koning, H. P. (2002) Different substrate recognition motifs of human and trypanosome nucleobase transporters. Selective uptake of purine antimetabolites. *Journal of Biological Chemistry* 277: 26149-26156.

Walmsley, A. R., Barrett, M. P., Bringaud, F., & Gould, G. W. (1998) Sugar transporters from bacteria, parasites and mammals: structure-activity relationships. *Trends in Biochemical Sciences*. 23: 476-481.

Wang, C. C. (1995) Molecular mechanisms and therapeutic approaches to the treatment of African trypanosomiasis. *Annual Review of Pharmacology and Toxicology* 35: 93-127

Weber, E., Rodriguez, C., Chevallier, M. R., & Jund, R. (1990) The purine-cytosine permease of *Saccharomyces cerevisiae*: primary structure and deduced protein sequence of the FCY2 gene product. *Molecular Microbiology* 4: 585-596.

Welburn, S. C., Fevre, E. M., Coleman, P. G., Odiit, M., & Maudlin, I. (2001) Sleeping sickness: a tale of two diseases. *Trends in Parasitology* 17: 19-24.

Williamson, J. (1970) Review of chemotherapeutic and chemoprophylactic agents. In: Mulligan, H. W. ed. *The African trypanosomiases*. George Allen & Unwin (London).

Witola, W. H., Inoue, N., Ohashi, K., & Onuma, M. (2004) RNA-interference silencing of the adenosine transporter-1 gene in *Trypanosoma evansi* confers resistance to diminazene aceturate. *Experimental Parasitology* 107: 47-57.

World Health Organisation. (2000) Report on Global Surveillance of Epidemic-prone Infectious Diseases.

World Health Organisation. (2001) Human African Trypanosomiasis Treatment and Drug Resistance Network: Report of the second and third meetings.

World Health Organisation. (2002) Human African Trypanosomiasis – A Guide for Drug Supply.

Wung, W. E. & Howell, S. B. (1980) Simultaneous liquid chromatography of 5-fluorouracil, uridine, hypoxanthine, xanthine, uric acid, allopurinol, and oxipurinol in plasma. *Clinical Chemistry* 26: 1704-1708.

Y

Yao, S. Y. M., Ng, A. M. L., Vickers, M. F., Sundaram, M., Cass, C. E., Baldwin, S. A., & Young, J. D. (2002) Functional and molecular characterization of nucleobase transport by recombinant human and rat equilibrative nucleoside transporters 1 and 2. Chimeric constructs reveal a role for the ENT2 helix 5-6 region in nucleobase translocation. Journal of Biological Chemistry 277: 24938-24948.

Appendices

Appendix A: Media, Buffers and Solutions**LB medium**

Tryptone	10 g/l
Yeast extract	5 g/l
NaCl	10 g/l

pH 7.0

Sterilisation by autoclaving

SOC medium

Bactotryptone	20 g/l	
Yeast extract	5 g/l	
NaCl	10 mM	
KCl	2.5 mM	
MgCl ₂	10 mM	} added after sterilisation by autoclaving
MgSO ₄	10 mM	
Glucose	20 mM	

Trypanosome assay buffer

HEPES	33 mM
NaCl	98 mM
KCl	4.6 mM
CaCl ₂	0.55 mM
MgSO ₄	0.07 mM
NaH ₂ PO ₄	5.8 mM
MgCl ₂	0.3 mM
NaHCO ₃	23 mM
Glucose	14 mM

pH 7.3

Erythrocyte assay buffer

NaCl	140 mM
KCl	5 mM
Tris	20 mM
MgCl ₂	2 mM
EDTA	0.1 mM

pH 7.4

Yeast assay buffer

HEPES	33 mM
NaCl	98 mM
KCl	4.6 mM
CaCl ₂	0.55 mM
MgSO ₄	0.07 mM
NaH ₂ PO ₄	5.8 mM
MgCl ₂	0.3 mM
NaHCO ₃	23 mM

pH 7.3

PSG (phosphate-buffered saline plus glucose)

PS buffer:

Na ₂ HPO ₄ (anhydrous)	13.48 g
NaH ₂ PO ₄ .2H ₂ O	0.78 g
NaCl	4.25 g

Make to one litre with dH₂O

Add six volumes of PS to four volumes of glucose solution to give final glucose concentration of 1%

pH 8.0 exactly

CBSS (Carter's balanced salt solution)

HEPES	25 mM
NaCl	120 mM
KCl	5.4 mM
CaCl ₂	0.55 mM
MgSO ₄	0.4 mM
Na ₂ HPO ₄	5.6 mM
D-glucose	11.1 mM

pH 7.4

HMI-9 (and purine nucleobase-free HMI-9)

(For 500ml of medium)

Iscoves MEM	365 ml
Hypoxanthine (or adenosine for purine nucleobase-free)	1 mM
Kanamycin	30 µg/ml
Penicillin	50 u/ml
Streptomycin	50 µg/ml
Bathocuprione disulphonic acid	50 µM
Thymidine	160 µM
Pyruvate	1 mM
β-mercaptoethanol	2 mM
Cysteine	1 mM
FCS (or dialysed FCS for purine nucleobase-free)	20%

SDM-79

(For 1 litre of medium)

S-MEM F14 powder	7 g
Medium 199 TC45 powder	2 g
MEM amino acids (50X)	8 ml
MEM non-essential Amino acids (100)	6 ml
Glucose	1 g
HEPES	8 g
MOPS	5 g
NaHCO ₃	2 g
Sodium pyruvate	100 mg
L-alanine	200 mg
L-arginine	100 mg
L-glutamine	300 mg
L-methionine	70 mg
L-phenylalanine	80 mg
L-proline	600 mg
L-serine	60 mg
L-taurine	160 mg
L-threonine	359 mg
L-tyrosine	100 mg
Adenosine	10 mg
Guanosine	10 mg
Glucosamine HCl	50 mg
Folic acid	4 mg
Para-aminobenzoic acid	2 mg
Biotin	0.2 mg
FCS	10%

pH 7.3

PFTM (purine-free trypanosome medium)

(For 1 litre of medium)

RPMI 1640 medium	130 ml
S-MEM powder	7 g
8ml MEM (50x) amino acids	8 ml
6ml MEM non-essential amino acids (100)	6 ml
CaCl ₂ .2H ₂ O	39 mg
Glucose	1 g
HEPES	8 g
MOPS	5 g
NaHCO ₃	2 g
Sodium pyruvate	0.2 g
L-alanine	0.2 g
L-arginine	0.1 g
L-glutamine	0.3 g
L-methionine	70 mg
L-phenylalanine	80 mg
L-proline	0.6 g
L-serine	60 mg
L-threonine	0.35 g
L-tyrosine	0.1 g
L-aurine	0.3 g
Glucosamine	50 mg
Folic acid	5 mg
<i>p</i> -aminobenzoic acid	20 mg
Biotin	0.2 mg
Sodium acetate	6.5 mg

pH 7.3

Supplement with 7.5 mg/l bovine hemin, 5% dialysed FCS and inosine (0.2 mM final)

YPAD (yeast extract - peptone - dextrose and adenine medium)

(For 600 ml of medium)

Yeast extract	6 g
Peptone	12 g
Glucose	12 g
Adenine hemisulphate	60 mg
dH ₂ O	to 600 ml

(For solid medium → Bacto-agar 10g)

pH 5.6

Autoclave

SC-URA (synthetic complete medium minus uracil)

(For 600 ml of medium)

Difco Yeast Nitrogen Base w/o amino acids	4 g
Glucose	12 g
Synthetic complete drop out mix	0.5 g
dH ₂ O	to 600 ml

(For solid medium → Bacto-agar 10g)

pH 5.6

Autoclave

Synthetic complete drop out mix minus uracil

Adenine hemisulphate	2 g (or 1.47 g adenine free base)
Arginine HCl	2 g
Histidine HCl	2 g
Isoleucine	2 g
Leucine	4 g
Lysine HCl	2 g
Methionine	2 g
Phenylalanine	3 g
Homoserine	6 g
Tryptophan	3 g
Tyrosine	2 g
Valine	9 g

SLB

NaCl	5 g/l
Yeast extract	20 g/l
Bactotryptone	35 g/l
[5.0 M] NaOH	1 ml/l

DNA extraction buffer

[1.0 M] Tris (pH8)	10 ml
[0.5 M] EDTA	2 ml
[5.0 M] NaCl	4 ml
dH ₂ O	to 200 ml

TBE running buffer

Tris	53.9 g
Boric acid	27.5 g
EDTA	2.3 g
dH ₂ O	to 5 litres

TE buffer

Tris	10 mM (0.605 g)
EDTA	1 mM (0.186 g)
dH ₂ O	to 500ml

pH 8.0

TFB1

Potassium acetate	30 mM
CaCl ₂	10 mM
MnCl ₂	50 mM
RbCl	100 mM
15% glycerol	

pH 5.8

TFB2

MOPS	10 mM
CaCl ₂	75 mM
RbCl	10 mM
15% glycerol	

pH 6.5

20x Northern gel buffer

Na ₂ HPO ₄	0.36 M (96.5 g heptahydrate per litre)
NaH ₂ PO ₄	0.04 M (5.5 g monohydrate per litre)

1x Northern gel buffer, 3% formaldehyde

20x Northern gel buffer	25 ml
Stock formaldehyde (37%)	44 ml
dH ₂ O	430 ml

RNA loading buffer

50% glycerol

1mM EDTA

0.4% bromphenol blue

Made up with DEPC-dH₂O and autoclaved**DEPC-dH₂O**0.1% DEPC in dH₂O

Incubated at room temperature overnight

Autoclaved

20x SSC

Sodium citrate 0.3 M

NaCl 3.0 M

pH 7.0

Autoclave

Denhardt's solution (x100)

(For 500 ml)

Ficoll 400 10 g

Polyvinylpyrrolidone 10 g

BSA 10 g

Trypanosome stabilates

50 ml of culture (1×10^6 cells/ml) centrifuged at 1200 rpm for 10 minutes and resuspended gently in 3-4 ml of fresh medium. An equal volume of freezing medium (10% glycerol in heat-inactivated FCS) mixed thoroughly but gently. Cell suspension transferred into cryotubes and placed in cotton wool-lined container. Container placed in -70 °C freezer overnight and then transferred to liquid nitrogen storage container.

Bacterial stabilates

600 µl of overnight LB culture mixed with 400 µl of 40% glycerol in LB broth. Tubes frozen at -20 °C and then stored at -70 °C until required.

Yeast stabilates

850 μ l of overnight broth culture mixed with 150 μ l of sterile glycerol. Tubes frozen at -20°C and then stored at -70°C .

Appendix B: Restriction Enzyme Recognition and Incision Sites

<i>BamHI</i>	G↓GATCC
<i>EcoRI</i>	G↓AATTC
<i>HindIII</i>	A↓AGCTT
<i>NotI</i>	GC↓GGCCGC
<i>PstI</i>	CTGCA↓G
<i>SalI</i>	G↓TCGAC
<i>Sau3AI</i>	↓GATC
<i>XbaI</i>	T↓CTAGA
<i>XhoI</i>	C↓TCGAG

Appendix C: Publications

Al-Salabi, M. I., Wallace, L. J. M., & De Koning, H. P. (2003) A *Leishmania major* nucleobase transporter responsible for allopurinol uptake is a functional homolog of the *Trypanosoma brucei* H2 transporter. *Molecular Pharmacology* 63: 814-820.

Burchmore, R., Wallace L. J. M., Candlish, D., Al-Salabi, M. I., Beal, P., Barrett, M. P., Baldwin, S. A., & De Koning, H. P. (2003) Cloning, heterologous expression and *in situ* characterization of the first high affinity nucleobase transporter from a protozoan. *Journal of Biological Chemistry* 278: 23502-23507.

De Koning, H. P., Anderson, L. F., Stewart, M., Burchmore, R. J., Wallace, L. J., Barrett, M. P. (2004) The trypanocide diminazene aceturate is accumulated predominantly through the TbAT1 purine transporter: additional insights on diamidine resistance in african trypanosomes. *Antimicrobial Agents and Chemotherapy* 48: 1515-1519.

Matovu, E., Stewart, M., Geiser, F., Brun, R., Mäser, P., Wallace, L. J. M., Burchmore, R. J., Enyaru, J. C. K., Barrett, M. P., Kaminsky, R., Seebeck, T. and De Koning, H. P. (2003) The mechanisms of arsenical and diamidine uptake and resistance in *Trypanosoma brucei*. *Eukaryotic Cell* 2: 1003-1008.

Natto, M. J., Wallace, L. J. M., Candlish, D., Al-Salabi, M. I., Coutts, S. E., & De Koning, H. P. Characterisation of allopurinol transport in *Trypanosoma brucei*: implications for resistance to purine antimetabolites. In submission.

Wallace, L. J. M., Candlish, D., & De Koning, H. P. (2002) Different substrate recognition motifs of human and trypanosome nucleobase transporters. Selective uptake of purine antimetabolites. *Journal of Biological Chemistry* 277: 26149-26156.

Woe is not me.